

Inaugural-Dissertation

zur Erlangung der Doktorwürde

der

Naturwissenschaftlich-Mathematischen Gesamtfakultät

der

Ruprecht-Karls Universität

Heidelberg

vorgelegt von

M. Sc. - Dipl. Chem. Mihaela Caprioara

aus Piatra Neamt/Rumänien

Tag der mündlichen Prüfung: 26.11.2007

**DNA-Based Ligands for Use in Asymmetric Catalysis and
Development of Metallo-(deoxy)Ribozymes**

**Gutachter: Prof. Dr. Andres Jäschke
Prof. Dr. Nils Metzler-Nolte**

Acknowledgments

I thank all my friends and colleagues from the University of Heidelberg and from other research groups who contributed to the work described in this thesis.

I express my sincere gratitude to my supervisor, Prof. Andres Jäschke, for giving me the opportunity to work in a very stimulating research group, on a highly interesting project, as well as for his continuous support, encouragement, and confidence at all stages of my work. Thank you for all suggestions that helped me to improve the quality of this thesis.

I would like to thank Prof. Nils Metzler-Nolte who agreed to review and co-examine this thesis.

I want to acknowledge Dr. Roberto Fiammengo and express my recognition for his guidance, expertise, determination, and understanding, which considerably added to my experience throughout all these years. He provided me with direction, stimulated me in being critical with my results, and had always prompt answers to my questions. I appreciate his work and patience to read the preliminary versions of my writings, including this thesis, and the assistance he provided through the most difficult correction steps.

I would like to acknowledge Prof. Nils Metzler-Nolte and Dr. Srecko Kirin who kindly provided the *N,N*-bis(2-picolyl)amine derivative, as well as Prof. Lutz Gade for generously providing the PYRPHOS ligand. I also thank Prof. Roland Krämer and Dr. Andriy Mokhir for helpful discussion and technical support in performing the MALDI TOF measurements. I am grateful to Dr. Marianne Engeser, University of Bonn, for our fruitful collaboration, for recording the electrospray mass spectra of the Rh(I)-PYRPHOS complex and the DNA-PYRPHOS conjugate, as well as for her help with the interpretation of the data.

I thank Dr. Mark Helm, Pierre Fournier, Stephanie Pfander and Anna Wiesmayr for generously offering to proof-read sections of my thesis. I appreciate their support, their rigorous and constructive corrections. I am grateful to Stephanie Pfander and Alexander Nierth for the linguistic improvements of the “Zusammenfassung” of my thesis.

I want to acknowledge Pierre Fournier with whom I shared the work in the lab, for the many helpful discussions about catalysis and for his enthusiasm in the times when difficult tasks came up.

Special thanks go to Dr. Richard Wombacher, Columbia University, for his continuous

interest in my project and for our scientific debates, knowledge exchange, and venting of frustration during our breaks. I also thank Dr. Barbara-Sylvia Weigand, Stephanie Pfander, Markus Petermeier for being supportive and understanding, for their friendship and encouragement over the last four years. I am grateful to all former and current colleagues for the stimulating working environment and for their contributions to the lab research standards.

This work would have been incomplete without the help of Sandra Suhm, Heiko Rudy, Tobias Timmerman, Besarta Nezaj, Marina Silbereis. I want to thank them for the great technical assistance in synthesis, mass spectrometry and NMR measurements, as well as for their excellent job to fulfil the needs of the lab.

My special thanks go to the office staff, in particular to Mrs. Viola Funk and Mrs. Karin Weiß, for all the instances in which their assistance helped me along the way and for all their support and advices at times of critical need.

Thanks to my family for their sincere encouragement and support they provided me through my entire life. In particular, I would like to thank my fiancé and my best friend, Razvan, for his patient support, encouragement, and for helping me finish this thesis.

This work was financially supported by Deutsche Forschungsgemeinschaft (SFB 623).

To my family

Summary

Caprioara, Mihaela; M. Sc. Chem.

Title: DNA-Based Ligands for Use in Asymmetric Catalysis and Development of Metallo-(deoxy)Ribozymes

1. Gutachter: Prof. Dr. Andres Jäschke

2. Gutachter: Prof. Dr. Nils Metzler-Nolte

The fascinating way nature relies on biomolecules, mostly proteins and sometimes RNA, to carry out sophisticated chemical processes led to more and more efforts to use the concepts of biology for preparing efficient chiral catalysts. The “hybrid catalyst” approach that combines the steric information derived from a protein scaffold with the catalytic activity of transition metal complexes offers a resourceful means of developing semisynthetic metalloenzymes for enantioselective applications. Since the discovery of nucleic acids with enzyme-like functions, the catalytic potential of nucleic acids is being revealed by *in vitro* selection and evolution of novel ribozymes and DNAzymes. Nucleic acids, especially RNA, appear to be versatile catalysts capable of accelerating a broad range of reactions and exquisitely discriminating between chiral targets. However, while proteins dominated the construction of hybrid catalysts, the application of DNA and RNA in asymmetric catalysis has hardly been explored.

This work aimed at exploring the chirality of nucleic acids and generating hybrid catalysts based on DNA and RNA. Towards the development of metallo-(deoxy)ribozymes assisted by combinatorial strategies (*e.g.*, SELEX), a straightforward synthetic way of embedding transition metal complexes in nucleic acids folds was established. DNA sequences carrying mono- and bidentate phosphine ligands as well as P,N-ligands were successfully prepared starting from amino-modified oligonucleotide precursors. The optimized “convertible nucleoside” approach allowed the parallel, high-yielding synthesis of various alkylamino-DNA conjugates differing in length and structure of the spacer. Coupling of amino-oligonucleotides with PYRPHOS, BINAP and PHOX ligands equipped with a carboxyl group led to the incorporation of phosphine moieties at predetermined internal sites. Moreover, the stability of the DNA-tethered BINAP and PHOX was reasonably high, which makes them attractive candidates for the development of transition metal-containing oligonucleotides. To this end, systematic studies on the behavior of phosphine- and PHOX-metal complexes in aqueous medium - a prerequisite of nucleic acid catalysts - were carried out. Two model organometallic transformations were selected that were compatible with the structure and chemistry of nucleic acids. The rhodium(I)-catalyzed 1,4-addition of phenyl boronic acid to 2-cyclohexen-1-one and iridium(I)-catalyzed allylic amination of the branched phenyl allyl acetate, respectively, proceeded efficiently in the presence of phosphorus-based ligands, in aqueous medium, at room temperature and low catalyst concentration. For the first model reaction, the best conversion (80%) was achieved with the isolated $[\text{Rh}(\text{nbd})\text{BINAP}]\text{BF}_4$ complex, in 6:1 dioxane/water, and TEA additive. On the basis of these data, a suitable system for assessing the catalytic potential of the DNA-BINAP ligand was implemented. In the second chosen reaction the *in situ* formed Ir(I)-PHOX complexes (0.05-0.1 mM) gave rise to racemic, branched allylic amination products in good yields (33-75%), in 3:7 dioxane/water. Kinetic resolution of the racemic substrate was then attempted by employing catalysts generated from the $[\text{Ir}(\text{cod})\text{Cl}]_2$ precursor and single- and double-stranded DNA-PHOX conjugates. Good conversions were obtained in the presence of G-poor DNA/DNA and RNA/DNA hybrids bearing the PHOX moiety, indicating a potential role of the G-N7 site in the first coordination sphere. With all tested DNA-PHOX conjugates, the levels of enantioselectivity remained modest. The results described in this work provide useful information for understanding the influence of nucleic acid sequence and covalent tethering on the reaction outcome. These are the first reported applications of DNA-based ligands in organometallic catalysis and they build the fundamentals for further development of selective nucleic acid catalysts, by means of rational design and *in vitro* selection approaches.

Zusammenfassung

Die faszinierende Art und Weise, in der die Natur auf Biomoleküle - meist Proteine und teilweise RNA - zurückgreift um anspruchsvolle chemische Prozesse auszuführen, hat zu immer mehr Bemühungen geführt, die Konzepte der Biologie für die Herstellung effizienter chiraler Katalysatoren zu nutzen. Die Verbindung dreidimensionaler Proteinstrukturen mit der katalytischen Aktivität von Übergangsmetallkomplexen ist eine interessante Herangehensweise in der Synthese sogenannter Hybrid-Katalysatoren für enantioselektiven Anwendungen. Seit der Entdeckung von Nucleinsäuren mit enzym-ähnlichen Funktionen wurde deren katalytisches Potential durch in vitro Selektion und Evolution neuer Ribozyme und DNAzyme deutlich gezeigt. Nucleinsäuren, insbesondere RNA, sind demnach vielseitige Katalysatoren, die in der Lage sind eine breite Palette an Reaktionen zu beschleunigen und außerordentlich gut zwischen chiralen Zielmolekülen zu unterscheiden. Während Proteine die Entwicklung von Hybrid-Katalysatoren jedoch weitgehend beherrschen, wurde die Anwendung von DNA oder RNA in der asymmetrischen Katalyse bisher kaum untersucht.

Das Ziel dieser Arbeit war die Synthese von Hybrid-Katalysatoren auf Basis eines DNA und RNA Gerüsts. Für die kombinatorisch-gestützte Entwicklung von Metallo-Ribozymen und -Deoxyribozymen (z. B. mittels SELEX) wurde ein direkter Syntheseweg zum Einbau von Übergangsmetall-Komplexen in Nucleinsäurestrukturen etabliert. DNA Sequenzen welche ein- und zweizählige Phosphin-Liganden sowie P,N-Liganden tragen, wurden ausgehend von amino-modifizierten Oligonucleotid Vorstufen erfolgreich synthetisiert. Der optimierte Ansatz mittels sogenannter „convertible nucleosides“ erlaubt die parallele Synthese verschiedener alkylamino-DNA Konjugate, welche sich in Länge und Struktur der Spacer unterscheiden. Die Kopplung der Amino-Oligonucleotide mit PYRPHOS-, BINAP- und PHOX-Liganden, welche mit einer Carboxylgruppe ausgestattet sind, führt zum Einbau der Phosphin Bausteine an einer zuvor festgelegten Stelle im Nucleotidstrang. Ferner macht die hohe Stabilität der DNA-gebundenen BINAP und PHOX Liganden diese zu attraktiven Kandidaten für die Entwicklung von Oligonucleotiden, die Übergangsmetall-Komplexe enthalten. Zu diesem Zweck wurden systematische Studien zum Verhalten von Phosphin- und PHOX-Metallkomplexen im wässrigen Medium durchgeführt - eine Voraussetzung für Katalysatoren auf Nucleinsäurebasis. Zwei metallorganische Transformationen, die mit der Struktur und den chemischen Eigenschaften von Nucleinsäuren kompatibel sind, wurden als Modellreaktionen ausgewählt. Die Rhodium(I)-katalysierte 1,4-Addition von Phenylborsäure zu 2-Cyclohexen-1-on und die Iridium(I)-katalysierte allylische Aminierung des verzweigten Phenylallylacetats verliefen erfolgreich in Anwesenheit von phosphorbasierten Liganden, in wässrigem Medium, Raumtemperatur und niedriger Katalysatorkonzentration. Für die erste Modellreaktion wurde die beste Umsetzung mit dem isolierten $[\text{Rh}(\text{nbd})\text{BINAP}]\text{BF}_4$ Komplex in 6:1 Dioxan/Wasser und unter TEA Zugabe erzielt (80 %). Auf Grundlage dieser Daten wurde ein geeignetes System erstellt, um das katalytische Potential von DNA-BINAP Liganden zu beurteilen. Bei der zweiten Modellreaktion führte der in situ gebildete Ir(I)-PHOX Komplex (0.05-0.1 mM) in 3:7 Dioxan/Wasser zu guten Ausbeuten (33-75 %) der racemischen, verzweigten Aminierungsprodukte. Bei der kinetischen Auflösung racemischer Substrate wurden Katalysatoren verwendet, die aus dem $[\text{Ir}(\text{cod})\text{Cl}]_2$ -Vorstufe und einfach- und doppelsträngigen DNA-PHOX Konjugaten hergestellt wurden. Gute Umsätze wurden in Anwesenheit von G-armen DNA/DNA und RNA/DNA Hybriden, die eine PHOX Gruppe tragen, erzielt, was auf eine mögliche Funktion der G-N7 Position in der ersten Koordinationssphäre hindeutet. Die Enantioselektivität blieb jedoch bei allen getesteten DNA-PHOX Konjugaten gering. Die Ergebnisse dieser Arbeit bieten hilfreiche Informationen für das Verständnis darüber, welchen Einfluss die Nucleinsäuresequenz und die kovalente Verknüpfung auf den Ausgang der Reaktion haben. Dies ist der erste Bericht über die Anwendungen von DNA-basierten Liganden in der metallorganischen Katalyse und setzt den Grundstein für die weitere Entwicklung selektiver Nucleinsäurekatalysatoren mittels der Methodik des rationalen Designs und der in vitro Selektion.

INDEX

1	INTRODUCTION.....	17
1.1	SYNTHESIS OF CHIRAL ORGANIC MOLECULES	17
1.1.1	<i>Asymmetric Catalysis with Phosphorus Ligands</i>	19
1.1.1.1	PYRPHOS Ligands.....	19
1.1.1.2	BINAP Ligands.....	21
1.1.1.3	PHOX Ligands.....	24
1.1.1.4	Phosphite and Phosphoramidite Ligands	26
1.1.2	<i>Biocatalysis</i>	27
1.1.2.1	Artificial Enantioselective Enzymes	28
1.1.2.2	Hybrid Catalysts.....	30
1.2	NUCLEIC ACID ENZYMES	33
1.2.1	<i>Chirality in the Structure of Nucleic Acids</i>	33
1.2.2	<i>In vitro Selection of Nucleic Acid-Enzymes</i>	38
1.2.3	<i>DNA-zymes</i>	40
1.2.4	<i>Ribozymes</i>	41
1.2.5	<i>DNA-Based Hybrid Catalysts</i>	43
1.3	TRANSITION METAL-DNA CONJUGATES	46
1.3.1	<i>Non-covalent Interactions</i>	46
1.3.2	<i>Covalent Attachment</i>	47
1.3.2.1	Post-synthetic Functionalization	47
1.3.2.2	Automated Solid-phase Synthesis.....	49
2	OBJECTIVES.....	53
3	RESULTS AND DISCUSSIONS	55
3.1	INCORPORATION OF METAL COMPLEXES INTO NUCLEIC ACIDS	55
3.1.1	<i>Functionalization of DNA with Phosphoramidite Ligand Precursors</i>	58
3.1.2	<i>DNA-Phosphine Ligands</i>	62
3.1.2.1	Amino-Functionalized Oligonucleotides	62
3.1.2.2	Duplex Stability of Amino-Tethered Oligonucleotides.....	65
3.1.2.3	Reactivity of Amino-Modified Oligonucleotides.....	68
3.1.2.4	Post-synthetic Functionalization of Amino-modified DNA with Phosphine Ligands.....	69
3.1.2.5	Duplex Stability of Bisphosphine-Tethered DNA.....	76
3.2	ORGANOMETALLIC TRANSFORMATIONS IN WATER.....	78
3.2.1	<i>Phosphine- and Phosphinooxazoline-Metal Complexes</i>	79
3.2.2	<i>Rhodium(I)-Catalyzed 1,4-Addition</i>	87

3.2.3	<i>Iridium(I)-Catalyzed Allylic Amination</i>	92
3.2.3.1	Preparation of Allylic Substrates and Products. Analytical Methods.....	95
3.2.3.2	Preliminary Results of Catalysis with Ir-PHOX Complexes.....	98
3.2.3.3	Allylic Amination with DNA-Appended Phosphinooxazoline Ligands.....	104
3.2.3.4	Allylic Amination with Double-stranded DNA-appended Phosphinooxazoline Ligands	110
4	CONCLUSIONS AND OUTLOOK	117
5	MATERIALS AND METHODS	127
5.1	STANDARD METHODS AND REAGENTS	127
5.2	SYNTHESIS OF PHOSPHORUS LIGANDS AND THEIR TRANSITION METAL COMPLEXES.....	128
5.2.1	<i>Synthesis of Phosphoramidite Ligands</i>	128
5.2.2	<i>Synthesis of PHOX Ligands</i>	130
5.2.3	<i>Synthesis of Palladium(II)- and Platinum(II)-Phosphine Complexes</i>	133
5.2.4	<i>Synthesis of Platinum(II)-, Palladium(II)- and Rhodium(I)-PYRPHOS Complexes</i>	134
5.2.5	<i>Synthesis of Rhodium(I)- and Iridium(I)-PHOX Complexes</i>	135
5.3	OLIGONUCLEOTIDES.....	137
5.3.1	<i>Automated Solid-Phase Synthesis</i>	138
5.3.2	<i>General Procedure for the Synthesis of Amino-Modified ODNs</i>	140
5.3.3	<i>General Procedure for the Synthesis of 7-deaza-G -containing Amino-Modified ODNs</i>	141
5.3.4	<i>General Procedure for the Synthesis of Complementary DNA</i>	143
5.4	SYNTHESIS OF DNA-BASED LIGANDS.....	144
5.4.1	<i>Incorporation of Phosphite Moiety by DNA Solid-phase Synthesis</i>	144
5.4.2	<i>Synthesis of DNA-Phosphine Conjugates</i>	146
5.4.3	<i>Synthesis of DNA-Appended N,N-bis(2-picolyl)amine Conjugates</i>	148
5.5	HIGH-PRESSURE LIQUID CHROMATOGRAPHY	150
5.5.1	<i>Reversed-Phase HPLC Purification of Oligodeoxynucleotides</i>	150
5.6	MASS SPECTROMETRY ANALYSIS OF OLIGONUCLEOTIDES	152
5.7	5'-RADIOACTIVE LABELLING OF OLIGONUCLEOTIDES	153
5.8	ANALYSIS AND QUANTIFICATION OF DNA.....	154
5.8.1	<i>Quantification of Oligonucleotides by UV Absorbance</i>	154
5.8.2	<i>Analysis of DNA Duplexes by Thermal Melting Curves</i>	155
5.8.3	<i>Polyacrylamide Gel Electrophoresis (PAGE)</i>	156
5.9	TRANSITION METAL-CATALYZED REACTIONS	157
5.9.1	<i>Conjugate Addition</i>	157
5.9.1.1	Synthesis of 3-Phenyl-1-cyclohexanone	157
5.9.1.2	General Procedure for 1,4-Addition of Phenylboronic Acid to 2-Cyclohexen-1-one	158

5.9.2	<i>Allylic Amination</i>	161
5.9.2.1	Synthesis and Stability of the Allylic Substrate	161
5.9.2.2	Synthesis of Linear and Branched Allylic Amines	162
5.9.2.3	Allylic Amination Catalyzed by Ir-PHOX Complexes	164
6	APPENDICES	169
6.1	LIST OF ABBREVIATIONS	169
6.2	INSTRUMENTS AND SPECIAL MATERIALS	172
7	REFERENCES	175

1 Introduction

1.1 Synthesis of Chiral Organic Molecules

“How would you like to live in a looking-glass house, Kitty? ... Perhaps looking-glass milk isn't good to drink.” (Lewis Carroll, *Through the Looking-Glass*)

„Chirality ... is an intrinsic universal feature of various levels of matter.“^[1]

Living world depends on molecular chirality, in that crucial biopolymers associated with life are made up of chiral monomers (L-amino acids in proteins, D-sugars in RNA and DNA).^[2, 3] Chirality was first described in 1848 by Louis Pasteur who demonstrated that tartrate enantiomers rotated the plane of the polarized light in different ways, and only the right-handed enantiomer was present in wine lees.

In living organisms, all chemical transformations, recognition or information processing involve chiral molecules, such as enzymes or hormones.^[4] Most physiological processes are based on precise molecular interactions between the chiral host molecules and the two enantiomeric guest molecules. Despite the structural similarity, two enantiomers behave and are recognized differently in a chiral environment. Biological chiral receptors, for example, interact mostly with drug molecules having the proper absolute configuration, leading to distinct biological activities of the two enantiomers. The importance of the relationship between pharmacological activity and chirality was demonstrated in the early 1960s, by the tragic administration to pregnant women of thalidomide (Figure 1.1), in the racemate form. The *R* enantiomer has the desired sedative properties, while (*S*)-thalidomide is teratogenic and led to fetal malformations.^[1] However, even in 2000, only 40% of synthetic chiral drugs were sold in single enantiomer dosage form.^[5]

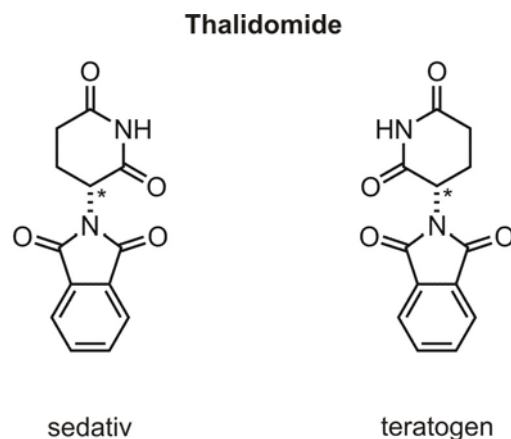


Figure 1.1. Thalidomide enantiomers and their biological properties.

The fascinating way nature is producing substances with chirality and the preference of one enantiomer over the other in the living matter have attracted considerable interest for developing synthetic routes to enantiomerically pure compounds, with the major goal of gaining significant clinical, scientific and industrial benefits. Three main strategies have been established: (i) enantiomer separation; (ii) transformation of a chiral precursor and (iii) enantioselective reactions. Enantiomerically pure substances were earlier obtained by the classical resolution of a racemate or chemical conversion of naturally occurring chiral compounds, such as tartaric and lactic acids, amino acids, carbohydrates, terpenes, or alkaloids. Nevertheless, the use of enantioselective catalysts became over years the most efficient and attractive approach.

For many years, the practical access to pure enantiomers relied on biochemical or biological methods. Nature utilizes enzymes for this purpose and relies on configurational and conformational optimization by structural variation of the chiral building blocks. The complex biological structures nature offers us have often modest applicability in chemical synthesis due to their limited substrate scope and operational stability.^[6] However, with the help of protein engineering techniques, such as mutation, selection, and directed evolution, enzymes have been successfully improved and biocatalysts with novel properties developed.^[7]

In parallel to this field, metal-catalyzed enantioselective transformations have received much attention. Transition metal catalysts possess great potential in synthesis of enantiopure compounds from achiral/prochiral precursors, namely through an asymmetric reaction^[8], or from racemic mixtures. Such metal catalysts usually consist

of a metal centre and a ligand carrying the stereochemical information in order to ensure the catalysis to proceed in a stereoselective manner.^[9] In 2001, Noyori, Sharpless and Knowles were rewarded with the Nobel Prize for their achievements in the field of asymmetric organometallic catalysis.^[1, 10, 11]

1.1.1 Asymmetric Catalysis with Phosphorus Ligands

The search for valuable asymmetric catalytic systems is one of the most active research areas in organic and bioorganic chemistry. A wide range of man-made catalysts has been constructed over the past four decades, and is mainly based on chiral metal complexes. The chiral information in the products prepared by enantioselective catalysis derives from the optically active ligands bound to the transition metal. Therefore, the proper design of the chiral ligands is the most important requirement for achieving high efficiency.^[12, 13] Much effort has been dedicated to the synthesis of new chiral ligands or tuning of existing ligands to obtain high selectivity and reactivity.

After the discovery of Wilkinson's homogeneous hydrogenation catalyst $[\text{RhCl}(\text{PPh}_3)_3]$ ^[14], phosphorus ligands have attracted considerable interest. A second development in the mid-1960s was made by Knowles and Horner who replaced the triphenylphosphine of the Wilkinson's catalysts with chiral monophosphines. These ligands were used in hydrogenation reactions, albeit with poor enantioselectivities. Few years later, monophosphines were successfully replaced due to the rapid development of chiral bisphosphorus ligands. Some of the most relevant phosphorus-based ligands will be reviewed here.

1.1.1.1 PYRPHOS Ligands

A large number of chelating bisphosphine ligands bearing a chiral carbon backbone has been synthesized and mainly employed in Rh-catalyzed asymmetric hydrogenation of dehydroamino acids. The discovery of 1,2-bisphosphine PYRPHOS-type (3,4-bis-diphenylphosphino-pyrrolidine) ligands^[15] enlarged the spectrum of substrates that could be processed with chiral bisphosphines in Rh-catalyzed hydrogenations (*e.g.* *N*-(acylamino)acrylates, enamides, enol acylates, and itaconic acids.^[16-18] A few selected examples of such ligands are illustrated in Figure 1.2.

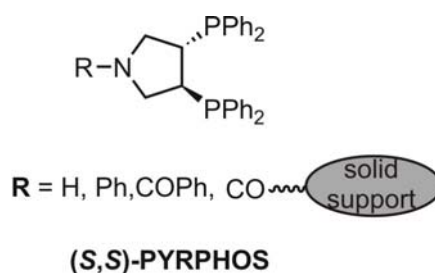


Figure 1.2. PYRPHOS ligands.

The majority of bisphosphine ligands consisting of a chiral carbon-backbone contain two aryl substituents attached to each phosphorus atom, which exert strong steric and electronic influences in their transition metal complexes. The orientation of the phenyl substituents has been reported to control the stereoselectivity and, therefore, the sterically congested phosphines possess remarkable catalytic properties. For example, PYRPHOS ligands, which contain a symmetrically placed nitrogen atom, generate rigid five-membered chelate rings with transition metals beneficial for the optimal transfer of chirality to the reaction centre. With Rh-PYRPHOS as catalyst, hydrogenation of *N*-(acetylamino)cinnamic acid to (*S*)-*N*-acetyl-phenylalanine proceeded with >99% yield and over 95% ee.^[15, 19] An important advantage of these ligands is that they can be readily tuned by variations of the *N*-substituent. Moreover, they can be easily attached to a linker through an amide bond and therefore facilitate the further immobilization of their transition metal complexes on polyethylene glycol supports,^[20] silica gel,^[15] gold surfaces,^[21] or at the end of dendrimers.^[18, 22] In general, the stereoselectivity of the immobilized systems was comparable to those obtained using analogue homogeneous transition metal catalysts. Interesting examples of PYRPHOS application have been reported by Gade and co-workers in early 2000s. Upon fixation of the ligand in the densely packed environment of a dendrimer, the resulting polynuclear complexes induced enantioselectivities of 74-93% in Rh(I)-catalyzed hydrogenation of *Z*-methyl-*N*-(acetylamino)cinnamate and dimethyl itaconate,^[18] and 69% in Pd(0)-catalyzed allylic amination of 1,3-diphenyl-1-acetoxypropene,^[22] respectively.

1.1.1.2 BINAP Ligands

Numerous studies have generally demonstrated that ligands with C_2 symmetry elements perform excellent stereochemical control,^[12] most likely due the reduced number of conformations the ligand can adopt in the coordination sphere of the metal. Noyori's pioneering work on atropisomeric C_2 -symmetric bisphosphine ligand BINAP (2,2'-bis(diphenylphosphino)-1,1'-binaphthyl)^[23] (Figure 1.3) and its successful applications in Rh-catalyzed hydrogenation of α -(acylamino)acrylic acids and esters^[24] (Table 1.1, entry 1) opened the way to a new class of fully aromatic chiral phosphorus ligands. The BINAP skeleton is conformationally flexible and can accommodate a large variety of transition metals, generating seven-membered rings that contain only sp^2 -hybridized carbon atoms. The rotational freedom around the donor atom-metal bond in the resulting chelate structures is therefore restricted. This feature, responsible for the chirality transfer to the metal coordination sites involved in the catalytic transformation, explains the high chiral recognition ability of BINAP ligands in numerous catalytic reactions.

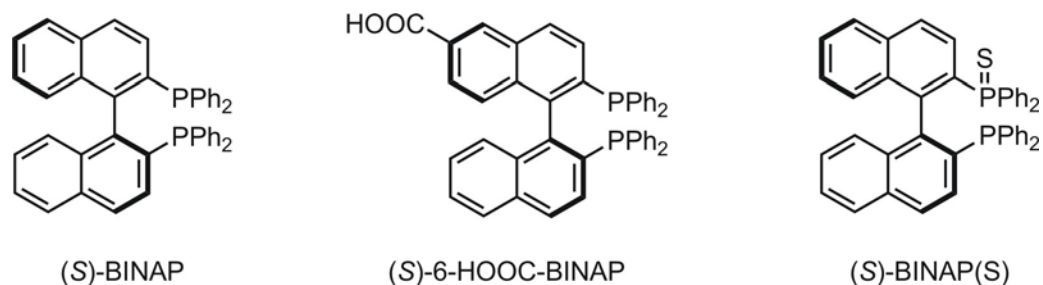
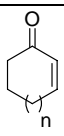
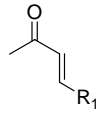
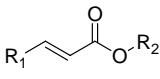
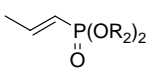


Figure 1.3. BINAP ligands.

Transition metal-BINAP complexes have been extensively employed to reduce prochiral C=O, C=N, or C=C bonds. Enantioselective hydrogenation of olefins with chiral rhodium or ruthenium catalysts is one of the most established methods in asymmetric catalysis. Examples of substrates processed with BINAP-based hydrogenation catalysts include functionalised olefins and ketones (*e.g.* α -dehydroamino acid derivatives,^[24, 25] (β -acylamino)acrylates,^[26] cyclic enamides,^[27, 28] α,β -unsaturated acids,^[29] allylic alcohols,^[30] itaconic acids, α or β -keto esters,^[31, 32] and imines.^[33]

Sato's preliminary work on Pd-catalyzed Heck reactions with BINAP ligands,^[34] followed by several studies on substrates variation,^[35-38] clearly demonstrated the potential of such chiral bisphosphines in enantioselective C-C bond forming processes. Although BINAP commonly induced modest regio- and stereoselectivity in asymmetric Heck reactions,^[39] its high catalytic performance has been confirmed in Rh-catalyzed conjugate 1,4-additions.

Table 1.1. Rh(I)-BINAP catalyzed asymmetric addition

Entry	Olefin	Ar	% ee
1 ^[40]	 $n = 0, 1, 2$	PhB(OH) ₂	93-97
2 ^[40]	 $R_1 = i\text{-Pr, Am}$	PhB(OH) ₂	92-97
3 ^[41, 42]	 $R_1 = \text{Me, } n\text{-Pr}$ $R_2 = \text{Me, Et, } t\text{-Bu, CH}_2\text{Ph}$	ArB(OH) ₂ Ar = Ph, 3-MeOC ₆ H ₄	87-95
4 ^[43]	 $R_2 = \text{Me, Et, Ph}$	(ArBO) ₃ Ar = C ₆ H ₅ , 4-CH ₃ C ₆ H ₅ , 3-ClC ₆ H ₅	91-96

In 1998, Miyaura and Hayashi described the conjugate addition of arylboronic acids to α,β -unsaturated ketones in the presence of a Rh-phosphine complex (Table 1.2).^[44] Under optimized reaction conditions, high yields and stereoselectivities were achieved for a wide range of substrates using BINAP as chiral ligand.^[40, 45] The stereochemical outcome of the enantioselective additions using BINAP is dictated by the formation of a chiral pocket containing the vacant coordination site in the highly distorted structure of the Rh complex.^[46] For this reason, BINAP ligands remain the most efficient bisphosphines examined in Rh-catalyzed conjugate addition,^[41] affording high yields and over 90% enantioselectivity with various types of cyclic or linear enones and

organoboronic acids.^[47] Several examples of electron-deficient olefins, including α,β -unsaturated ketones or esters, and phosphonates, as well as organoboron/boroxine reagents employed in Rh-BINAP catalyzed asymmetric 1,4-additions, are summarized in Table 1.1.

A common aspect of Rh-catalyzed 1,4-additions is that they are usually accelerated by the presence of water as cosolvent. Therefore, the development of water-soluble organometallic catalysts has attracted considerable attention. A typical example is introduction of water-soluble functional groups onto BINAP. This strategy has been used to generate BINAP analogues (*i.e.*, diguanidinium-BINAP,^[48] the bromohydrate form of the 6,6'-dimethylamino-BINAP^[49]) for Rh- or Ru-mediated hydrogenation reactions, while aqueous 1,4-addition employs a resin-bound Rh-BINAP variant. The connection of BINAP with the amphiphilic polymer having an amino group was done via amide bond formation, using a BINAP-carboxylic acid derivative (Figure 1.3).^[50] The resulting polymer-supported BINAP-Rh catalyst afforded high yield (71-95%) and high enantioselectivity (91-97%) in water for the 1,4-addition of phenylboronic acid to α,β -unsaturated ketones.

An interesting family of heterobidentate chiral P,S-ligands, BINAP(S) (Figure 1.3), generated by conversion of BINAP to mono-sulfides, was reported in the early 2000s.^[51] With such ligand systems, highly selective Pd-catalyzed racemate resolution,^[52, 53] as well as asymmetric amination of allylic substrates was obtained (Figure 1.4).^[53, 54] The observed regioselectivity in case of allylic substrates containing rather small substituents was in contrast to the traditional regioselectivity of Pd systems, and branched products were predominantly formed. These intriguing results, together with the induced high regio- and stereoselectivities, made BINAP(S) a ligand of choice for further development in the field of allylic substitution reactions, where usually chiral P,N-ligands are used.

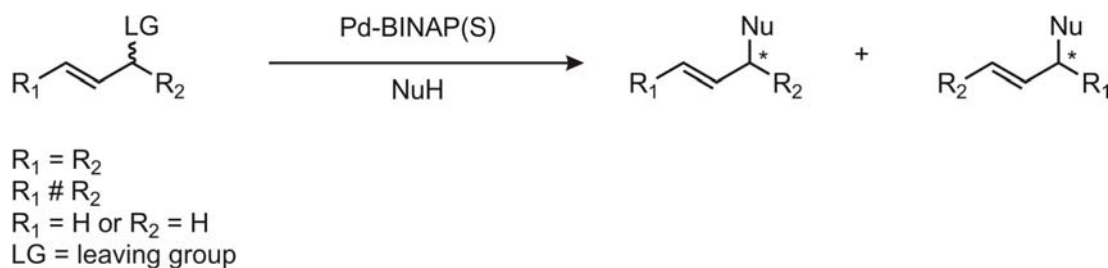


Figure 1.4. Pd-catalyzed allylic substitution with BINAP(S) ligand.

1.1.1.3 PHOX Ligands

A powerful class of chiral bidentate P,N-ligands,^[55] namely phosphinooxazolines (PHOX) (Figure 1.5), structurally similar to Crabtree's catalysts combines a hard, N (oxazoline) with a soft, P (phosphine) donor and has been introduced by Helmchen in 1993.^[56]

PHOX chirality derives from an asymmetric centre placed in the oxazoline ring directly connected to an aromatic phosphine moiety. Upon transition metal coordination, PHOX ligands form six-membered chelates that bind the substrate in a stereoselective manner. It has been assumed that such nonsymmetrical ligands would allow more enantiocontrol than C_2 -symmetric ligands^[57] that dominated for long time asymmetric catalysis.

Chiral PHOX ligands were initially used in Pd-catalyzed allylic alkylation of symmetrically substituted allyl acetates,^[56] yielding complete substrate conversion and high enantioselectivity. Additionally, they induced excellent enantioselectivities in Ir-catalyzed asymmetric hydrogenation of unfunctionalized olefins^[58-60] for which classical Rh or Ru-BINAP catalysts were not efficient. Promising results were also obtained with olefins lacking a polar group,^[61] and imines,^[62] as substrates for hydrogenation.

Remarkable contributions from the groups of Helmchen and Pfaltz demonstrated the great catalytic properties of PHOX ligands in transition metal-catalyzed C-C and C-N bond formation, including allylic substitutions and Heck reactions. Due to their modular structure, a number of very effective PHOX ligands were readily generated by varying the substituent at the stereogenic centre of the oxazoline moiety, responsible for catalyst reactivity.^[63, 64] Commonly, high conversions were obtained with bulky groups located next to the metal centre. PHOX ligands with W, Mo, Pd, and Ir precursors have been tested for various allyl systems, either symmetrically substituted,^[56, 65, 66] or monosubstituted linear substrates^[67, 68] in reaction with nucleophiles, such as dimethyl malonate,^[57] amines,^[65] nitro compounds,^[69] and sulfinates.^[70] High enantiomeric excess and metal-dependent regioselectivity were mainly achieved with arylallyl derivatives.^[57] Furthermore, interesting results were obtained in intramolecular aminations,^[71] in spite of long reaction times generally required in PHOX-Ir catalyzed

allylic substitutions with amines.^[72] So far, conversion of racemic monosubstituted allyl compounds to a single enantiomer through kinetic resolution in the presence of chiral PHOX ligands has not been reported.

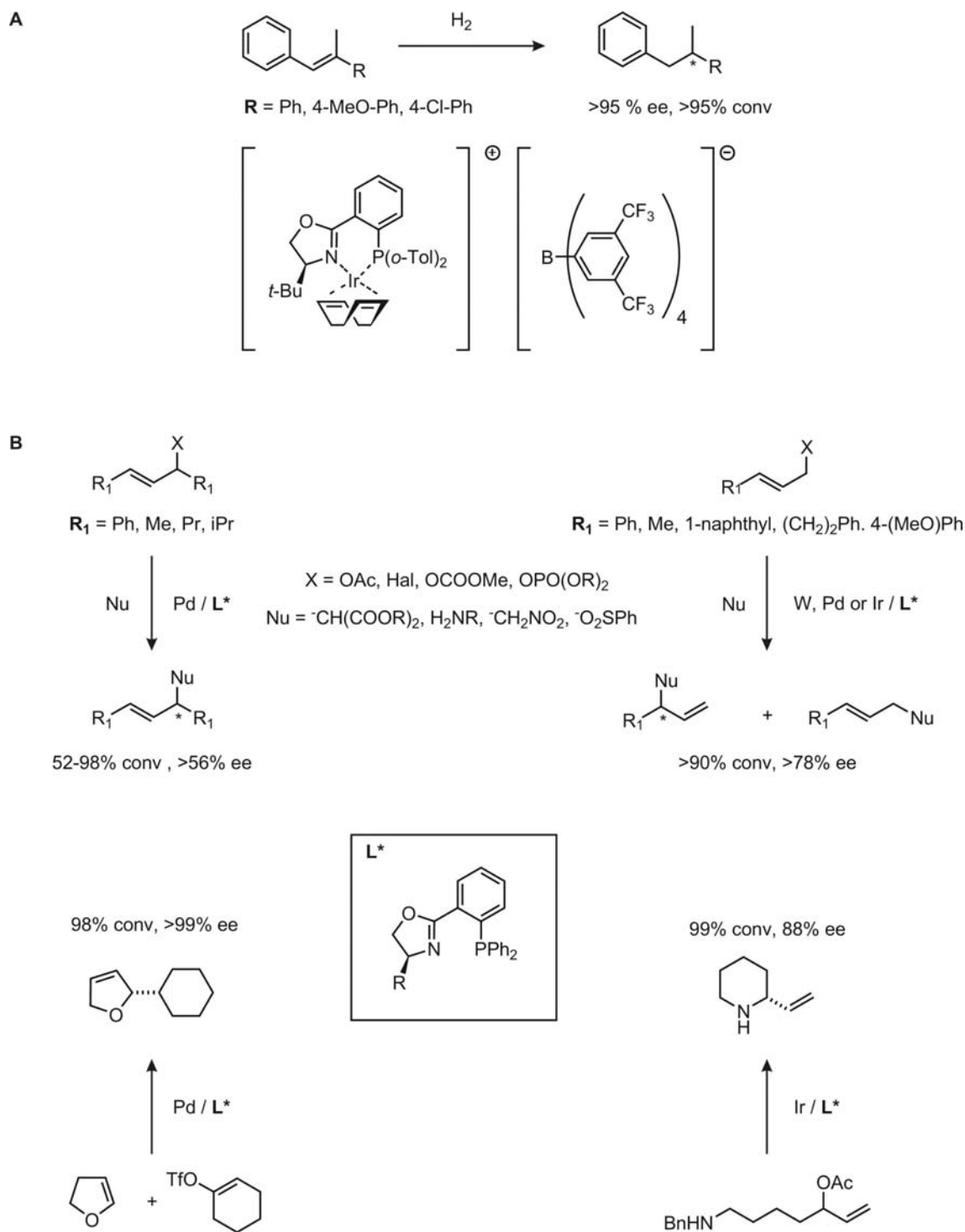


Figure 1.5. (A) Enantioselective hydrogenation in the presence of PHOX-Ir complexes. (B) Transition metal-catalyzed allylic alkylations and Heck reactions using PHOX ligands.

Although impressive enantioselectivities have been also observed in Pd-catalyzed Heck reactions, the use of PHOX ligands in such transformations appeared to be limited due to their low reactivity.^[63] Figure 1.5 illustrates several applications of PHOX complexes in asymmetric catalysis.

1.1.1.4 Phosphite and Phosphoramidite Ligands

Traditionally, chelating phosphine ligands with a -PPh₂ moiety, appeared to be ideal in many asymmetric transformations, but P-O and P-N containing monodentate phosphorus ligands, such as monophosphites and phosphoramidites, were often found to be as effective. This type of ligands benefits of straightforward preparation, modular construction for tuning of properties, high π -acidity, and, in contrast to phosphine analogues, resistance to oxidation.^[73, 74] Although the relative instability, especially in protic solvents, noticeably limited their utility, within the last decade several new classes of phosphite and phosphoramidite ligands of high stability have been developed. Such ligands are capable of rate acceleration and stereoselectivity in a number of essential organic transformations, such as allylic substitution, hydrogenation and conjugate addition.^[74]

Some of the most simple and, at the same time, selective monophosphite ligands are the biaryl-derived species (Figure 1.6). In combination with an iridium catalyst precursor, triphenylphosphites were found to induce high rate acceleration and regioselectivity in favour of the branched product for both aryl and alkyl substrates in allylic substitution reactions.^[75-77] Chiral biaryl-derived phosphites gave excellent results in Ir-catalyzed transformations of unsymmetrical allylic substrates.^[78, 79] Structurally related phosphite-phosphine combinations have been successfully applied to Pd-catalyzed allylic transformations of symmetrically disubstituted substrates.^[80]

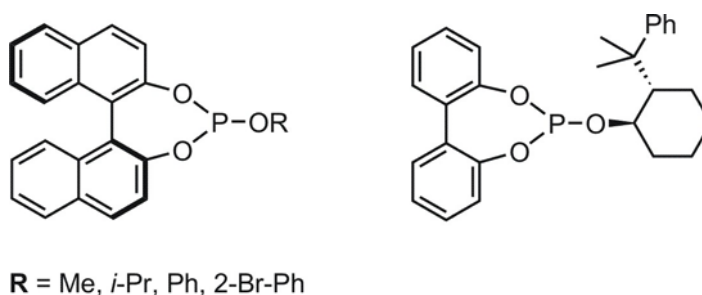


Figure 1.6. BINOL and biphenyl-derived monophosphite ligands.

The use of BINOL-derived structures appeared to be important for achieving high enantioselectivity. For example, chiral BINOL-derived monophosphites afforded high levels of enantioselectivity in Rh-catalyzed hydrogenation of itaconic acid.^[81, 82]

Furthermore, P-O/N bond containing ligands have been demonstrated to be very good chiral sources for use in asymmetric conjugate addition reactions. After the successful applications of Cu(II)-phosphoramidite complexes based on the BINOL scaffold,^[83-88] structurally related phosphite ligands containing a biphenolic unit and a chiral P-bonded alcohol were also screened in Rh-catalyzed 1,4-additions of arylboronic acids to enone. In aqueous media and under basic conditions, phosphites afforded excellent yields but only moderate enantioselectivities, albeit higher than the corresponding phosphoramidites.^[89]

1.1.2 Biocatalysis

An attractive alternative to enantioselective metal catalysts is offered by biological systems. Natural enzymes catalyze biological transformations with remarkable specificity and efficiency, using a limited number of functional groups in the protein structure. Given that enzymes are products of evolution, they mostly function with high selectivity only with polar, polyfunctional natural substrates (*e.g.*, carbohydrates, acid derivatives, and biopolymers), and under physiological conditions. Furthermore, the single-handed orientation and lock-and-key specificity of the proteins significantly reduce the substrate pool of catalysis, and might often cause severe product inhibition. By this means, natural enzymes are generally not optimal catalysts.

One example of highly versatile class of natural enzymes used in synthesis of optically pure compounds consists of hydrolases, namely lipases and esterases.^[90-92] Many of them were found to perform well even in organic solvents. Although lipases/esterases can generally accommodate various synthetic substrates and maintain their chiral recognition properties, they do not always exhibit satisfying catalytic performance, in terms of activity, stability and most importantly, enantioselectivity.

1.1.2.1 Artificial Enantioselective Enzymes

Protein engineering has been employed to generate artificial enzymes that are modified to be compatible with a desired chemical process. Two main approaches, namely (i) rational design for fine-tuning existing biocatalysts, and (ii) combinatorial techniques based on libraries and suitable selection methods^[93] have been developed. In the first approach, one or few amino acids in the enzyme are rationally either replaced with the remaining natural amino acids by using site-directed mutagenesis techniques,^[94, 95] or chemically modified.^[96] However, this method is rather challenging as it requires a thorough understanding of the structure and mechanism of the targeted enzymes. An efficient alternative to rational protein design was developed, namely the directed evolution^[95, 97, 98] (Figure 1.7). Large libraries were generated by random mutagenesis (*e.g.*, error-prone PCR)^[99] of the gene encoding the catalyst, or recombinative methods of gene fragments (*e.g.*, DNA-shuffling).^[100] The resulting mutants were then subjected to gene expression and high-throughput screening methods^[101, 102] in order to identify improved variants. The mutant gene of the optimal enzyme variant can be resubmitted to mutagenesis/expression/screening cycles until biocatalysts with improved properties are obtained.

The first example of an *in vitro* evolved enantioselective enzyme was reported by Reetz in 1997.^[103] The isolated lipase afforded >90% *ee* in hydrolytic kinetic resolution of chiral esters, while the wild-type enzyme from *Pseudomonas aeruginosa* gave only 2%.^[103, 104] Several enantioselective enzymes, such as lipases,^[105, 106] esterases,^[107] aldolases,^[108] or oxygenases,^[109] were optimized by *in vitro* evolution and mainly employed in biological transformations.

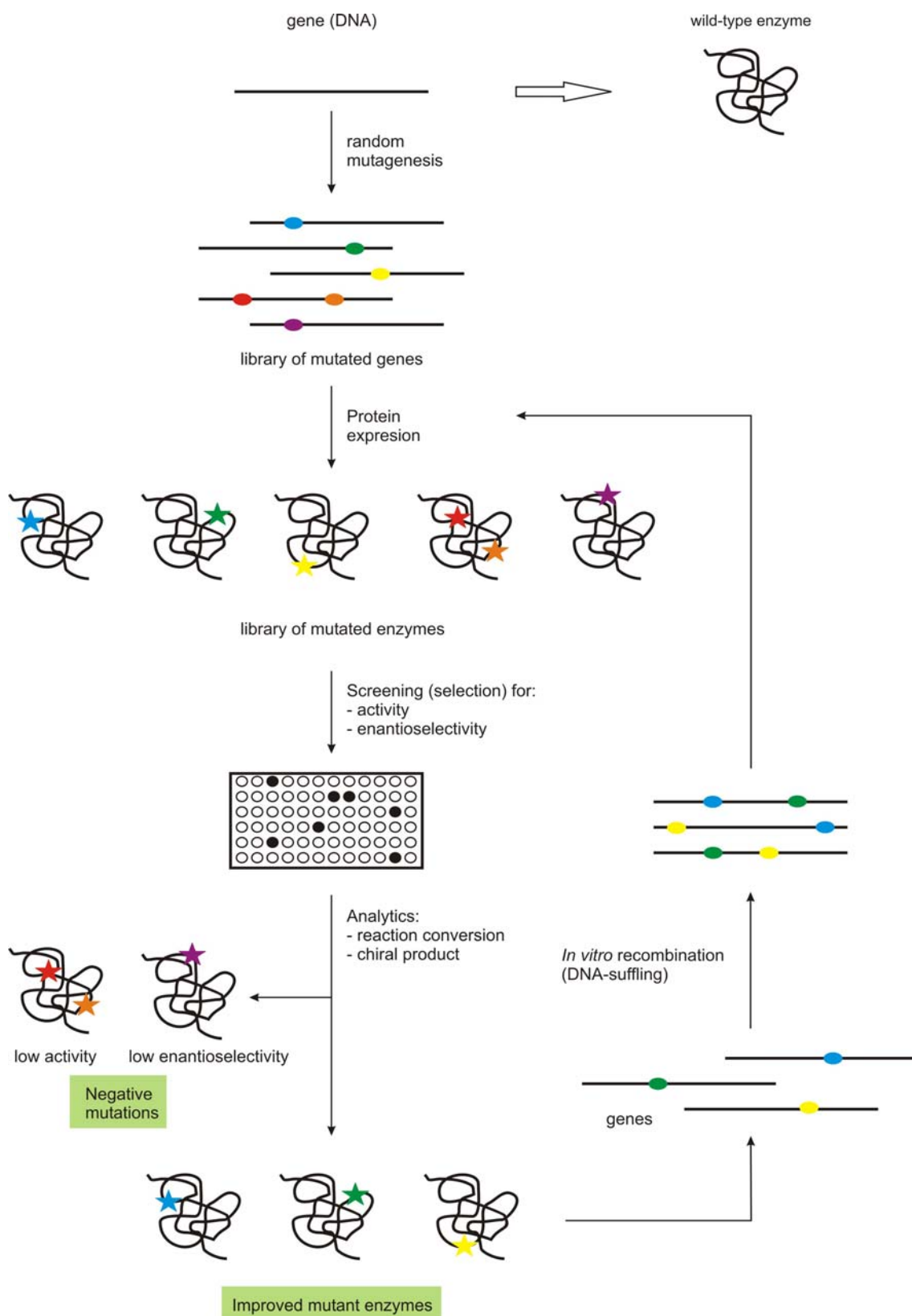


Figure 1.7. Directed evolution of (enantioselective) enzymes.

1.1.2.2 Hybrid Catalysts

The applications of the artificial enantioselective enzymes in chemical processes were expanded by the development of “hybrid catalysts” for use in transition-metal catalyzed organic reactions. This term was introduced by Reetz in 2002,^[110, 111] and consists in embedding ligands and metal complexes thereof at a specific site in a protein. This approach was inspired by Whitesides’ work, who showed that asymmetric catalytic hydrogenations of α -acetamido-acrylic acid could be performed by anchoring an achiral diphosphinerhodium(I) complex, via a biotin carrier, in a chiral cavity of the protein avidin^[112] (Figure 1.8). A similar system based on interaction of enantiopure biotinylated PYRPHOS-rhodium(I) complex with the host protein avidin, was used as catalyst in asymmetric hydrogenation of itaconic acid.^[113] In both cases, the chirality of the protein induced modest levels of enantioselectivity, with observed ee values ranging between 33 and 44%, but definitely proved the principle of hybrid catalysts.

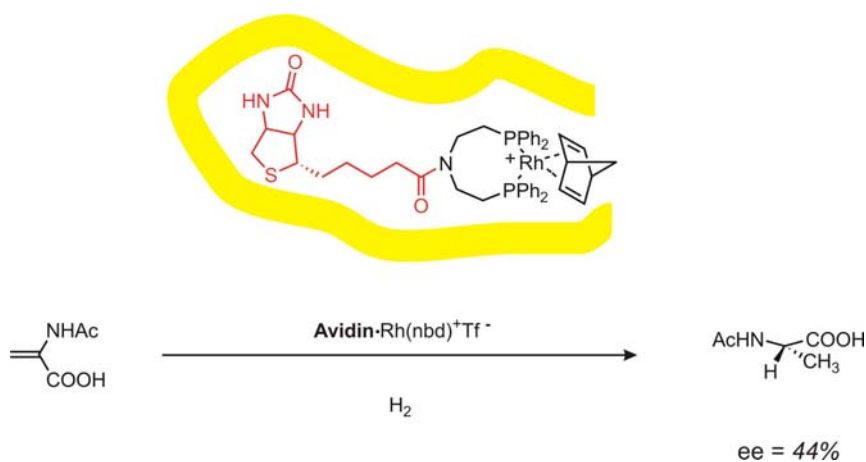


Figure 1.8. Asymmetric hydrogenation with avidin containing biotinylated phosphine-rhodium (I) complex.

The enantioselectivity was later significantly improved by chemical tuning and rational protein design. Ward introduced different spacers between biotin and the achiral diphosphinerhodium(I) complexes, replaced avidin with streptavidin - a similar protein with a deeper binding pocket - and, upon site-directed mutagenesis, obtained 96% enantioselectivity in hydrogenation of α -acetamido-acrylic acid.^[114, 115] Using the same chemo-genetic optimization procedure,^[96] enantioselective hydrogenases for Ru-catalyzed reduction of prochiral ketones have been developed (97% ee).^[116]

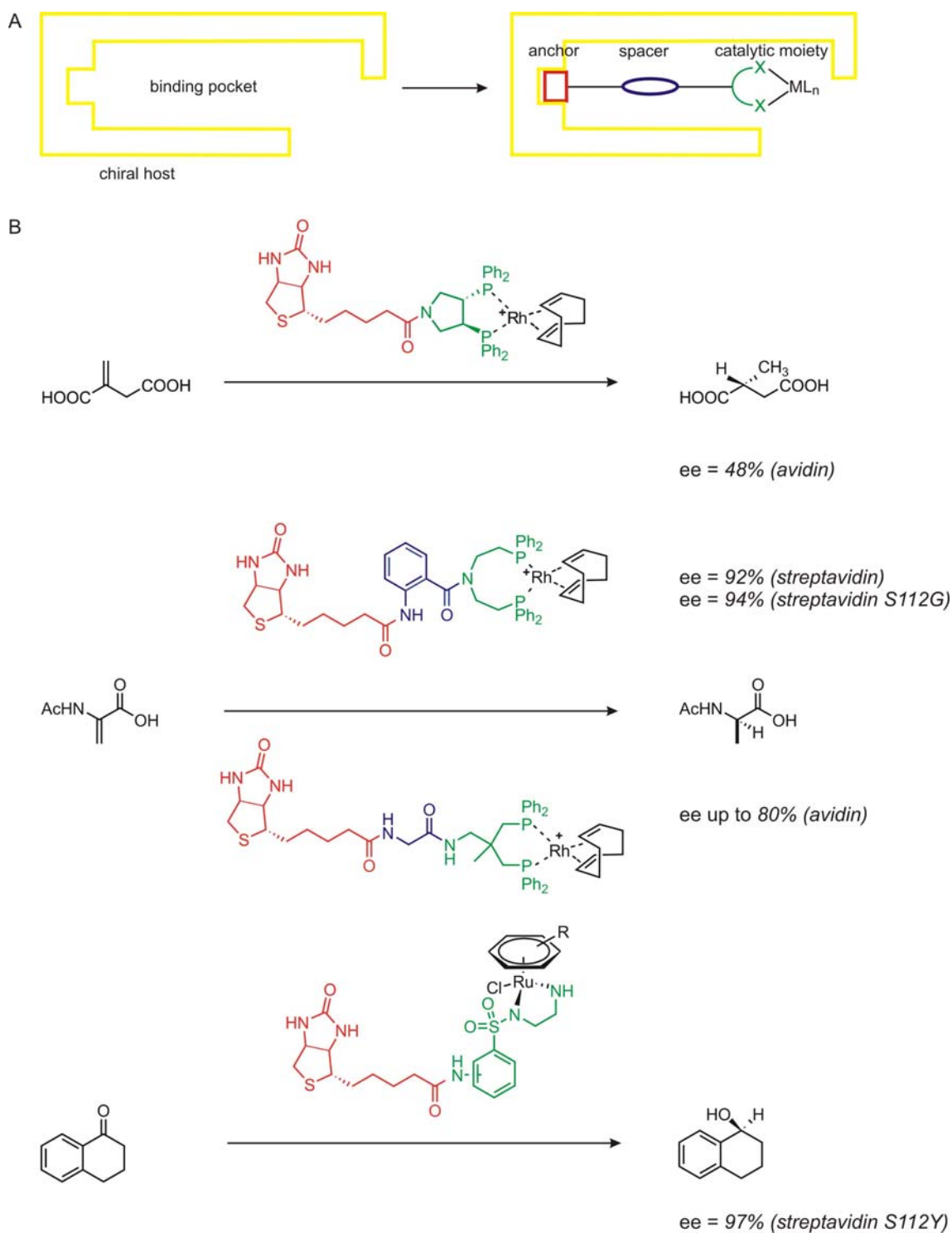


Figure 1.9. (A) Non-covalent anchoring of an active catalyst within a chiral host (hybrid catalyst). (B) Examples of artificial metalloenzymes in asymmetric catalysis.

Transport proteins, such as serum albumins, are another class of efficient host proteins able to strongly bind hydrophobic guests, for example porphyrins. Albumin-conjugated manganese(III) and copper(II) complexes were found to catalyze sulfoxidation reactions

and, respectively, Diels-Alder cycloadditions, with moderate to good enantioselectivities.^[117-119] Non-covalent insertion of chromium(III)-salophen complexes into apomyoglobin mutants yielded metalloenzymes with low catalytic efficiency in asymmetric sulfoxidation (27-83% yield, ee <13%).^[120]

Reetz and co-workers applied the directed evolution approach for tuning the enantioselectivity of hybrid catalysts, using the Whitesides system and streptavidin.^[110, 111, 121] A library of mutant hybrid catalysts was produced via random mutagenesis, and posttranslational, non-covalent modification with metal complexes. Iterative cycles of mutagenesis coupled with enantioselective screening procedure led to an improved protein mutant, showing 65% ee.^[121] A few examples of evolved artificial metalloenzymes generated by non-covalent anchoring to protein cavities are depicted in Figure 1.9 B.

In parallel to non-covalent anchoring strategies, covalent incorporation of transition metal catalysts ensures an unambiguous localization of the metal centre in the host protein. For this purpose, proteins with a single accessible reactive amino acid residue, typically cysteine or serine, are site-specific functionalized with appropriately modified ligand moieties. Di Stefano reported an artificial metalloenzyme obtained by attachment of 1,10-phenanthroline to the cysteine residue of the adipocyte lipid-binding protein for use in Cu-catalyzed enantioselective hydrolysis of amides and esters (31-86% ee).^[122] Using this approach, Reetz introduced salen and dipyrindine moieties in the binding site of papain^[111, 123] (Figure 1.10). Preliminary studies showed that hybrid manganese-salen and rhodium-dipyrindine catalysts were active in epoxidation and hydrogenation, albeit with low enantioselectivities (ee <10%).

De Vries described the covalent anchoring of a monophosphite to the cysteine residue of papain (Figure 1.10), that yielded 100% racemic product in Rh-catalyzed reduction of methyl-acetamidoacrylate.^[124]

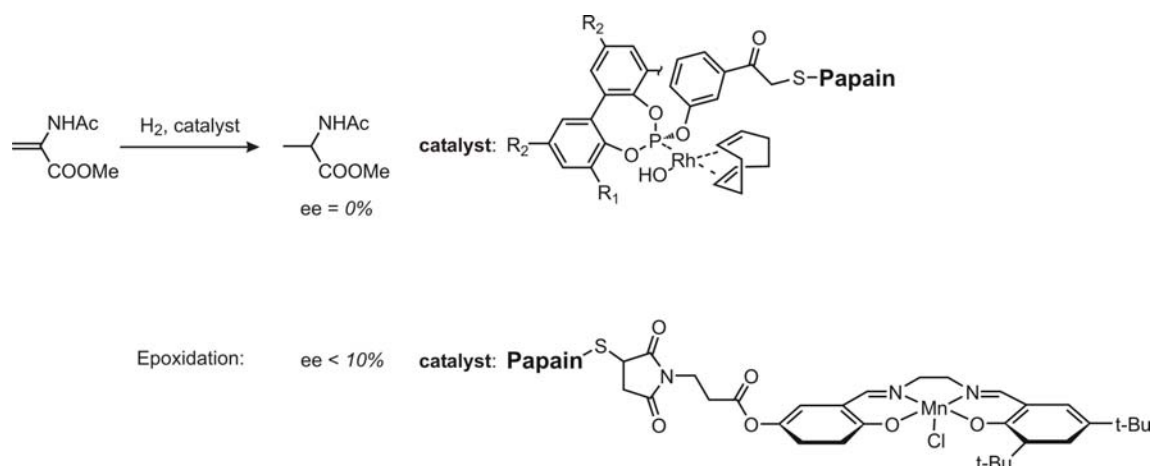


Figure 1.10. Catalysis with transition metal complexes covalently attached to proteins. Rhodium-phosphite- (top) and manganese-salen-functionalized papain (bottom).

Alternatively, diphosphine ligands carrying a *p*-nitrophosphonate moiety were covalently linked to the serine residue in the active site of lipase. However, this functionalization turned out to be reversible, and undesired hydrolysis of the phosphonate moiety was observed.^[111]

1.2 Nucleic Acid Enzymes

1.2.1 Chirality in the Structure of Nucleic Acids

Nucleic acids are polymers composed of a polar, negatively charged sugar-phosphate backbone and hydrophobic nucleobases (Figure 1.11). This amphiphilic nature, together with the hydrogen bonding and stacking potential of nucleosides, determines the assembly and maintenance of secondary and tertiary structures within nucleic acids.

The asymmetric D-ribose and D-2-deoxyribose sugars contain stereogenic centres, whose pucker configuration is important for the overall DNA or RNA structure. Typically, DNA adopts a double helical, antiparallel structure, via Watson-Crick base pairing (Figure 1.12), whereas RNA exists mainly in a single-stranded form. However, double helix elements are also a common feature of RNA structure and are fundamental in biological functions of RNA.

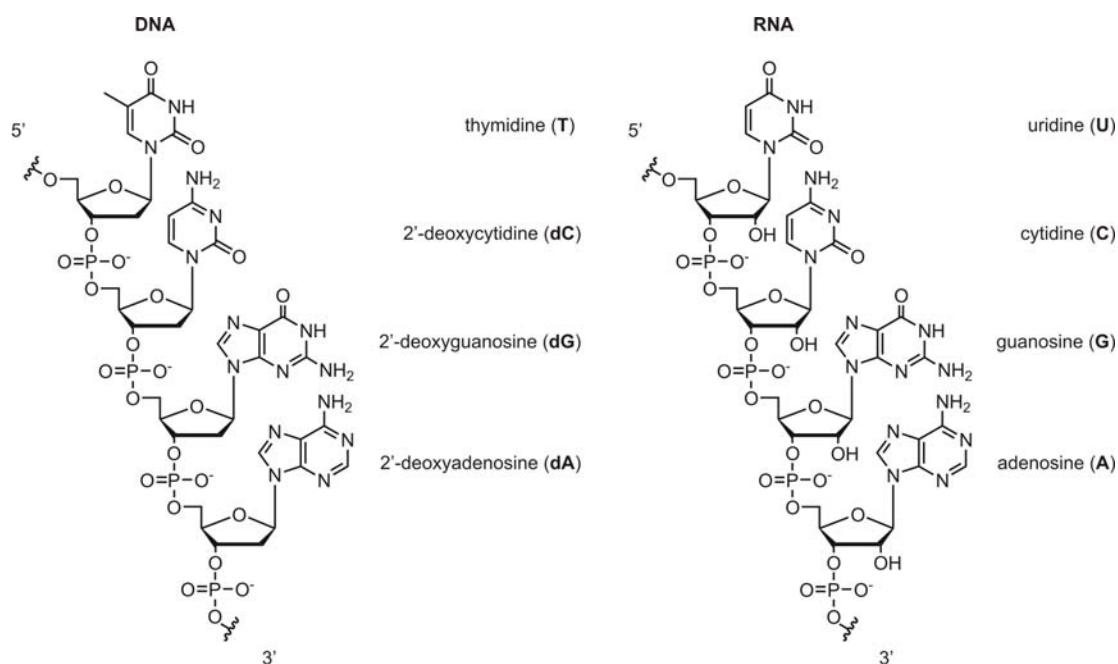


Figure 1.11. Constitution of DNA and RNA, with the name of the monomeric nucleoside units.

The most common DNA conformations are the B- and the A-forms (Figure 1.13), both right-handed, but with different sugar conformation (C2'-endo for B-DNA and C3'-endo for A-DNA, Figure 1.14). In addition, each form displays distinctive helical parameters, such as diameter, pitch, twist and tilt angles.^[125, 126] The B-DNA appears as a compact cylinder with a hydrophobic interior of base pairs stacked nearly perpendicular to the helix axis at 3.4 Å intervals, achieving a complete rotation after 10 base pairs.^[127, 128] An important feature of the B-form is the presence of two distinguishable minor and major grooves providing selective surfaces for the binding of ligands such as proteins or small molecules. The A-DNA is wider and shorter than the B-helix, and its bases are tilted to the helix axis (Figure 1.13). This form is characterized by a complete turn after eleven base pairs and a reduced rise per base pair of 2.6-3.3 Å.^[127, 129] In this channel-type arrangement the minor groove is smaller, while the major groove becomes deeper and narrower. This A-type helical orientation is preferred by double-stranded regions of RNA (as in hairpins), RNA-DNA hybrids, as well as by DNA-DNA duplexes containing one or more ribose units. A third conformation type, although not very common in nature, is the left-handed Z-DNA. It is generated by alternating conformations of the ribose rings (C2'-endo and C3'-endo) and of the nucleobases (*syn* and *anti*) (Figure 1.14), and contains only one deep helical groove.

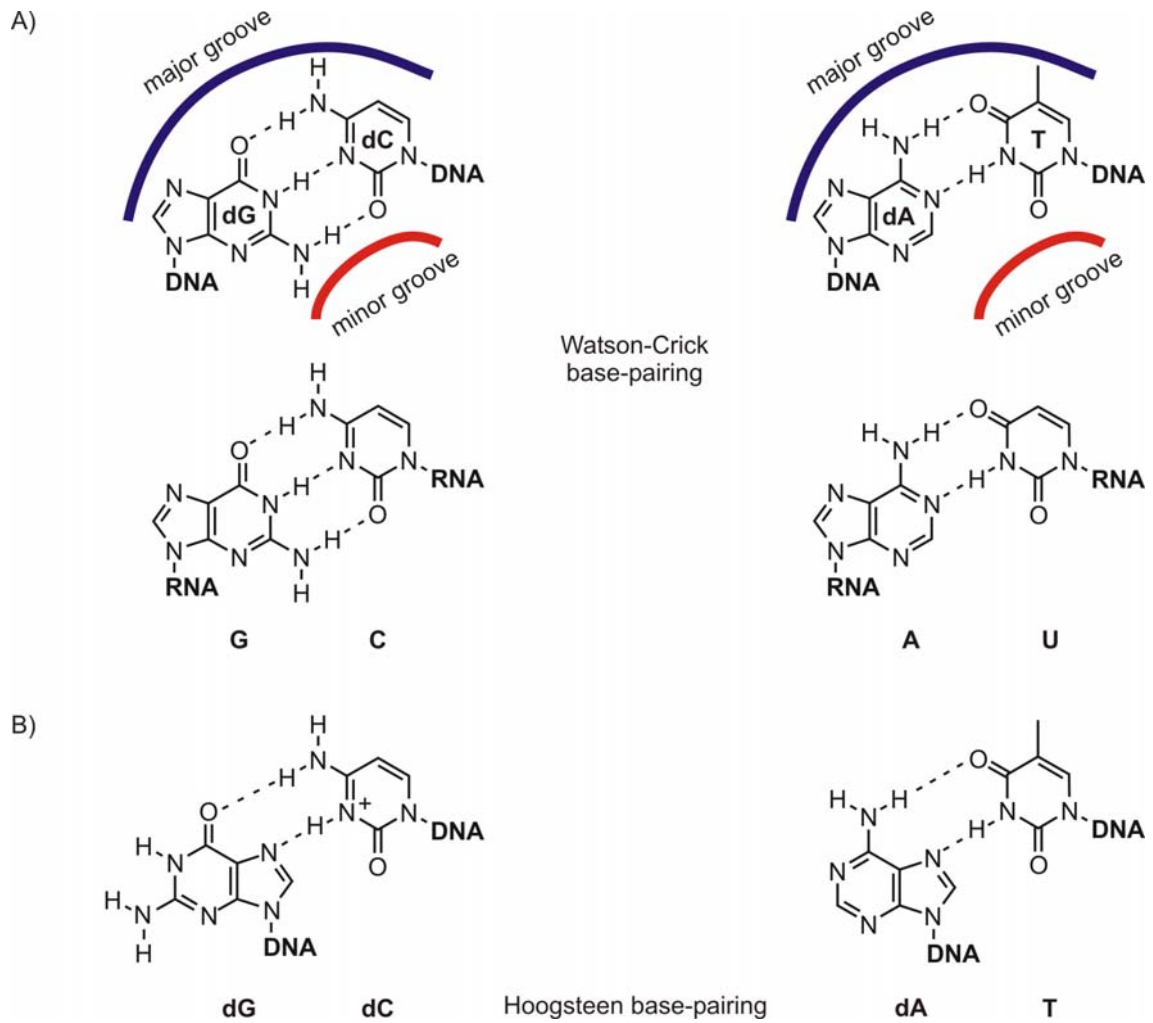


Figure 1.12. A) Watson-Crick base pairs in DNA (top) and RNA (bottom). B) Hoogsteen base pairs in DNA.

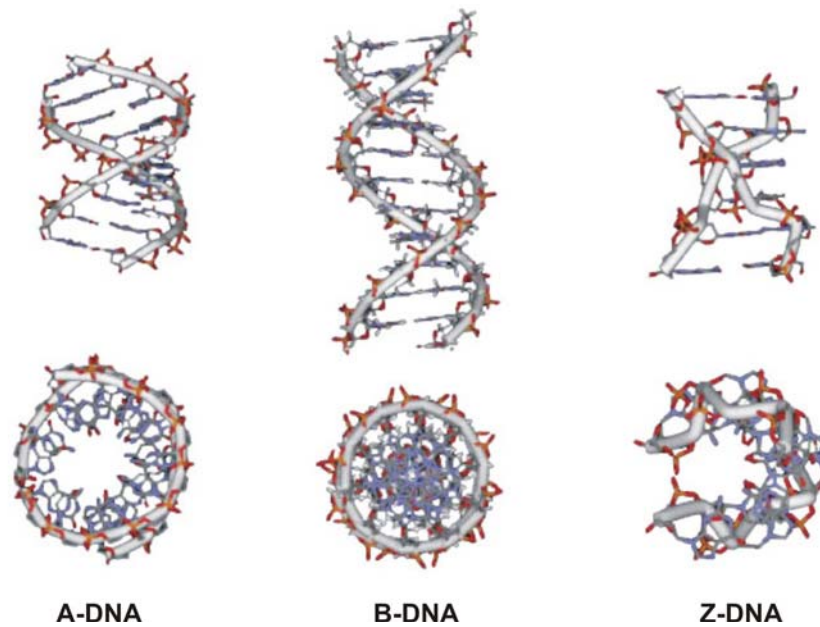


Figure 1.13. Different DNA helices.

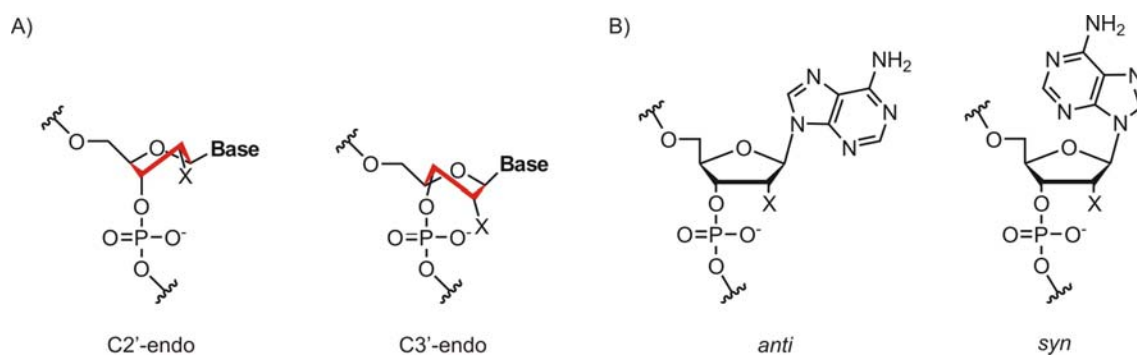


Figure 1.14. A) C2'-endo or C3'-endo conformations of the ribose ring, B) *anti* and *syn* base orientation (exemplified by adenine).

Beside the standard double helix form, DNA can adopt a number of different, more complex structures, such as triplexes (through Hoogsteen base-pairing (Figure 1.12 B), at low pH), quadruplexes (by folding of a guanosine-rich single chain), and Holliday junctions (of four DNA strands),^[126, 130, 131] important for interaction with biological components, such as proteins. By comparison to DNA, RNA possesses higher structural and dynamic flexibility and has a higher the propensity to fold and form 3D higher-ordered structures that alternate helices and single-stranded regions or loops.

These structural features confer distinctive properties to nucleic acids and provide numerous discriminatory intermolecular contacts with target molecules. In particular, chirality plays a crucial role on the interactions of nucleic acids with chemical species, such as drugs, or metal complexes,^[125] determining the DNA/RNA molecular recognition, binding affinity, and, if applicable, enantiodiscrimination.

For example, nucleic acids are able of forming precise binding pockets for the specific recognition of substrates and cofactors. Therewith, combinatorial chemistry has been used to identify nucleic acid sequences, namely aptamers, which recognize and bind targets ranging from simple ions and small molecules, to peptides and single proteins. A large number of small-molecule RNA aptamers have been isolated that can interact with nucleotides and free nucleobases, amino acids, cofactors, basic antibiotics, and transition-state analogues.^[132] Single-stranded DNA can also recognize a variety of small molecules, including ATP, organic dyes, porphyrins, and arginine.^[133]

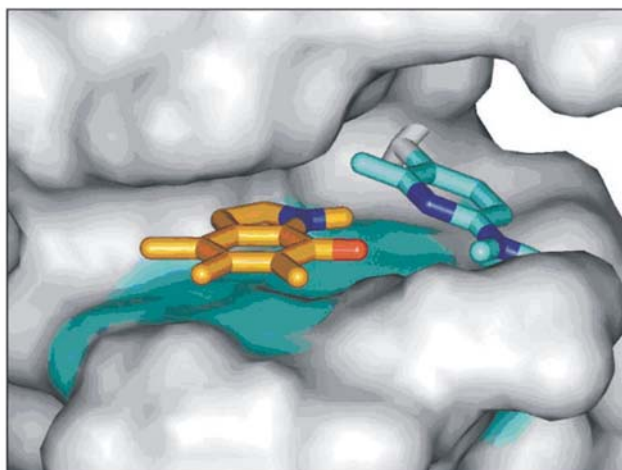


Figure 1.15. Binding pocket of the theophylline-RNA aptamer complex.^[134, 135]

Structural studies have revealed that, upon contacting the ligand and conformational change, the aptamers are able of forming precise, highly-ordered pockets, consisting mainly of purine-rich loops. These elements are highly conserved and, by interactions with spatially close nucleotides, often engaged in forming triplex, quadruplex, junctions or pseudoknot structures.^[136] Since planarity of the target molecules, presence of H-bond donors and acceptors, and positively charged groups appear to be the main factors involved in molecular recognition, molecules bind with different affinities depending on their geometry, hydrophobicity and overall charge. Aminoglycoside antibiotics with multiple primary amino groups,^[137, 138] as well as the nucleotides,^[139] and nucleobases^[140] are among the high-affinity ligands. In addition, many RNA aptamers show high substrate specificity and can differentiate among closely related molecules. The theophylline aptamer (Figure 1.15), for example, discriminates against caffeine, which has only one additional methyl group, by 10^4 -fold.^[141]

Some aptamers can discriminate enantiomers of the target molecules, such as amino acids and synthetic drugs, and bind them with high enantioselectivity. Examples of small ligand enantiomers include L-arginine,^[142] L-histidine,^[143] or (*R*)-thalidomide.^[144] Small molecules can interact with the minor groove of B-DNA (*e.g.*, polyamides^[145]), or intercalate between the base pairs. DNA intercalators contain a planar aromatic heterocyclic functionality (achiral) which can insert and stack between the base pairs of helical DNA. Their conjugation with chiral moieties can lead to a stereochemical preference for interaction. Beside small chiral molecule recognition, nucleic acids structures offer potential chiral environment,^[146, 147] or chiral template for asymmetric

synthesis.^[148, 149] However, this field of research is practically unexplored. Nevertheless, exploring the chirality of nucleic acids in combination with *in vitro* evolution and selection methodologies is a promising approach and may lead to a new generation of bio-inspired functional molecules.

1.2.2 *In vitro* Selection of Nucleic Acid-Enzymes

Protein enzymes have dominated for a long time the field of biocatalysis. The 20 amino acid components, in addition to the hydrogen bonding ability of the polyamide backbone ensure substantial chemical diversity and structural versatility in enzymatic catalysis. In contrast to proteins, nucleic acids with just four monomers and few functional groups are restricted to hydrogen bonding, π -stacking, and metal-ion coordination (Figure 1.16) for folding and interactions with potential substrates,^[150] and therefore catalytically limited. Only a few nucleic acid enzymes are found in nature, all of them being RNA enzymes (ribozymes) (*e.g.*, hammerhead ribozyme, hepatitis delta virus ribozyme, group I self-splicing introns, and the ribosome).^[151-153] They mediate phosphodiester bond cleavage/formation and are responsible for peptide bond formation in protein biosynthesis.^[154-156] DNA is less catalytically competent than RNA, in part since it lacks the 2'-hydroxyl group that can engage in hydrogen bonding as both donor and acceptor (Figure 1.16). Moreover, the DNA double-helical form restricts the structural flexibility and the potential of folding permitted by single-stranded conformations and possibly required in catalysis.

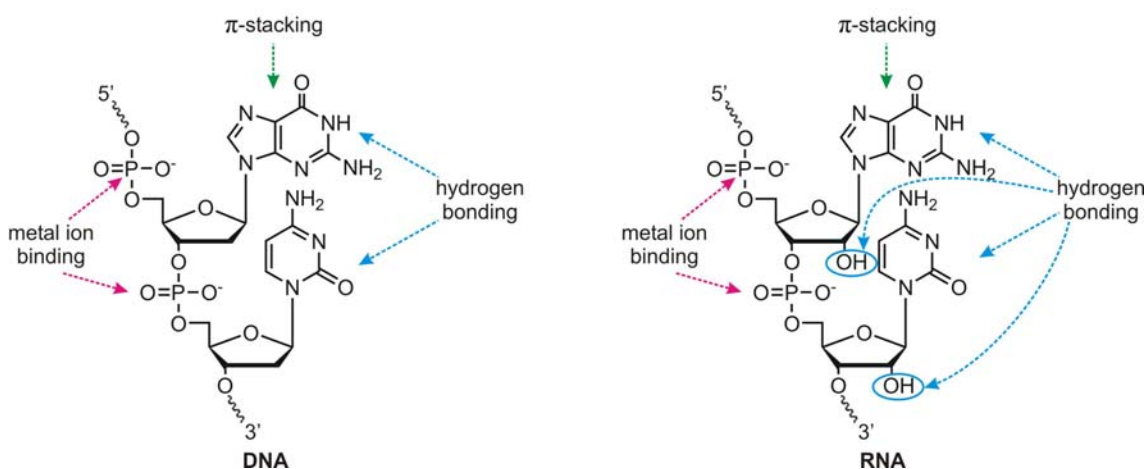


Figure 1.16. Interactions occurring in DNA and RNA structures and that can contribute to catalysis.

Directed evolution^[157] and *in vitro* selection strategies have led to the development of DNA and RNA molecules with specific molecular recognition properties and catalytic abilities. Various DNA enzymes (DNAzymes) and an even larger number of ribozymes able of catalyzing a broad range of chemical reactions have been isolated using SELEX techniques (Systematic Evolution of Ligands by EXponential enrichment).^[151, 158-162]

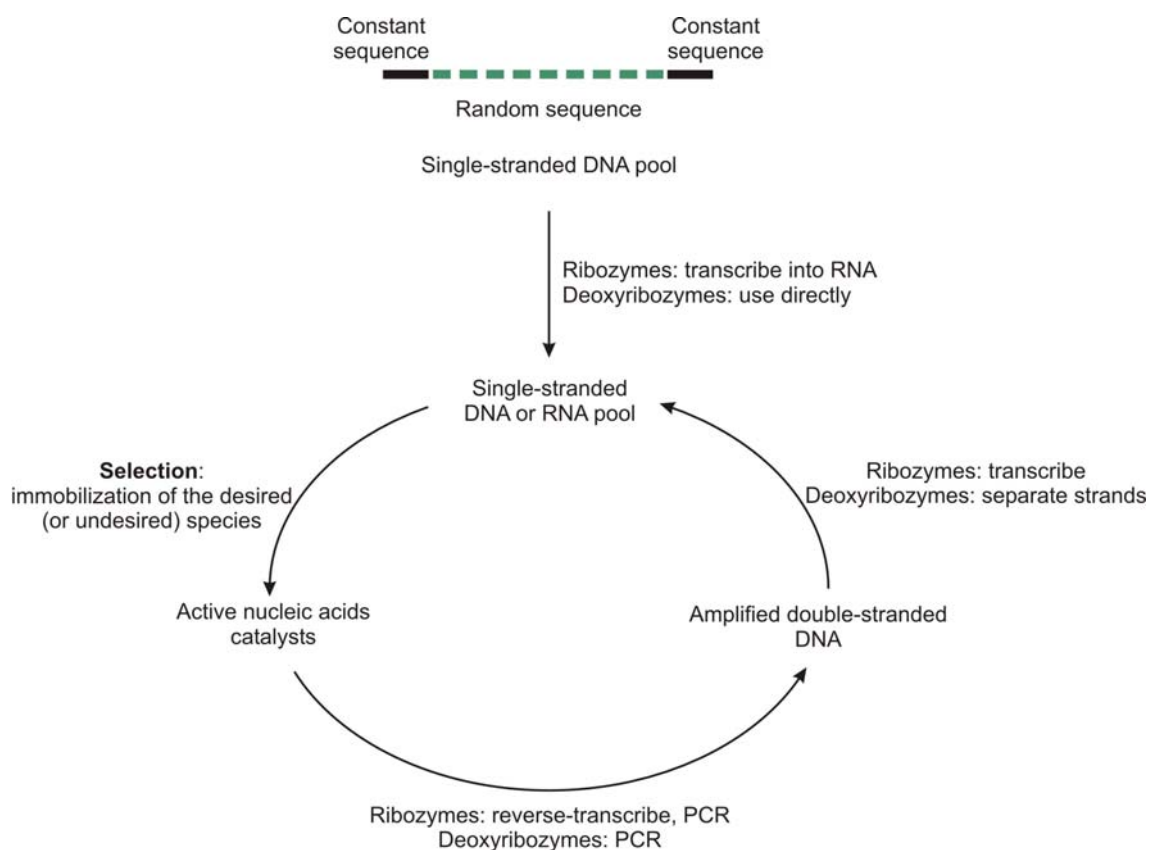


Figure 1.17. *In vitro* selection of nucleic acids. The enriched DNA pool re-enters the selection cycle.

A general *in vitro* selection approach is shown in Figure 1.17. SELEX involves screening of combinatorial libraries containing random sequences. For a given reaction, one substrate (bond forming) or product molecule (bond cleavage) is attached to the population of potential catalysts. A chemical tag (*e.g.*, biotin) is appended to the other substrate or to the product, so that a bond-forming reaction results in joining the tag to the catalyst, whereas a bond-breaking reaction results in releasing the tag from the catalyst. The tag is typically captured by affinity chromatography (*e.g.*, streptavidin-coated support). The applied selection procedure is tag specific, retaining tagged molecules in case of a bond-forming reaction or rejecting tagged molecules in case of

bond-cleavage reaction. The active species are isolated, forming an enriched library, which is then amplified. After iterated selection-amplification cycles, the individual catalytically active species are identified by cloning and sequencing protocols, and further optimized by rational design.

1.2.3 DNA-zymes

Deoxyribozymes isolated from pools of random-sequence DNAs catalyze the Pb^{2+} -dependent cleavage of RNA^[163] and the oxidative Cu^{2+} -mediated cleavage of DNA,^[164] facilitate the 3',5'-linkage between two chemically activated DNA sequences in the presence of Zn^{2+} or Cu^{2+} ,^[165] formation of 3'-5' and 2'-5' junctions and of linear (Figure 1.18) and branched RNA,^[166] promote the metallation of porphyrin rings,^[167] and display peroxidase activity upon binding to hemin (Fe(III)-protoporphyrinIX).^[168] Many other reactions involving nucleic acid covalent modification are catalyzed by DNA: ATP-dependent self-phosphorylation,^[169] DNA adenylation (capping),^[170] and site-specific deglycosylation (depurination).^[171] Overall, deoxyribozymes appeared to generate rate enhancements similar to that of typical RNA enzymes, albeit inferior to their protein counterparts.^[172]

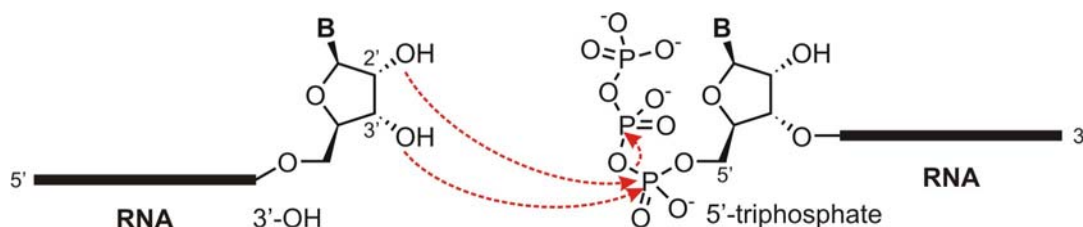


Figure 1.18. RNA ligation catalyzed by deoxyribozymes. Formation of 2'-5' and 3'-5' junctions between readily available termini results in a linear RNA product.

Nearly all DNAzymes require metals for catalysis. Monovalent, divalent and even lanthanide metal ions^[173] can assist the optimal folding of DNA to form complex tertiary structures. Moreover, divalent metal ions and lanthanides behave as Lewis acid catalysts or general acid/base catalysts and trigger the reaction at the active site of the enzyme.^[173, 174]

To compensate for the lack of chemical moieties present in proteins, additional amino acid cofactors have been incorporated into DNA. For example, an L-histidine dependent deoxyribozyme has been reported to catalyze RNA transesterification in the absence of

divalent metal ions.^[175] Histidine might act as general base catalyst to assist in deprotonation of the target-site 2'-hydroxyl group.

Several approaches make use of modified nucleotides to expand the array of chemical functionality of DNA. For example, imidazole and primary amino groups have been incorporated into DNA (Figure 1.19) as surrogates for histidine and lysine. These modified DNAs are able to catalyze RNA hydrolysis independently of a divalent cation.^[176, 177] The same amino-modified deoxyribozyme was found to effect scission of DNA containing abasic sites and display apurinic/aprimidinic lyase-endonuclease-activity.^[178]

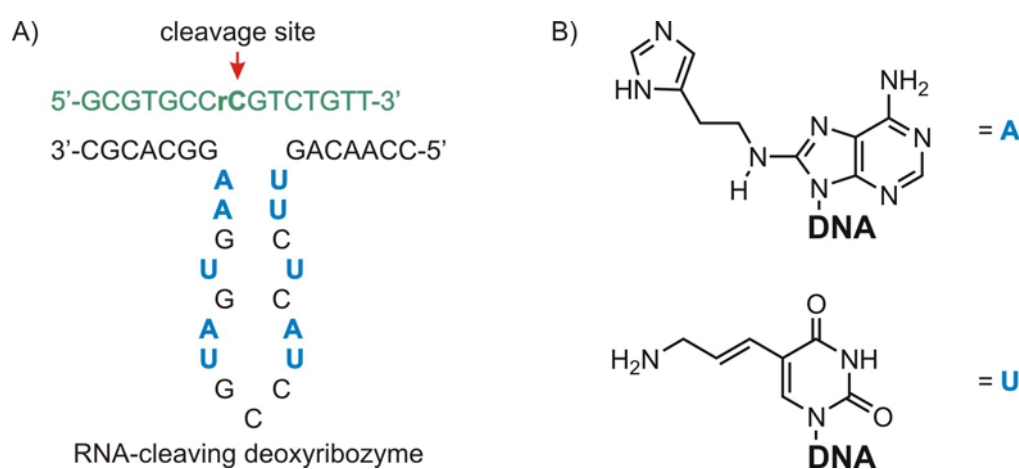


Figure 1.19. A) RNA-cleaving modified deoxyribozyme (black, modified nucleotides are shown in blue) and its target sequence (green). B) Structures of the modified nucleotides: histaminyldeoxyadenosine (A) and aminoallyl-deoxyuridine (U).

1.2.4 Ribozymes

Since the discovery of catalytic properties of natural RNAs 25 years ago^[179, 180], a large number of ribozymes with novel catalytic properties has been developed by means of *in vitro* selection. The chemical transformations catalyzed by RNA range from classical reactions such as RNA hydrolysis and ligation to reactions including redox catalysis,^[181] urea synthesis,^[182] glycosidic bond formation and nucleotide synthesis,^[183, 184] RNA polymerisation,^[185, 186] and aminoacylation of tRNA with aminoacids.^[187, 188] Moreover, it has been demonstrated that C-C bond forming reactions could be also accelerated by RNAs. Examples include Diels-Alder reaction,^[189-191] Michael addition,^[192] and aldol condensation.^[193]

The impressive catalytic potential of RNA comes from its ability to fold into 3D structures and form binding cavities for various substrates and metal ions.^[194] In the presence of divalent ions, RNAs can properly fold in very stable and rigid conformations. In some cases, metal ions are involved directly in catalysis, by stabilizing leaving groups or transition states.

Interesting examples of nucleic acids interactions with metal ions in aid of activity regulation are revealed by the metal-binding allosteric ribozymes. Breaker described several hammerhead ribozymes that are triggered and regulated selectively by binding of certain metal ions (Figure 1.20), such as Cd^{2+} , Co^{2+} , Mn^{2+} , Ni^{2+} , Zn^{2+} , Fe^{2+} .^[195]

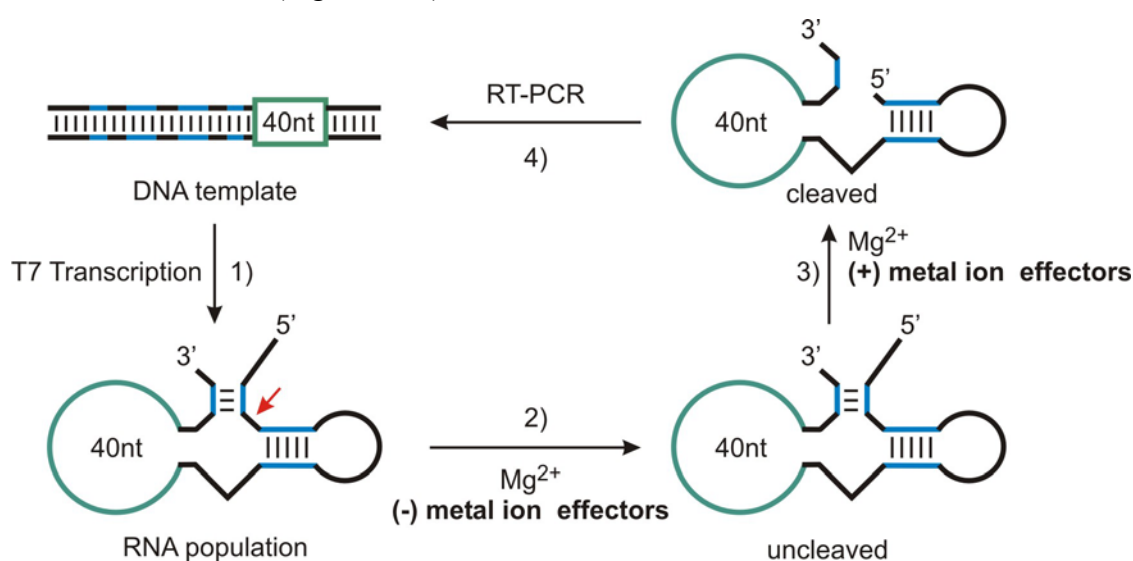


Figure 1.20. Selection scheme for the isolation of cation-dependent ribozymes. The ribozyme core contains a 40 nucleotide random-sequence domain (40nt). The RNA population is prepared by T7 transcription (1) and submitted to negative (no metal effectors) selection (2) and positive (with metal effectors) (3) selection. The RNA species enriched for allosteric function are amplified by RT-PCR. Mg^{2+} ions (steps 2 and 3) are included in the selection cycle to promote high catalytic activity of the hammerhead ribozyme.

The important role of metal ions as cofactors has been demonstrated not only in reactions involving phosphodiester chemistry, as in the Pb^{2+} -dependent 2'-O-mediated RNA self cleavage or the 2',3'-cyclic phosphate hydrolysis. For example, ribozymes showing alcohol dehydrogenase activity,^[181] or catalyzing racemic aldol reactions^[193] were selected in the presence of Zn^{2+} . The catalytic activity of the Diels-Alder ribozyme evolved in Eaton's group was dependent on the presence of Cu^{2+} and 4-pyridyl modified uracil residues. Likely, Cu^{2+} and Ni^{2+} play a key role either in the structure of RNA or in catalysis by providing Lewis acid sites upon coordination to the pyridyl moieties.^[196]

^{197]} In contrast, the Diels-Alder ribozyme isolated by Jäschke's group showed fast multiple turnovers without requiring transition metals or replacement of the natural nucleotides. In this case, hydrophobic interactions, electronic and proximity effects were responsible for achieving catalysis. The crystal structure revealed the presence of a preformed catalytic pocket almost perfectly complementary to the reaction product.^[198] Furthermore, this is the single reported example where the chiral binding cavity of a selected RNAzyme directed the reaction towards one enantiomer of the chiral product, resulting in an enantiomeric excess of 89%^[147] (Figure 1.21).

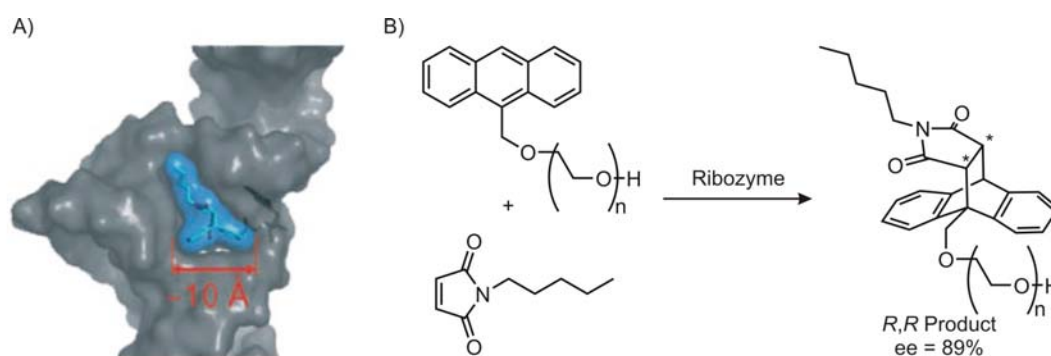


Figure 1.21. A) Diels-Alder ribozyme crystal structure. B) Diels-Alder reaction between oligo(ethylene glycol)anthracene derivatives and *N*-pentylmaleimide catalyzed by the ribozyme.^[147]

The observation that RNA is capable of stereodiscrimination was also supported by Eaton's work on in vitro selection of RNA urea synthase. This ribozyme, that promotes the formation of a urea bond between peptide phosphonate substrates and the exocyclic amino group of the 3'-terminal cytidine, can stereoselectively recognize peptide substrates for catalysis.^[182]

1.2.5 DNA-Based Hybrid Catalysts

While proteins proved to be suitable chiral scaffolds to form hybrid catalysts and induce enantioselectivity in asymmetric catalysis, attempts of employing nucleic acids in a similar context have been only recently described. In 2005, Feringa and co-workers reported on a supramolecular catalyst generated by intercalation of a copper-based Lewis acid in salmon testes DNA (Figure 1.22). The double helical DNA provides then enantioselectivity in Lewis acid catalyzed Diels-Alder cycloaddition of aza-chalcone to cyclopentadiene, in water.^[146, 199] Feringa's work provided the first example of the use

of DNA as source of chirality in asymmetric catalysis.

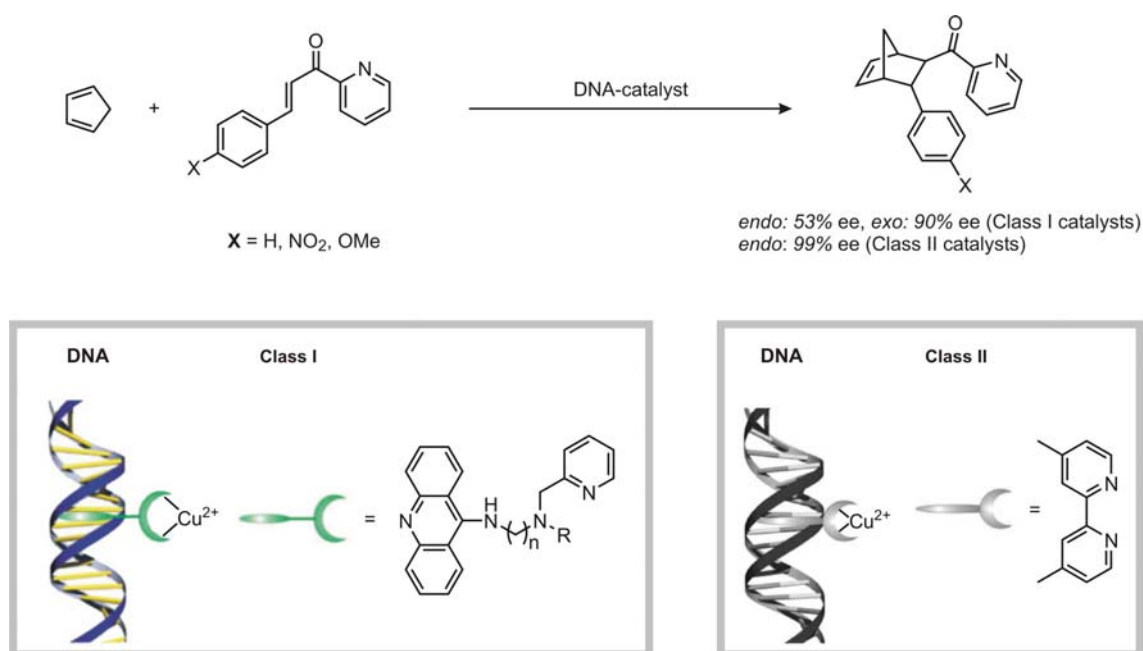


Figure 1.22. Diels-Alder reaction of cyclopentadiene with aza-chalcone catalyzed by copper complexes in the presence of DNA.

In this approach two classes of catalysts have been investigated. In the first case, achiral bidentate pyridine ligands for Cu²⁺ coordination were attached via short spacers to 9-amino acridine, a DNA intercalating moiety (Figure 1.22). As a result, the active Cu²⁺ centre is brought into close proximity to the DNA chiral environment and allows for transferring the chirality from DNA to the reaction product. With such catalysts, moderate to good enantiomeric excesses were achieved: 53% for the major isomer (*endo*) and up to 90% for the minor (*exo*) isomer.^[146] Interestingly, the design of the metal binding ligand and the distance between the metal complex and the DNA helix considerably affected the enantioselectivity. Thereby, aryl- and naphthyl-containing ligands induced preference for the synthesis of opposite enantiomers. Elongation of the spacers (n=3) resulted in change of the enantiopreference observed with a short linker (n=2), while longer linkers (n=5) gave unsatisfactory results.

Optimization studies led to a second class of DNA-based catalysts (Figure 1.22), by replacing the intercalator-spacer-ligand system with a bipyridine-containing moiety, which behaves both as intercalator and bidentate ligand. In this system, the catalytic metal centre is accommodated much closer to the DNA backbone. The obtained *endo*-selectivities and enantioselectivities were dependent on the size and DNA binding

strength of the aromatic ligands. The best results (>99% *endo* isomer, >99% ee) were given by smallest ligands, indicating that a shorter distance between Cu²⁺ and DNA is beneficial for chirality transfer. In addition, the most active catalysts contained medium DNA binders, suggesting that some flexibility in the binding of the complex favours a preferred orientation of the reaction product.^[199, 200]

The chirality transfer is explained by two possible mechanisms. In a one step mechanism, the chiral DNA environment directs the orientation of the diene towards one of the prochiral faces of the copper-bound dienophile. This pathway might correspond to catalysts where Cu²⁺ is positioned very close to the DNA, which is achieved by binding to intercalating ligands. Alternatively, in a two step mechanism, the DNA chirality could be transmitted to the achiral ligand, leading to enantiodiscrimination and different DNA binding affinities of the resulting chiral metal complex. A preferred chiral conformation of the catalyst would then translate into enantioselectivity in the catalyzed reaction.

However, in these systems the exact position of the metal complexes within the DNA is not defined, making a thorough understanding of the role of DNA difficult. Towards this end, a well-defined positioning of the metal complex and a precise control of the coordination environment are essential. This prerequisite has been addressed by Kamer who, at the beginning of 2007, reported on site-specific incorporation of monophosphine ligands into DNA trimers.^[201] Solid-phase bound synthetic oligonucleotides containing internal 5-iodo-2'-deoxyuridine have been reacted with diphenylphosphine under Pd-catalyzed cross-coupling conditions. The resulting trinucleotide-phosphine ligands have been tested in Pd-catalyzed allylic substitution, in 25% aqueous medium, giving <83% conversion and <12% stereoselectivity. In these systems, the stereocontrol comes from the ribose moiety and not from the DNA folding. Nevertheless, in the absence of more elaborate systems with well-defined secondary structures, the application of nucleic acids as catalysts or scaffolds for transition metal catalysts remains rather limited.

1.3 Transition Metal-DNA Conjugates

Although it became clear that DNA and RNA could optimally fit substrates or transition states in a binding pocket and induce enantioselectivity, the catalytic potential of nucleic acids in asymmetric catalysis remained practically unexplored. So far, the incorporation of transition metal complexes into DNA and RNA was only considered for the development of functional biomolecules with potential applications as therapeutics, artificial nucleases, and as nanotechnology construction material. Metal complexes can bind to nucleic acids via both noncovalent interactions and covalent attachment.

1.3.1 Non-covalent Interactions

Metal complexes are a very interesting class of reagents, which can site-specifically target double-stranded DNA and RNA. Therefore, they found useful applications as luminescent probes for DNA, mismatch recognition tools and structural probes for RNA.

A labile ligand of the transition metal complex can be substituted by a nucleophile in DNA, leading to formation of metal-DNA adducts. Nucleobases or phosphate groups are available for direct coordination to the metal centre. Certain highly reactive metal complexes are known to possess therapeutic effects due to irreversible binding to DNA. One of the best examples is *cis*-platinum (*cis*-PtCl₂(NH₃)₂), a square planar complex, which is a very effective anticancer drug. *Cis*-platinum targets the nuclear DNA, forming a critical lesion by cross-linking two adjacent guanines or an adenine and a guanine on the same strand, through coordination of the platinum ion to the N7 nitrogen.^[125, 202] Furthermore, antitumor activity and pronounced metastatic properties were observed with ruthenium analogues, such as *cis*- and *trans*-Ru^{II}Cl₂(DMSO)₄, Ru^{II}(bpy)₂Cl₂, Ru^{III}(tpy)Cl₃, and [Ru^{II}(NH₃)₅Cl]Cl.^[203, 204]

On the other hand, metal complexes interact with DNA via electrostatic binding, surface binding to the minor or major groove, or intercalation of planar aromatic ligand into the stacked base pairs.^[205] In this category, coordinatively saturated octahedral complexes of Ru²⁺ and Rh³⁺ containing phenanthroline units have been extensively employed as

luminescent reporters,^[205] DNA cleaving,^[206] or cross-linking agents,^[207] and for the study of long range energy and electron-transfer processes through DNA.^[208] Complexes in which one phenanthroline moiety is replaced by 9,10-phenanthrenequinone diimine (phi) or extended by two aromatic rings such as in dipyridophenazine (dppz) ligand are among the most studied major groove metallo-intercalators. Rhodium, ruthenium, and osmium complexes containing phi ligands promote cleavage of DNA and RNA sites upon photoirradiation, and can be used as probes for nucleic acids structure.^[205] $[\text{Ru}((\text{phen})_2\text{dppz})]^{2+}$ possesses interesting photophysical properties, and induces a “light-switch” effect, upon DNA intercalation.^[209] Minor groove binding molecules, such as bis(1,10-phenanthroline)copper(I),^[210, 211] Fe(II)-bleomycin,^[212] and metal-porphyrins, display DNA strand scission without irradiation.^[213]

The coordination chirality of octahedral complexes gives rise to different binding constants and recognition properties for the two enantiomers of the same metal complex. The enantioselectivity in DNA binding was clearly established by Barton *et al.* An interesting example refers to tris(2,7-diphenylphenanthroline)ruthenium(II), whose enantiomeric forms specifically target right-handed B-DNA, and left-handed Z-DNA, respectively, suggesting a correlation between the handedness of the complex and that of the host DNA.^[214]

1.3.2 Covalent Attachment

The requisite for metal complexes to target nucleic acids in a sequence-specific fashion has led to the development of synthetic strategies for precise incorporation. The most attractive way of achieving this goal involves tethering metal complexes to nucleic acids via covalent attachment. In principle, metal binders can be appended to oligonucleotide sequences either at the 5'- or 3'-termini or internally, at the nucleobase residue or at the ribose 2'-position (Figure 1.23).

1.3.2.1 Post-synthetic Functionalization

Covalent attachment has been traditionally accomplished by post-synthetic strategies, namely conjugation of a functionalized oligonucleotide with either a metal-chelator,

followed by metal complexation (1), or directly with a metal complex (2) (Figure 1.23). In both cases, the post-synthetic derivatization has been commonly addressed by reacting oligonucleotides containing 3' or 5'-terminal amines or amine-tethered nucleosides, with activated esters. These approaches afford nucleic acids that carry for example metal-based cleavage reagents,^[215] luminescent probes and redox-active species.^[216-218] Several examples are briefly described here (Figure 1.23).

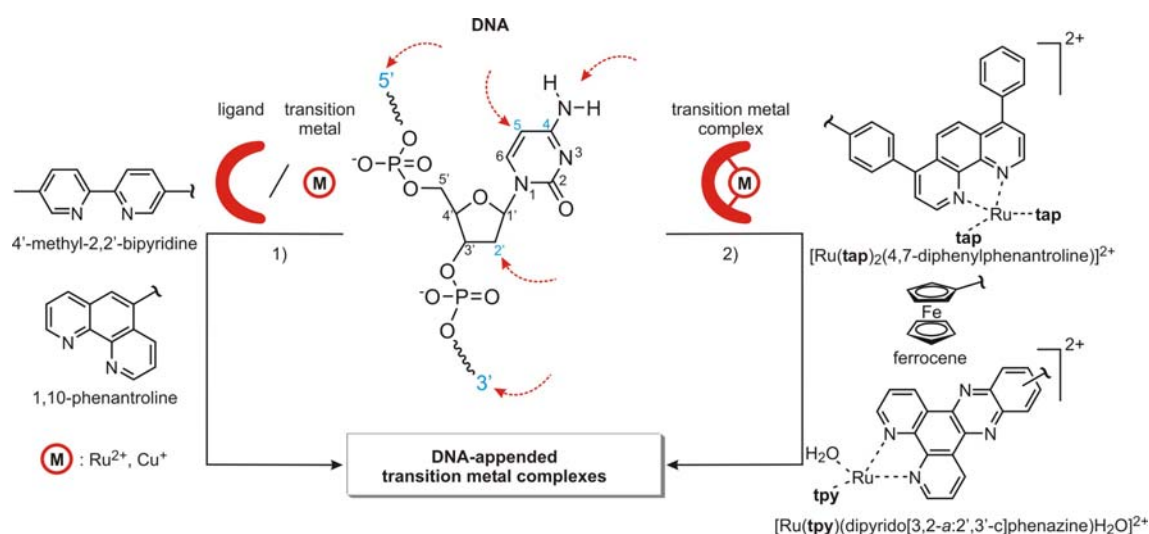


Figure 1.23. Functionalization of DNA with transition metal complexes: 1) ligand attachment followed by metallation, and 2) conjugation with transition metal complex. The DNA sites for attachment are shown in blue. **tap** = 1,4,5,8-tetraazaphenanthrene, **tpy** = 2,2':6',2''-terpyridine.

Sigman reported on 5'-terminal attachment of 1,10-phenanthroline ligand to DNA (Figure 1.23 left), which upon hybridization with an RNA target, induced site-directed Cu^{2+} -mediated hydrolysis of RNA and DNA.^[219, 220] Internal modifications of DNA with metal binding moieties has been described by Telser *et al.* *N*-hydroxysuccinimidyl (NHS) esters of bipyridine ligands for ruthenium coordination (Figure 1.23 left) have been attached to DNA sequences containing 4- or 5-amino modified cytidine, respectively deoxyuridine residues.^[216] Recently, Liu *et al.* developed a method for introduction of monophosphines into 3'- or 5'-amino tethered oligonucleotides.^[221, 222] Chemically stable metal complexes (*e.g.*, ferrocene, Ru(II) complexes) (Figure 1.23 right) have been incorporated into DNA by postsynthetic derivatization of appropriate amino-modified oligonucleotide precursors at position 5 of a thymine,^[217, 223] 3'/5'-termini,^[218, 224] or at internucleotide positions.^[218]

Post-synthetic solid phase strategies proved to be very efficient for attachment of sensitive metalating species, due to the fact that all manipulations could be performed in organic solvents. Oligonucleotides equipped with a 3'- or/and 5'-alkylamino functionality were successfully derivatized with $[\text{Rh}(\text{phi})_2(\text{bpy}')]^{3+}$ and $[\text{Os}(\text{phen})(\text{byp}')(\text{Me}_2\text{-dppz})]^{2+}$ complexes (phi = 9,10-phenanthrene quinonediimine, bpy' = 4-butyric acid-4'-methyl bipyridyl; phen = 1,10-phenanthroline, Me₂-dppz = 7,8-dimethyldipyridophenazine), while still attached onto the solid support^[225] (Figure 1.24).

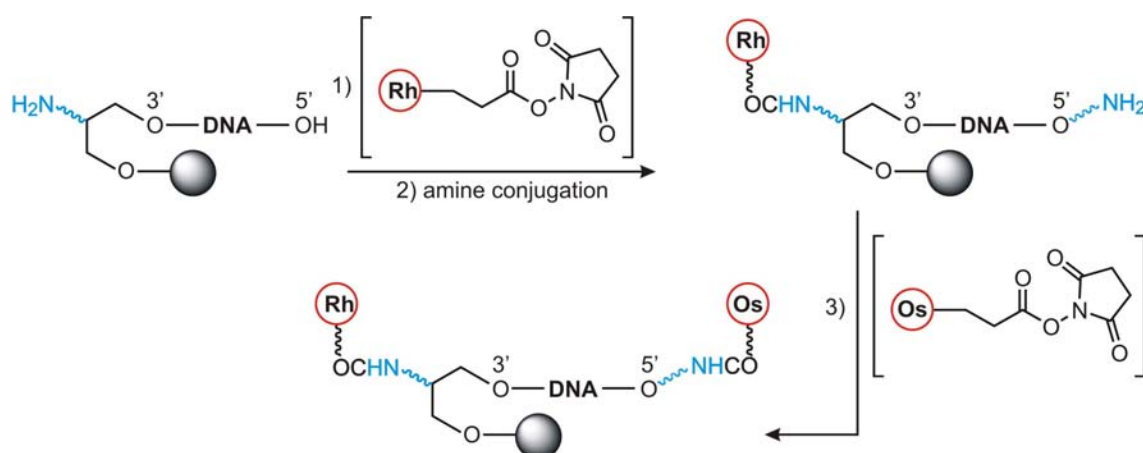


Figure 1.24. Solid phase synthesis of DNA-tethered rhodium and osmium complexes: 1) coupling of 3'-amino modified DNA with the NHS ester of $[\text{Rh}(\text{phi})_2(\text{bpy}')]^{3+}$ complex, 2) 5'-amino functionalization of the resin bound DNA, 3) coupling of the 5'-amino modified oligonucleotide with $[\text{Os}(\text{phen})(\text{byp}')(\text{Me}_2\text{-dppz})]^{2+}$ complex. DMT = 4,4'-dimethoxytrityl.

A similar approach was very recently reported by the group of Kamer. Resin-bound trinucleotide DNA containing 5-iodo-2'-deoxyuridine was functionalized with triphenylphosphine under Pd(0)-catalyzed cross-coupling conditions.^[201]

1.3.2.2 Automated Solid-phase Synthesis

Interesting approaches of “on-column” derivatization have been established by Grinstaff *et al.*, in which metal complexes were incorporated into DNA during automated solid phase synthesis. These methods couple an alkyne functionalized-ferrocene,^[226, 227] or $\text{Ru}(\text{bpy})_3^{2+}$,^[228] to a solid phase-bound oligonucleotide, containing 5-iodo-deoxyuridine (Figure 1.25).

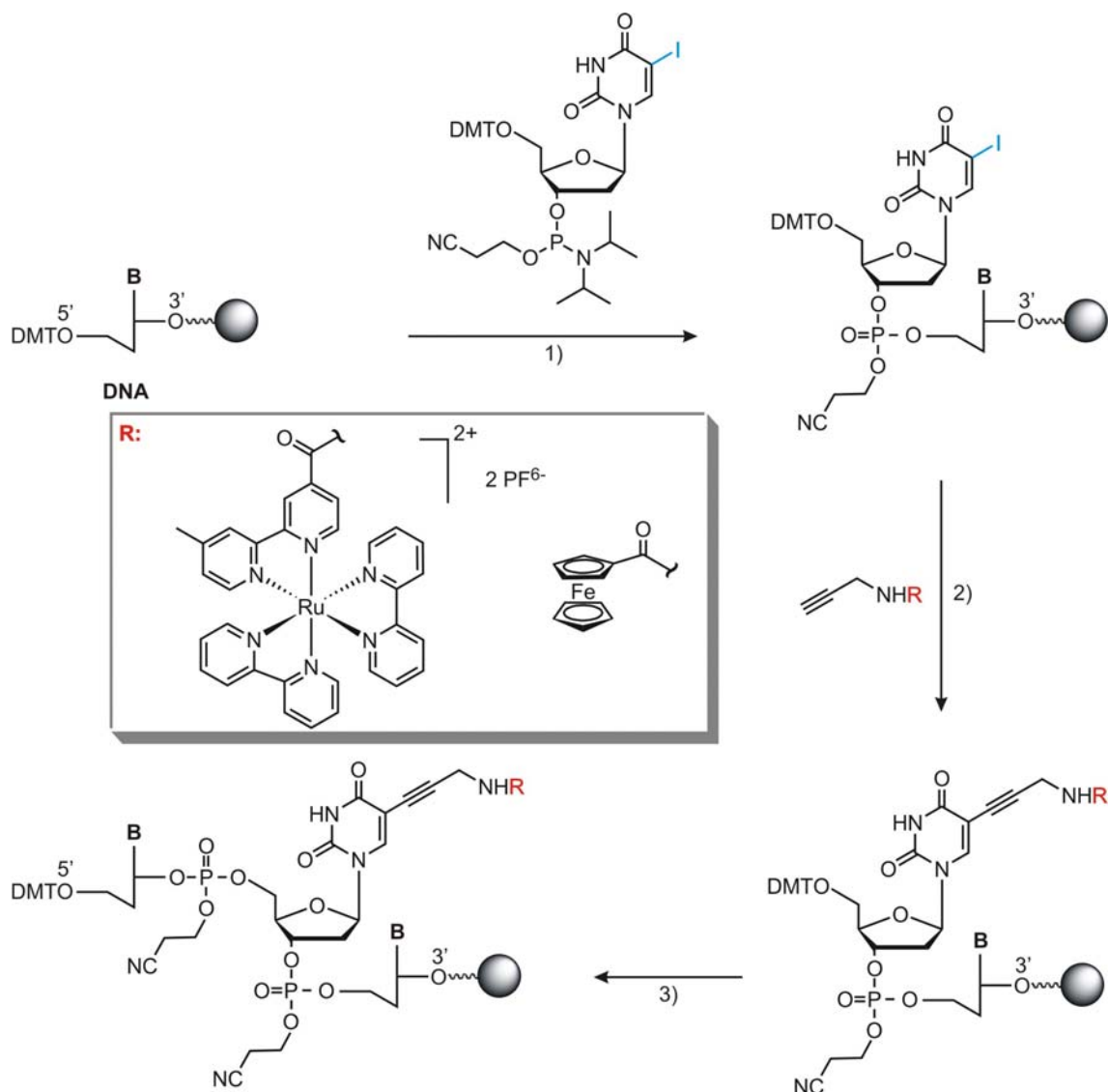


Figure 1.25. Conjugation of ferrocene and $\text{Ru}(\text{bpy})_3^{2+}$ complexes (**B** = A, C, G or T): 1) incorporation of 5-iodo-2'-deoxyuridine phosphoramidite during standard DNA synthesis, 2) Pd(0) cross-coupling of alkyne functionalized metal complex and the resin-bound 5-iodo-2'-deoxyuridine, 3) normal oligonucleotide synthesis is resumed.

Alternatively, solid-phase methodologies have utilized ligand-tethered or metallated nucleoside analogues or metal-coordinating nucleoside mimics for subsequent use in automated DNA assembly. Non-nucleoside based moieties such as 2,2'-bipyridine,^[229] phenanthroline or terpyridine^[230] ligands, for Ru(II) and Cu(II) coordination, have been converted into phosphoramidite building blocks and introduced via automated synthesis at internal positions into DNA sequences. In other approaches, conjugation of EDTA with C5-amino-modified thymidine via amide bond formation,^[231] and coupling of phenanthroline to the N2 position of deoxyguanosine,^[232] followed by standard solid-

phase phosphoramidite chemistry, afforded oligonucleotides to promote Fe(II)-mediated sequence-specific cleavage of DNA. Bipyridine ligands have been attached to nucleobases (*e.g.*, C5-iodo-deoxyuridine) by Sonogashira coupling, resulting in ethynyl-linked conjugates.^[233] A similar strategy has been employed by Tor's group for site-specific incorporation of Ru(II) donor and Os(II) acceptor polypyridine complexes as tools to study photoinduced energy transfer in DNA duplexes.^[234] Under Pd-catalyzed cross-coupling conditions, ferrocene was tethered to 5-iodo-deoxyuridine and incorporated into DNA using automated synthesis techniques.^[227, 235]

Beside metallated phosphoramidite monomers that can be incorporated during solid-phase synthesis, customized solid supports containing metallonucleosides, such as 2'-Ru(bpy)₂-deoxyuridine, have instead been prepared to initiate DNA synthesis, yielding 3'-metallated oligonucleotides.^[236]

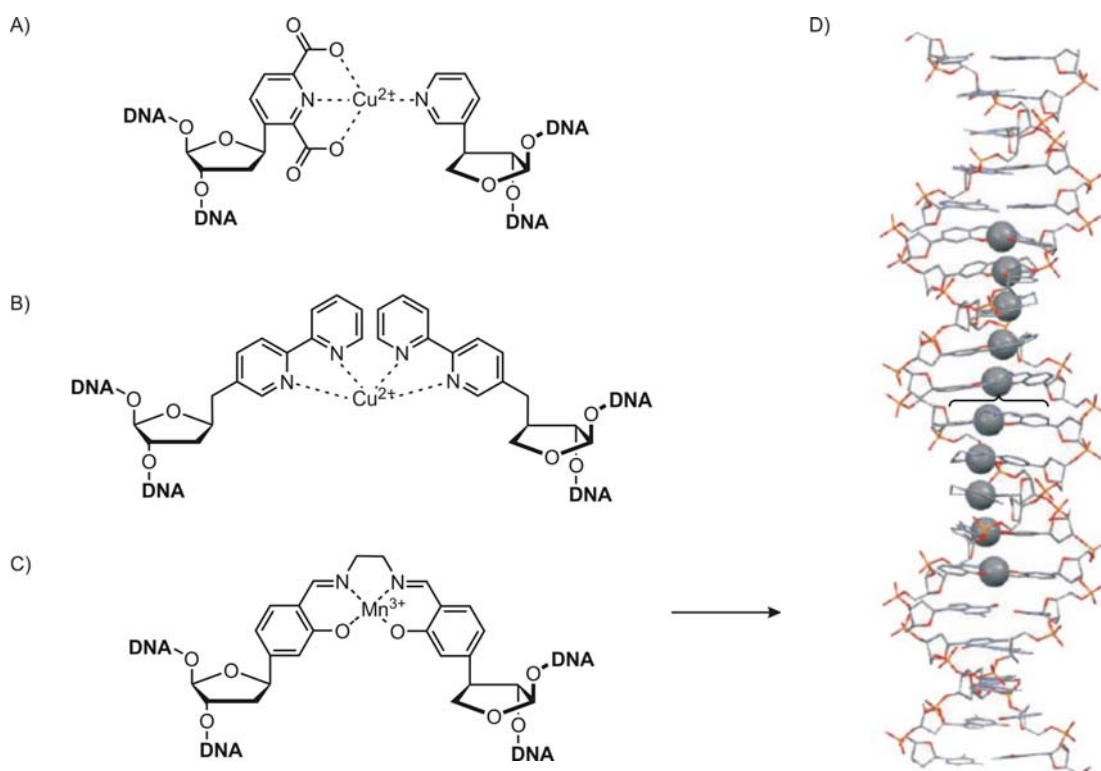


Figure 1.26. Modified oligonucleotides containing pyridine (A), 2,2'-bipyridine (B) and salen (C) ligandosides coordinated to copper and manganese ions. D) The assembly of ten metal-salen base pairs inside a DNA duplex.

Recently, the groups of Shionoya, Schultz, Sheppard, Tor and Carell reported metal-coordinating nucleic acids consisting of nucleoside mimics, called ligandosides, where the heterocyclic base is replaced by a strong chelator. Moreover, such metal-binding

nucleosides could pair through metal coordination and replace the natural hydrogen-bonded base-pairs. In particular, pyridines,^[237] bipyridines,^[237, 238] and salicylaldehyde derivatives, precursors of salen ligands,^[239-241] were coupled to the ribose units, converted into phosphoramidites, and finally assembled into DNA sequences by solid phase synthesis (Figure 1.26). Metal-mediated (*e.g.*, Pd²⁺, Cu²⁺, Ni²⁺, Zn²⁺, and Mn²⁺) ligand-bridged base pairing were then formed, affording stable DNA assemblies. In these structures the metal is located inside the duplex structure. In addition, polynuclear metal complexes could be formed in a predictable manner by incorporation of consecutive metal-base pairs, thereby creating a double helix DNA where five copper,^[242] or ten manganese^[243] (Figure 1.26 D) ions are stacked on top of each other. Such assemblies are presumably precursors of molecular devices, such as molecular magnets and wires.

Despite several advantages of the solid-phase synthesis methodology, including versatility, high yields of metal incorporation, and routine product isolation, the success of this approach depends on the synthesis of individual metallated monomers, compatible with automated DNA synthesis. A severe limitation is the requirement for stable ligands that can survive the conditions used during synthesis, like deprotection, oxidation, capping, or isolation. Therefore, the known repertoire of metal-binding functionalities is rather scarce and consists mainly of nitrogen- and oxygen-donor ligands. Moreover, the majority of metal complexes conjugated to oligonucleotides are kinetically inert or without catalytic activity, except for their Lewis acidity.

The development of an efficient and flexible synthetic strategy for the incorporation of other interesting classes of ligands would therefore be beneficial for the further progress of the field and facilitate the generation of novel metalloribozymes and -DNAzymes.

2 Objectives

The continuous interest in isolation of RNA and DNA molecules with novel catalytic activities, in particular in chemical processes not existing in the biological world, and the success of semisynthetic metalloenzymes in asymmetric catalysis prompted us to become interested in the design of nucleic acid-based hybrid catalysts for organometallic transformations.

This project aims at introducing metal-binding ligands into RNA and DNA folds and developing transition metal complexes in which the activity is primarily dictated by the organometallic catalyst precursor, while the selectivity is governed by the chiral cavity created in the host nucleic acid molecule. The molecular recognition power of nucleic acids, combined with the catalytic properties of transition metal complexes, is assumed to facilitate catalytic reactions for which no enzymes or ribozymes are known. Since in this case, a rational design approach could not span all possible structures, the application of combinatorial methods is expected to generate artificial metallo-DNAzymes and -ribozymes with the desired activity and selectivity. The combinatorial selection of RNA-based hybrid catalysts is, however, a long term goal, which requires a well-matched selection scheme. Unlike the known ribozymes, the *in vitro* selection of RNA-hybrid catalysts needs an overall system that combines structural and functional information from both nucleic acids and organometallic chemistry. For this, the following major subjects have to be challenged:

- well defined positioning of the metal complex in the RNA molecules
- suitable reactions compatible with the structure and chemistry of nucleic acids
- low stereoselectivity provided by the transition metal catalyst in the absence of nucleic acids.

Towards this end, several specific questions should be addressed. For the selection of RNA-transition metal catalysts the use of relatively short DNA/RNA hybrids is envisioned as a way to provide the system with the necessary ligand for a transition metal ion. The main focus of this work is aimed at the development of versatile methods for the site-specific incorporation of metal-binding functionalities into nucleic acids.

These approaches will be applied to covalently attach phosphites, mono- and bidentate phosphines, as well as P,N-ligands either at the termini or at specific internal positions of oligonucleotides and also in combination with various structural parameters. This will allow expanding the repertoire of DNA sequences specifically interacting with transition metals and afford attractive precursors for the development of metallo-(deoxy)ribozymes. Studies on metal complex formation with phosphine and phosphinoxazoline ligands in aqueous mixtures are carried out in order to explore the suitability of phosphorus ligands for nucleic acid-based transition metal catalysis.

Moreover, a major target is the selection of suitable model reactions, namely transition metal-catalyzed transformations that can be performed in water, and subsequently in combination with DNA- and RNA-based ligands. In addition, rigorous analytical methods need to be established that allow the detection of activity and selectivity with pmol amount of catalyst. Since the steric course of the reaction is expected to be influenced by the nucleic acid fold, transition metal complexes are chosen/selected that catalyze the background reaction with modest or, preferably, no stereoselectivity. Towards this end, the synthesis, characterization, and evaluation of the ligand systems and transition metal complexes thereof, as well as of the reaction substrates will be carried out and discussed in detail.

Implementation of achiral ligands in these systems and therefore the exploitation of the nucleic acid scaffold as the only source of chirality are severely restricted by the covalent attachment of the ligand to the biopolymer. Therefore, this work aims at assessing to what extent the stereogenic information carried by a chiral ligand will be complemented by that of the nucleic acid part. On the way to the goal of creating nucleic acid-based catalysts, the influence of DNA and RNA on the activity and selectivity of the tethered metal complexes will be investigated by employing rationally designed model compounds. Due to the inherent chirality of the DNA backbone, DNA-based ligands may effect transfer of chiral information to the chemical reaction. Additionally, from the design and synthesis standpoint such DNA conjugates are attractive systems to work with. Finally, exploring the DNA sequence design, ligand tethering and nucleic acid helix properties is anticipated to aid in gaining insights into the structural basis of DNA-transition metal interactions and to provide tools for designing DNA-based catalysts with improved properties.

3 Results and Discussions

3.1 Incorporation of Metal Complexes into Nucleic Acids

Design of RNA-transition metal system

In the particular case of RNA-hybrid catalysts, the selection procedure requires an additional step for embedding transition metal complexes within RNA sequences (Figure 3.1). Furthermore, a well-defined localization of the transition metal in the nucleic acid scaffold is essential for a clear understanding and, later on, for manipulating the RNA's role in catalysis.

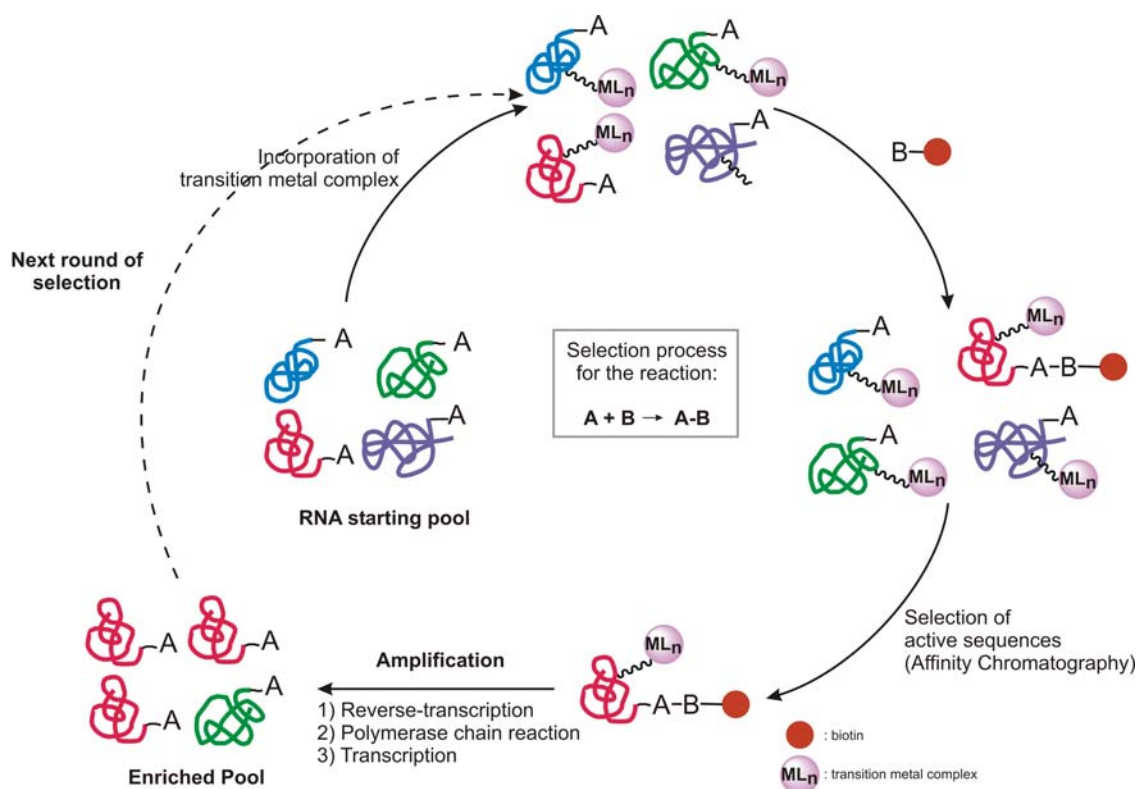


Figure 3.1. General scheme for *in vitro* selection of RNA-based hybrid catalysts.

Therefore, we aim at creating precise metal binding sites in RNA by careful placement of ligands (preferably achiral) within the context of the overall tertiary structure. For

that, two possible approaches were considered: 1) incorporation of metal-binders at a particular nucleotide site within the random region of each sequence of the RNA pool (Figure 3.1 and 3.2 A); 2) co-selection in the presence of a stoichiometric amount of DNA functionalized with a ligand for metal coordination (Figure 3.1 B).

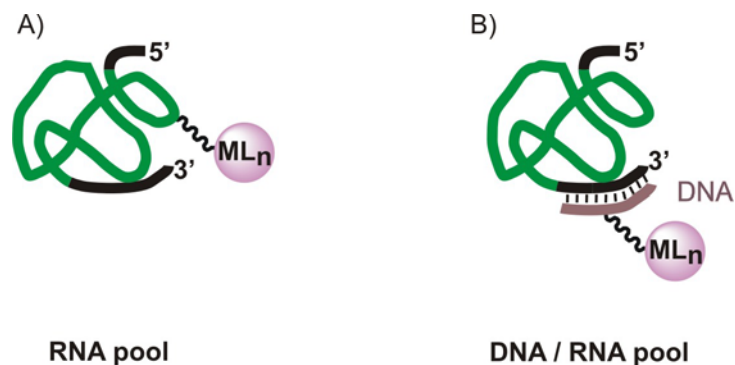


Figure 3.2. Site-specific incorporation of transition metal complexes into RNA and DNA.

The first approach requires either ligand-tethered nucleotides or modified nucleotides bearing functionalizable groups for post-transcriptional modification with metal chelators. For that, one must take into account the factors affecting the synthetic accessibility of the unnatural nucleotides in the form of triphosphates,^[244-246] their compatibility with the known polymerases^[247] involved in the selection cycle, and the stability of metal complexes during enzymatic manipulation.^[248] Additionally, substituting an unnatural base in the DNA or RNA template involves a novel hydrogen-bonding pattern in order to retain the high-fidelity in transcription, PCR and reverse-transcription reactions and to afford the site-specific introduction of its corresponding complement. Therefore, establishing a unique, convenient base-pairing system to be reproducibly incorporated at a site-specific occurrence during each selection cycle appears very challenging and time-consuming.^[249]

As an alternative to achieve precise positioning of the transition metal complex in the RNA fold, a double-stranded DNA/RNA hybrid based on a short modified DNA fragment that matches the 3'-end constant region (cDNA priming site) of the original random-sequence population was chosen (Figure 3.2 B). With the help of a transition metal-DNA carrier a new selection scheme could be designed. In this case, the localization of the DNA-tethered metal complex to the RNA sequence is primarily directed by proximity and Watson-Crick base-pairing. However, these hybridization methods are necessarily limited to reaction conditions compatible with DNA/RNA

duplex formation, such as aqueous environment, precluding a large number of potential chemical transformations. Therefore, the DNA/RNA hybrid approach requires the study of a model reaction, in which proper conditions for RNA folding, proximity effects and tertiary interactions, important for generating local binding sites and catalytic pockets, are maintained.

Criteria of ligand choice

The design of the ligand should produce a structure which can be synthesized fairly readily and appropriately for incorporation into DNA/RNA. Furthermore, the choice of the ligand must take into account the factors affecting the stability of metal complexes in close location to nucleophilic sites in nucleic acids. Nucleobases or phosphate groups in nucleic acids are available for direct coordination to the metal centre. Thus, they can substitute and prevent the ligands from binding, and finally dramatically influence the reactivity of transition metal catalysts. It is anticipated that strong metal binders might overcome this problem by reducing the lability of metal complexes with respect to simple substitution, and dominate the control on metal coordination environment by virtue of the electron-rich nature and chelate effects.

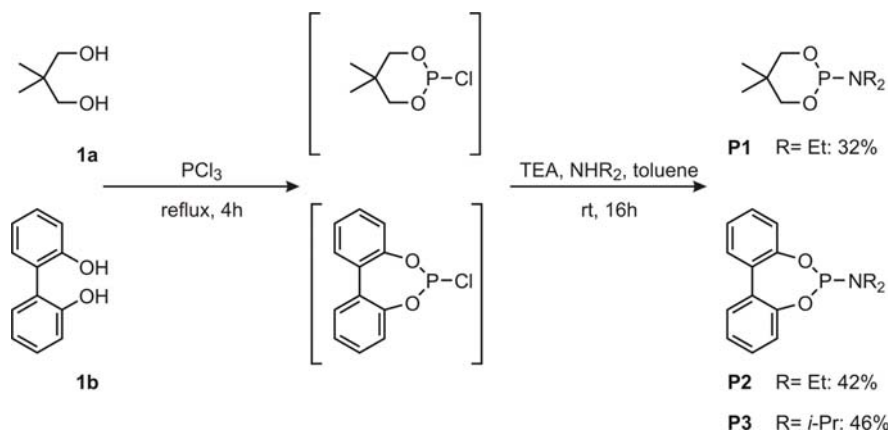
An efficient approach to the modification of DNA with transition metal chelators needs to fulfill the following requirements: (1) generality - the incorporation of ligands for metal coordination at any position along the DNA should be possible; (2) structural stability - the modification should ensure minimal structural perturbation of the DNA duplexes; (3) versatility and tunability - various metal binders as well as tethers for attachment to the DNA should be accessible; (4) simplicity - synthetic approach compatible with the chosen ligands; and (5) high yielding and regioselective DNA functionalization.

Phosphorus ligands possess high affinity for transition metals and are among the most efficient and extensively used ligands in transition metal catalysis. Attracted by the broad applicability of this class of ligands, we attempted the preformation of phosphite-containing oligonucleotides (ODN) and also prepared DNA conjugates carrying mono- and bidentate phosphine and phosphinooxazoline ligands as precursors for introducing metal centres at well-defined positions in DNA and RNA sequences.

3.1.1 Functionalization of DNA with Phosphoramidite Ligand Precursors

Cyclic phosphites were initially chosen as target ligands for incorporation into DNA employing solid-phase synthesis. This approach involves the synthesis of phosphoramidites analogues **P1-3** (Scheme 3.1) and their sequence-specific incorporation into oligonucleotides using the phosphoramidite chemistry. The choice of such ligands originated from the following criteria: (1) low sensitivity to oxidation compared to phosphines and (2) straightforward synthesis from phosphoramidite precursor.

Cyclic phosphoramidites **P1-3** were obtained by direct phosphitylation of appropriate diols with neat phosphorus trichloride, resulting in a chlorophosphite, followed by displacement with amines (Scheme 3.1). The phosphoramidites were purified by flash chromatography over silicagel. These building blocks were thus obtained in high purity (important for high coupling efficiency during oligonucleotides synthesis) and characterized by ^1H and ^{31}P NMR.



Scheme 3.1. Synthesis of phosphoramidites **P1-3**.

As model systems we have chosen to covalently attach the aromatic phosphoramidite **P2** at the 5'-end of pentanucleotide DNA sequences using standard solid phase phosphoramidite DNA synthesis conditions and to generate a phosphite-type linkage (Scheme 3.2). Attachment of an achiral phosphoramidite precursor (**P1**) or chiral but configurationally fluxional P-bonded biphenol unit (**P2,3**)^[82, 89] would result in chiral DNA-based ligands in which the chirality is exclusively dominated by the nucleic acid

oligonucleotide synthesis. Upon iodine-oxidation the presumably formed phosphite linkage would result in a highly stable phosphate ester-type functionality (Scheme 3.2), unproblematic for post-synthetic manipulations.

As a result, removal of the DNA from the solid support using concentrated ammonium hydroxide, followed by overnight incubation at room temperature yielded a single product as observed in the HPLC chromatogram (Figure 3.3 B). Owing to the hydrophobicity added by the phosphite moiety, the modified DNA conjugate eluted with later retention time ($t_R = 29.9$ min) compared to the unmodified DNA ($t_R = 18.0$ min). The isolated product was then analyzed by mass spectrometry and, corresponded indeed to the biphenyl-phosphate containing DNA conjugate **sODN1-P2(O)** (overall yield: 45%; calculated $[M-H]^-$: 1691, measured: 1710).

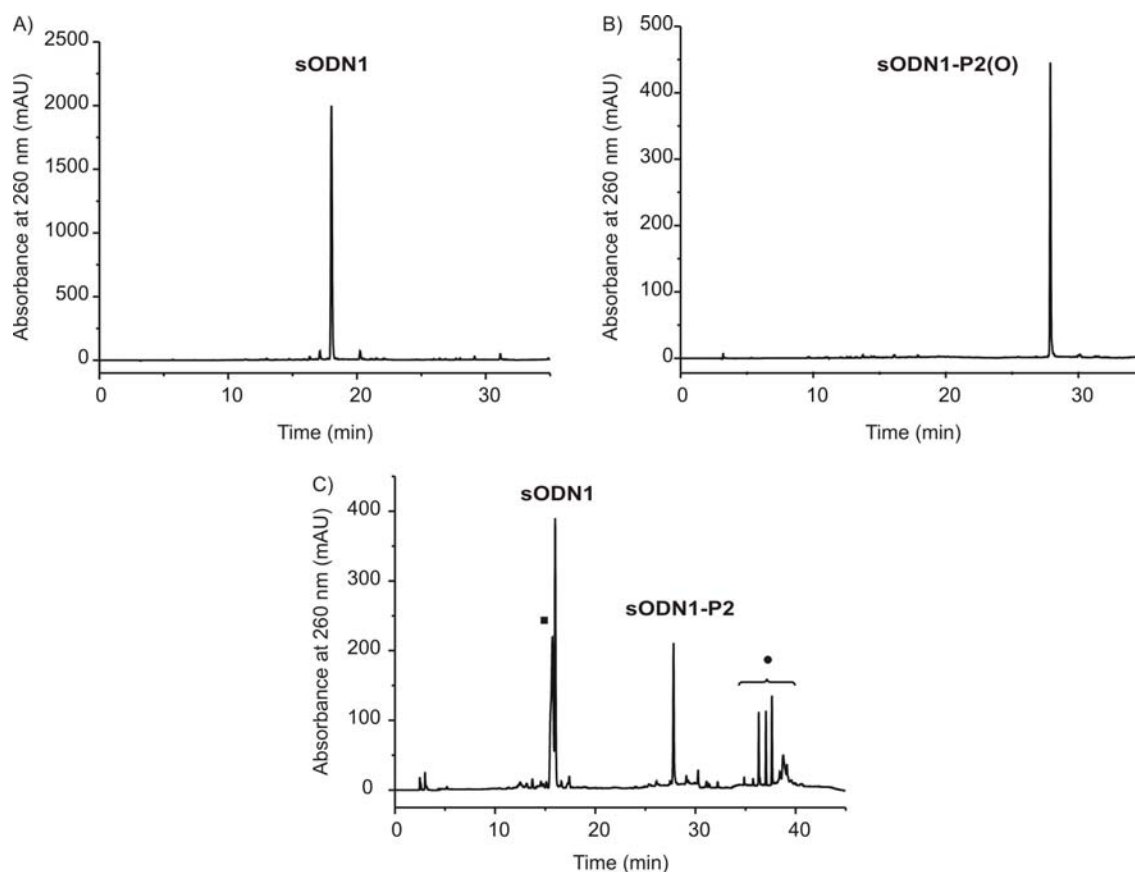


Figure 3.3. HPLC chromatograms of the attempted DNA solid-phase derivatization (no iodine oxidation) with **P2** (A), the phosphate-containing DNA conjugate **sODN1-P2(O)** (iodine oxidation) (B), and the crude DNA product obtained after treatment of resin-bound DNA-phosphite **sODN1-P2** with $[\text{Rh}(\text{cod})\text{Cl}]_2$, followed by ammonium hydroxide deprotection. ■ Failure DNA sequences obtained by automated solid-phase synthesis and 5'-OH unmodified **sODN1**; ● protected oligonucleotide and residual organic molecules.

Having demonstrated the coupling of **P2** phosphoramidite, we were still confronted with stability and isolation of DNA-phosphite conjugates. At this point, we assumed that long time exposure to basic conditions required by post-synthetic DNA cleavage and deprotection might lead to decomposition of the DNA-appended phosphite.

It is known that compounds containing P–O/N bonds have proved to some extent unstable, being able to undergo hydrolysis in protic solvents and lead to either cyclic *H*-phosphonates or ring-cleavage products^[251] due to the tendency of phosphorus to form P=O bonds. For example, Feringa reported on stability of phosphoramidite ligands which after heating to 100 °C for 5 hours in dioxane/H₂O 10:1 were completely hydrolyzed, whereas their corresponding rhodium(I) complexes remained unchanged despite the drastic conditions.^[252] This observation was also confirmed in the case of phosphite ligands that appeared to be fully stable in protic solvents upon coordinating transition metals.^[253]

Prompted by these findings, we made use of the phosphites ability to bind transition metals and form stable complexes, as a way to overcome the problematic isolation of phosphite-containing DNA from aqueous mixtures. Complex formation between the DNA-appended phosphite and 1,5-cyclooctadienylrhodium(I) chloride dimer was attempted by simply combining the solution of [Rh(cod)Cl]₂ precursor in acetonitrile with the CPG beads coated with the DNA conjugate and stirring the resulting suspension. In this approach, the phosphate moieties of the DNA backbone were all protected as cyanoethyl esters so the oligonucleotide was uncharged and well solvated by organic solvents. The crude DNA was liberated from the bead and the protecting groups removed by treatment with aqueous ammonia. This final step was monitored by reversed-phase HPLC under the same conditions employed for analysis of unmodified oligonucleotides. Figure 3.3 C shows the chromatogram of the crude DNA product after 30 minutes incubation at 65°C with ammonium hydroxide. Several early-eluting side products that did not contain the hydrophobic biphenolic moiety, likely failed sequences in the DNA synthesis, and the 5'-OH unmodified **sODN1** oligonucleotide were obtained. Additional DNA products with higher retention times might correspond to protected oligonucleotide likely due to insufficient deprotection time. The single DNA conjugate (*t_R* = 27.8 min) not belonging to any of these two categories was isolated in 18% yield, lyophilized and characterized by MALDI-TOF mass spectrometry. The mass

spectrum confirmed that the isolated species was the pure **sODN1-P2** phosphite-DNA conjugate (**sODN1-P2**: calc. $[M-H]^-$ 1675, found 1685) and no trace of decomposition products could be detected.

These results indicate that the Rh complex was formed, in a certain extent, and was fairly stable under the conditions employed in the deprotection and cleavage protocol. However, the moderate yield does not exclude the presence of free DNA- phosphite in the crude reaction mixture because free phosphite ligand hydrolyses in water, leading to 5'-OH unmodified **sODN1**, which was observed during HPLC analysis. Furthermore, the isolation of rhodium complexes on reversed-phase chromatography appears difficult and generally results in displacement of the transition metal ion from the complex due to the hemilability of P-Rh bond.

All these observations directed our attention to phosphine ligands, known to be more stable against hydrolysis, albeit highly sensitive to oxidation, as suitable metal-binding moieties for DNA functionalization.

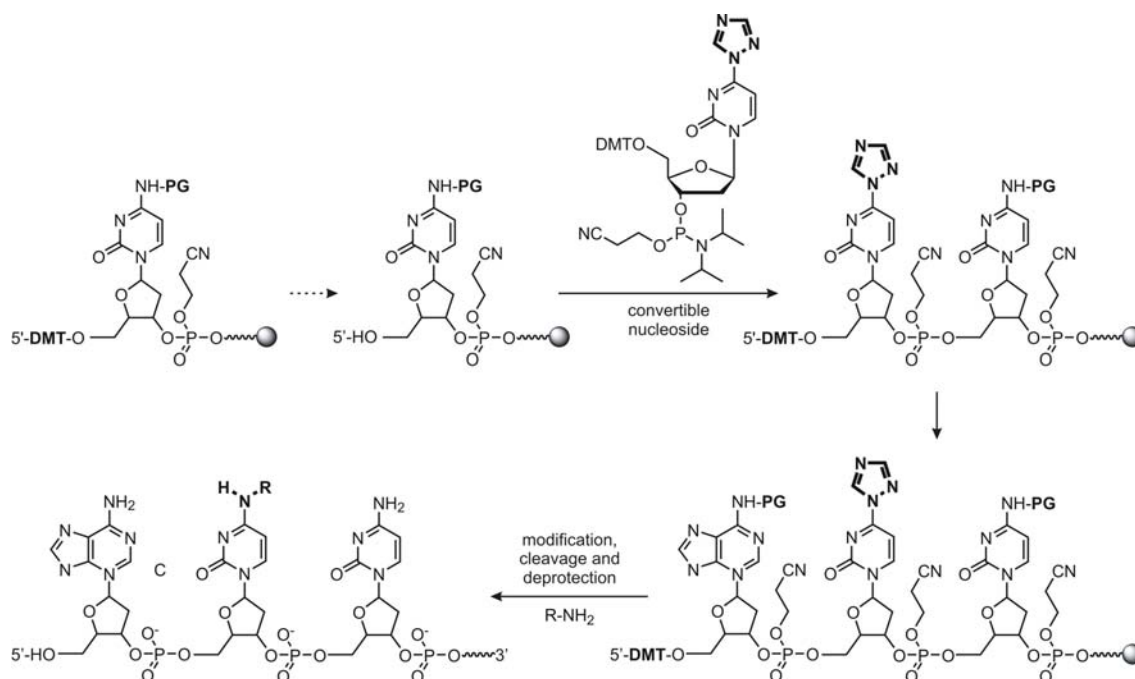
3.1.2 DNA-Phosphine Ligands

Obviously, phosphine ligands need to be incorporated after DNA synthesis to avoid exposure to the oxidation step during automated solid-phase synthesis. We envisioned the post-synthetic modification of oligonucleotides as the most suitable and versatile approach for the preparation of phosphine-carrying DNA conjugates. Various aminoalkyl-modified oligonucleotides have been successfully reacted at predetermined internal sites with carboxylate derivatives of PYRPHOS, BINAP and PHOX ligands (Figure 2.3), affording the first examples of DNA sequences carrying mono- and bidentate phosphine ligands as well as P,N-ligands.^[254]

3.1.2.1 Amino-Functionalized Oligonucleotides

For the preparation of amino-modified oligonucleotides, we employed the “convertible nucleoside” approach developed by Verdine^[255] and Swann.^[256] The oligonucleotide chain is elongated using a building block that is a precursor of the amino-functionalized nucleoside, a so-called “convertible nucleoside”. This precursor may be transformed into a range of differently modified nucleosides in the final steps of the synthesis^[257-259]

(Scheme 3.3). This strategy applies to the modification of exocyclic positions, such as the 4-position of deoxycytidine, a biologically important site as it is directly involved in DNA Watson-Crick base pairings.^[255, 256, 260, 261]



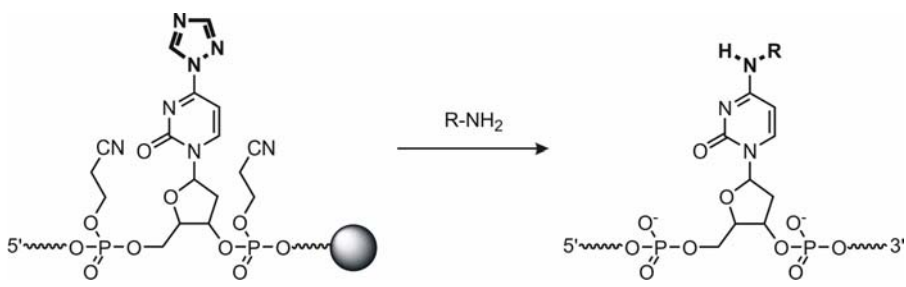
Scheme 3.3. Synthesis of amino-modified oligonucleotides using the “convertible nucleoside” approach (convertible nucleoside = 4-triazolyl-2'-deoxyuridine). **PG** = protecting group, ● = CPG.

The “convertible nucleoside” approach (Scheme 3.3) involves three steps: (1) preparation of a versatile monomer containing a suitable leaving group on the nucleobase, such as 4-triazolyl-deoxyuridine; (2) incorporation of the monomer into oligomers; (3) replacement of the leaving group after DNA synthesis with diamines. This approach offers the advantage that the triazolyl leaving group is stable during DNA synthesis and subsequent deblocking step and only post-synthetically convertible to introduce the required alkylamino group on the base.

In our case, the “convertible nucleoside” strategy was adapted and optimized. Oligomers containing 4-triazolyl-deoxyuridine were prepared by automated DNA synthesis, on 1 μ mol scale. No modification was made for the incorporation of the modified monomer compared to the natural ones, for which a satisfactory coupling yield, mostly over 95%, was obtained. All oligonucleotides were synthesized with retained 5'-terminal trityl group that simplifies the purification of the desired full-length products.

In order to facilitate the removal of the protecting groups from normal bases, we chose to use base-labile monomers, in which dA, dG and dC are protected with the *t*-butylphenoxyacetyl (TAC) group. This protecting group can be readily removed by concentrated aqueous ammonia solution within 2 h at room temperature or 15 min at 55°C (Proligo's protocol). Together with other non-standard phosphoramidite building blocks (e.g., a decaethyleneglycol spacer molecule **S** as for **ODN3**), or 7-deaza-guanosine monomer (**ODN5a,b**), this protocol allowed moderate to high-yielding syntheses of long ODNs with the convertible nucleotide at varying internal positions. After synthesis, the ODNs were treated with suitable diamines (Table 3.1): ethylenediamine, 1,4-butanediamine, and 1,13-diamino-4,7,10-trioxatridecane, affording conversion of the 4-triazolyl-dU to different 4-alkylamino-dC derivatives that can base-pair like a normal cytidine nucleotide.^[260] At the same time, the ODN is cleaved from the support and deprotected.

Table 3.1. Preparation of amino-modified **ODN1-5**.^[a]



ODN	Sequence	R	Yield ^[b] [%]
ODN1a		$\text{H}_2\text{N}-\text{CH}_2\text{CH}_2\text{CH}_2\text{CH}_2-\text{OH}$	35
ODN1b	5'-GC AGT GAA GGC ^R TGA GCT CC-3'	$\text{H}_2\text{N}-\text{CH}_2\text{CH}_2\text{CH}_2-\text{OH}$	42
ODN1c		$\text{H}_2\text{N}-\text{CH}_2\text{CH}_2-(\text{O}-\text{CH}_2\text{CH}_2)_2-\text{O}-\text{CH}_2\text{CH}_2-\text{OH}$	40
ODN2	5'-GC AGT GAA GGC TGA GCT CCT AC ^R C-3'	$\text{H}_2\text{N}-\text{CH}_2\text{CH}_2\text{CH}_2\text{CH}_2-\text{OH}$	32
ODN3 ^[c]	5'-GC AGT GAA GGC TGA GCT CCS C ^R C-3'	$\text{H}_2\text{N}-\text{CH}_2\text{CH}_2\text{CH}_2\text{CH}_2-\text{OH}$	30
ODN4a		$\text{H}_2\text{N}-\text{CH}_2\text{CH}_2\text{CH}_2-\text{OH}$	25
ODN4b	5'-GC AGC GAT AAC ^R TAA GCG CT-3'	$\text{H}_2\text{N}-\text{CH}_2\text{CH}_2\text{CH}_2\text{CH}_2-\text{OH}$	21
ODN4c		$\text{H}_2\text{N}-\text{CH}_2\text{CH}_2-(\text{O}-\text{CH}_2\text{CH}_2)_2-\text{O}-\text{CH}_2\text{CH}_2-\text{OH}$	22
ODN5a ^[d]	5'-GC AGT GAA XXC ^R TXA GCT CC-3'	$\text{H}_2\text{N}-\text{CH}_2\text{CH}_2\text{CH}_2-\text{OH}$	14 ^[e]
ODN5b ^[d]		$\text{H}_2\text{N}-\text{CH}_2\text{CH}_2\text{CH}_2-\text{OH}$	5 ^[e]

[a] Reaction conditions: 5 M aqueous solution of 1,4-diaminobutane or ethylenediamine, r.t., 4 h or neat 1,13-diamino-4,7,10-trioxatridecane, r.t., 4 h (followed by additional treatment with water, 5 h). [b] Isolated yields after solid phase synthesis (1 μmol), conversion and purification. [c] A decaethylene glycol unit **S** was incorporated during solid phase synthesis. [d] **X** denotes 7-deaza-guanosine nucleotide. [e] Moderate yields due to low coupling efficiency of the **X** monomer.

To investigate the reaction time required for complete deprotection, cleavage and replacement of the triazolyl group, the resin-bound DMT-on *ODNI* was treated with 1,4-butanediamine at room temperature and monitored by reversed-phase HPLC (Figure 3.4). The desired amino-modified oligomer as confirmed by MALDI-TOF mass spectrometry was obtained in 4 hours and longer reaction times did not improve the yields of deprotection, cleavage and conversion.

Compared to reported methods, this mild one-pot conversion, deprotection and cleavage procedure gives consistently high yields of amino-modified DNA sequences in short reaction times.

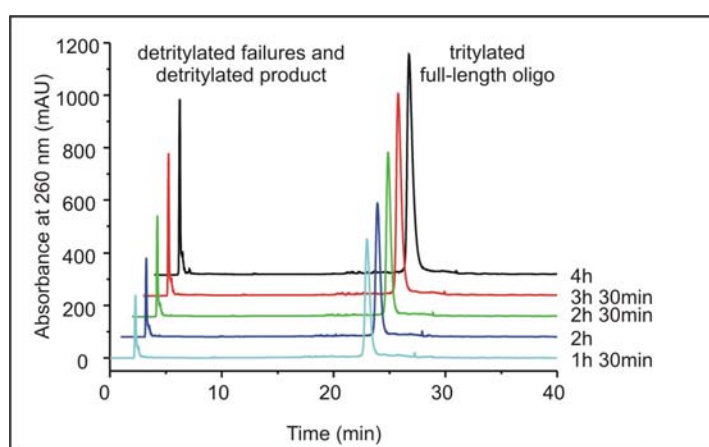


Figure 3.4. Reversed-phase HPLC chromatograms of the crude tritylated *ODNIa* at different reaction times.

Furthermore, our synthetic approach allows the parallel synthesis of various conjugates differing in length and structure of the spacer, which may be of particular relevance in determining the interaction between the transition metal complex and the biopolymer.^[146]

3.1.2.2 Duplex Stability of Amino-Tethered Oligonucleotides

It is well known that in B-DNA form, the non-base-paired substituent on the N4-position of deoxycytidine projects directly into the central space of the major groove (Figure 3.5) and provides an excellent location for the attachment of DNA-interacting ligands.^[255] At the same time, it corresponds to one of the least sterically demanding positions available on a DNA base.

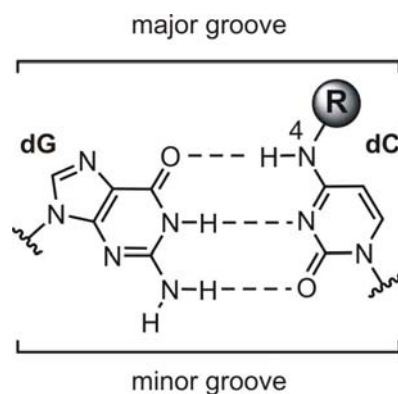


Figure 3.5. *N*-alkyl tethers attached to the exocyclic amine of dC, allowing the major groove to be targeted without interfering with Watson-Crick base-pairing.

Therefore, attachment of a tether at this site should induce little steric perturbation of duplex DNA structure as demonstrated by X-ray crystallographic studies on duplex DNA containing the related N6-methyladenine.^[262] Figure 3.6 illustrates the positioning of the tether in a 4-thioethyl-dC containing B-DNA model.

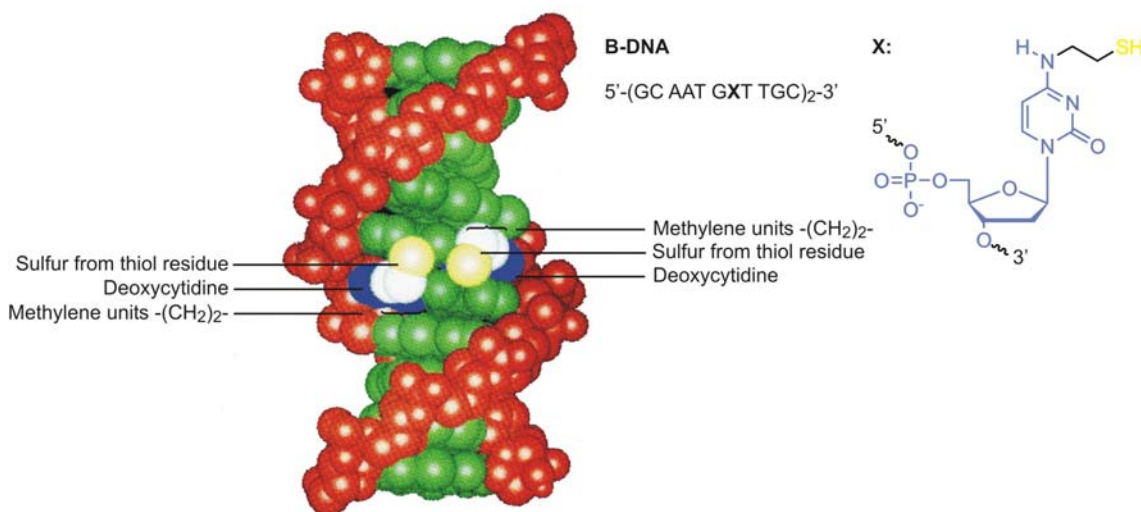


Figure 3.6. Location of N4-ethylthiol in dC-tethered B-DNA.^[255]

However, it has been shown that N4-alkylamine and -alkylthiol substituents (Figure 3.6) do destabilize duplex DNA, in some extent, on the basis of electronic factors. For example, a destabilizing effect of 6-7°C has been observed for a 15mer double-stranded DNA, each strand containing either a N4-butylamino- or ethylamino-modified 2'-deoxycytidine residue. Therefore, in many applications the effects of single unnatural bases of this type on DNA duplex stability have been considered relatively modest.

Moreover, it has been assumed that further derivatization and subsequent covalent attachment of DNA-interacting moieties would not exert a strong effect on duplex stability.

These systems resemble very well our amino-modified oligonucleotides **ODN1a** and **ODN1b**, respectively. Therefore, we assumed that also in our case the effect of alkylamine tethers on **DNA** stability would be low in aqueous solutions containing salts. Since we aim at performing organometallic transformations in the presence of DNA hybrids, we were uncertain what amount of organic solvent would be optimal for our system. The amino-modified oligonucleotide **ODN1a** precursor (Table 3.1) which contains an intermediate C4-linker was used to study the effect of organic solvents on the double-helical DNA conformation. We then prepared the complementary DNA strand **cDNA1** (5'-GG AGC TCA GCC TTC ACT GC- 3') using standard solid-phase synthesis and deprotection procedures (Chapter 5.3.4). The duplexes were formed by combining equimolar amounts (2 nmol) of each strand in Hepes buffer (15 mM, pH 7.5)^[263] in the presence of dioxane (0-30% v/v), annealing them together by heating to 90 °C and gradually cooling to room temperature. The results are depicted in Figure 3.7.

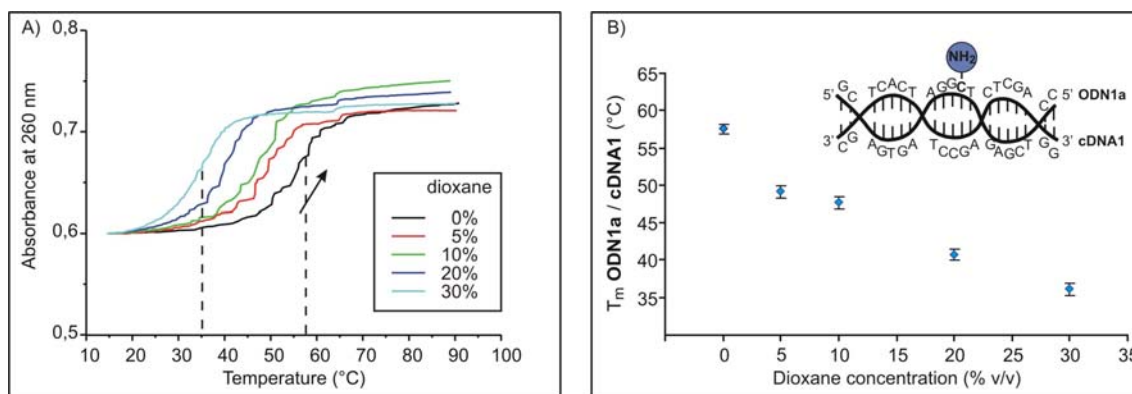


Figure 3.7. A) Melting profiles of the **ODN1a/cDNA1** duplex in the presence of various concentrations of dioxane. B) Plot of melting temperature versus dioxane concentration.

The black curve in Figure 3.7 A shows the change in absorbance at 260 nm of the **ODN1a/cDNA1** duplex dissolved in 100% buffer containing 150 mM NaClO₄ and 7.5 mM Mg(ClO₄)₂ when subjected to heating from 15 to 90°C at 5°C per min (control experiment). The shape of the curve resembles a typical DNA denaturation curve.^[264] Thermal denaturation involves unstacking of the bases, which gives rise to an increase in absorbance. The T_m value determined for this curve in Figure 3.7 B is 57.6±0.6°C.

When the DNA duplex pre-formed in 5-30% dioxane was subjected to the same heating/cooling annealing procedure as in water, it yielded the same sigmoidal dependence as the black curve in Figure 3.7 A, indicating that annealings in neat water and in dioxane/water mixtures show the same behaviour.^[265, 266] Under these conditions the melting profiles of double-stranded amino-modified DNA were substantially shifted with increasing concentration of organic solvent. However, the hyperchromicities remained unchanged, indicating that the organic solvent did not alter the DNA integrity significantly at room temperature.

The melting temperatures were plotted as a function of the volume percentage of dioxane. Figure 3.7 B shows an almost linear dependence of the T_m values on the dioxane concentration, in agreement with literature data that supported a linear decrease of the thermal stabilities of DNA/DNA and RNA/DNA duplexes with increasing concentration of formamide.^[267]

Our results demonstrated that **ODN1a/cDNA1** still preserved its double-helical conformation in 30% aqueous dioxane, at high salt concentration, although its thermal stability was lower than in 100% water, as reflected by a 21.4°C reduction in the T_m value (Figure 3.7 B). We estimate that structurally related DNA/DNA and DNA/RNA duplexes, for example functionalized with metal-chelating moieties, would show similar behaviour in aqueous-dioxane mixtures as their amino-tethered double-stranded DNA precursors.

3.1.2.3 Reactivity of Amino-Modified Oligonucleotides

Before studying the phosphine systems and their attachment to DNA, which were expected to require anaerobic conditions, the coupling reaction of amino-modified ODNs with carboxylic acid groups and amide bond formation were initially investigated using the *N,N'*-bis(2-picolyl)amine derivative **bpa**^[268], highly stable against oxidation.

Thus, **ODN1a**, **ODN2** and **ODN3** were reacted with the *in situ* formed *N*-hydroxysuccinimide (NHS) ester (100-200 equiv) of **bpa** in 66.7% DMF, pH = 8.5, for 48 hours, at room temperature (Scheme 3.4). Precautions were taken in the pH adjustment of the reaction mixture, because at high pH competing hydrolysis of the NHS ester bond occurs. Under our conditions, the coupling of **bpa** to **ODN2** and **ODN3** proceeded to completion, as demonstrated by the PAGE. In the case of coupling to

ODN1, the reaction conversion could not be estimated due to co-migration of excess **bpa** activated ester with the amino-modified DNA starting material.

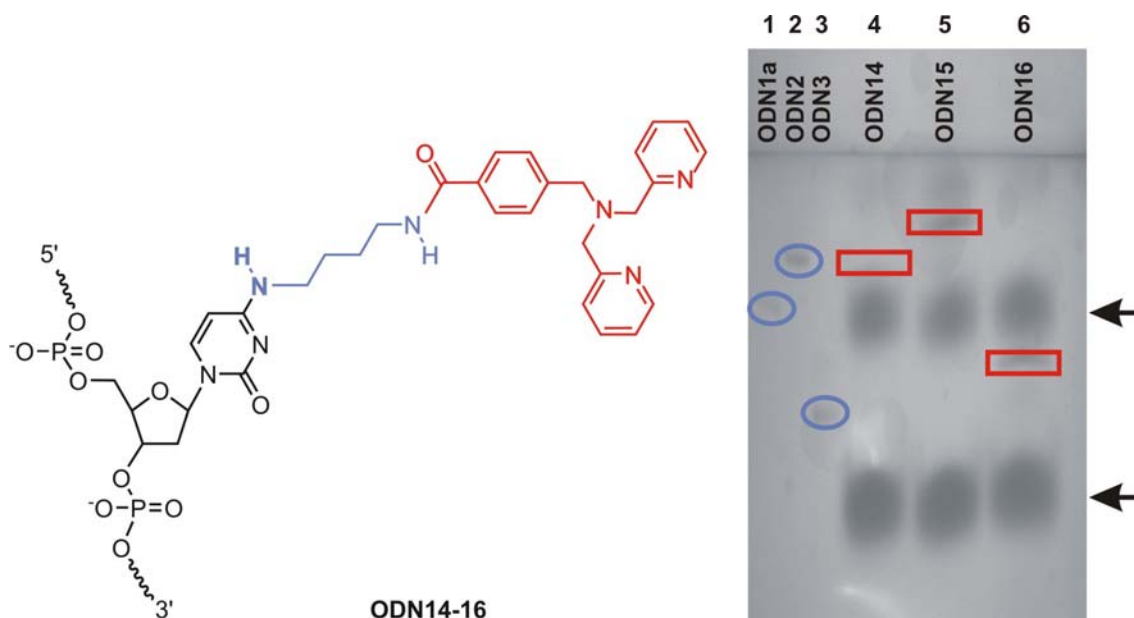


Figure 3.8. UV-shadowing of the 18% PAGE gel ($\lambda = 254$ nm) used for analysis of the DNA-appended **bpa** conjugates **ODN14-16**. Lane 1 - control amino-modified **ODN1a**; lane 2 - control amino-modified **ODN2**; lane 3 - control amino-modified **ODN3** (see **Table 3.1** for abbreviations). Coupling reaction of **bpa** after 48 hours incubation, at room temperature with amino-modified **ODN1a** - lane 4, **ODN2** - lane 5, and **ODN3** - lane 6, respectively. The arrows indicate excess **bpa** NHS-activated ester and hydrolyzed ester, respectively.

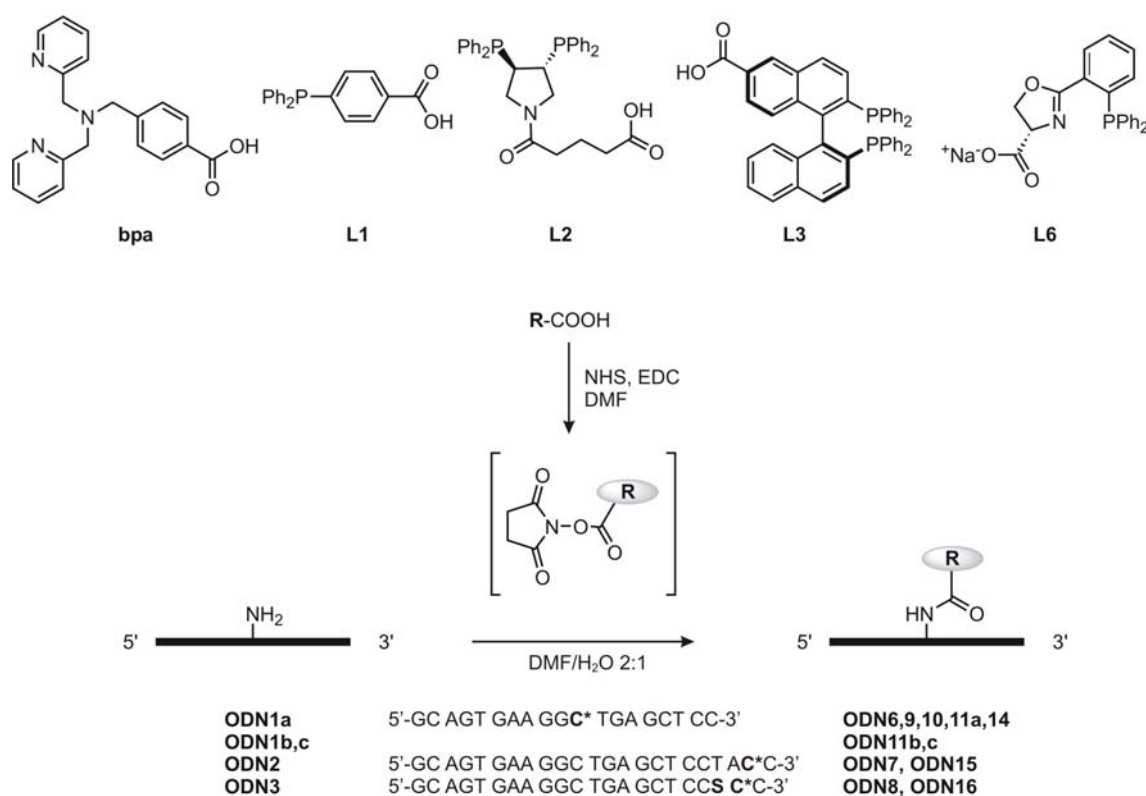
Figure 3.8 depicts an analytical denaturing polyacrylamide gel comparing the retarded bands corresponding to *N,N'*-bis(2-picolyl)amine-containing DNA conjugates **ODN14-16** to the starting amino-modified **ODN1a**. Due to the increased mass, the electrophoretic mobility of **ODN14-16** is lower than of the oligonucleotide precursor.

3.1.2.4 Post-synthetic Functionalization of Amino-modified DNA with Phosphine Ligands

Having demonstrated the reactivity of amino-modified ODNs, amide bond formation between **ODN1a** and commercially available 4-(diphenylphosphino)-benzoic acid **L1** was chosen as the model reaction to investigate the coupling of phosphine-based ligands (Scheme 3.4). Phosphine **L1** was first activated by using *N*-(3-dimethylaminopropyl)-*N'*-ethylcarbodiimide (EDC) in the presence of *N*-hydroxysuccinimide (NHS), and the *in situ* generated active ester was directly added to the **ODN1a** solution.

The coupling reaction was analyzed by reversed-phase HPLC and proceeded to completion, affording 60% of the desired DNA-phosphine conjugate **ODN6**. Not surprisingly, a fraction ($\leq 20\%$) of **ODN6** was oxidized to the corresponding phosphine oxide **ODN6(O)**, presumably during workup. Small amounts of byproducts were observed that did not carry a phosphine moiety, suggesting slight degradation of the starting material (Figure 3.9).

The desired phosphine-containing oligonucleotide could be easily isolated by HPLC and was stable under the purification conditions. While HPLC purification as described here does not cause oxidation of the phosphine-DNA, sample preparation, collection and manipulation should be performed in oxygen free conditions. MALDI-TOF mass spectrometry of the HPLC purified **ODN6**, however, gave only the mass of the oxidized product **ODN6(O)** (Table 3.2).



Scheme 3.4. Post-synthetic functionalization of amino-modified ODN with *N,N'*-bis(2-picolyl)amine **bpa**, phosphines **L1-3** and phosphinoxazoline **L6**. **C*** = N4-alkylamino-modified 2'-deoxycytidine. **S** = decaethylene glycol unit.

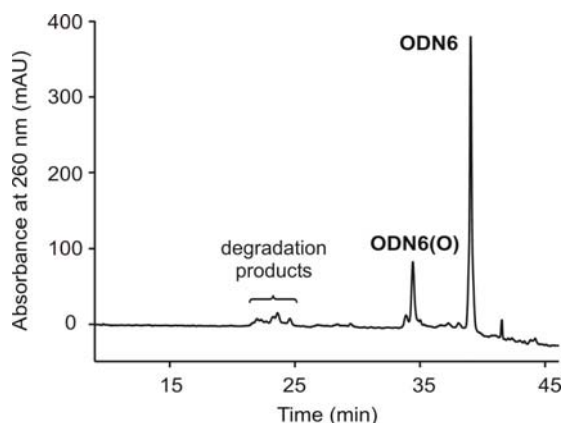


Figure 3.9. HPLC chromatogram of **ODN6** pre-purified by chloroform extraction and ethanol precipitation to remove the excess of coupling reagents. Trace amounts of degradation products elute between 20 and 24 min, similarly to the starting material **ODN1a** ($t_R = 21.9$ min) (for HPLC conditions see Chapter 5.5.1).

To prove the identity of the oligonucleotide eluting with $t_R = 39.0$ min as phosphine-DNA conjugate **ODN4a**, the HPLC eluate was treated with sulfur^[269] to yield the air-stable phosphine sulfide analogue **ODN6(S)** with $t_R = 38.0$ min. The MALDI mass spectrum clearly confirmed that the isolated species was the pure phosphine-DNA **ODN6** and no trace of the oxide **ODN6(O)** was detected.

Amino-modified oligonucleotides **ODN2** and **ODN3** were also reacted with phosphine **L1**. The coupling reactions proceeded consistently well, affording 65% and 68% of **ODN7** and **ODN8** respectively (Table 3.2).

Table 3.2. Isolated yields and MALDI-TOF analysis of **ODN6-8**.^[a]

Entry	Conversion [%]	Isolated yield [%]	ODN(O) ^[b]		ODN(S) ^[c]	
			calcd	obsd	calcd	obsd
ODN6	>99	60	6228	6234	6244	6249
ODN7	96	65	7424	7430	7440	7447
ODN8	>99	68	7328	7332	7344	7350

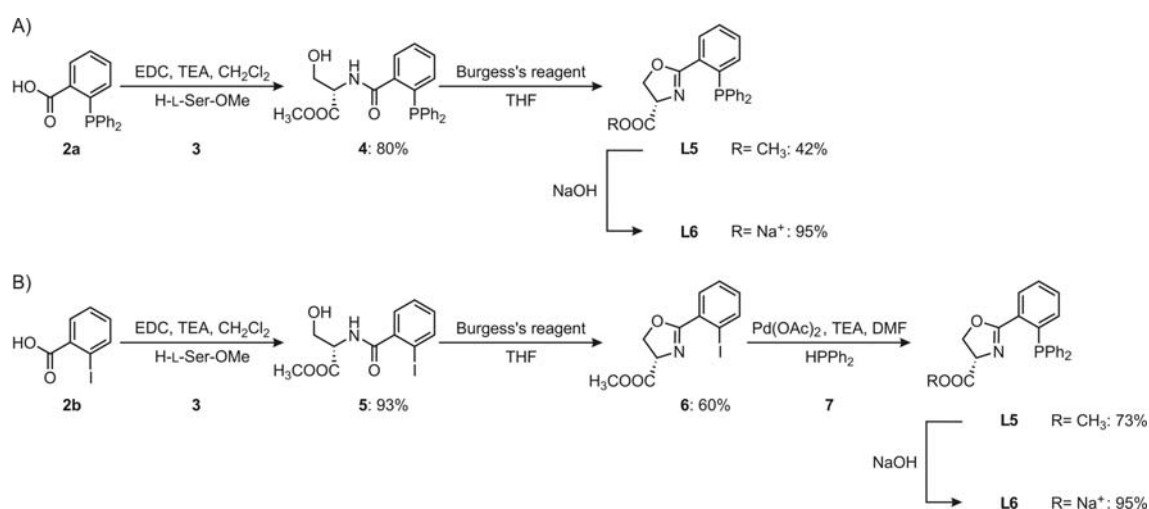
[a] **ODN7** and **ODN8** are the coupling products of **L1** with **ODN2** and **ODN3**, respectively. [b] **ODN(O)**: DNA-phosphine oxide. [c] **ODN(S)**: DNA-phosphine sulfide.

Having established the optimal conditions for coupling the monophosphine derivative **L1** to DNA, we then studied the reaction of **L2,3** and **L6** with **ODN1a** (Scheme 3.4).

Bisphosphines **L2**^[19] and **L3**^[50] are derivatives of the well-known ligands PYRPHOS and BINAP, respectively, extensively used in organometallic catalysis,^[13, 18, 21, 22, 40]

while **L6** belongs to the family of PHOX ligands with applications in allylic substitution, hydrogenation and asymmetric Heck reactions.^[57, 63]

Compound **L6** was synthesized starting either from commercially available 2-(diphenylphosphino)-benzoic acid **2a** (Scheme 3.5 A) or 2-iodo-benzoic acid **2b** (Scheme 3.5 B) and L-serine methyl ester hydrochloride **3** (H-L-Ser-OMe), followed by oxazoline ring closure in the presence of Burgess's reagent. In the second synthetic approach, the PPh₂-group was introduced by palladium-catalyzed P-C cross coupling reaction with diphenylphosphine **7**.^[270] The phosphinooxazoline was isolated as sodium salt **L6**, since acidification results in oxazoline ring opening.^[271]



Scheme 3.5. Synthesis of phosphinooxazoline **L6**.

The coupling reactions of **L2**, **L3** and **L6** to **ODN1a** were monitored by reversed-phase HPLC and proceeded with 98% and 95% conversion for **L2** and **L6**, respectively. The amounts of oxidized species (mono- and bisoxide for **ODN9** and monoxide for **ODN11a**) were below 10%. In case of **L3**, the observed conversion was lower (55%), most probably due to the limited solubility of the BINAP derivative in the aqueous reaction mixture (Table 3.3). Oxidation products (mono- and bisoxide of **ODN10**) were found to be formed in <7% yield. Conjugates **ODN9**, **ODN10** and **ODN11a** were purified and isolated by reversed-phased HPLC. Figure 3.10 A illustrates typical HPLC chromatograms obtained for the coupling of **L2**, **L3** and **L6**. The isolated products were analyzed by mass spectrometry (Table 3.3) in the form of the corresponding phosphine sulfide analogues. All other byproducts generated by full or partial oxidation were also isolated and characterized: phosphine bisoxides (for **L2** and **L3**) and phosphine

monoxides (for **L6**; and for **L2** and **L3** characterized as monoxide-monosulfide).

Table 3.3. Isolated yields and MALDI-TOF MS analysis of **ODN9-11a**.

Entry	Coupled ligand	Isolated yield [%]	ODN(O) _n ^[a]		ODN(O)(S) m/z ^[b]		ODN(S) _n ^[a]	
			calcd	obsd	calcd	obsd	calcd	obsd
ODN9	L2	74	6489	6491	6508	6510	6524	6528
ODN10	L3	38	6605	6610	6621	6626	6637	6637
ODN11a	L6	78	6297	6296	-	-	6313	6314

[a] n = 2 for **L2** and **L3**, and n = 1 for **L6**. [b] **ODN9** and **ODN11a** detected in negative mode ([M-H]⁻), **ODN10** in positive mode ([M+H]⁺). DNA sequence: 5'-GC AGT GAA GGC* TGA GCT CC-3', C* = N4-PHOX-appended 2'-deoxycytidine.

While MALDI mass spectrometry was found unsuitable for the direct detection of phosphine conjugates, ESI-MS analysis gave in the only one case attempted (**ODN9**) the main peak corresponding to the non-oxidized phosphine, indicating that this technique might be suitable for the characterization of phosphine-DNA species without the need of sulfur treatment (Figure 3.11).

DNA-phosphine conjugates **ODN6-11a** are generally air sensitive and must be manipulated under oxygen-free conditions, as commonly done with phosphine ligands. Nevertheless, the observed rates of oxidation are notably different, depending on the attached ligand. The relative stabilities and the conditions under which these conjugates could be handled were investigated by an HPLC assay. Oligonucleotides **ODN6**, **ODN9**, **ODN10** and **ODN11a** were isolated by HPLC, the eluates stored at room temperature for 1 h under argon, and then re-analyzed by HPLC. This allowed measuring the extent of oxidation caused by oxygen dissolved in the HPLC solvents from the very moment after their isolation. Oligomers **ODN6** and **ODN9** showed disappointingly low stabilities, yielding large amounts of fully oxidized species (60 and 90%, respectively). In contrast, **ODN10** and **ODN11a** were found to be stable under these conditions, giving <10% of oxidized product in case of **ODN10** and no detectable amount for **ODN11a** (Figure 3.10 B). These results demonstrate that the stability of the DNA-appended BINAP and PHOX conjugates, **ODN10** and **ODN11a**, respectively, is high enough to allow manipulations of such conjugates even under suboptimal conditions, e.g., outside a glove box.

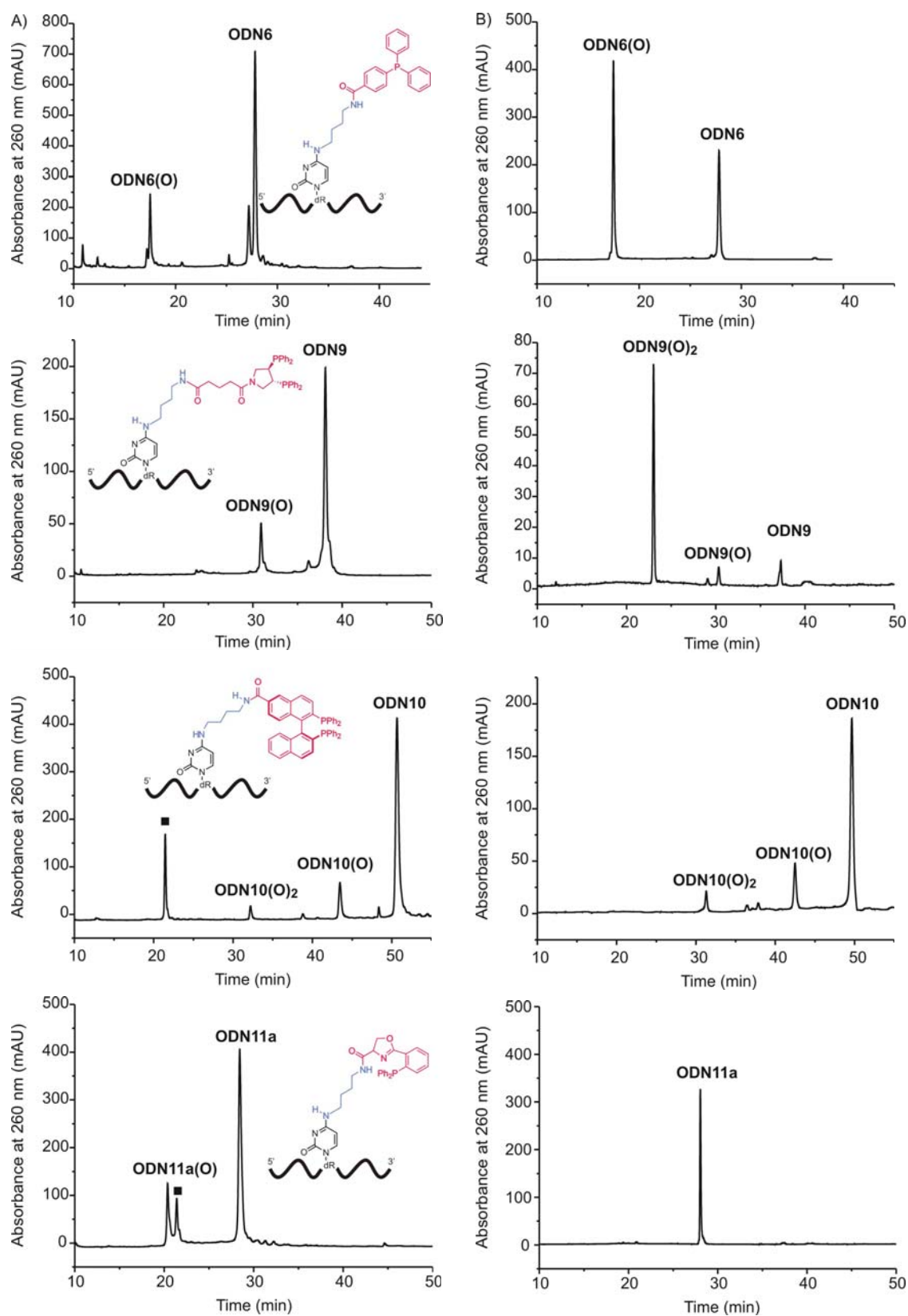


Figure 3.10. HPLC chromatograms of the phosphine and phosphinoxazoline derivatized DNA conjugates **ODN6**, **ODN9**, **ODN10** and **ODN11a**. A) Crude product after chloroform extraction and ethanol precipitation. ■ Trace impurity from the starting material **ODN1a**. B) HPLC purified product, after 1 h at r.t.

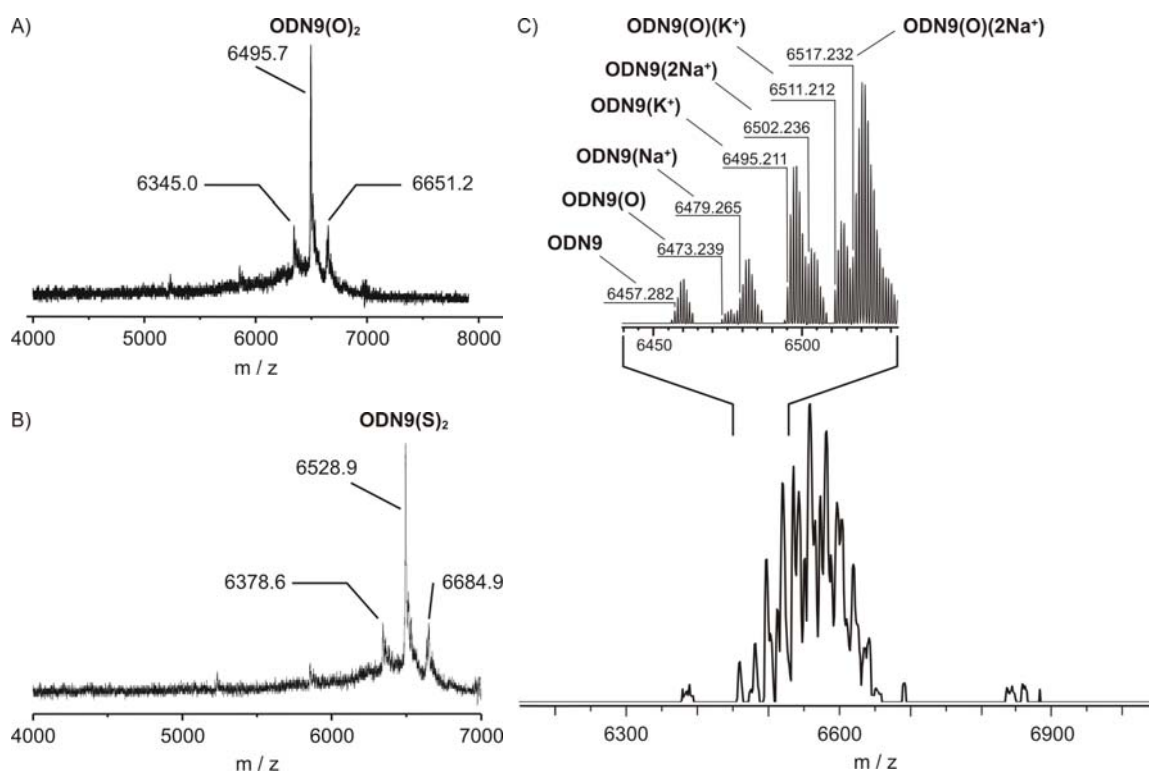


Figure 3.11. Mass spectrometry analysis of **ODN9**. A) MALDI-TOF spectrum of **ODN9(O)₂** (HPLC isolated **ODN9**). B) MALDI-TOF spectrum of **ODN9(S)₂**. C) ESI MS spectrum (part of the deconvoluted spectrum) of **ODN9** (measured: 6457.28, calculated: 6457.27).

The stability of DNA-tethered BINAP and PHOX ligands makes them attractive precursors for the development of metal-containing oligonucleotides. Moreover, we chose to generate a series of DNA-based phosphinoxazoline ligands with variable spacer length to ensure a reasonably large spectrum of DNA-transition metal interactions.

Beside the four-carbon linker (**ODN1a**) employed so far for DNA ligand attachment, two more flexible linkers were chosen, namely a short two-carbon tether (**ODN1b**) and a 13-atom spacer (**ODN1c**), respectively (Table 3.1). Amino-modified oligonucleotides **ODN1b** and **ODN1c** were then reacted with the phosphinoxazoline derivative **L6** (Scheme 3.4), yielding 58% and 75% **ODN11b** and **ODN11c** respectively, and below 10% oxidized products (Figure 3.12). In case of **ODN11b**, the observed conversion was lower (71%) compared to **ODN11c** (94%), likely due certain steric hindrance caused by the shorter linker used for functionalization.

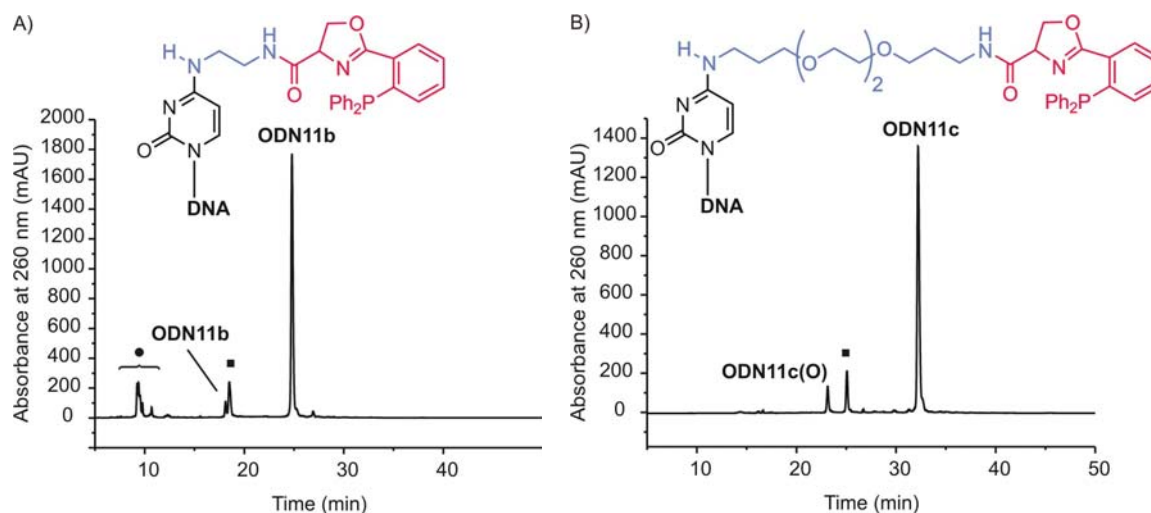


Figure 3.12. HPLC chromatogram of **ODN11b** and **ODN11c** pre-purified by chloroform extraction and ethanol precipitation to remove the excess of coupling reagents. ■ Trace impurity from the starting material **ODN1b** and **ODN1c** respectively. ● Trace amounts of unreacted starting material ($t_R = 8.9$ min) and degradation products (for HPLC conditions see Materials and Methods, Chapter 5.5.1)

It is reasonable to think that the most useful tethers for attaching metal complexes are relatively short since a short tether permits more stereoselective control of the DNA scaffold. In our amino-modified oligonucleotides strategy, the two-carbon tether was the shortest tether that could be introduced to provide reactive amine functional groups for subsequent derivatization. A long tether might also prove beneficial for achieving enough flexibility to reach catalytic pockets in applications involving DNA/RNA (pool) hybrids (Figure 3.2) and *in vitro* selection. However, for a rational design approach, it would be rather difficult to predict the influence of long tethers on the transfer of chirality from the DNA to the metal centre. For example, long spacers may provide too little interaction between the DNA and the transition metal complex appended onto the tether. In addition, a long tether may introduce too much flexibility into the DNA, thereby precluding the goal of a structural constraint.

3.1.2.5 Duplex Stability of Bisphosphine-Tethered DNA

Although it has been generally assumed that further derivatization of N4-alkyl-dC residues does not interfere with formation of B-form duplex DNA, several factors, such as steric effects, may still influence the relative stability of the modified oligonucleotides. For example, the presence of large aromatic ligands in the major groove might cause a destabilization effect by repelling water molecules and bound

small cations. However, the introduction of a positively charged metal complex is expected to cancel this effect and to electrostatically stabilize the duplex.^[234]

The PYRPHOS-appended DNA **ODN9** was tested in its ability to form duplexes with complementary **cDNA1** and **cRNA1**, as it would be later required according to its use in the selection scheme (Figure 3.1).

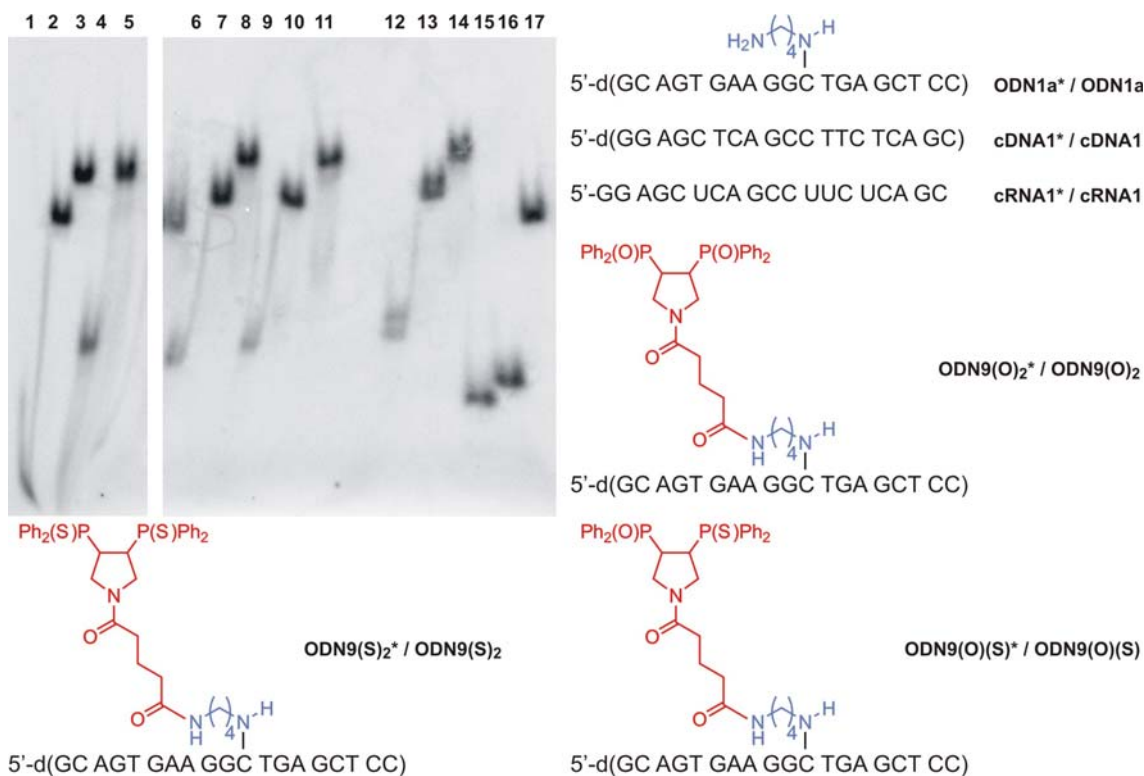


Figure 3.13. Native PAGE showing the formation of duplexes between PYRPHOS-appended DNA **ODN1a** and complementary **cDNA1** or **cRNA1**. Asterisks indicate the presence of a radioactive ³²P label at the 5'-end of the oligonucleotides. From left to right: Lane 1 - **ODN1a***; lane 2 - **ODN1a*/cDNA1**; lane 3 - **ODN1a*/cRNA1**; lane 4 - **cRNA1***; lane 5 - **ODN1a/cRNA1***; lane 6 - **ODN9(O)₂***; lane 7 - **ODN9(O)₂*/cDNA1**; lane 8 - **ODN9(O)₂*/cRNA1**; lane 9 - **ODN9(S)₂***; lane 10 - **ODN9(S)₂*/cDNA1**; lane 11 - **ODN9(S)₂*/cRNA1**; lane 12 - **ODN9(O)(S)***; lane 13 - **ODN9(O)(S)*/cDNA1**; lane 14 - **ODN9(O)(S)*/cRNA1**; lane 15 - **ODN1a***; lane 16 - **cDNA1***; lane 17 - **ODN1a*/cDNA1**. Hybridization buffer: 100 mM HEPES pH 7.5, 200 mM NaCl, 1 mM EDTA.

The hybridization experiments were conducted with only one of the two oligonucleotides 5'-³²P-labelled, using standard denaturation/reannealing cycles (see Materials and Methods, Chapter 5.8.3). As reference, the amino-modified **ODN1a** was used. Due to the fact that all manipulations had to be carried out in air, the bisoxide, bisulfide and monoxide-monosulfide analogues, **ODN9(O)₂**, **ODN9(S)₂**, and **ODN9(O)(S)** respectively, were used as replacement for **ODN9** to avoid mixtures of non-oxidized, partially and fully oxidized products. The formation of duplexes was

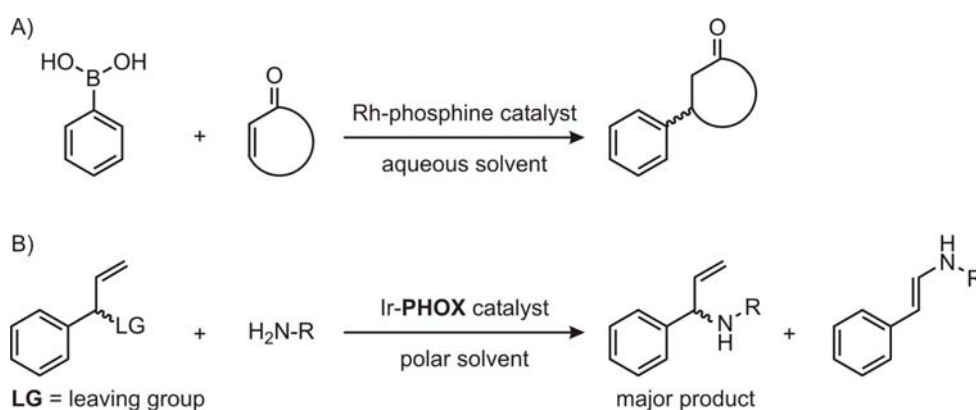
controlled by native 16% PAGE (Figure 3.13).

The results of these experiments clearly show that attachment of the ligand does not prevent the formation of duplexes. In all cases the hybridization appears to be quantitative under the conditions employed.

3.2 Organometallic Transformations in Water

Together with synthetic approaches for the incorporation of chelating functionalities and, subsequently, of transition metal centres at well-defined positions in DNA or RNA sequences, appropriate model reactions for the use of nucleic acid-based ligands are also required.

Most organometallic transformations have been traditionally conducted in polar or nonpolar organic solvents. Water has been less used either because of sensitivity of organometallic catalysts to water, or because most organic compounds are not easily soluble in water. The observations of reaction rate enhancement as well as the possibility of achieving new selectivities in water led to an increased interest in exploring the properties of water in organometallic-catalyzed reactions.^[272-274] A number of homogeneous transition metal-catalyzed reactions, such as rhodium(I)-catalyzed hydrogenation, palladium(II)-catalyzed amination, rhodium(I)-catalyzed 1,4-addition, copper(II)-catalyzed Diels-Alder cycloaddition, and aldol condensation have been successfully carried out in aqueous mixtures, and mainly in the presence of water soluble phosphorus ligands.^[274] However, a clear understanding of the nature of the interactions occurring in aqueous media has still to be worked out.



Scheme 3.6. A) Rhodium(I)-catalyzed 1,4-conjugate addition of phenylboronic acid to α,β -unsaturated ketones. B) Iridium(I)-catalyzed allylic amination.

The reactions we selected as model systems for the development of nucleic acid based hybrid catalyst were: rhodium(I)-catalyzed 1,4-addition of boronic acids to α,β -unsaturated carbonyl compounds and iridium(I)-catalyzed allylic amination (Scheme 3.6), because of their compatibility with the aqueous environment. Preliminary studies were devised using these model reactions to study the catalytic competence of the new DNA-phosphine and phosphinoxazoline ligands **ODN9-11**.

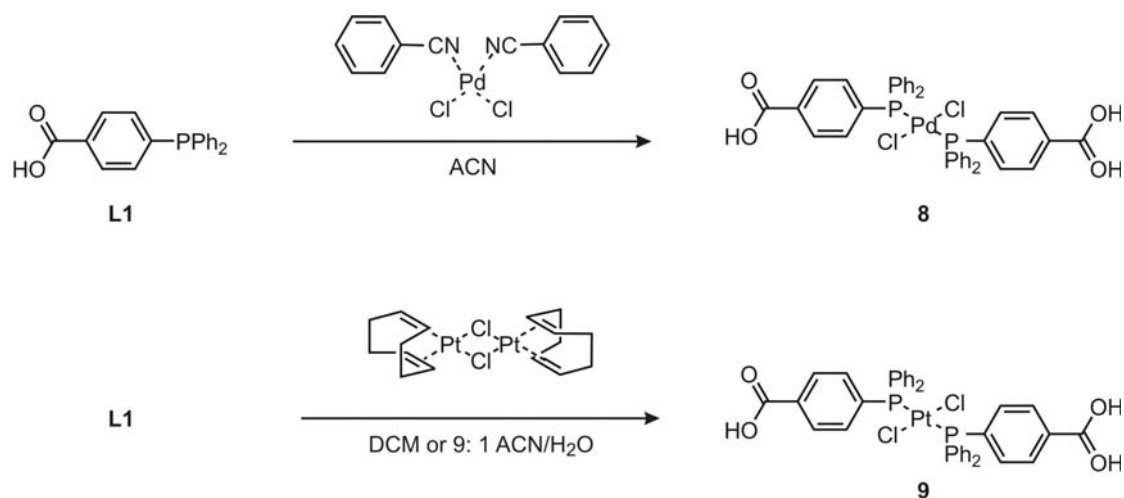
3.2.1 Phosphine- and Phosphinoxazoline-Metal Complexes

Phosphine and phosphinoxazoline-metal complexes were prepared using various transition metal precursors and standard synthetic procedures. Preliminary assays concerning the synthesis and behaviour of such complexes in the presence of water were conducted to demonstrate whether such catalysts could be formed and were stable enough under these conditions. In addition, maintaining anaerobic conditions during handling air-sensitive phosphine ligands and metal complexes thereof in small reaction volumes (as required by the use of nucleic acids), in an adequate reaction setup and outside a glove box is not trivial. The standard Schlenk techniques and degassing of reaction mixtures were found sufficient to avoid air contamination even in reduced scale reactions (*e.g.*, <100 μL).

The first control experiments involved the monophosphine ligand **L1**. Reaction of palladium(II) $\text{PdCl}_2(\text{PhCN})_2$ with **L1** in neat acetonitrile led to the formation of complex $\text{PdCl}_2(\text{L1})_2$ (**8**) (Scheme 3.7), showing a singlet in the ^{31}P NMR spectrum ($\text{DMSO-}d_6$, $\delta = 24.6$ ppm). Also, a single complex (**9**) was obtained when **L1** was reacted with $[\text{Pt}(\text{cod})\text{Cl}]_2$ in neat dichloromethane (Scheme 3.7), showing a singlet in the ^{31}P NMR spectrum at $\delta = 14.3$ ppm (CD_3OD), with platinum-phosphine coupling (satellite $J_{\text{Pt,P}} = 1852$ Hz) characteristic of a trans complex.^[201] When the same complex was formed in aqueous mixture 93:7 acetonitrile/ H_2O - likely suitable conditions to prepare DNA-metal complexes - the ^{31}P NMR spectrum showed a singlet at $\delta = 18.4$ ppm ($\text{DMSO-}d_6$) indicative for phosphorus-platinum coordination.

The palladium and platinum complexes were formed quantitatively and no oxidized products were observed. Moreover, the interaction between the phosphine **L1** and the solvent appeared to remain unchanged in water. The platinum complex **9** could be

easily prepared in water and was stable under the conditions employed.



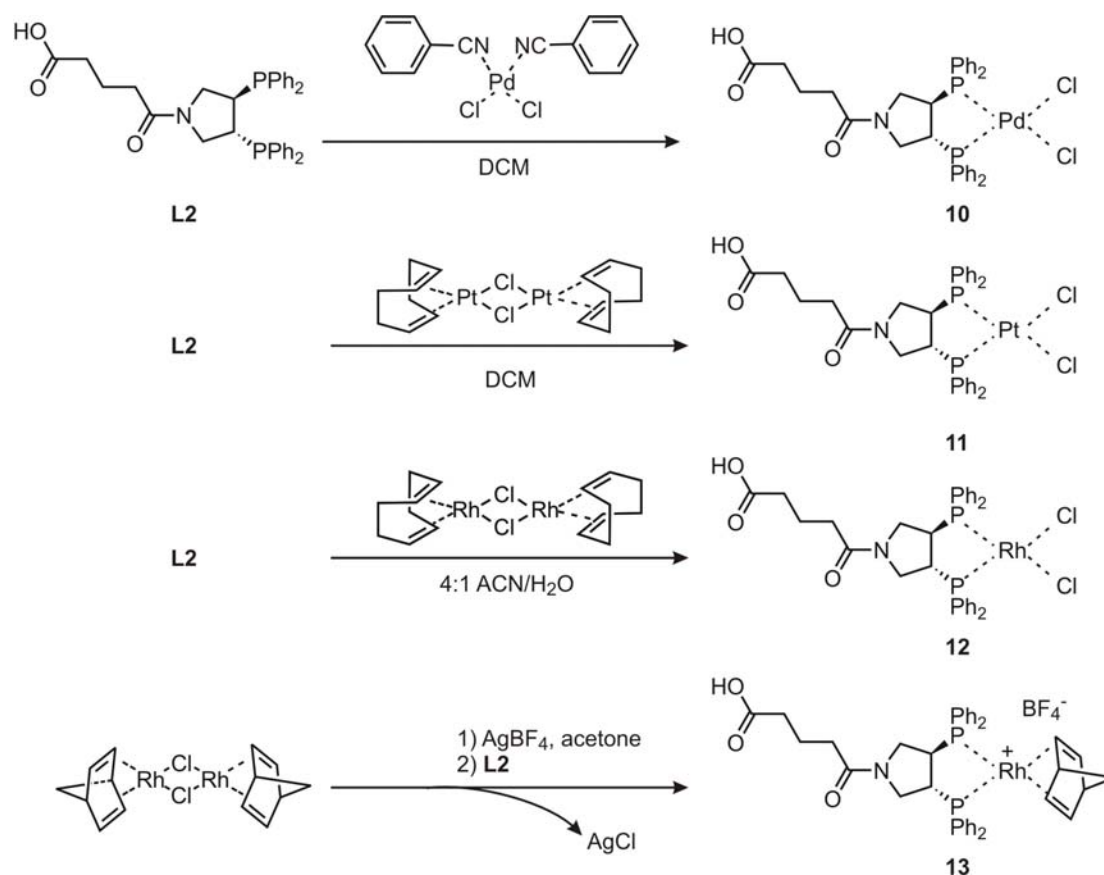
Scheme 3.7. Synthesis of palladium(II)- and platinum(II)-L1 complexes.

The PYRPHOS ligand **L2** was first treated with one equivalent of $\text{PdCl}_2(\text{PhCN})_2$ or half equivalent of $[\text{Pt}(\text{cod})\text{Cl}]_2$ per bisphosphine unit, at ambient temperature in neat dichloromethane to afford palladium(II) or platinum(II) complexes **10** and **11** (Scheme 3.8). The complex formation was monitored by ^{31}P NMR spectroscopy. The ^{31}P NMR spectra demonstrated the absence of unreacted PYRPHOS after the complete conversion and displayed a single coordination-shifted resonance at $\delta = 42.6$ ppm ($\text{DMSO}-d_6$) and 26.4 ppm (CD_3OD) for **10** and **11** respectively ($\delta = -11.0$ to -12.2 for the non-metallated phosphine.^[18] For complex **11** the platinum-phosphorus coupling constant $J_{\text{Pt,P}} = 1163$ Hz corresponded to the expected range of such phosphine-platinum compounds. The absence of 1,5-cyclooctadiene and benzonitrile resonances in the ^1H NMR spectrum indicated that in both isolated complexes the coordination sites were likely occupied by chlorine atoms.

The binding capability of PYRPHOS ligand **L2** was also investigated in aqueous solvent. Stirring **L2** with $[\text{Rh}(\text{cod})\text{Cl}]_2$ (one equivalent bisphosphine per Rh) at room temperature, in 40% water with acetonitrile cosolvent, gave the metallated complex **12** (Scheme 3.8). The complete reaction was confirmed by the ^{31}P NMR spectrum. The resonance of the free phosphine unit was shifted to lower field (ABX system^[18]; CD_3OD , $\delta_{\text{A}} = 38.2$ ppm, $\delta_{\text{B}} = 36.8$ ppm) due to the metal complexation. The signal splitting was attributed to $\text{Rh}(I = 1/2)/\text{P}$ coupling. The $J_{\text{Rh,P}}$ constants of 150 and 153 Hz are within the expected range for such phosphinerhodium compounds.

To further investigate the stability of rhodium(I)-PYRPHOS complex towards air and

aqueous media, complex **13** was prepared using $\text{Rh}(\text{nbd})\text{BF}_4$ as metal precursor. This precursor was generated from $[\text{Rh}(\text{nbd})\text{Cl}]_2$ and AgBF_4 in acetone (Scheme 3.8) followed by removal of the precipitated AgCl . The resulting complex $[\text{Rh}(\text{L2})(\text{nbd})]^+\text{BF}_4^-$ was analyzed by ^1H and ^{31}P NMR. The NMR spectra confirmed the desired metal complex (Acetone- d_6 , P resonances: $\delta_{\text{A}} = 36.9$ ppm, $\delta_{\text{B}} = 35.6$ ppm).



Scheme 3.8. Synthesis of palladium(II), platinum(II) and rhodium(I)-L2 complexes.

The complex **13** was immediately dissolved in acetonitrile and analyzed by ESI mass spectrometry. In this case, the base peak corresponds to a complex without norbornadiene ligand (Figure 3.14 A). Instead, two solvent molecules seem to coordinate the metal. An additional peak could be assigned to oxidized species. Other signals could not be attributed so far. A certain level of decomposition of the Rh(I) complex **13** was observed after one week storage in acetonitrile, at room temperature and air. However, under these conditions, the main compound still formed the most abundant signal (Figure 3.14 B).

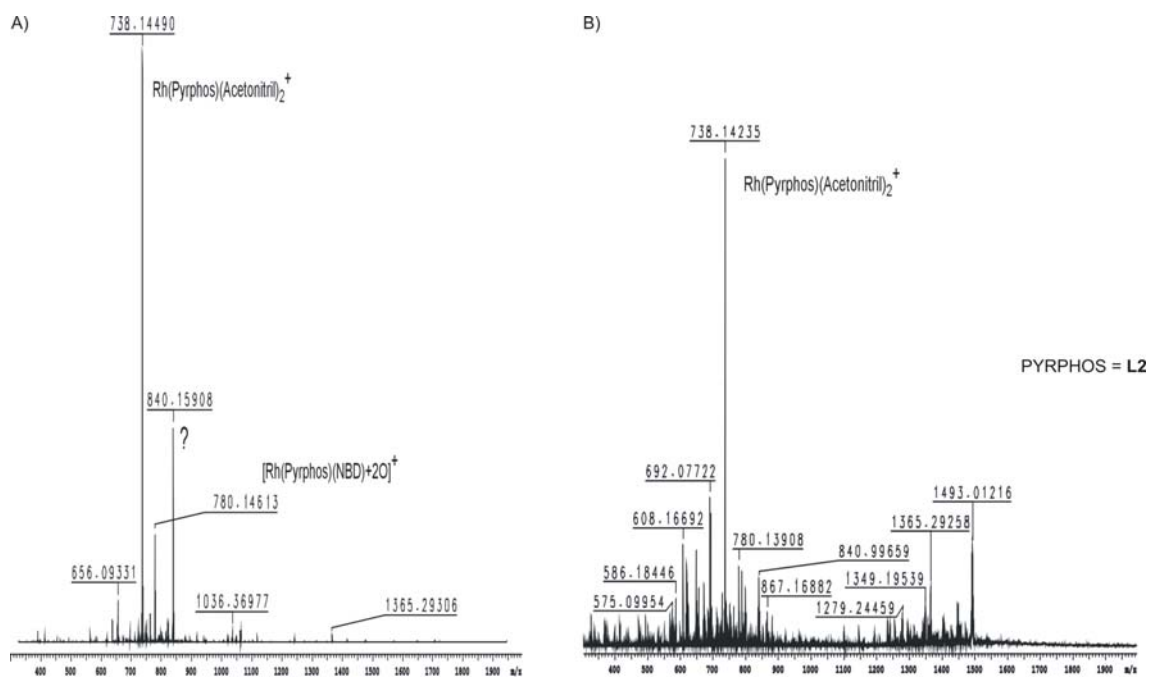


Figure 3.14. ESI MS spectrum of complex **13**: A) in acetonitrile, immediately sprayed; B) sprayed after one week storage in acetonitrile at ambient temperature and air.

To verify the hypothesis of solvent molecules as ligands instead of norbornadiene, two other solvents were tested. Firstly, the complex was dissolved in acetone. After storage for one week at room temperature and air, the solution was analyzed by ESI MS (Figure 3.15 A). In this case, the base peak is due to a Rh-complex similar to the one observed in acetonitrile: $\text{Rh}(\mathbf{L2})(\text{acetone})_2^+$ (m/z : calcd. 772.18, obsd. 772.17). Three other signals could be readily assigned: $\text{Rh}(\mathbf{L2})(\text{acetone})^+$ (m/z : calcd. 714.14, obsd. 714.13), $\text{Rh}(\mathbf{L2})^+$ (m/z : calcd. 656.10, obsd. 656.09) and $\text{Rh}(\mathbf{L2})(\text{water})^+$ (m/z calcd. 674.11, obsd. 674.10). Unlike the spectrum recorded in acetonitrile (inhomogeneous solution), the impurities containing the oxidized species showed higher intensities. When the Rh-complex was dissolved in methanol and immediately sprayed, the results were similar to the acetone solution, the coordinated solvent molecules being now methanol (Figure 3.15 B).

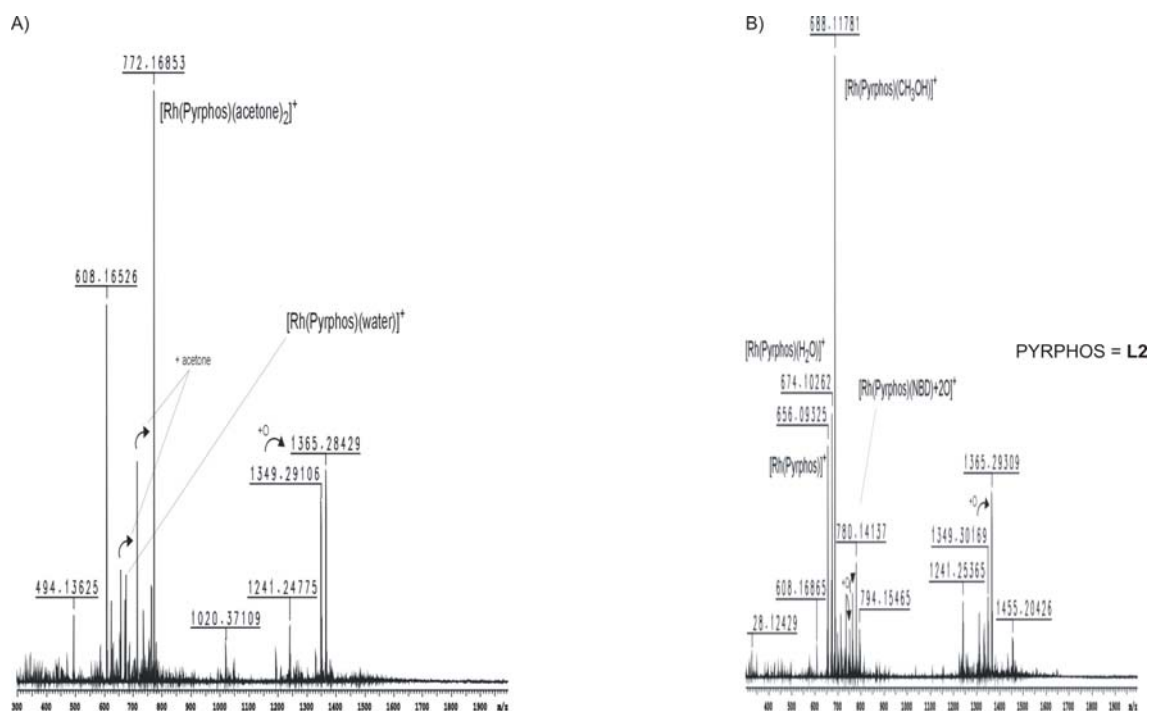


Figure 3.15. ESI MS spectrum of complex **12**: A) sprayed after one week storage in acetone at ambient temperature and air; B) in methanol, immediately sprayed.

Finally, the CID-MS/MS of the isolated ion m/z 772.17 sprayed from acetone was recorded to give additional evidence for the formation of Rh(I)-PYRPHOS complex, and, implicitly, $\text{Rh}(\text{L2})(\text{acetone})_2^+$ species. The observed pattern perfectly matched the expectations and two acetone molecules were sequentially lost (Figure 3.16).

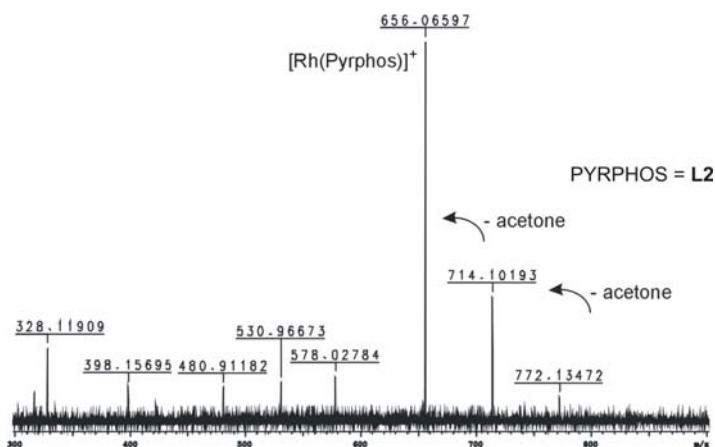
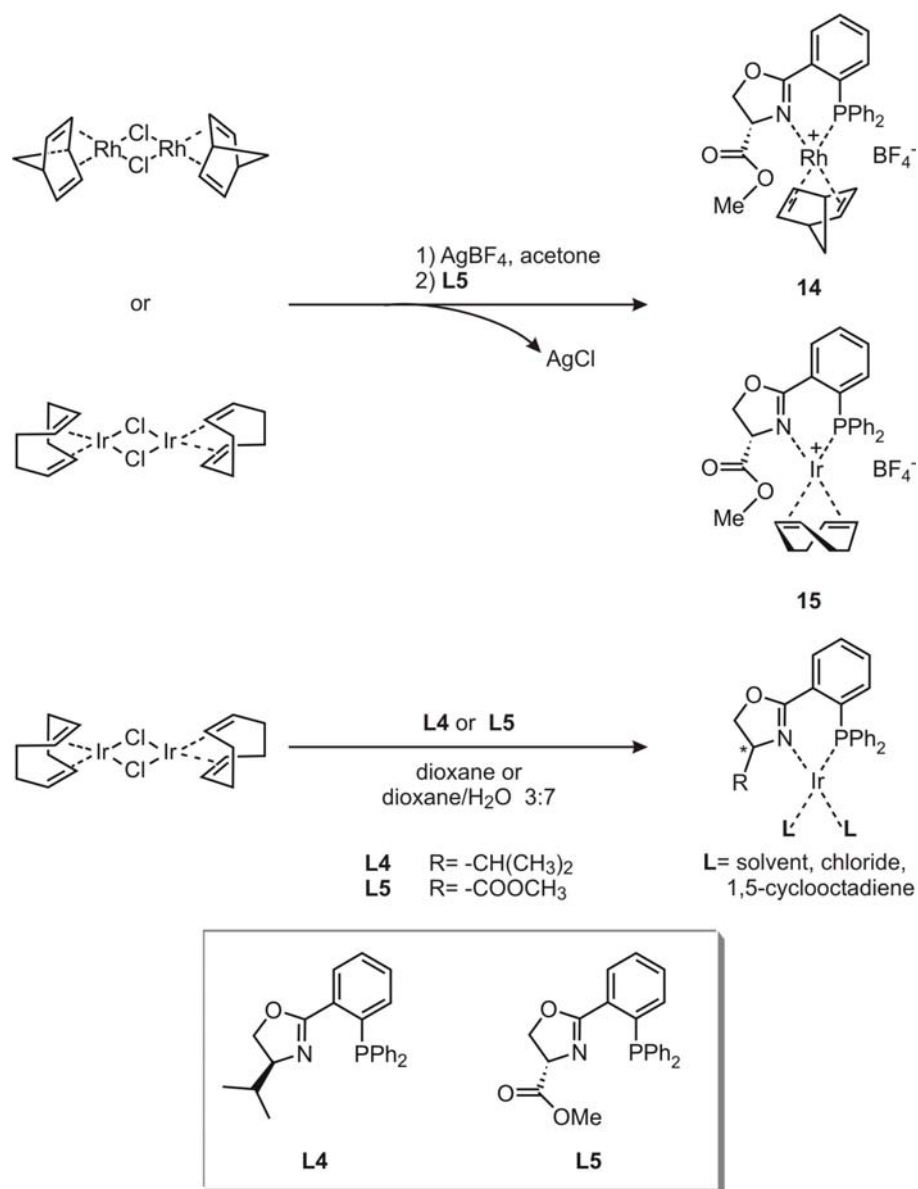


Figure 3.16. CID-MS/MS spectrum of $\text{Rh}(\text{L2})(\text{acetone})_2^+$.

In conclusion, the rhodium(I)-PYRPHOS complex can be analyzed by ESI-MS in acetone and in acetonitrile. The proposed cation structure $\text{Rh}(\text{L2})(\text{nb})^+$ could not be

confirmed. No norbornadiene ligand was found attached to the rhodium centre. Instead, up to two solvent molecules, either acetone or acetonitrile or methanol or water were coordinated. Norbornadiene as ligand was observed only in complexes with partially oxidized **L2**. These results could indicate that **L2** binds to rhodium not only via the phosphorus atoms, but also with one or two carbonyl groups. In all cases, significant amounts of degradation were observed after one week in solution at room temperature and in air, but in each case, the original compound was stable enough to still be detectable without difficulties.

It was also interesting to investigate the stability of phosphinooxazoline-based complexes against oxidation. Control experiments in organic solvent were initially carried out. For solubility reasons, we chose to evaluate metallation of phosphinooxazoline **L5** which contains a methylester functionality (Scheme 3.9), instead of the **L6** carboxylate analogue. Reaction of the complex $[\text{Rh}(\text{nbd})\text{Cl}]_2$ with AgBF_4 in acetone proceeded with cleavage of the chloride bridges, followed by exchange of the chloride ion with BF_4^- to give the monomeric precursor $\text{Rh}(\text{nbd})\text{BF}_4$. Reaction with one equivalent **L5** yielded the compound $[\text{Rh}(\text{L5})(\text{nbd})]^+\text{BF}_4^-$ **14** (Scheme 3.9) as confirmed by ESI mass spectrometry (m/z : calcd. 584.09, obsd. 584.09), and no additional (oxidation) byproducts were observed. Also according to ^{31}P NMR of the isolated complex, only one product was formed. The coordination of the phosphorus donor atom to the rhodium was evident due to the characteristic downfield shift of the phosphorus resonance $\delta = 31.9$ compared to -4.8 ppm (CDCl_3) of the free **L5**. The iridium(I) complex **15** was prepared in a similar way starting from $[\text{Ir}(\text{cod})\text{Cl}]_2$ (Scheme 3.9). Also in this case, the desired complex $[\text{Ir}(\text{L5})(\text{cod})]^+\text{BF}_4^-$ was obtained as demonstrated by ^{31}P NMR analysis (CDCl_3 $\delta = 14.8$). Both complexes were stable against air and moisture and could be easily handled in the laboratory atmosphere. The isolated solid products are fine powders, and our attempts to grow crystals have been fruitless to date.



Scheme 3.9. Synthesis of rhodium(I) and iridium(I)-**L4/L5** complexes.

We next attempted the formation of iridium(I) complexes in aqueous media, using the well-described, commercially available compound **L4** in comparison with our ligand **L5** (Scheme 3.9). Control experiments were also performed in neat organic solvent. Both ligands were dissolved in either neat dioxane or 3:7 dioxane/water. After addition of $[\text{Ir}(\text{cod})\text{Cl}]_2$ (0.1 mM final concentration of Ir-complex, as later used in catalytic attempts), the metallation was complete within seconds, as was evident from the change of color from orange-yellow to dark red, and monitored by ^{31}P NMR spectroscopy. In most of the cases the ^{31}P NMR spectrum indicated the presence of single species. The observed phosphorus resonances were in good agreement with those reported in

literature for similar Ir(I)-PHOX complexes in neat organic solvents:^[275, 276] 10.3 ppm (dioxane, 10% CDCl₃) and 15.7, 15.6 ppm (3:7 dioxane/water, 10% D₂O) for **L4**, and 8.8 ppm (dioxane, 10% CDCl₃) and 15.2 ppm (3:7 dioxane/water, 10% D₂O) for **L5**, respectively (Figure 3.17).

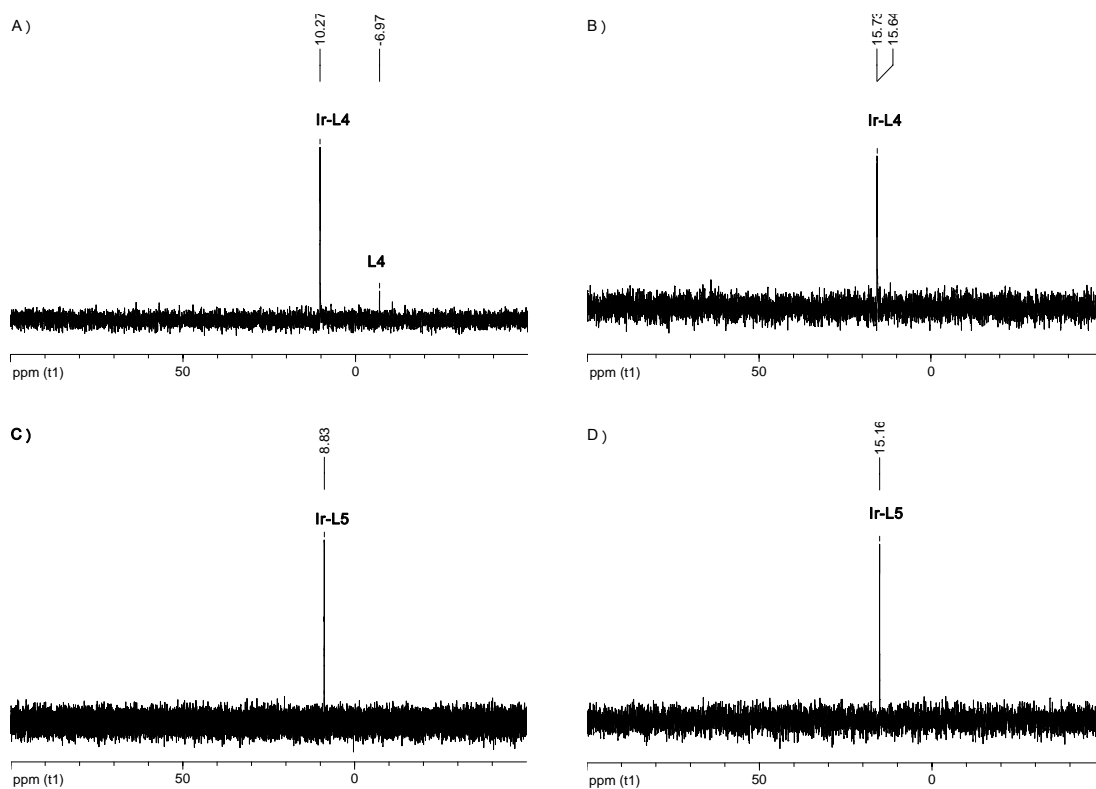


Figure 3.17. ³¹P NMR spectra of iridium(I)-phosphinoxazoline complexes showing phosphorus metallation: A) Ir-**L4** in dioxane, B) Ir-**L4** in 3:7 dioxane/water, C) Ir-**L5** in dioxane, D) Ir-**L5** in 3:7 dioxane/water.

Phosphinoxazoline complexes of Ir(I) have not been so far characterized in the presence of water. Moreover, catalytic applications of such complexes in aqueous environment have not been reported until now. Our preliminary analyses provide useful information about the metallation process in water, although additional work has to be done to elucidate the role of the solvent in coordination and interaction with the metal centre.

These studies concerning the synthesis and stability of phosphine and phosphinoxazoline complexes in aqueous media supports the hypothesis that such complexes are reasonably stable and suitable for organometallic asymmetric reactions performed in the presence of water.

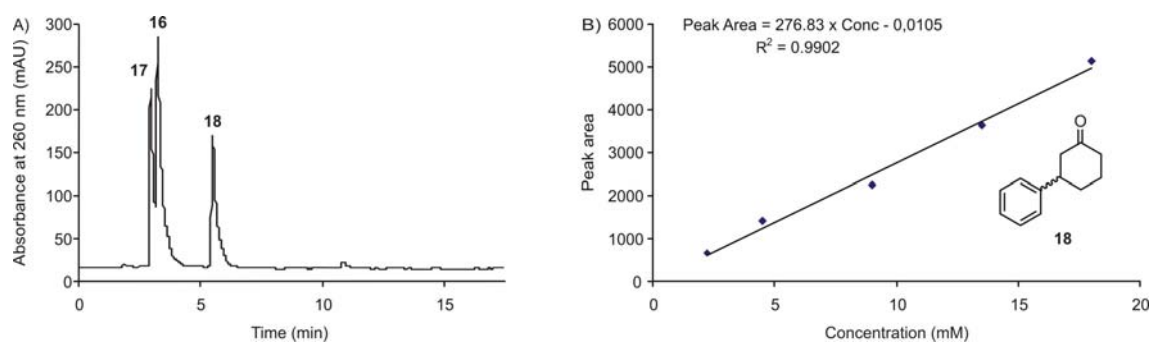


Figure 3.18. A) Reversed-phase HPLC analysis of 1,4-addition of phenylboronic acid **16** to 2-cyclohexen-1-one **17** (Elution: 30% water, 70% acetonitrile; $t_R(\mathbf{17}) = 3.0$ min, $t_R(\mathbf{16}) = 3.3$ min, $t_R(\mathbf{18}) = 5.1$ min). B) Calibration curve with 3-phenyl-1-cyclohexanone product **18**.

Initial studies were focused on the optimization of reaction conditions, including temperature, solvent, phosphorus ligands and Rh-complexes thereof (Figure 3.19), for carrying out addition of phenylboronic acid **16** to 2-cyclohexen-1-one **17** to obtain 3-phenyl-1-cyclohexanone **18**.

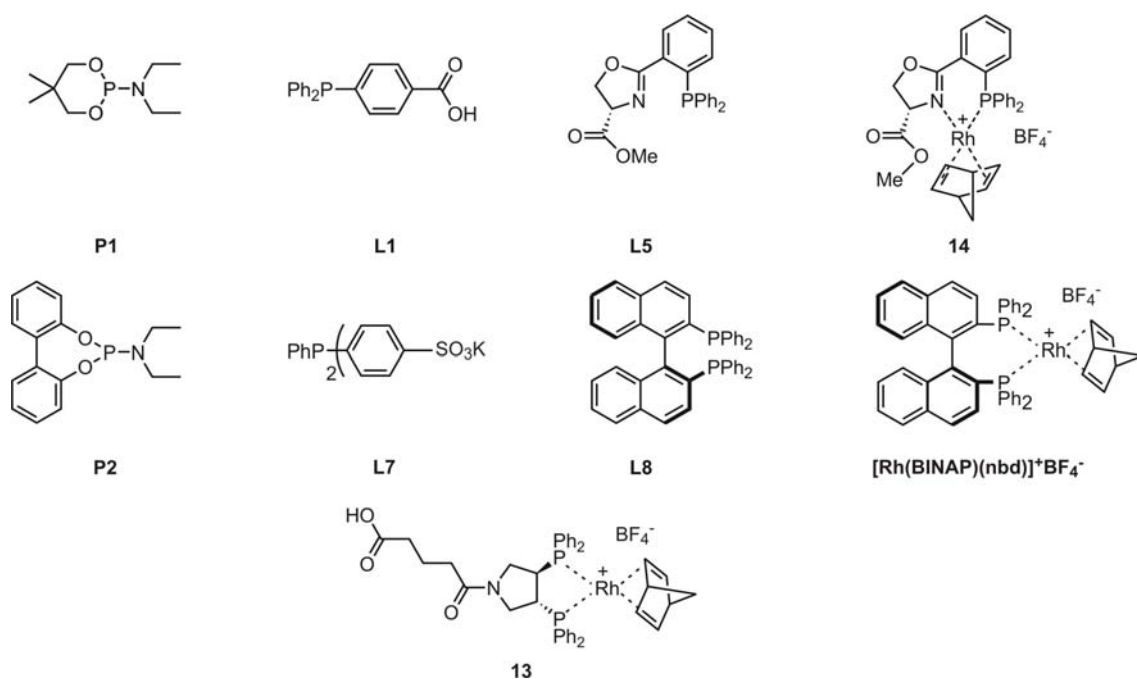


Figure 3.19. Phosphorus-based ligands and Rh(I) complexes screened for activity in 1,4-addition reaction.

The phosphoramidites **P1** and **P2** were screened initially, under standard reaction conditions,^[252] in 10:1 dioxane/water, using 1.5 mol% [Rh(cod)Cl]₂ and 7.5 mol% of ligands (Rh/L= 1:2.5), without basic additives. The reaction was also performed under increased concentration of water at room temperature for 24-72 hours. All experiments

were carried out under argon atmosphere without pre-degassing the solvents and reagents. A few selected results are presented in Table 3.4.

Table 3.4. Rh-catalyzed conjugate addition of arylboronic acid **16** to 2-cyclohexen-1-one **17** with phosphoramidite **P1** and **P2** ligands.

Entry	Ligand	Dioxane/water	Temp. [°C]	Time [h]	Conversion ^[c] [%]
1	P1	10:1	60	2	80%
2	P1	1:5	60	24	70%
3	-	1:10	rt	24	<5%
4	P1	1:10	rt	72	20%
5	P2	1:10	rt	24	<5%
6 ^[b]	P1	1:10	rt	72	<5%

[a] Reaction conditions: 0.08 mmol **17**, 0.25 mmol **16** (3.0 equiv - excess due to competitive hydrolysis), 3 mol% catalyst loading, 2.2 mL reaction volume. [b] 0.5 mol% [Rh] catalyst loading. [c] The conversions were estimated by ¹H NMR analysis with *i*-propanol as internal standard (entries 1-2 and 4-6) and by thin-layer chromatography (entry 3).

In general, the catalysts were efficient when the reaction was carried out at 60°C in 10:1 or 1:5 dioxane/water (70-80% conversion) (Table 3.4, entries 1-2), while at room temperature and 1:10 dioxane/water the conversion dropped dramatically even after long reaction times (Table 3.4, entries 4-5). Moreover, the catalyst precursor [Rh(cod)Cl]₂ was found almost inactive (Table 3.4, entry 3), although, under the conditions employed by Miyaura *et al.*, the same catalyst showed high reactivity.^[278] In a parallel test reaction, the Rh catalyst loading was reduced to 0.5 mol%, and after 72 hours reaction time only trace amount of product was formed (Table 3.4, entry 6).

Surprisingly, biphenolic phosphoramidite **P2** seemed to be less active than the **P1** ligand, although structurally related ligands have been reported as efficient systems in similar transformations, albeit in 10:1 dioxane/water.^[89] The reduced yields could be explained by the fact that the Rh-phosphoramidite catalysts were generated *in situ* in 1:10 dioxane/water mixtures, where ligand hydrolysis might compete in a higher extent with metal complex formation. In addition, under these conditions, the system became heterogeneous, making the results unreproducible. However, in the absence of the base, high temperature appeared to be absolutely necessary for achieving good conversions. Prolonging the reaction time did not improve the yields due to the competitive hydrolytic deboronation of arylboronic acids with water (Table 3.4, entry 4 versus 3 and 5).

For homogeneity reasons we chose to attempt 1,4-addition with water-soluble phosphine ligands.^[279] Rhodium complex [Rh(cod)Cl]₂ was combined with the

commercially available phosphine ligand TPPDS **L7** (0.38 mol % catalyst) 1:10 dioxane/water mixture and reacted with **17**, 2.5 equivalents of phenylboronic acid **16**, and 2.1 equivalents of K_2CO_3 at 37°C for 48 hours. To prevent hydrolytic deboronation of **16** to unreactive benzene, a phase transfer reagent, *i.e.* sodiumdodecyl sulfate (SDS, 0.5 equivalent), was added to the reaction mixture.^[279] As alternative to aqueous solution of K_2CO_3 , Tris buffer (20 mM, pH 8.0) was used instead. The same reaction conditions were also employed only with $[Rh(cod)Cl]_2$ precursor. In parallel, 1,4-addition reaction was conducted with monophosphine **L1** ligand, under reduced concentration of organic solvent, *i.e.* 1:1 dioxane/water and 1:1 methanol/water, at 50° and with 3.85 mol% catalyst loading. The results are illustrated in Table 3.5.

Table 3.5. Rh-catalyzed conjugate addition of arylboronic acid **16** to 2-cyclohexen-1-one **17** with monophosphines **L1** and **L7**.^[a]

Entry	Ligand	Solvent	Base	Phase transfer reagent	Temp. [°C]	Time [h]	Conversion ^[c] [%]
1	L7	dioxane/water 1:10	-	-	37	48	<1
2	L7		-	SDS	37	48	<1
3	L7		K_2CO_3	SDS	37	48	10
4	-		Tris	SDS	37	48	41
5	L7		Tris	SDS	37	48	7
6 ^[b]	L1	dioxane/water 1:1	-	SDS	50	19	3
7 ^[b]	L1	methanol/water 1:1	-	SDS	50	19	1

[a] Reaction conditions: 0.52 mmol **17**, 1.3 mmol **16** (2.5 equiv), 0.38 mol% catalyst loading, 2.2 mL reaction volume. [b] 3.85 mol% [Rh] catalyst loading. [c] The conversions were determined by reversed-phase HPLC (elution: 30% water, 70% acetonitrile), using the calibration curve showed in Figure 3.18 B.

The best results were obtained with $[Rh(cod)Cl]_2$ which gave **18** in 41% yield (Table 3.5, entry 4). The fairly high activity of the Rh catalyst in 91% water might be explained by the basic conditions provided by K_2CO_3 and also by reduced competitive hydrolytic deboronation due to the presence of SDS. However these additives appeared to be inefficient in combination with Rh-phosphine complexes. Although the Rh-TPPDS complex was highly reactive in 1,4-addition reactions in neat water,^[279] in our case, the addition of organic cosolvent (9-50%) with the sulfonated phosphine ligand **L7** or with triphenylphosphine **L1** resulted in almost no reaction after 48 hours (Table 3.5, entries 4 and 5-7).

Literature data on Rh(I)-catalyzed addition of phenylboronic acids to olefins in the presence of sulfonated ligands or triphenylphosphine showed that the use of cosolvents or neat organic solvents with such ligands resulted in very low conversions.^[279] In these systems, the reactivity could be restored by changing to 100% aqueous environment.

However, such conditions would not be appropriate for our system due to the poor solubility of the product and substrates.

Finally, we attempted 1,4-addition reactions with Rh-bisphosphine complexes **13**, **14**, and $[\text{Rh}(\text{BINAP})(\text{nbd})]^+\text{BF}_4^-$ ^[250] (Figure 3.19) at 3 mol% catalysts loading, in 6:1 dioxane/water mixture. Using either $[\text{Rh}(\text{cod})\text{Cl}]_2$ precursor or the synthesized $[\text{Rh}(\text{BINAP})(\text{nbd})]^+\text{BF}_4^-$ complex, the observation of high activity in the presence of triethylamine was again confirmed by our experiments. Good conversions, 77 and 80% respectively, were obtained after 6 hours in the presence of one equivalent of triethylamine, while in its absence the product was formed only in 47% (Table 3.6, entries 2 and 6 versus 1). The $[\text{Rh}(\text{cod})\text{Cl}]_2$ precursor showed again high activity without additional ligand (Table 3.6, entries 1-2).

Table 3.6. Effect of oxygen-free conditions^[a], ligand and Rh-complex on the 1,4-addition of phenylboronic acid **16** to 2-cyclohexen-1-one **17**.^[b]

Entry	Rh(I) precursor	L	Isolated Rh(I)-complex	Base ^[c]	Solvent diox/H ₂ O	Temp [°C]	Time [h]	Conv ^[d] [%]
1	$[\text{Rh}(\text{cod})\text{Cl}]_2$	-	-	-	6:1	37	16	47
2	$[\text{Rh}(\text{cod})\text{Cl}]_2$	-	-	NaHCO ₃		37	16	47
3	-	-	13	TEA		rt	6	0
4	-	-	$[\text{Rh}(\text{L8})(\text{nbd})]^+\text{BF}_4^-$	-		rt	6	0
5	-	-	$[\text{Rh}(\text{L8})(\text{nbd})]^+\text{BF}_4^-$	TEA		rt	6	0
6	-	-	$[\text{Rh}(\text{L8})(\text{nbd})]^+\text{BF}_4^-$	TEA	6:1	rt	6	80
7	$[\text{Rh}(\text{nbd})\text{Cl}]_2$	L8	-	TEA		rt	19	12
8 ^[e]	-	-	14	TEA	3:7	rt	4	0
9 ^[e]	$[\text{Rh}(\text{C}_2\text{H}_4)\text{Cl}]_2$	L5	-	TEA		rt	4	0

[a] Reactions 1-5 were carried out under argon atmosphere with undegassed solvents and reagents. Reactions 6-9 were conducted under oxygen-free conditions. [b] Reaction conditions: 1.0 mmol **17**, 1.5 mmol **16** (1.5 equiv), 3 mol% catalyst loading, 3.5 mL reaction volume, unless otherwise stated. [c] 0.1 equiv NaHCO₃ or 1.0 equiv TEA. [d] Determined by reversed-phase HPLC analysis (elution: 30% water, 70% acetonitrile, $t_{\text{R}}(\text{18}) = 5.1$ min) with the calibration curve showed in Figure 3.18 B, unless otherwise stated. [e] Reaction conditions: 41.0 μmol **17**, 61.5 μmol **16** (1.5 equiv), 2.4 mol% catalyst loading, 1.0 mL reaction volume. Conversion determined by reversed-phase HPLC analysis (elution: 50% water, 50% acetonitrile, $t_{\text{R}}(\text{18}) = 11.0$ min) in the presence of internal standard.^[250]

It was also found that the isolated $[\text{Rh}(\text{BINAP})(\text{nbd})]^+\text{BF}_4^-$ complex was superior to the rhodium complex *in situ* generated by mixing $[\text{Rh}(\text{nbd})\text{Cl}]_2$ with 1.5 equivalents of (*S*)-BINAP **L8** per rhodium, in 6:1 dioxane/water and 1.0 equiv TEA, at room temperature, which gave only 12% conversion (Table 3.6, entry 6 versus 7). It was also possible to show that it was certainly necessary to run these reactions in an absolutely oxygen-free environment (Table 3.6, entry 5 versus 6). Unlike the $[\text{Rh}(\text{cod})\text{Cl}]_2$ precursor (Table 3.6, entries 1 and 2), the Rh-PYRPHOS (**13**) and -BINAP complexes were completely inactive in the presence of oxygen, independently of TEA additive (Table 3.6, entries 3-

5). Some of the intermediates formed during the catalytic cycle^[280] must therefore be very sensitive to oxidation, since $[\text{Rh}(\text{PYRPHOS})(\text{nbd})]^+\text{BF}_4^-$ (**13**) and $[\text{Rh}(\text{BINAP})(\text{nbd})]^+\text{BF}_4^-$ complexes have been shown to remain reasonably unchanged in solution in the presence of air and at room temperature for at least one week (Figure 3.14 B).^[250]

Other bidentate ligands, such as PHOX ligand **L5**, did not catalyze the 1,4-addition, no matter whether its isolated Rh(I)-complex **14** or *in situ* generated complex from $[\text{Rh}(\text{C}_2\text{H}_4)\text{Cl}]_2$ and 1.1 equivalents **L5** per rhodium were used under similar conditions (1.0 equiv TEA, 2.4 mol% catalyst loading), albeit in 70% water (Table 3.6, entries 8 and 9).

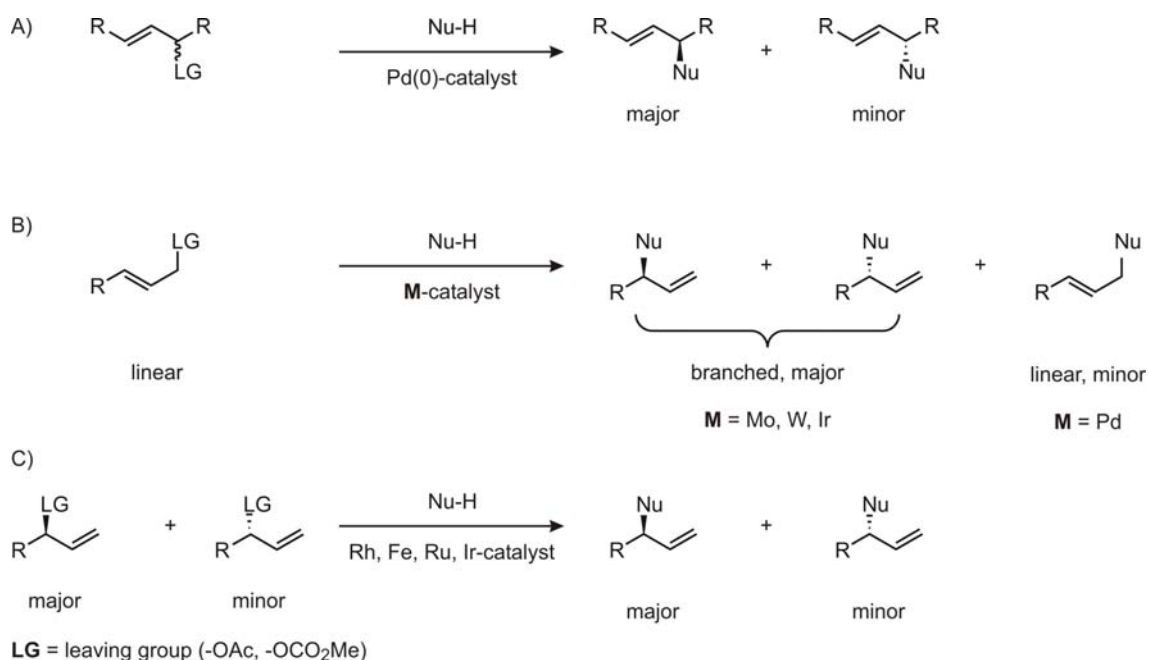
The synthesized Rh-BINAP complex afforded so far the best yield of the addition product under oxygen-free conditions, at 3 mol% catalyst loading (10 mM) and with TEA additive, while in the presence of free BINAP **L8** low conversion was observed. These results represent a solid starting point for studies involving DNA-BINAP conjugates, such as **ODN10** synthesized from amino-DNA **ODN1a** and the BINAP-carboxylic acid derivative **L3** (Scheme 3.4). Based on all informations, it seems that the best way of preparing a DNA-appended Rh(I)-BINAP complex will consist in the pre-treatment of $[\text{Rh}(\text{cod})\text{Cl}]_2$ or $[\text{Rh}(\text{nbd})\text{Cl}]_2$ precursor with AgBF_4 and then addition to the DNA-phosphine ligand. The concentration of dioxane could not be reduced lower than 30% due to the limited solubility of reagents. However, this value seems to be well tolerated by double-stranded nucleic acids, as demonstrated in our studies on DNA duplex stability in the presence of organic solvents (Chapter 3.1.2.2, Figure 3.7).

3.2.3 Iridium(I)-Catalyzed Allylic Amination

Transition metal catalyzed asymmetric allylic substitutions are among the most important carbon-carbon and carbon-heteroatom bond forming reactions in organic synthesis.^[281] Two classes of allylic compounds have been enantioselectively transformed with chiral catalysts: (1) symmetrically substituted racemic and (2) monosubstituted linear or branched (racemic) allylic substrates (Scheme 3.11).

While Pd(0)-catalysts have been typically used in the former case, the monosubstituted allylic substrates were less often employed with such systems because of

regioselectivity in favour of linear achiral products. The regioselectivity control of allylic substitution reactions is mainly governed by the choice of the transition metal ion. For example, with Pd(0)-catalysts, linear products were generally produced (Scheme 3.11 A, while Mo-^[72, 282-284] or W-based catalysts^[285] yielded chiral branched products from monosubstituted linear substrates, giving therefore asymmetric induction (Scheme 3.11 B). Rh,^[286] Fe,^[287] or Ru^[288, 289] complexes were commonly used to catalyze substitutions of enantiomerically enriched branched substrates, yielding branched products with retention of configuration and a high degree of conservation of enantiomeric excess (“memory effect”) (Scheme 3.11 C).



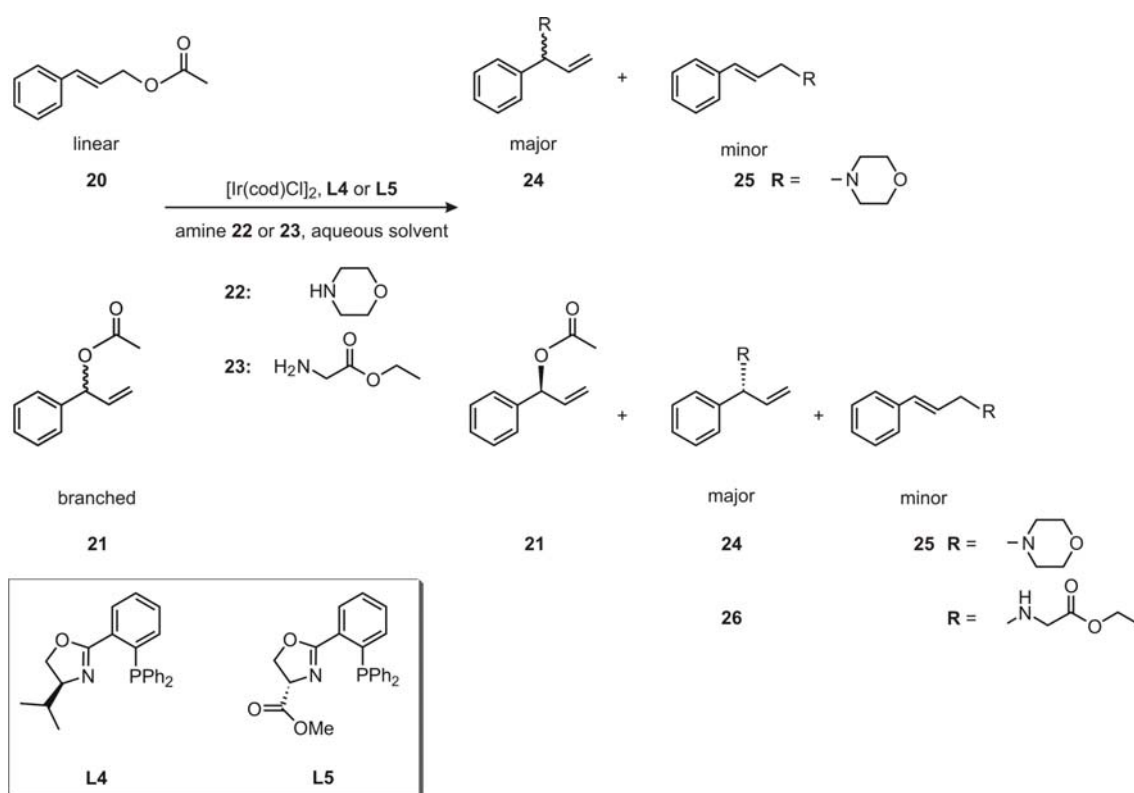
Scheme 3.11. Transition-metal catalyzed allylic substitution of A) symmetrically substituted, B) monosubstituted linear and C) monosubstituted branched substrates.

In 1997, Takeuchi reported the first use of Ir-catalysts in allylic substitution, combining [Ir(cod)Cl]₂ precursor with triphenylphosphite ligand to achieve excellent regioselectivities in favour of the branched product from linear allylic substrates.^[290] In the same year, Helmchen reported the first asymmetric version of allylic substitution using chiral phosphinooxazoline ligands.^[67] Achiral linear aryl acetates were transformed into branched chiral products (Scheme 3.11 B), with high regioselectivity and enantiopurity. However, the reaction was slower in comparison to the reaction catalyzed by the [Ir(cod)Cl]₂/P(OPh)₃ system or even [Ir(cod)Cl]₂ precursor alone.^[76]

^{291]} Since then, Ir-catalysts have received much attention in asymmetric allylic substitution.

A large number of catalytic systems consisting of Ir precursors and chiral monodentate phosphoramidite ^[292-297] or achiral phosphite^[75, 76] ligands have been developed. In contrast, further investigations on Ir-PHOX complexes gave disappointing results especially in transformations involving alkyl-substituted allylic substrates: aminations were generally slow^[72] and interesting results could only be achieved in intramolecular aminations.^[71]

Although not many examples of Ir-PHOX-catalyzed allylic aminations have been published so far, we chose to study this system with DNA-based catalysts for the following reasons: (1) these reactions require polar solvents,^[76] (2) bidentate PHOX ligands should reduce competition of nucleic acids donor groups in binding the transition metal due to their strong chelating properties, (3) the modest catalytic performance of the Ir-PHOX systems in allylic amination might be enhanced in combination with nucleic acid properties, as finally aimed by our hybrid catalyst approach.



Scheme 3.12. Iridium(I)-catalyzed allylic amination of linear **20** and branched **21** phenyl-allyl acetates with morpholine **22** and glycine ethyl ester **23**, using chiral phosphinoxazoline ligands **L4** and **L5**.

As test reactions for probing the catalytic performance of PHOX ligands **L4** and **L5**, iridium-catalyzed allylic substitutions of monosubstituted phenyl-allyl acetates **20** and **21** with amine nucleophiles morpholine **22** and glycine ethyl ester hydrochloride **23** were selected (Scheme 3.12).

When monosubstituted allyl substrates (*e.g.* **20** and **21**) are used in allylic amination reactions, the possibility of two regioisomeric products arises: the linear isomer and the branched isomer. With iridium(I)-catalysts the branched-to-linear-ratio can be shifted to the formation of the branched isomer as major product, affording the chance to observe asymmetric induction from achiral substrates. We were also interested in the ability of Ir-PHOX complexes to effect kinetic resolution^[298] of racemic branched substrate, *e.g.* compound **21**, and to yield enantiomerically enriched product and substrate, respectively. The general principle of kinetic resolution, namely achievement of partial or complete resolution by virtue of unequal rates of reaction of the enantiomers in a racemate with a chiral catalyst, is illustrated in Figure 3.20. The maximum theoretical yield is 50% due to the consumption of only one enantiomer.

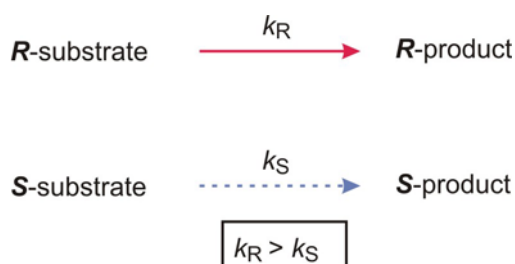
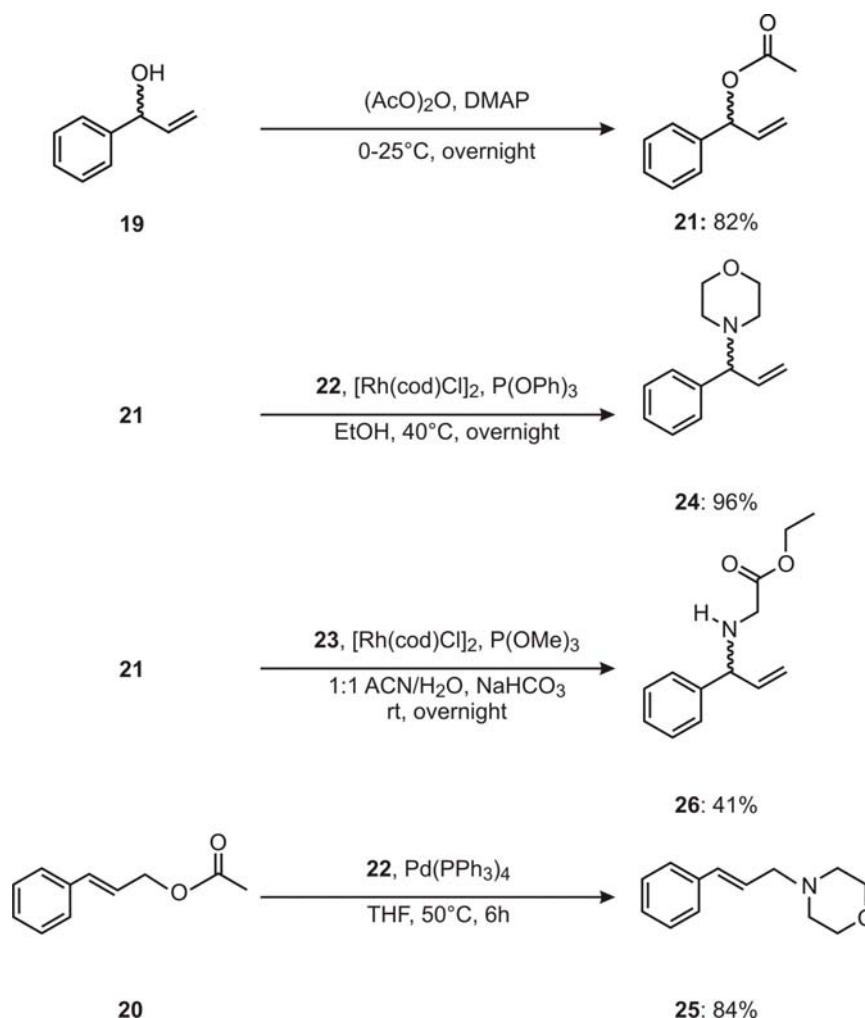


Figure 3.20. Principle of the classic kinetic resolution.

3.2.3.1 Preparation of Allylic Substrates and Products. Analytical Methods

The branched substrate **21** was prepared by esterification of the commercially available α -benzylvinyl alcohol **19** (Scheme 3.13). Reference products **24-26** were prepared as described in Scheme 3.12. Branched product **24** was obtained as racemic mixture from **21** via amination with morpholine **22**, in ethanol, using a catalyst *in situ* generated from $[\text{Rh}(\text{cod})\text{Cl}]_2$ and triphenyl phosphite. Achiral linear product **25** was prepared in a similar way, involving amination of the commercially available cinnamyl acetate **20**

with **22** in dry THF, with Pd(PPh₃)₄ catalyst. The synthesis of the branched product **26** was performed starting from the racemic allylic acetate **21** and glycine ethyl ester **23** (hydrochloride form), in 1:1 acetonitrile/water with 2.0 equiv NaHCO₃, using [Rh(cod)Cl]₂ and trimethyl phosphite ligand.



Scheme 3.13. Synthesis of phenyl-allyl substrate **21** and of amination products **24-26**.

In a large number of studies, allylic carbonates are usually the substrates of choice, while allylic acetates are less often used, owing to their lower reactivity and selectivity.^[292] Preliminary attempts in our group showed that branched methylcarbonate derivatives could undergo isomerisation and cleavage of the carbonate moiety in aqueous environment.^[250] These observations prompted us to use acetate substrates instead. Since we aim at carrying out allylic aminations in aqueous solvent, at basic pH, the stability of substrate **21** against saponification under these conditions had to be initially investigated. Solutions of **21** in 1:1 water/acetonitrile and 0.1 M aqueous

NaHCO₃/acetonitrile were incubated at room temperature for 9 hours and systematically analyzed by reversed-phase HPLC (Figure 3.21).

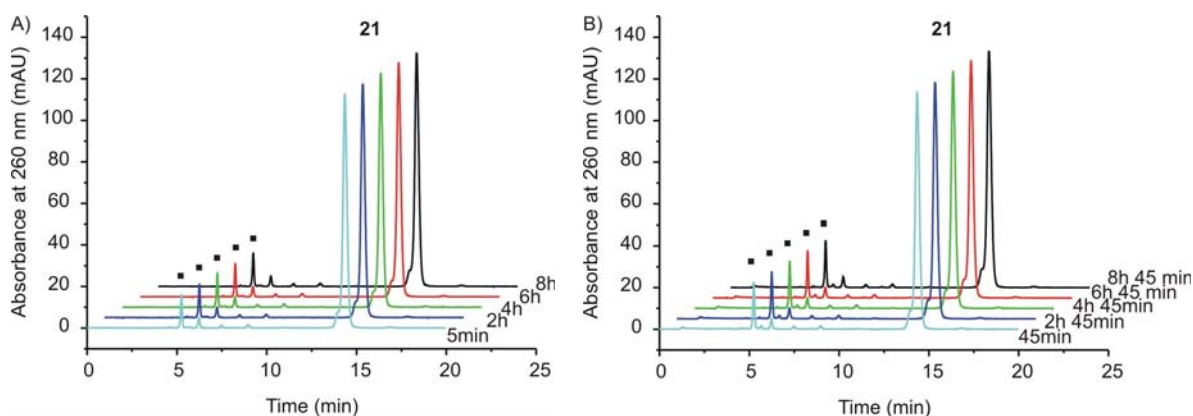


Figure 3.21. Stability of allylic acetate **21** in A) 1:1 water/acetonitrile and B) 0.1 M aqueous NaHCO₃/acetonitrile. Gradient: 50% water and 50% acetonitrile, $t_R(\mathbf{21}) = 14.4$ min. ■ Impurity.

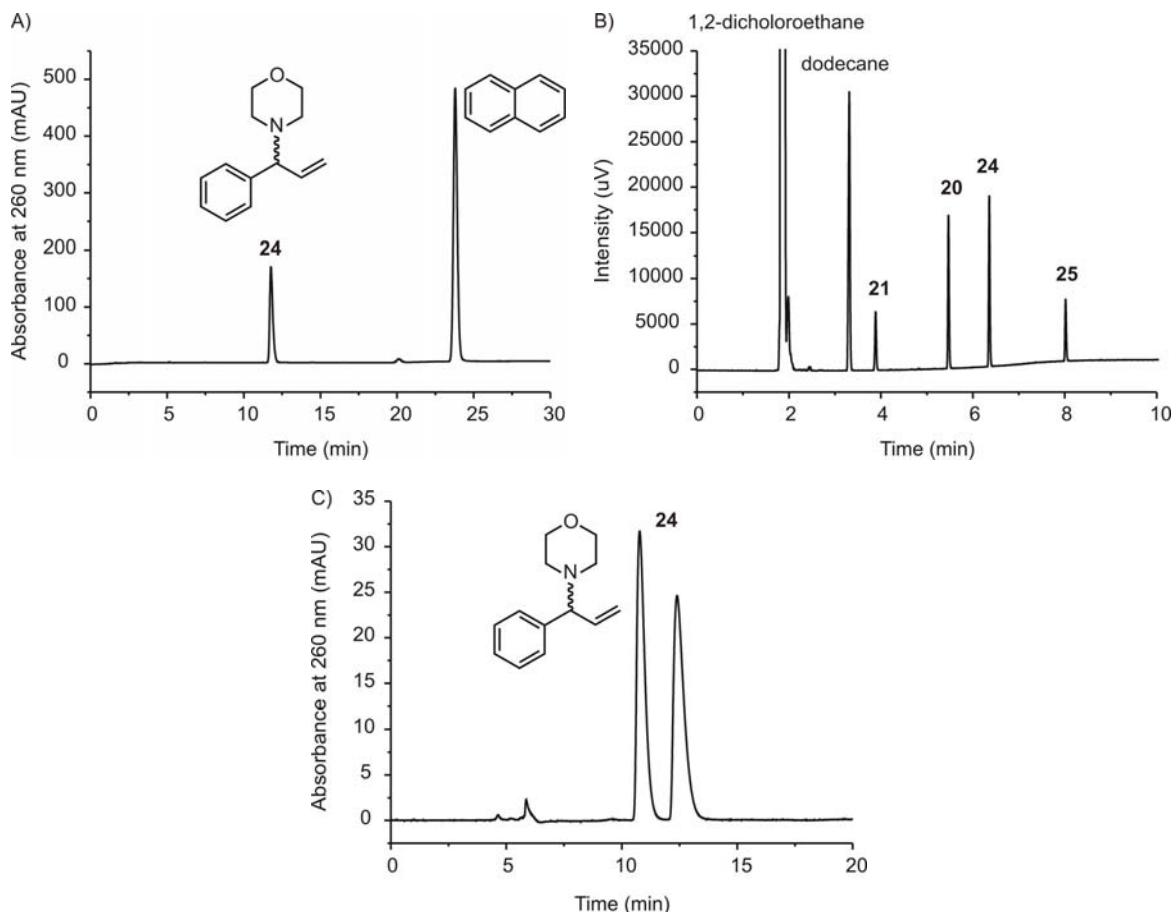


Figure 3.22. A) Reversed-phase HPLC analysis of branched amination product **24** with naphthalene as internal standard. B) Gas chromatography analysis of mixture of branched **21** and linear **20** allylic substrates and branched **24** and linear **25** amination products with dodecane as internal standard. C) HPLC chiral separation of racemic branched product **24**.

The HPLC chromatograms show similar behaviour of allylic acetate **21** in both water (Figure 3.21 A) and NaHCO₃ mixtures (Figure 3.21 B). Even after long incubation times, the allylic acetate remained reasonably stable, making it a suitable substrate for carrying out aminations in aqueous solvent, under basic conditions.

The reference substrates and products were then employed to establish analytical methods for following the reaction and determining the enantioselectivity: 1) reversed-phase HPLC, elution with 50:50 acetonitrile/water, $t_R = 11.8$ min (**24**), 24.0 min (naphthalene as internal standard) (Figure 3.22 A); 2) gas chromatography, gradient: 2 min at 150°C, increase to 230°C with 15°C/min; $t_R = 3.3$ min (dodecane as internal standard), 3.9 min (**21**), 5.5 min (**20**), 6.4 min (**24**) and 8.0 min (**25**) (Figure 3.22 B); 3) HPLC chiral separation, elution with *n*-hexane/*i*-propanol 99:1, $t_R(\mathbf{24}) = 10.8, 12.4$ min (Figure 3.22 C).

3.2.3.2 Preliminary Results of Catalysis with Ir-PHOX Complexes

The development of allylic substitutions in water has generally received little attention. The main reason for that is likely the hydrolysis of the electrophile reactant that may compete with the desired nucleophilic substitution.^[299] Only few reports of palladium-catalyzed allylic substitutions (aminations) in water have been published. The best results were obtained with a heterogeneous system based on immobilized phosphine or P₃N-chelate ligands.^[300-302] Uemura and coworkers reported on a homogeneous version of palladium-catalyzed allylic substitutions in water, in which a phosphinite-oxazoline ligand afforded moderate to high yields and good enantiomeric excess (85%).^[303] However, this system proved to be more efficient in acetonitrile alone (92% ee) rather than in water or water/acetonitrile mixtures.

Our first studies were conducted to determine if Ir-PHOX catalysts impart activity and stereoselectivity in allylic aminations carried out in aqueous media. Allylic aminations of phenyl-allyl acetates **20** and **21** catalyzed by [Rh(cod)Cl]₂, [Ir(cod)Cl]₂ and combinations of these complexes with **L5** were initially investigated. The phosphinooxazoline **L5** is the precursor of **L6** derivative used for attachment to the DNA.

Table 3.7. Effect of transition metal precursor and catalyst concentration on amination of branched allylic substrate **21** with amines **22** and **23**.^[a]

Entry	Catalyst precursor	Ligand	Nucleophile	Cat.conc. [mM]	Solvent ACN/H ₂ O	Conv ^[b] [%]
1	[Rh(cod)Cl] ₂	-	22	10	1:1	20
2 ^[c]	Rh(nbd)BF ₄	L5	22	10	1:1	40
3	[Ir(cod)Cl] ₂	-	22	10	1:1	>95
4	[Ir(cod)Cl] ₂	L5	22	10	1:1	>95
5 ^[d]	[Ir(cod)Cl] ₂	L5	23	10	1:1	50 ^[e]
6	[Ir(cod)Cl] ₂	L5	22	1.0	1:1	>95
7	[Ir(cod)Cl] ₂	L5	22	1.0	3:7	>95
8	[Ir(cod)Cl] ₂	L5	22	0.5	3:7	>95

[a] Reaction conditions: 0.05 mmol **21**, 0.07 mmol **22** (1.5 equiv), 2 mol% [Ir(cod)Cl]₂, 4.2 mol% **L5**, 1.0 mL reaction volume, r.t., 14 hours, unless otherwise stated. [b] Conversion estimated by thin-layer chromatography, unless otherwise stated. [c] Isolated Rh(I) complex **14** from Rh(nbd)BF₄ and **L5**. [d] 0.07 mmol **23** (hydrochloride form) (1.5 equiv), 0.07 mmol NaHCO₃ (1.5 equiv). [e] Conversion determined by reversed-phase HPLC, elution with 50% water and 50% acetonitrile, t_R(**26**) = 12.4 min.

In the first set of experiments, substrate **21** was reacted with morpholine **22** and glycine ethyl ester **23**. The results, summarized in Table 3.7, clearly show that the complex formed *in situ* by combining [Ir(cod)Cl]₂ and **L5** is highly active in the presence of 50-70% water (entries 4 and 6-8). Moreover, complete conversion was achieved with morpholine **22** (3.0 equiv) as nucleophile even at 0.1 mol% catalyst loading, that corresponds to a [Ir] catalyst concentration of 0.5 mM (Table 3.7, entry 7). The reaction rate was significantly higher with morpholine **22** than with glycine ethyl ester **23** (Table 3.7, entry 4 versus 5).

High conversion was also induced by [Ir(cod)Cl]₂ without additional ligand (Table 3.7, entry 3). In addition, the [Ir(cod)Cl]₂ precursor was superior to [Rh(cod)Cl]₂ which under the same conditions gave only 20% product formation (Table 3.7, entry 3 versus 1). With the isolated cationic complex [Rh(**L5**)(nbd)]⁺BF₄⁻ **14** (Table 3.7, entry 2) the results were distinctly better than with the [Rh(cod)Cl]₂ catalyst precursor, slight rate acceleration being observed (entry 1).

Because of the low reactivity of glycine ethyl ester **23**, the next studies were focused on aminations with morpholine nucleophile **22**.

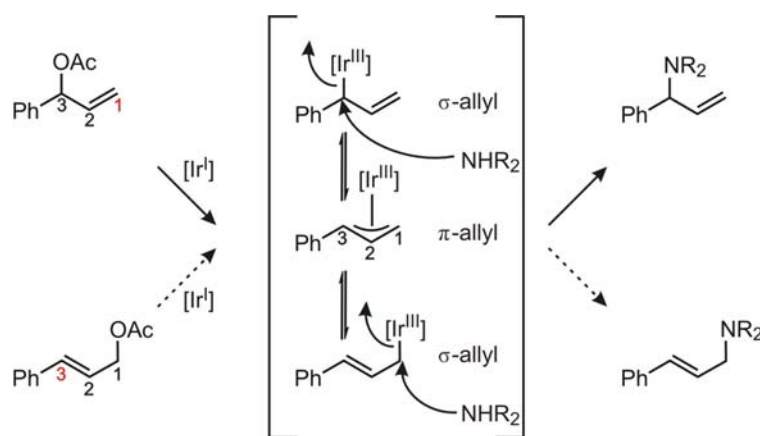
Following the results obtained with the branched substrate **21**, we next attempted the amination of linear allyl acetate **20**, using the same Ir(I) catalyst prepared *in situ* from [Ir(cod)Cl]₂ and **L5**. Test reactions were carried out in both standard conditions (neat organic solvent), and 70% aqueous solvent as in our early experiments. The results are shown in Table 3.8.

Table 3.8. Allylic amination of linear (**20**) and branched (**21**) substrates with morpholine **22** in neat organic solvent and 70% water, with $[\text{Ir}(\text{cod})\text{Cl}]_2$ and ligand **L5**.^[a]

Entry	Allylic substrate	Ligand	Solvent	Temp. [°C]	Conv. ^[b] [%]
1	20	-	acetonitrile	rt	<1
2	20	L5	acetonitrile	rt	<1
3	20	-	dioxane	rt	<1
4	20	L5	dioxane	rt	<1
5 ^[c]	20	-	3:7 dioxane/water	rt	<1
6 ^[c]	20	L5	3:7 dioxane/water	rt	<1
7 ^[c]	21	-	3:7 dioxane/water	rt	96
8 ^[c]	21	L5	3:7 dioxane/water	rt	98
9 ^[c]	20	L5	3:7 dioxane/water	50	5

[a] Reaction conditions: 0.05 mmol **20** or **21**, 0.15 mmol **22** (3.0 equiv), 1.4 mol% **L5**, 0.5 mM [Ir] catalyst, 1.0 mL reaction volume, r.t., 14 hours, unless otherwise stated. [b] Conversion determined by gas chromatography. [c] 6 hours reaction time.

The reaction rate was significantly higher for the branched substrate **21**, and complete conversion was achieved in 70% aqueous solvent, in 6 hours (Table 3.8, entries 7 and 8), while the isomeric linear substrate was found in all cases unreacted even after 14 hours reaction time (entries 1-6). The attempt to enhance the reaction rate at elevated temperature failed: the amination of the linear substrate remained sluggish, even at 50°C, leading to only 5% conversion (entry 9).

**Scheme 3.14.** Ir(I)-catalyzed allylic amination of branched and linear substrates via σ - and π -allyl intermediates.

Differences in reaction rates between branched and linear substrates have been generally observed in Ir(I)-^[77] and Rh(I)^[286]-catalyzed allylic substitutions. They have been attributed to the $\text{S}_{\text{N}}2'$ mechanism occurring in the formation of the π -allyl intermediate during the catalytic cycle proposed by Helmchen *et al.*^[67] (Scheme 3.14). Therefore, the oxidative addition of the substrate to Ir(I) and Rh(I) species is expected to be faster in the case of the branched isomer due to a less sterically congested

environment imposed by the substituents at the end of the allylic system.^[286]

Our results were in good agreement with the only one reported example of amination reactions with Ir-PHOX complexes. Helmchen *et al.* observed that the Ir-catalyst generated from $[\text{Ir}(\text{cod})\text{Cl}]_2$ and the phosphinoxazoline ligand (*S*)-*i*-Pr-PHOX (**L4**) was ineffective in the intramolecular amination of linear allyl acetates, whereas high yield and moderate to high enantioselectivity were obtained with the branched homologues (albeit after long reaction times: 4-6 days).^[71]

These observations prompted us to evaluate the above-described catalyst mixture of $[\text{Ir}(\text{cod})\text{Cl}]_2$ and classical PHOX ligand **L4**,^[67] extensively used in Ir(I)-catalyzed asymmetric allylic substitutions, versus the structurally-related **L5**. The aminations of the branched allyl acetate **21** were performed in neat dioxane or 3:7 dioxane/water mixture containing 100 mM NaClO_4 and 5 mM $\text{Mg}(\text{ClO}_4)_2$ (the presence of salts is later required by the use of nucleic acid-based systems). In addition, test reactions were carried out in order to assess the reactivity of Ir-PHOX system at low catalyst concentration that is an essential condition for creating DNA-based catalysts. The results are presented in Table 3.9.

Table 3.9. Allylic amination of branched substrate **21** with morpholine **22** according to Scheme 3.12, using PHOX ligands (*S*)-**L4** and (*S*)-**L5**.^[a]

Entry	PHOX Ligand	[Ir] [mM]	Solvent ^[b]	Time [h]	Conv ^[c] [%]	Ee ^[d] [%]
1	L4	1.0	dioxane	1.5	<2	n.d.
2	L4	1.0	3:7 dioxane/water	1.5	99	n.d.
3	L5	1.0	3:7 dioxane/water	1.5	99	6
4 ^[e]	L4	1.0	3:7 dioxane/water	13	50	3
5	-	0.1	3:7 dioxane/water	13	73	-
6	L4	0.1	3:7 dioxane/water	13	71	5
7	L5	0.1	3:7 dioxane/water	13	67	1

[a] Reaction conditions: 0.05 mmol **21**, 0.15 mmol **22** (3.0 equiv), 2.5 mol% **L5** (entries 1-4) and 0.25 mol% **L5** (entries 5-7), 1.0 mL reaction volume, r.t., unless otherwise stated. [b] 100 mM NaClO_4 , 5 mM $\text{Mg}(\text{ClO}_4)_2$ aqueous solution. [c] Conversion determined by gas-chromatography with dodecane as internal standard. [d] Determined by HPLC, $t_R(\mathbf{24}) = 10.8, 12.4$ min. [e] Kinetic resolution conditions: 0.5 equiv **22**.

Although dioxane is a common solvent in allylic substitutions, reaction in neat dioxane with the standard Ir-**L4** catalyst gave almost no product (entry 1). At the same catalyst concentration, reaction in 3:7 dioxane/water mixture proceeded smoothly, affording complete conversion with both **L4** and **L5** ligands, in only 1.5 hours (entries 2 and 3). Under these conditions, the amination proceeded efficiently even at lower catalyst concentration (0.1 mM), affording 67-73% conversion (entries 5-7). However, no effect

on the catalyst activity due to **L4** or **L5** ligand could be observed, since similar conversion was obtained also with only $[\text{Ir}(\text{cod})\text{Cl}]_2$ precursor (entry 6).

The isolated branched amine product **24** obtained with chiral phosphinooxazolines **L4** and **L5** was submitted to chiral separation. The very low observed enantioselectivities (Table 3.9, entries 3 and 6,7) are consistent with a strong memory effect of the Ir-catalyst obtained from a racemic starting material, as previously observed in similar transformations with malonate nucleophile.^[298] We therefore attempted to use such memory effects in a kinetic resolution reaction, either by allowing the reaction to proceed only to 50% conversion or using half equivalent of amine nucleophile. Disappointingly, treatment of the racemic starting material **21** with half equivalent of morpholine **22** gave the branched amine product **24** in only 3% ee (Table 3.9, entry 4). As already mentioned in the introduction of this chapter, allylic aminations can be accelerated by polar solvents (*e.g.* alcohols, acetonitrile). It was argued that such solvents were involved in the stabilization of transition states of the oxidative addition to Ir(I) species and the nucleophilic attack of the amine.^[76] Because of these solvent effects, both oxidative addition and nucleophilic attack might be enhanced. Intriguingly, Ir(I)-catalyzed intramolecular aminations with **L4** PHOX ligand became slower and also less selective when polar solvents (*e.g.*, dimethylformamide or acetonitrile) were used as alternative to toluene.^[71]

The results collected in Table 3.9 clearly show that in our system water is a better solvent than dioxane, and likely a “participating” solvent in catalysis.^[299] The unique solvating properties of water, and its potential contribution to the electronic properties as well as the steric environment of the catalytic system, exerted through direct binding to iridium ion, or/and second coordination sphere interactions, might account for the outcome of the allylic amination. However, the precise reason for the effect of water on the steric course of the reaction remains unclear.

Beside the solvent effect, the lack of stereoselectivity observed in our catalytic attempts (Table 3.9, entries 3,4 and 6,7) might be attributed to ligand, or/and amine^[76] nucleophile. Although in the majority of asymmetric allylic substitutions with PHOX ligands, the relative bulkyness of the oxazoline substituent at the chirality centre appears one of the decisive factors for achieving selective catalysts, with **L4**-based complex being one of them,^[57, 304] in our case the enantioselectivity induced by **L4** was

unsatisfactory. The structurally related chiral PHOX ligand **L5** also displayed weak selective properties. The steric effect of the amine nucleophile might additionally influence the stereocontrol of the reaction, as previously observed by Takeuchi:^[76] the stereoselectivity decreases as the steric bulk of the amine decreases.

Unlike most transition metal catalyzed processes, allylic aminations do not exclusively rely on a single mechanism as a source of asymmetry. A possible catalytic cycle for the Ir(I)-catalyzed allylic amination is illustrated in Figure 3.23. The following general steps have been proposed by Helmchen *et al.*^[67]: 1) *in situ* formation of the Ir(I) catalyst (complex A), 2) oxidative addition of the substrate to the metal centre and formation of π -allyl complexes (complex B/B'), and c) attack of the nucleophile (Nu), *trans* to phosphorus. It has also been proposed that these reactions proceed with double inversion, via σ -allyl or π -allyl complexes, which undergo σ - π - σ isomerisation^[57, 77] (Scheme 3.15).

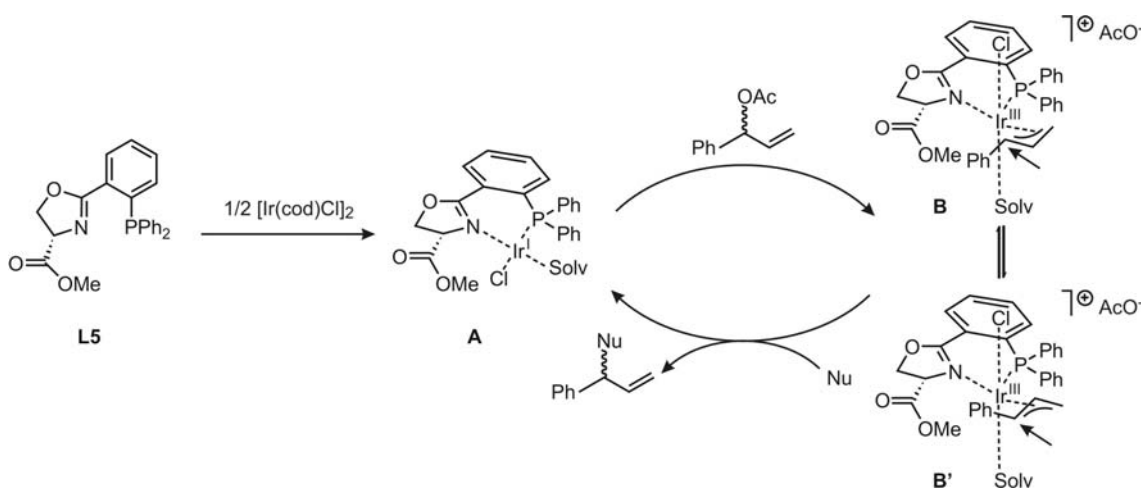
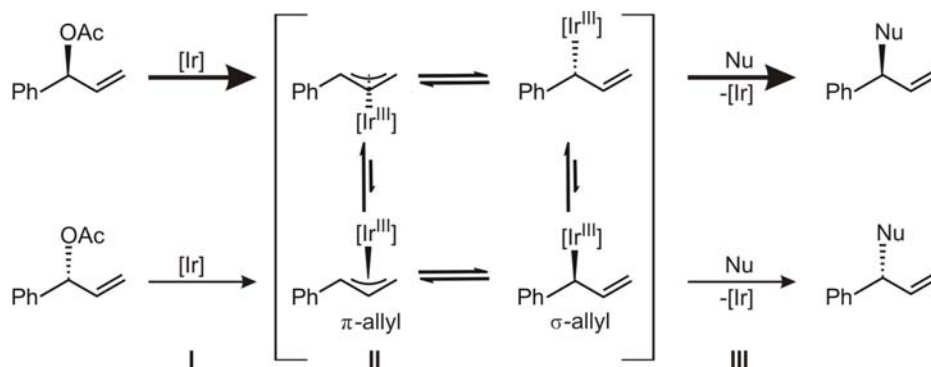


Figure 3.23. Proposed mechanism for the allylic amination of a branched racemic allyl substrate using Ir(I)-**L5** complex.

Although the preference for one of the allylic substrate faces (kinetic control) (Scheme 3.15 I) could be one possible mechanism,^[57] the source of the enantioselectivity is complicated by the possibility that one or more steps in the catalytic cycle may be the enantiodiscriminating step(s). Enantioselection can also derive from a certain degree of isomerisation between the π -allyl intermediates (thermodynamic control), or/and a stereospecific nucleophilic attack (kinetic control) (Scheme 3.15 II and III, respectively).



Scheme 3.15. Enantiocontrol in Ir(I)-catalyzed allylic amination.

Our attempt to reduce the rate of the nucleophilic attack by lowering the nucleophile concentration (Table 3.9, entry 7), and thereby install the stereocontrol likely promoted by the enantioface preference of our catalyst, was so far unsuccessful. At this stage, the mechanism by which the Ir-PHOX catalyst imposes its chirality upon the branched amination product is difficult to understand.

However, our results lead to the following conclusions: 1) the Ir(I)-catalyzed allylic amination is compatible with the use of nucleic acids; 2) the *in situ* formed Ir(I)-**L5** complex is active in 70% aqueous mixtures, in the presence of salts, at room temperature and at low catalyst concentration (100 μ M); 2) the Ir(I)-catalyst generated with a chiral PHOX ligand, either **L4** or **L5**, does not provide enantioselectivity in amination of racemic branched allylic substrate with morpholine. Nevertheless, these promising findings represent a convenient starting point for the development of DNA- or RNA-based asymmetric catalysts, in which the nucleic acid fold can possibly contribute to the stereoselectivity of the process.

3.2.3.3 Allylic Amination with DNA-Appended Phosphinooxazoline Ligands

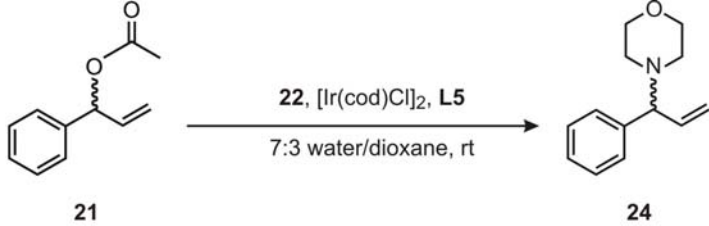
Iridium(I)-phosphinooxazoline complexes are among the most powerful catalysts employed in allylic substitutions, albeit never used in combination with DNA or RNA scaffolds.

The promising results obtained with the catalyst formed with $[\text{Ir}(\text{cod})\text{Cl}]_2$ and ligand **L5** led us to investigate the ability of DNA-appended PHOX conjugates to generate enantioselective catalysts for amination of racemic branched allyl acetate with

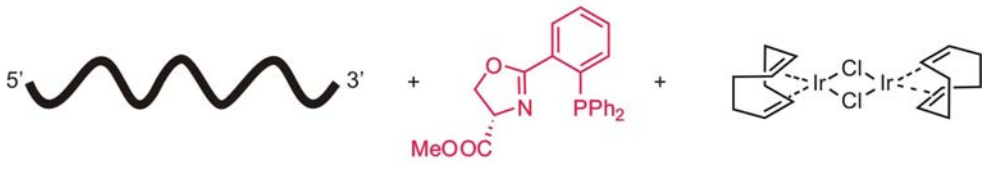
morpholine, assuming that the DNA chirality would provide the stereocontrol of the reaction.

To limit the non-specific binding of $[\text{Ir}(\text{cod})\text{Cl}]_2$ to the DNA, maximum one equivalent of iridium precursor has to be used for complex formation with DNA-based PHOX ligands. However, since the DNA strands are anionic, non-specific electrostatic attractions between these strands and cationic species, including the iridium ion, might occur. More importantly though, the DNA heterocyclic bases have a variety of nitrogen and oxygen donor atoms which can coordinate iridium and influence its catalytic properties. It has been reported that adenine derivatives, for example, can form rhodium-complexes with N1, N6 and N7 as binding sites.^[305]

Control experiments were conducted to determine if in our case DNA interferes with iridium binding and leads to catalytically inactive species. Amination reactions were performed in the presence of 1.1-1.4 equivalents of synthetic unmodified DNA (23 mer, **cDNA2**: 5'-GG AGC TCA CAA GTC CTT CAC TGC-3'), which was either firstly combined with the **L5** ligand, followed by addition of $[\text{Ir}(\text{cod})\text{Cl}]_2$ precursor, or directly added to the pre-formed Ir-**L5** complex. The experiments were carried out on 100 μL scale and the catalyst concentration was maintained in the range of 50-100 μM . Early assays showed that the solution of metal precursor $[\text{Ir}(\text{cod})\text{Cl}]_2$ must be freshly prepared each time. A stock solution of metal precursor $[\text{Ir}(\text{cod})\text{Cl}]_2$ in the presence of phosphinoxazoline ligand **L5**, in dioxane, could be instead used for at least one month when stored at -20°C without noticing any difference in catalytic activity. All reactions were performed in water/dioxane 7:3, and/or in the presence of 100 mM NaClO_4 and 5 mM $\text{Mg}(\text{ClO}_4)_2$. This solvent mixture resembles the conditions used in the stability assays of double-stranded DNA (Chapter 3.1.2.2), the presence of the salts being important for maintaining DNA/DNA or DNA/RNA constructs in helical conformation. Moreover, since the amount of mono- and divalent cations is relatively high, we assume that the charged phosphate connecting units are compensated by metal ions. Localizing metal ions along the DNA phosphodiester backbone may increase the chance that DNA will be shielded from the iridium ion. In this case, the potential interactions of the iridium ion with the DNA would be restricted to nucleobase coordination.

Table 3.10. Effect of DNA on Ir(I)-catalyzed amination of branched allylic substrate **21** with morpholine **22**.^[a]


$$\text{21} \xrightarrow[\text{7:3 water/dioxane, rt}]{\text{22, [Ir(cod)Cl]}_2, \text{L5}} \text{24}$$



Entry	Ligand	cDNA2		L5		Salts	Time [h]	Conversion ^[c] [%]
		[Ir] [μM]	[DNA] ^[b] [μM]	[Ir] [μM]	[DNA] ^[b] [μM]			
1	L5	50	-	-	-	-	19	20
2	L5	50	53.3	-	-	-	19	24
3	L5	50	-	-	+	+	16.5	37
4	L5	50	53.3	-	+	+	16.5	33
5	-	100	-	-	-	+	6	75
6	-	100	135	-	-	+	6	67
7	L5	100	-	-	-	+	6	67
8 ^[d]	L5	100	135	-	-	+	6	72

[a] Reaction conditions: 5 μmol **21**, 15 μmol **22** (3.0 equiv), 100 μL reaction volume, r.t., unless otherwise stated. [b] Pre-formed Ir-**L5** catalyst was added to the DNA (1.1-1.4 equiv) solution. Experiments performed at least in duplicate. [c] Conversion determined by gas chromatography with dodecane as internal standard. [d] [Ir(cod)Cl]₂ was added to a 1:1 PHOX/DNA solution.

The results shown in Table 3.10 confirmed that the catalytic activity of both [Ir(cod)Cl]₂ precursor and pre-formed Ir-**L5** complex was preserved in the presence of DNA (entries 2, 4, and 6). Interestingly, the presence of salts in the reaction milieu led to a slight increase in rate acceleration (entry 3 versus 1). However, no significant salt-dependent effect on the reaction conversion could be observed when the DNA was added to the reaction mixture (entry 4 versus 2). This finding indicated that the DNA phosphate groups, apparently available for interactions with the iridium ion, did not trigger formation of catalytically inactive species. Furthermore, it appeared that the catalytic complex *in situ* generated from [Ir(cod)Cl]₂ and **L5** was formed in the presence of one equivalent of DNA per PHOX ligand, since no decrease in conversion was observed (entry 8 versus 7). On the other hand, this result can also be argued by the high catalytic activity of the [Ir(cod)Cl]₂ precursor without additional ligand (shown in the previous chapter: Table 3.9, entry 5 versus 6 and 7), which anyway is not disturbed by the presence of DNA (Table 3.10, entry 5 versus 6). Therefore, under these conditions, the

ability of the DNA coordinating sites to compete with the PHOX ligand in iridium-binding could not be entirely excluded, although a bidentate phosphinooxazoline is expected to be a superior ligand relative to the nucleobases and the phosphate groups are likely to be shielded by the mono- and divalent ions present in the reaction mixture. Importantly, our data clearly demonstrated that the interactions, if any, between the unmodified synthetic 23mer DNA and the $[\text{Ir}(\text{cod})\text{Cl}]_2$ precursor or the pre-formed Ir-**L5** complex, were negligible since they did not alter the catalytic properties of the system. Encouraged by these results, we then tested the DNA-based PHOX ligands in our model reaction with the branched allyl acetate **21** and morpholine nucleophile **22**. It has been assumed that the DNA-appended PHOX ligand would provide chelating control on the iridium ion, and favour its precise positioning into the DNA chiral environment. We screened DNA-PHOX constructs containing diverse linker units, four-carbon, two-carbon, and 13-atom spacer (**ODN11a-c**) (Chapter 3.1.2.4), and attempted to study the influence of the linker length on the catalytic properties of the resulting DNA-tethered iridium complex as well as on the transfer of chirality from the DNA scaffold.^[146, 199]

The Ir(I) complexes were prepared by mixing 2.2-2.6 equivalents of HPLC purified **ODN11a-c** conjugates with $[\text{Ir}(\text{cod})\text{Cl}]_2$ in a degassed aqueous solution of 143.0 mM NaClO_4 and 7.0 mM $\text{Mg}(\text{ClO}_4)_2$ (see Materials and Methods, Chapter 5.9.2.3). In order to rule out decomposition of DNA-PHOX ligands caused by the oxidation of the phosphinooxazoline moiety during the reaction, as well as possible side reactions of DNA with components of the reaction mixture, the DNA-appended Ir(I) complexes were incubated with the allyl substrate **21** and morpholine **22**, under the same conditions used for the amination reaction, and then analyzed by HPLC. The presumably formed Ir(I)-PHOX complex is expected to be stable towards oxidation.

Figure 3.24 illustrates the HPLC chromatograms obtained for the **ODN11a** under the above-described conditions. The oxidation proceeded slowly, from <10% (A) immediately after addition of $[\text{Ir}(\text{cod})\text{Cl}]_2$ to the DNA to 54% after overnight incubation in the presence of the substrates (B). Similarly, slight amount of oxidized DNA-PHOX conjugate (<10%) was also obtained in the case of **ODN11b** and **ODN11c** soon after treatment with $[\text{Ir}(\text{cod})\text{Cl}]_2$, while high levels of oxidation, 50% and 70%, respectively, were observed after carrying out the amination reaction. However, the amount of the observed oxide **ODN11a-c(O)** in the HPLC assays is probably overestimated. Beside

the long incubation time, a certain level of oxidation that might occur during HPLC sample preparation (outside a glove-box) and due to the oxygen dissolved in the HPLC solvents must be also considered.

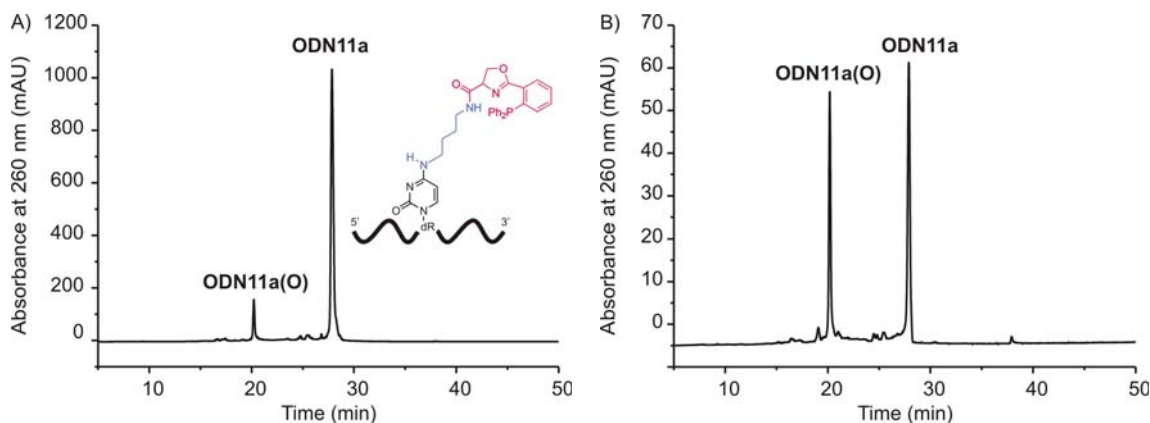


Figure 3.24. HPLC chromatograms of the phosphinoxazoline-derivatized DNA conjugate **ODN11a**. A) HPLC purified product immediately after redissolving in aqueous salt solution and addition of 0.5 equivalent $[\text{Ir}(\text{cod})\text{Cl}]_2$. B) Overnight incubation at room temperature with allylic substrate and morpholine. DNA sequence: 5'-GC AGT GAA GGC* TGA GCT CC-3', C* = N4-PHOX-appended 2'-deoxycytidine.

We assumed that in all cases the remaining amount of non-oxidized DNA-PHOX conjugate (approx. 50%) was high enough to ensure appropriate conditions for carrying out allylic amination reactions in the presence of **ODN11a-c**. The reactions were performed on a 50 or 100 μL scale, in 7:3 water/dioxane, at room temperature. The concentration of DNA-appended PHOX ligand was maintained between 66 and 130 μM , considering 1.1-1.3 equivalents of ligand per iridium and only 90% purity of the DNA-conjugate due to inevitable oxidation. The results are shown in Table 3.11.

Disappointingly, in all cases when the DNA-tethered PHOX ligand was used, the catalyst activity was highly reduced (<28% conversion) compared to both $[\text{Ir}(\text{cod})\text{Cl}]_2$ precursor (entry 1) and pre-formed Ir-**L5** complex (entry 2) and additionally, no enantioselectivity was observed (entries 3, 4, and 6-8). The best conversion (28%) was obtained with the DNA conjugate containing the longest spacer between the PHOX moiety and the DNA scaffold, **ODN11c** (entry 8). This result reflects the higher flexibility introduced by the Ir(I)-PHOX-tethered linker, apparently important for preventing coordination of the iridium ion with the DNA electron donor atoms, and finally preserving the catalytic activity.

Table 3.11. Iridium(I)-catalyzed allylic amination of branched allyl acetate **21** with morpholine **22** with DNA-appended PHOX ligand **ODN11a-c**.^[a]

Entry	Ligand	[Ligand] [μM]	[Ir] [μM]	Conversion ^[b] [%]	E _c ^[c] [%]
	-	-	100	73	-
2 ^[e]	L5	140	100	82	<1
3	ODN11b	130	100	12	5
4	ODN11a	130	100	<1	n.d.
5	-	75	60	84	n.d.
6	ODN11b	78	60	10	2
7	ODN11a	78	60	9	<1
8	ODN11c	78	60	28	<1

[a] Reaction conditions: 5 μmol **21**, 5.5 μmol **22** (1.1 equiv), 100 mM NaClO_4 , 5 mM $\text{Mg}(\text{ClO}_4)_2$, 100 μL reaction volume, r.t., 16 hours. [b] Conversion determined by gas chromatography with dodecane as internal standard. [c] Determined by HPLC, detection wavelength $\lambda = 254$ nm, $t_{\text{R}}(\mathbf{24}) = 10.8, 12.4$ min. [e] 0.5 mol% **L5**.

These results were inconsistent with our previous findings that clearly supported the assumption that (unmodified) DNA does not participate in iridium coordination (Table 3.10), or at least the existing interactions are not detrimental for catalytic activity. To explain the results obtained with PHOX-carrying DNA sequences, one could consider that the formation of the DNA-appended Ir(I)-PHOX complex would result in close localization of the metal centre relative to the DNA and, consequently, in proximity to a plethora of ligands, such as the nonbridging phosphoryl oxygens and the 19 hydroxyl groups of the backbone, as well as the nitrogens and oxygens of the purine or pyrimidine bases. In this case, new iridium-DNA interactions, that haven't been observed so far, might emerge. Based on reasons discussed before, it was reasonable to assume that such interactions would preferentially involve the nucleobases. In order to prevent undesirable coordination, we chose to use double-stranded DNA constructs,

where the complementary strand sequesters most of the heteroatoms of the nucleobases through Watson-Crick base-pairing, making them no more available for metal coordination.

3.2.3.4 Allylic Amination with Double-stranded DNA-appended Phosphinooxazoline Ligands

We envisaged the Watson-Crick base-pairing of DNA as a tool to provide a particular steric environment for the transition metal. In this case, the flexibility of the single-stranded DNA given by a substantial degree of bond rotation occurring in the phosphodiester backbone linkages is considerably reduced. As a result, the structural constraints generated upon duplex formation are expected to facilitate the transfer of chirality from the DNA helix to the catalytic centre.

A series of oligonucleotides (19mers) containing the phosphinooxazoline ligand moiety attached to the deoxycytidine-19 residue (direction 5'-3') via three different spacers (**ODN11a-c**) were hybridized with the complementary DNA strand **cdNA1** (Figure 3.25 A). Two additional complementary oligonucleotides **cdNA2** and **cdNA3** were chosen, that upon hybridization generated small bulges (3-4 nt) on either the unmodified (**cdNA2**) or the PHOX-tethered DNA strand (**ODN11a-c**), in close vicinity to the ligand attachment site (Figure 3.25 B and C). This design based on introducing elements of flexibility of particular size and location within the duplex was anticipated to bring about shape changes and provide more complex structures for catalysis.

Confident to our previous observations regarding the B-DNA duplex stability in mixtures containing 30% water-miscible organic cosolvents in aqueous buffers (Figure 3.7), all double-stranded DNAs were used in Ir(I)-catalyzed allylic amination of branched acetate substrate **21** with morpholine **22**, in 70% aqueous solvent. Treatment of DNA-PHOX conjugates with equimolar amounts of complementary strands (typically 2.0-4.0 nmol) at room temperature, in aqueous salt solution, results in spontaneous assembling of DNA duplexes. After complexation with $[\text{Ir}(\text{cod})\text{Cl}]_2$ precursor and *in situ* formation of Ir(I)-catalyst (1.1-1.3 equivalents of DNA-appended PHOX ligand per iridium), the amination reactions were started by addition of acetate substrate **21** and morpholine nucleophile **22**. Parallel test reactions with single-stranded

DNA-PHOX conjugates were also performed, as previously described, to allow a more accurate comparison of the catalytic systems. Some results are shown in Table 3.12.

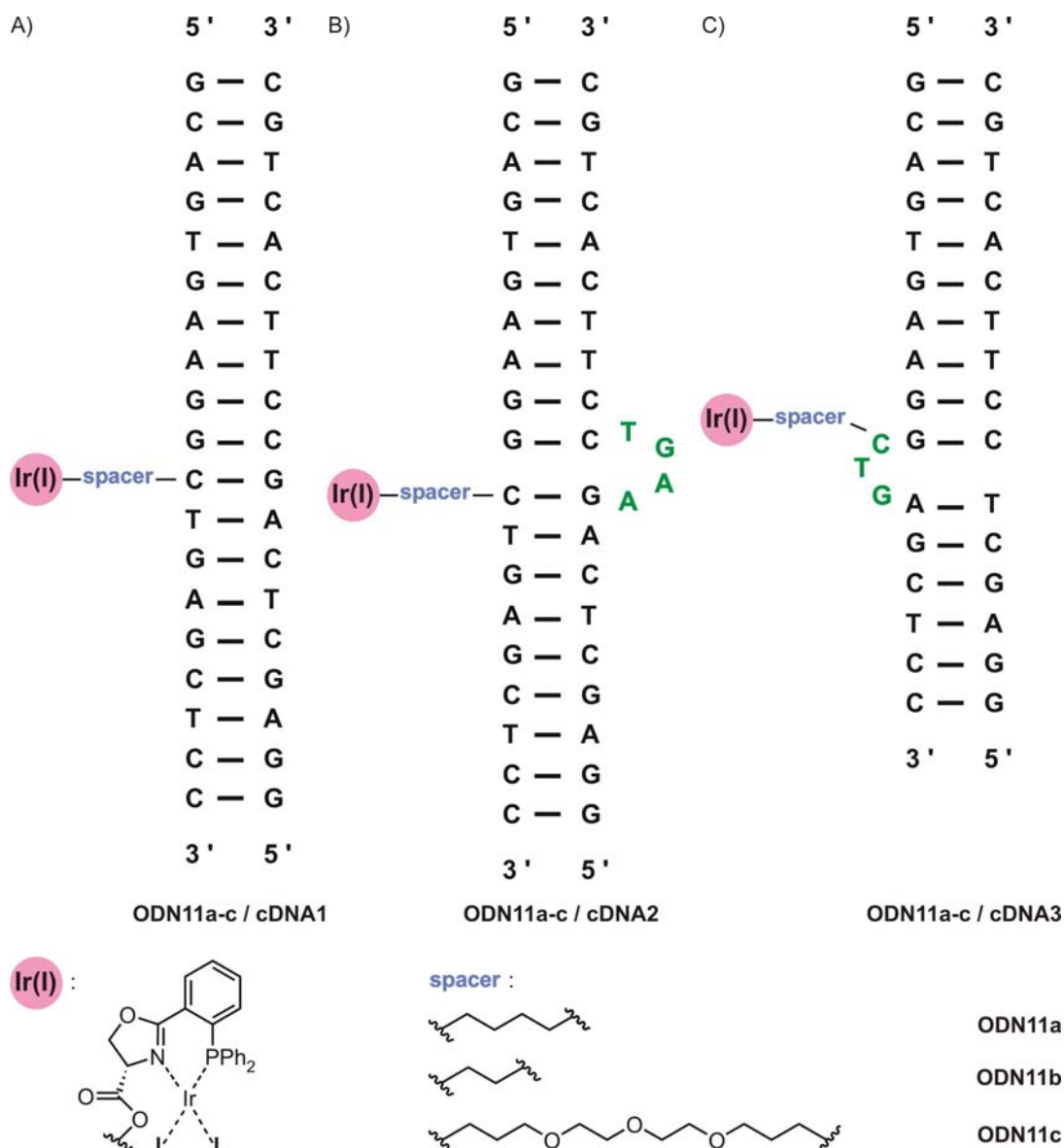


Figure 3.25. Double-stranded DNA-appended Ir(I)-phosphinooxazoline complexes. **L** denotes solvent molecule, chloride ion (from the $[\text{Ir}(\text{cod})\text{Cl}]_2$ precursor), or other coordinating species.

Contrary to our expectations, the catalytic activity of DNA-bound Ir-PHOX complexes could not be restored by blocking the oxygens and nitrogens on the Watson-Crick edge of the purine or pyrimidine bases by DNA duplex formation (entries 6-14 vs 3 and 4). It seems that all designed double-stranded DNA constructs still provide coordinating moieties responsible for formation of catalytically inactive species (entries 6-14 vs 1

and 2). At first glance, we assumed that the only available donor atoms after Watson-Crick base pairing are the N7 nitrogen atoms of deoxy-adenosine and -guanosine residues. Moreover, these sites are localized at the floor of the major groove of the B-DNA duplex (one example of dG=dC base-pair positioning towards the B-DNA major and minor grooves is shown in Figure 3.5). It is known that a functional tether attached at the N4-exocyclic amine of deoxycytidine residue protrudes out into the major groove space.^[255, 306, 307] Therefore we expect that the phosphinooxazoline moiety and its resulting iridium-complex would be specifically positioned in the major groove in close proximity to the presumably coordinating N7 atoms of adjacent dG and dA nucleobases^[305] (Figure 3.26 A).

Table 3.12. Iridium(I)-catalyzed allylic amination of branched allyl acetate **21** with morpholine with double-stranded DNA-appended PHOX ligand.^[a]

Entry	PHOX	DNA-PHOX	Complementary DNA			Conversion ^[b] [%]	E _c ^[c] [%]
	Ligand	Ligand	cDNA1	cDNA2	cDNA3		
1	-	-	-	-	-	44	n.d.
2	L4	-	-	-	-	65	<1
3	-	ODN11a	-	-	-	8	3
4	-	ODN11b	-	-	-	14	2
5	-	ODN11c	-	-	-	23	<1
6	-	ODN11a	+	-	-	8	<1
7	-	-	-	+	-	3	3
8	-	-	-	-	+	7	2
9	-	ODN11b	+	-	-	22	<1
10	-	-	-	+	-	7	7
11	-	-	-	-	+	15	<1
12	-	ODN11c	+	-	-	18	<1
13	-	-	-	+	-	3	6
14	-	-	-	-	+	6	n.d.

[a] Reaction conditions: 0.25 μmol **21**, 0.63 μmol **22** (1.1 equiv), 100 mM NaClO₄, 5 mM Mg(ClO₄)₂, 50 μL reaction volume, 0.5 mol% [Ir(cod)Cl]₂, 1.2 mol% **L4** (entry 2), 1.4 mol% **ODN11a-c** (entries 3-14), r.t., 19 hours. [b] Conversion determined by gas-chromatography with dodecane as internal standard. [c] Determined by HPLC, detection wavelength $\lambda = 220$ nm, t_R(**24**) = 10.8, 12.4 min.

Molecular modelling was further used to gain insight into possible intramolecular interactions within these molecules. Theoretical models based on quantum mechanical calculations have been proposed for the amino tether-functionalized Ir-**L5** complexes. The energy-minimized structures, that fairly resemble the published X-ray crystal structure of homologues π -allyl Ir(III)-complexes,^[68] were then used to estimate the distance between the iridium atom and the carbon C1 of the linker, directly attached at the dC nucleobase (Figure 3.26 B). This measurement gives the theoretical, linker-dependent distance of the metal centre within the DNA duplex, and consequently the

maximal interaction sphere with nucleobases. Based on these calculations, we assumed that the iridium ion can reach either the deoxyguanosine residues present above and below the modified deoxycytidine ($5' \rightarrow 3'$, dG = dC base pairs 9, 10, and 13) or the dG directly involved in Watson-Crick pair with the PHOX-tethered dC (dG = dC base pair 11) (Figure 3.26 A).

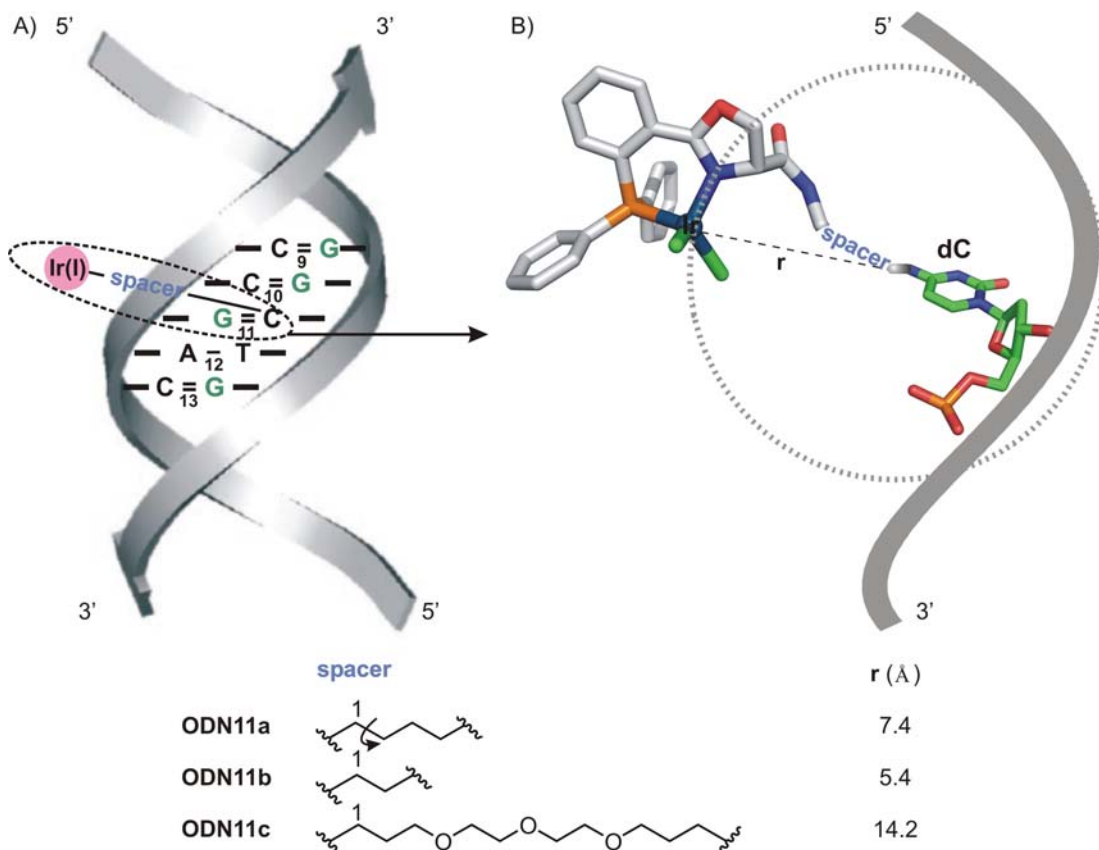


Figure 3.26. A) Localization of the Ir(I)-L5 complex inside the B-DNA duplex (left). B) Theoretical model of the dC-tethered-Ir(I)-L5 complex within the DNA. The model of the Ir-PHOX complex was constructed in Chem3DDraw and MM2+ minimized (two coordinating chlorine atoms were chosen for simplicity of the model). The theoretical maximal free rotation (r) allowed by the spacer was estimated in Chem3DDraw using energy-minimized structures.

To confirm this hypothesis, we focused on applying specific structural changes in the nucleotide sequence of the DNA-based PHOX ligands. Two new sets of DNA-PHOX conjugates were prepared, in which the above-mentioned potentially coordinating residues located on the sense strand were replaced by either the weakly coordinating 2'-deoxyadenosine or the non-coordinating 7-deaza-ribo-guanosine. Moreover, the base composition was slightly changed in the former case, in order to ensure a dG/dC content and a subsequent thermal stability comparable to the initial duplexes. For the second type of substitution, the remaining DNA sequence was conserved.

40 μM and the reactions were carried out on a 50 μL scale. The results of the catalysis attempts are given in Table 3.14.

Table 3.14. Iridium(I)-catalyzed allylic amination of branched allyl acetate **21** with morpholine **22** with single- and double-stranded DNA-appended PHOX ligand **ODN12a-c** and **ODN13**.^[a]

Entry	DNA-PHOX Ligand	[Ir] [μM]	Complementary DNA or RNA ^[b]			Conversion ^[c] [%]
			cDNA3	cDNA4	cRNA	
1	-	40	-	-	-	34
2	ODN12a	40	-	-	-	30
3	ODN12b	40	-	-	-	24
4	ODN12b	40	-	+	-	20
5	ODN12b	40	-	-	+	18
6 ^[d]	ODN12a	20	-	+	-	16
7 ^[d]	ODN12a	20	-	-	+	11
8 ^[d]	ODN12c	23	-	+	-	8
9 ^[d]	ODN12c	23	-	-	+	18
10 ^[e]	ODN13	30	+	-	-	36

[a] Reaction conditions: 0.25 μmol **21**, 0.63 μmol **22** (1.1 equiv), 100 mM NaClO_4 , 5 mM $\text{Mg}(\text{ClO}_4)_2$, 50 μL reaction volume, r.t., 19 hours, 1.0 mol% **ODN12a,b**, unless stated otherwise. [b] **cDNA3**: 5'-GG AGC TCC TTC ACT GC-3'; **cDNA4**: 5'-AG CGC TTA GTT ATC GCT GC-3'; **cRNA**: 5'-AG CGC UUA GUU AUC GCU GC-3'. [c] Conversion determined by gas-chromatography with dodecane as internal standard. [d] 0.5 mol% **ODN12a,c**. [e] 0.8 mol% **ODN13**.

The data show that by substituting the dG nucleotides on the sense strand in close proximity to the metal complex attachment site, the catalytic activity of the DNA-tethered Ir-PHOX complexes attached to DNA could be generally restored. Nevertheless, it appears that the dA residue exhibits weak iridium binding strength through its N7 site, as indicated by the slightly lower conversion obtained with the **ODN12a,b** conjugates (entries 2-7 versus 1). The DNA domain controlled by the long tether carrying the phosphinooxazoline moiety in **ODN12c** includes several remote dG residues that, beside those involved in the dG=dC base-pairs 9, 10, and 13, are apparently in charge of interactions with the iridium ion, leading to reduced catalytic activity, as observed with the **ODN12c/cDNA4** duplex (entry 8). However, the DNA/RNA analogue, generated from **ODN12c** and its complementary **cRNA** appeared to behave differently and higher reaction conversion was attained (entry 9). Since these two constructs adopt distinct helical forms, one can speculate that the specific accommodation of the attached Ir-**L5** complex in the A-DNA duplex rules out to some extent the unfavourable interactions with the DNA coordinating sites. Notably, the best result was achieved with the 7-deaza-ribo-guanosine-containing DNA construct **ODN13/cDNA3** (entry 10). In this case, the two-carbon linker-appended Ir-PHOX complex positions itself into the bulge, approaching only the nucleobases that can not

compete for metal coordination: 7-deaza-G above and dT below the tethering site. This results in no observable inhibition effect on the catalytic activity. All these studies need to be reconciled in order to fully understand whether all three ^9dG , ^{10}dG , and ^{13}dG nucleobases or combinations of them are responsible for disrupting the distinct binding motif provided by the bidentate DNA-appended phosphinoxazoline ligand.

The enantioselectivity was in all cases very poor (<3%). The length of the linker carrying the iridium complex seems to play an important role in the stereoselectivity of the catalytic species.^[146, 200] At this point, we believe that all three chosen tethers are too long and they presumably minimize the interactions between the DNA and the bound iridium(I) catalyst, yielding a weak transfer of chirality from the DNA backbone to the metal active site.

4 Conclusions and Outlook

The incorporation of transition metal complexes into DNA and RNA is an important objective for the development of functional biomolecules with potential applications as therapeutics, artificial nucleases, and as nanotechnology construction material. Inspired by the seminal work of Whitesides, who showed that asymmetric catalytic hydrogenations could be performed by anchoring an achiral Rh^{I} complex in a chiral cavity of the protein avidin, we aimed at embedding transition metal complexes in nucleic acids folds in order to generate nucleic acid-based hybrid catalysts. In addition, the use of combinatorial methods in the later stages of the project is expected to assist the quick development of artificial metallo-DNAzymes and -ribozymes with the desired activity and selectivity.

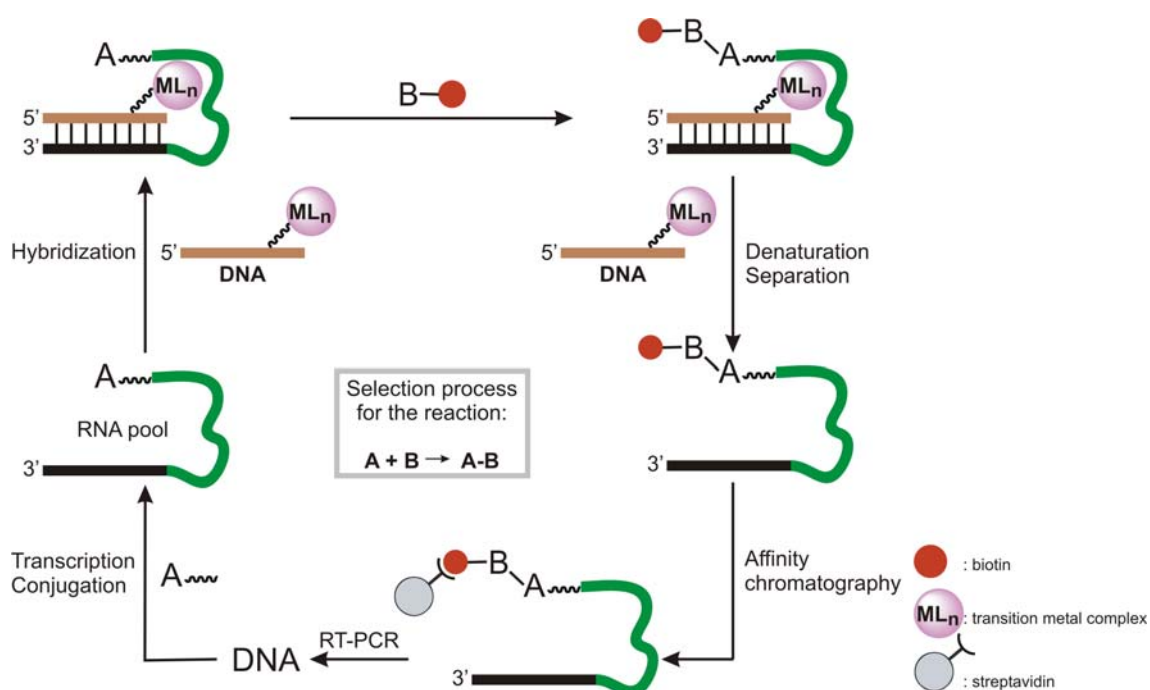


Figure 4.1. *In vitro* selection of RNA-based hybrid catalysts with DNA-appended transition metal complexes.

In this respect, a SELEX-type strategy devised for screening combinatorial libraries of up to 10^{15} metal-binding nucleic acids, followed by PCR amplification (Figure 4.1) (and, in some cases, diversification), would be a valuable tool towards hybrid catalysts, exclusive of the high-throughput-screening systems required by the evolutive

development of enantioselective enzymes. *In vitro* selection of RNA-hybrid catalysts remains probably a difficult approach since it requires a proper combination of structural and functional information from both nucleic acids and organometallic chemistry. In order to establish a robust selection scheme, several strategies were sought to allow for a precise positioning of the metal complex within the RNA fold. As discussed in the first part of Chapter 3.1, the most suitable way to provide the system with the necessary ligand for transition metal coordination consists of employing short DNA/RNA hybrids, with the DNA acting as a metal chelator-carrier oligonucleotide. This is the key step in the selection cycle, where a modified RNA library is created by simply carrying out a hybridization step with a suitably functionalized DNA strand (Figure 4.1).

At the moment we started this work, there was no precedent for nucleic acid-based hybrid catalysts. The major challenges in the development of hybrid catalysts based on DNA or RNA and transition metal complexes are in the field of asymmetric catalytic carbon-carbon and carbon-heteroatom bond forming reactions. Since the most powerful catalysts for these reactions are based on phosphorus ligands, we attempted to covalently attach achiral phosphite units at the 5'-terminus of the DNA sequences. Despite the successful assembling of such DNA conjugates using solid-phase synthesis and phosphoramidite ligand precursors, the desired DNA-appended phosphite could not be isolated due to its very low stability under the conditions used in purification. However, the problematic isolation of these conjugates could be overcome by the pre-formation of the corresponding rhodium(I) complex that was reasonably stable during the deprotection and cleavage of the resin-bound, functionalized oligonucleotide (Chapter 3.1.1)

The derivatization of DNA with a second class of phosphorus based ligands, namely phosphines, has been then envisioned as a suitable approach to modifying oligonucleotides with versatile ligands for transition metal coordination. An efficient post-synthetic strategy for the site-specific incorporation of mono- and bisphosphine, as well as phosphinoxazoline ligands into DNA sequences has been established. Parallel synthesis of various DNA precursors bearing a primary alkylamino functionality that can be selectively addressed was achieved by the one-pot conversion, deprotection and cleavage of convertible nucleoside-containing oligomers with diamines (Chapter

3.1.2.1). The subsequent coupling of amino-modified oligonucleotides with PYRPHOS, BINAP and PHOX ligands equipped with a carboxyl group allowed the attachment of the phosphine moieties at defined predetermined internal sites (Figure 4.2) (Chapter 3.1.2). Phosphine-containing oligonucleotides and their phosphine sulfide analogues were characterized by mass spectrometry (MALDI-TOF and FT-ICR-ESI) and their stability after purification and isolation systematically investigated. While the DNA-appended PYRPHOS ligand was quickly oxidized, BINAP and PHOX conjugates showed high stabilities, making them useful precursors for the development of metal-containing oligonucleotides. The approach described here provides new chelating functionalities for introducing metal centres at well-defined positions in DNA or RNA sequences and a unique collection of DNA-based phosphine ligands for creating efficient catalysts (Chapter 3.2.3). In addition, the combination with spacers differing in length and structure (Figure 4.2) might be relevant for the interactions between the transition metal complex and the biopolymer backbone.

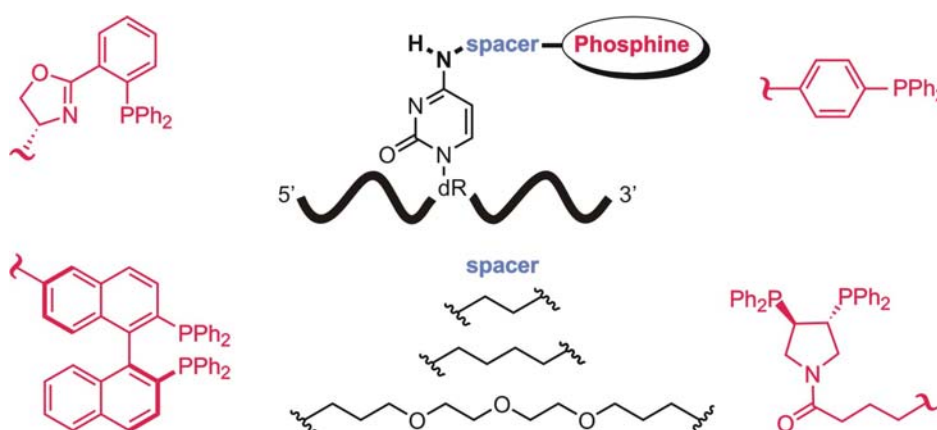


Figure 4.2. Site-specific incorporation of phosphine ligands into DNA sequences.

In addition to the synthetic challenges for incorporation of transition metal complexes, one barrier to expanding the applications of DNA and RNA in asymmetric organometallic catalysis stems from finding suitable target reactions that proceed in the presence of water and are compatible with the use of nucleic acids. Although an increasing number of transition metal-catalyzed transformations in aqueous mixtures are being reported, several reaction parameters and conditions had to be systematically examined and revised in order to achieve proper model systems compatible with the structure and properties of nucleic acids. Our studies on the preparation and stability of

mono- and bisphosphine- and phosphinooxazoline-based complexes with transition metals (*e.g.*, palladium, platinum, rhodium, iridium) demonstrated that these systems tolerated well water as cosolvent and could be easily handled in the laboratory atmosphere (Chapter 3.2.1). These findings together with the high affinity for transition metals make phosphorus ligands certainly the entities of choice for embedding transition metal complexes in DNA and RNA folds and creating metal-based catalytic nucleic acids.

From the wide range of homogeneous processes that phosphine- and phosphino-oxazoline-transition metal complexes can accelerate, commonly in neat organic solvent, two model reactions were selected. The rhodium(I)-catalyzed 1,4-addition and iridium(I)-catalyzed allylic amination proceeded efficiently in aqueous medium (*e.g.*, up to 70% water in allylic aminations), at room temperature, even with low catalyst concentration (*e.g.* 0.1 mM concentration of iridium catalyst). These findings were a successful event in our long-standing efforts to establish optimal systems, which wellmatch nucleic acids properties. In our hands, the ligand of choice for the 1,4-addition of phenyl boronic acid to 2-cyclohexen-1-one (Scheme 3.10) appeared to be the BINAP ligand **L8**. The best conversion was obtained with the isolated $[\text{Rh}(\text{nbd})\text{BINAP}]\text{BF}_4$ catalyst which was found superior to the related complex generated from the PYRPHOS ligand (Chapter 3.2.2). Our preliminary results using mono- and biphosphine ligands stimulate the applications of the DNA-appended BINAP in rhodium-catalyzed conjugate additions. For the convenient test of the DNA-based systems, additional optimization of the reaction conditions (concentration of the catalyst and substrates, water content) and investigation of the degree of enantioselectivity induced by the BINAP itself have still to be done.

In the second model reaction employed in this work, the *in situ* prepared Ir(I)-PHOX complexes afforded amination products in good yields, starting from the branched racemic phenyl allyl acetate, while the catalyst was found ineffective with the isomeric linear substrate (Scheme 3.12). Significant rate acceleration was observed when 70% water was used as cosolvent in aminations of the branched substrate with morpholine. Under the same conditions, the linear acetate remained unreactive, albeit slight enhancement of the reaction rate was observed at elevated temperature. Although the achieved conversion is very modest by conventional catalysis' standards, this system

introduces an interesting approach towards *in vitro* evolution of nucleic acid hybrid catalysts on the basis of stability and activity at high temperature. More in detail, SELEX-type techniques could aid to the isolation of thermostable nucleic acid sequences that, upon recruiting the Ir(I)-PHOX complex, are capable of complementing its catalytic activity and finally make unreactive substrates accessible.

The very good conversions (>98%) afforded by Ir(I) complexes in the aminations of the branched starting material, under environmentally friendly conditions, and at low catalyst loading (0.5 mM) (Chapter 3.2.3.2) contribute to the continued efforts of expanding the scope of biocatalysis. In addition, the novel chiral PHOX derivatives **L5** and **L6** reported in this work are attractive candidates for applications in organometallic catalysis, such as hydrogenations, Heck reactions or hydrosilylations. The ligand **L6** possesses suitable functionality for further derivatization, such as dendrimer fixation, and finally generation of metallodendrimer catalysts. By the virtue of the so called “dendrimer effect”, high levels of selectivity in asymmetric transformations can be enforced. On the other hand, this PHOX derivative can undergo functionalization with solid supports and assist formation of immobilized catalysts. This approach would allow new applications of PHOX ligands in heterogeneous catalysis.

Importantly for our purposes, the Ir(I)-PHOX(**L5**) complex (0.05-0.10 mM) remained highly active in the allylic amination reaction in the presence of unmodified DNA and high concentration of salts. This observation led to the conclusion that no undesired interactions between the transition metal ion and the DNA coordinating sites occurred that could shut down the reaction. Interestingly, no kinetic resolution on the branched racemic substrate and, implicitly, enantioselectivity could be achieved, despite the stereogenic nature of the PHOX-based catalysts. Since allylic amination reactions do not exclusively rely on a single mechanism as source of asymmetry, the origin of stereoselectivity remains difficult to understand at this stage. The mechanism by which the ligand can transfer its chirality with high fidelity to the amination product, or by which the steric effects of the amine nucleophile contribute to enantiodiscrimination make definitely the object of interesting upcoming studies.

Nevertheless these data open the way for exploring the catalytic potential of nucleic acids. As already outlined in the “Objectives” section of this work, the low levels of enantioselectivity induced by conventional transition metal catalysts could be surpassed

by making use of biopolymers. Two possibilities may arise: 1) the biopolymer exerts exclusive stereocontrol on the reaction outcome, or 2) the steric information carried by a chiral ligand is enriched by that of the biopolymeric part.

We attempted to assess to what extent synthetic 19mer DNA sequences may assist the transfer of chirality in allylic amination reactions. We considered that the DNA-based ligands were attractive scaffolds for transition metal catalysts due to the fact that they could be easily engineered and well-defined secondary structures based on Watson-Crick base pairing could be designed. Single-stranded DNA-PHOX conjugates were initially tested in the allylic amination of the branched racemic allyl acetate with morpholine, in 70% water, as model reaction. Preliminary attempts, in which DNA sequences containing a 2'-deoxyguanosine-rich domain in close proximity to the ligand attachment site were employed, yielded lower conversions compared to those obtained when the non-bound iridium(I)-PHOX complex was used instead (Chapters 3.2.3.2 and 3.2.3.3). A similar trend was observed for all tethered DNA-PHOX systems, independently of the length of the spacer carrying the ligand. These results evoked several key questions: 1) Can the iridium(I) complex be selectively formed with the DNA-appended bidentate PHOX ligand? 2) Can other binding sites for the transition metal be found in the DNA molecule? 3) Can the phosphate units and nucleobase heteroatoms contribute to the first coordination sphere? One possible answer might come from our early observations discussed above, on conserved catalytic activity of both $[\text{Ir}(\text{cod})\text{Cl}]_2$ precursor and pre-formed Ir(I)-PHOX complex in the presence of unmodified DNA. According to these results, one could assume that complex formation between the iridium(I) precursor and the DNA-appended PHOX ligand rendered a more precise and closer localization of the metal ion next to potential coordinating sites of the DNA backbone. As a result, the adjacent phosphate units or/and the nucleobase heteroatoms might directly participate in coordination and drastically influence the catalytic properties of the transition metal complex. Since mono- and divalent cations were used in large excess in the catalytic reactions, it has been assumed that the phosphodiester linkages were apparently shielded. In this case, it is mainly the nucleobase nitrogen and oxygen donor atoms to compete for the free metal coordination sites. To support this hypothesis, we have selected DNA/DNA and DNA/RNA hybrid systems (Chapter 3.2.3.4) in which the complementary strand sequesters most of the

nucleobase heteroatoms through Watson-Crick base-pairing, making them inaccessible for metal coordination. In addition, structural diversity has been introduced in the DNA systems and oligonucleotide sequences have been designed that upon simple hybridization induced the formation of three or four nucleotides bulge motifs. In these constructs, the transition metal complex is embedded in the double helix structure, and additionally located within the bulge in the sense strand or flanked by the bulge of the antisense strand (Figure 3.25). In all cases, no observable catalytic effect of the DNA-anchored iridium(I)-PHOX complex was obtained (Chapter 3.2.3.4). Based on these results we concluded that the N7 nitrogen atoms from the non-Watson Crick edge of the purines might be the single sites prone to direct coordination and formation of catalytically inactive species. To shed light on these observations, we evaluated the putative interaction sphere of the iridium ion with the nucleobases within the DNA helical model, based on the translational and rotational mobility induced by the covalent tethering of the metal complex (Figure 3.26). Indeed, several 2'-deoxyguanosine residues are directly located within this domain, in close proximity to the ligand attachment site. Notably, by exchanging particular neighbouring dGs for either the 7-deaza-ribo-guanosine or 2'-deoxyadenosine, the catalytic performance of the Ir-PHOX complexes anchored to the DNA could be restored (Chapter 3.2.3.4). Interestingly, the dG nucleotide directly involved in Watson-Crick base-pairing with the complementary PHOX-appended dC is apparently accepted for maintaining efficient catalytic properties. However, in all cases, no chiral induction was obtained starting from racemic substrates, probably owing to the lack of structural constraints and also intimate contact between the DNA helix and the catalytic metal centre. This might be explained by the flexibility and rather long distance introduced by the linkers carrying the metal complex, although a two-carbon spacer was expected to confer stereodiscriminating abilities on the system.

The results presented here are the first examples on applications of oligonucleotides-based ligands in organometallic catalysis and they contribute to the fundamentals of exploring the potential of nucleic acids in asymmetric transformations. Several possibilities could therefore be considered for the future. Firstly, the catalytic performance of the DNA-based ligands can be improved by rationally designing the nucleotide sequence, the modification position, the tether length and the secondary

structure elements. For example, DNA constructs ranging from simple, structurally distinct DNA/DNA and DNA/RNA hybrids to nucleic acid systems containing highly-structured motifs (*e.g.* branched DNA, hairpins, internal loops, three- and four-way junctions) (Figure 4.3) offer access to a large variety of chiral, readily available targets for covalent anchoring of transition metal complexes.

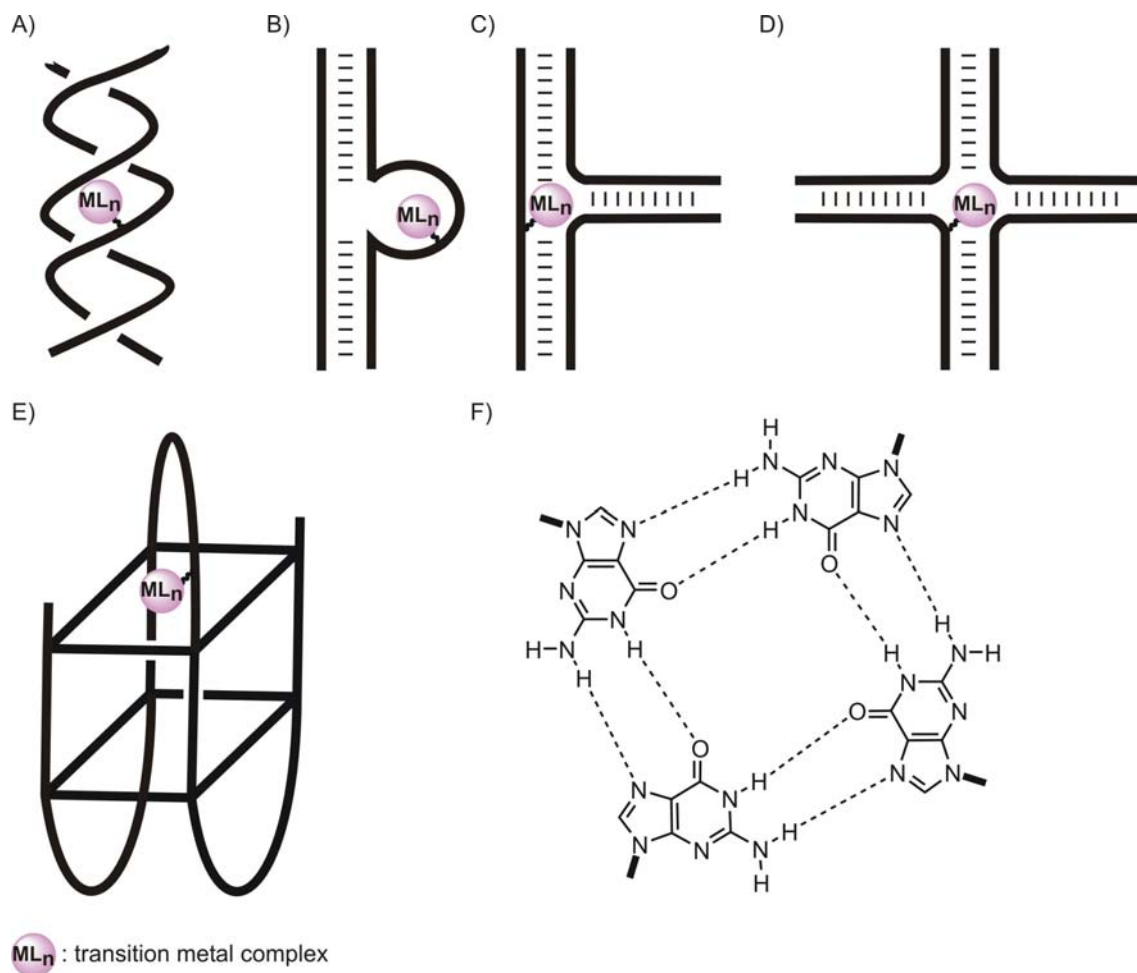


Figure 4.3. Proposed structures for embedding transition metal complexes and construction of DNA-based catalysts. A) DNA/DNA or DNA/RNA duplexes. B) Double helix structure with internal loop. C) Three-stem junction DNA structure. D) Four-stem junction DNA structure. E) DNA G-Quadruplex. F) Hydrogen bonding pattern of the G-tetrad.

Our modular synthetic strategy of DNA-ligand assembling from convertible nucleotide, diamine and functionalized ligand components could be further tuned for introducing shorter or conformationally constrained tethers and, finally creating selective DNA-based catalysts. Moreover, the data described above provide valuable information regarding the nucleobase requirements for adequate DNA sequence design and minimization of the critical first sphere coordination interactions that lead to inhibition

of the catalytic activity. Nevertheless, the distinct structural features of the G-quadruplexes (structural elements found in the telomere ends of the chromosomes) (Figure 4.3) might offer an intriguing alternative approach to the design of G-poor stretches as a tool of preventing purine coordination. More in detail, one poly(G) strand can assemble in a three-dimensional structure containing two (or more) G-quartets (or G-tetrads), the strand contributing four G residues to each G-tetrad. The guanine tetrads can stack upon each other to form four-stranded structures with a guanine tetrad core. This type of intermolecular arrangement may adopt a basket-like conformation, in which a distinct loop connecting diagonally related strands is formed (Figure 4.3). This particular structural element could be engineered to accommodate a phosphine ligand-tethered dC residue and to allow for subsequent location of the transition metal ion in a precise, resourceful cavity. Since each G residue of the core is involved in both Watson-Crick and Hoogsteen base-pairing (Figure 4.3), one might assume that a G-quadruplex would also provide a favourable coordination environment. The excellent recognition properties of G-quadruplexes could then be used for effecting transfer of chirality to the metal-catalyzed reaction.

The *de novo* synthesis of nucleic acid catalysts entirely based on rational design, combined with the rather time-consuming screening for activity and selectivity can be a difficult task. Combinatorial techniques, often called “shotgun” techniques, offer a valuable alternative based on the probability that the desired catalyst is represented in a library of randomly synthesized molecules. The experimenter’s efforts required by the conventional screening of rationally designed sequences are eliminated in a SELEX-type strategy, by the use of “column chromatography” methods to isolate the catalytically active species, as described at the beginning of this chapter. Hence, conducting *in vitro* selection of RNA hybrid catalysts, assisted by the ligand-DNA carrier and the transition metal precursor, is anticipated to facilitate the discovery of novel catalysts for organometallic transformations. The capacity of RNA to fold, provide particular coordination cavities and binding pockets and thereby to exquisitely tailor the first- as well the second coordination sphere of the active site is expected to be explored through combinatorial strategies. The optimal transfer of chiral information from the RNA scaffold to the chemical reaction can be then achieved. The RNA catalyst could be subsequently evolved to a more selective/active species to generate artificial

ribozymes with custom-made properties. The SELEX scheme proposed in this work implies selection of RNA species exclusively based on their ability of accelerating the desired transformation. The isolated catalysts will be then submitted to screening systems for determining the level of stereoselectivity. Ideally, besides effecting control on the electronic properties, the selected RNA molecules will also be able to impart the desired steric information. Alternatively, a methodology that allows for simultaneous selection for stereoselectivity has to be implemented.

With only little precedent in the field of nucleic acid-based hybrid catalysts, the results reported here represent a step forward in the development of metallo-ribozymes and -deoxyribozymes and allow new research at the interface between the fields of transition metal catalysis and biocatalysis.

5 Materials and Methods

5.1 Standard Methods and Reagents

Standard methods, such as DNA/RNA ethanol precipitation, polyacrylamide gel electrophoresis (Rotiphorese DNA sequencing system), NAP G25 - gel filtration, spectrophotometric quantification of oligonucleotides, gel elution of nucleic acids, UV-shadowing, were carried out according to published protocols.^[308, 309] All reagents were purchased from Aldrich, Fluka, Acros Organics or Proligo (for oligonucleotide synthesis) and used without further purification. DMF and THF were purchased from Fluka in septum sealed bottles and kept under inert atmosphere (dry solvents over molecular sieves).

Reactions with air-sensitive compounds were performed under argon atmosphere using standard Schlenk techniques. Degassing of solvents and reaction mixtures containing O₂-sensitive phosphines was achieved through a minimum of three successive freeze-pump-thaw cycles.

TLC analyses were carried out using silica gel plates Polygram[®] Sil G/UV₂₅₄ (40×80 mm) from Macherey-Nagel. Flash chromatography was carried out on silica gel 40 μm from J.T. Baker. NMR spectra were recorded on Mercury Plus 300, Varian VNMR S 500, Bruker AC-300, or DRX-300 spectrometers. ¹H and ¹³C{¹H} NMR spectra were calibrated to TMS on the basis of the relative chemical shift of the solvent as an internal standard. ³¹P{¹H} NMR spectra were calibrated to an external standard (85% H₃PO₄). Abbreviations used are as follows: s = singlet, d = doublet, t = triplet, m = multiplet, bs = broad singlet, bd = broad doublet. FAB and EI mass spectra were recorded on a JEOL JMS-700 sector field mass spectrometer. MALDI-TOF mass spectra were recorded on a Bruker BIFLEX III spectrometer. ESI MS analysis for small compounds was performed on a Finnigan MAT TSQ 700 spectrometer.

5.2 Synthesis of Phosphorus Ligands and their Transition Metal Complexes

(2-Diphenylphosphine)-4-benzoic acid **L1** and disodium bis(4-sulfonato-phenyl)phenylphosphine (TPPDS) **L7** were purchased from Sigma-Aldrich. Bisphosphines **L2**^[18, 19] and **L3**^[50, 310] are derivatives of the well-known ligands pyrphos and BINAP, and were prepared according to literature procedures. Compound **L2** was synthesized starting from (*R,R*)-3,4-bis(diphenylphosphano)pyrrolidine. For **L3** and **L8** preparation, the commercially available (*S*)-2,2'-dihydroxy-1,1'-binaphthalene was used.^[250] Phosphinooxazoline ligand (*S*)-2-[2-(diphenylphosphino)phenyl]-4-(1-methylethyl)-4,5-dihydrooxazole (**L4**), [Pt(cod)Cl]₂, PdCl₂(PhCN)₂, [Rh(cod)Cl]₂, [Rh(nbd)Cl]₂, [Rh(C₂H₄)₂Cl]₂ and [Ir(cod)Cl]₂ were purchased from Strem Chemicals. Rhodium(I)-complex [Rh**L8**(nbd)]⁺BF₄⁻ was prepared in our group.^[250] Compounds **L1-4** and **L7-8** are shown in Figure 5.1.

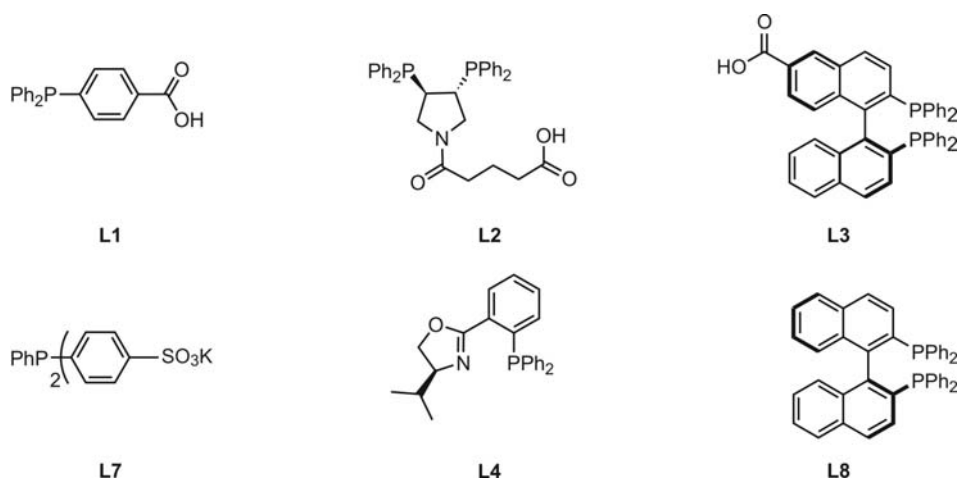


Figure 5.1. Phosphines **L1** and **L7**, bisphosphines **L2-3** and **L8**, and phosphinooxazoline **L4** ligands.

5.2.1 Synthesis of Phosphoramidite Ligands

The synthesis of phosphoramidite ligands **P1-3** (Figure 5.2) was accomplished according to published procedures,^[311, 312] by heating the commercially available neopentyl glycol (for **P1**) or 2,2'-biphenol (for **P2** and **P3**) with phosphorus trichloride, followed by treatment with appropriate amines (diethylamine, or *N,N'*-

diisopropylamine) according to Scheme 3.1.

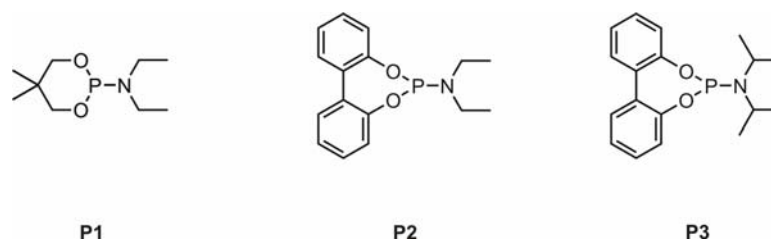


Figure 5.2. Phosphoramidites **P1-3**.

General procedure for the synthesis of phosphoramidites P1-3. A solution of diol (5.1 mmol), neopentyl glycol for **P1** (**1a**), or 2,2'-biphenol for **P2,3** (**1b**) in PCl_3 (4 mL, 45 mmol, 8.8 equiv) was refluxed for 4 h. The excess of PCl_3 was removed by distillation and the residual foam consisting of the phosphoryl chloride of the diol was diluted with toluene and concentrated (3 x 5 mL) to remove the excess of PCl_3 . The resulting yellow oil was dissolved in dry toluene (4 mL) and added to a solution of diamine (6.6 mmol, 1.3 equiv DEA (680 μL) for **P1,2** or DIPA (920 μL) for **P3**) and TEA (3 mL, 21 mmol, 4.1 equiv) in 5 mL dry THF. After being stirred for 16 h at room temperature, the reaction mixture was concentrated under vacuum and the crude product was purified by flash chromatography (column preconditioned with the eluent containing 1% TEA).

1,3-Propanediol-2,2-dimethyl-*N,N'*-diethylphosphoramidite (P1) The crude product was purified by flash chromatography (elution with EA/*n*-hex 3:97). Yield: 32%. Colorless oil. ^1H NMR (300 MHz; acetone- d_6) δ 3.81 (bd, 2H), 3.62 (dd, 2H), 3.13 (m, 4H), 1.21 (s, 3H), 1.07 (t, 6H), 0.75 (s, 3H). ^{31}P NMR (122 MHz; acetone- d_6) δ 147.62.

***O,O'*-(1,1'-Biphenyl-2,2-diyl)-*N,N'*-diethylphosphoramidite (P2)** The crude was purified by flash chromatography (elution with EA/*n*-hex 4:96). Yield: 42%. White solid. ^1H NMR (300 MHz; DMSO- d_6) δ 7.07 (d, 2H), 6.95 (t, 2H), 6.82 (t, 2H), 6.73 (d, 2H), 2.50 (m, 4H), 0.54 (t, 6H). ^{31}P NMR (122 MHz; DMSO- d_6) δ 149.67.

***O,O'*-(1,1'-Biphenyl-2,2-diyl)-*N,N'*-diisopropylphosphoramidite (P3).** The crude product was purified by flash chromatography (elution with EA/*n*-hex 5:95). Yield: 46%. White solid. ^1H NMR (300 MHz; acetone- d_6) δ 7.58 (d, 2H), 7.44 (m, 2H), 7.28 (dd, 4H), 3.58 (m, 2H), 1.25 (d, 12H). ^{31}P NMR (122 MHz; acetone- d_6) δ 152.12.

5.2.2 Synthesis of PHOX Ligands

Phosphinooxazolines **L5,6** (Figure 5.3) were synthesized starting from commercially available 2-(diphenylphosphino)-benzoic acid **2a** and L-serine methyl ester hydrochloride (H-L-Ser-OMe) **3**, followed by oxazoline ring formation in the presence of Burgess's reagent (*Route A*). An alternative synthetic route was also employed, starting from commercially available 2-iodo-benzoic acid **2b** and H-L-Ser-OMe (*Route B*), followed by oxazoline ring formation and palladium-catalyzed P-C cross coupling reaction with diphenylphosphine,^[270] according to Scheme 3.5.

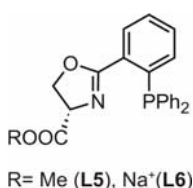


Figure 5.3. Phosphinooxazolines **L5-6**.

Route A

Preparation of (S)-N-(2-Hydroxy-1-carboxymethyl-ethyl)-2-(diphenylphosphino)-benzamide (4). To a stirred solution of 2-(diphenylphosphane)benzoic acid **2a** (1.5 g, 4.9 mmol, 1.1 equiv) and L-serine methyl ester hydrochloride **3** (0.693 g, 4.45 mmol) in CH₂Cl₂ (40 mL) were added TEA (0.68 mL, 4.9 mmol, 1.1 equiv) and EDC (0.94 g, 4.9 mmol, 1.1 equiv). The reaction mixture was stirred for 4 h at r.t., until the starting material was consumed according to TLC (EA/*n*-hex 1:1). The mixture was diluted with 100 ml CH₂Cl₂, washed with 5% NaHCO₃ (50 mL), 1 M HCl (50 mL) and brine (2 × 50 mL), dried over Na₂SO₄, filtered and concentrated under reduced pressure. The product was chromatographed on silica gel eluting with EA/*n*-hex 1:1 to yield the amide **4** (1.6 g, 3.92 mmol, 80%) as a white, amorphous solid. ¹H NMR (500 MHz; CDCl₃) δ 7.65 (dd, *J* = 7.4, 3.7 Hz, 1H), 7.42-7.29 (m, 12H), 7.01 (dd, *J* = 7.6, 4.3 Hz, 1H), 6.87 (bd, *J* = 7.0, 1H), 4.71 (m, 1H), 3.88 (m, 2H), 3.74 (s, 3H), 2.82 (bs, 1H). ¹³C NMR (126 MHz; CDCl₃) δ 170.62, 168.88, 140.79 (d, *J*_{C,P} = 25.3 Hz), 136.38 (d, *J*_{C,P} = 18.9 Hz), 136.31 (d, *J*_{C,P} = 19.1 Hz), 135.58 (d, *J*_{C,P} = 18.3 Hz), 134.23, 133.98, 133.82, 133.66, 130.52, 129.14, 129.03, 128.97, 128.79, 128.74, 128.66, 128.61, 127.87, 127.83, 62.86, 55.35, 52.73. ³¹P NMR (202 MHz; CDCl₃) δ -10.51. FAB MS: *m/z* 408.1 [M]⁺ (calcd

for $[\text{C}_{23}\text{H}_{22}\text{NO}_4\text{P}]^+$ 408.13).

Preparation of (S)-Methyl-2-(2-diphenylphosphino-phenyl)-4,5-dihydrooxazolo-4-carboxylate (L5). To a stirred solution of **4** (1.0 g, 2.5 mmol) in dry THF (20 mL) was added (methoxycarbonylsulfamoyl)triethylammonium hydroxide, inner salt^[313] (Burgess' reagent, 0.703 g, 2.95 mmol, 1.2 equiv). After being refluxed for 4 hours (TLC control: EA/*n*-hex 3:7), the reaction mixture was allowed to cool down to room temperature and diluted with 200 mL EA. The resulting solution was washed with water (2×100 mL) and brine (100 mL), and dried over Na_2SO_4 . Removal of the solvent under reduced pressure afforded the crude product as brownish oil. Purification by flash chromatography (elution with EA/*n*-hex 3:7, column preconditioned with the eluent containing 1% TEA) gave phosphinooxazoline **L5** as colorless oil (0.401 g, 1.13 mmol, 42%). ^1H NMR (500 MHz; CDCl_3) δ 7.92 (ddd, $J = 7.5, 3.5, 1.5$ Hz, 1H), 7.36-7.30 (m, 12H), 6.91 (ddd, $J = 7.6, 4.3, 1.0$ Hz, 1H), 4.69 (dd, $J = 10.6, 8.2$ Hz, 1H), 4.38 (t, $J = 8.4$ Hz, 1H), 4.26 (dd, $J = 10.5, 8.6$ Hz, 1H), 3.68 (s, 3H). ^{13}C NMR (126 MHz; CDCl_3) δ 171.08, 166.45, 139.30 (d, $J_{\text{C,P}} = 25.9$ Hz), 137.69 (d, $J_{\text{C,P}} = 11.9$ Hz), 137.50 (d, $J_{\text{C,P}} = 10.4$ Hz), 134.28, 134.11, 134.02, 133.85, 133.67 (d, $J_{\text{C,P}} = 1.9$ Hz), 130.95 (d, $J_{\text{C,P}} = 19.0$ Hz), 130.94, 130.36 (d, $J_{\text{C,P}} = 2.8$ Hz), 128.74, 128.61, 128.52, 128.46, 128.41, 128.35, 128.00, 69.10, 68.45, 52.50. ^{31}P NMR (202 MHz; CDCl_3) δ -4.80. EI MS: m/z 389.0 $[\text{M}]^+$ (calcd for $[\text{C}_{23}\text{H}_{20}\text{NO}_3\text{P}]^+$ 389.12).

Preparation of (S)-2-(2-diphenylphosphino-phenyl)-4,5-dihydrooxazolo-4-carboxylic acid sodium salt (L6). Compound **L5** (0.35 g, 0.90 mmol) was stirred in a 0.5 M solution of NaOH (3 mL) 6 hours at r.t. The reaction mixture was diluted with water (3 mL) and the product was precipitated by slow addition of acetone. After filtration and drying under vacuum, 0.34 g of the sodium salt **L6** was recovered (0.85 mmol, 95%, white solid). ^1H NMR (500 MHz; D_2O) δ 7.66 (dd, $J = 7.4, 3.0$ Hz, 1H), 7.10 (t, $J = 7.5$ Hz, 1H), 6.98-6.78 (m, 10H), 6.70 (t, $J = 7.5$ Hz, 1H), 6.55-6.50 (m, 1H), 4.17-4.11 (m, 1H), 3.97 (t, $J = 8.3$ Hz, 1H), 3.88-3.81 (m, 1H). ^{13}C NMR (126 MHz; D_2O) δ 178.16, 166.89, 137.24 (d, $J_{\text{C,P}} = 19.7$ Hz), 136.11 (d, $J_{\text{C,P}} = 7.9$ Hz), 135.87 (d, $J_{\text{C,P}} = 7.6$ Hz), 133.88, 133.75, 133.72, 133.59, 133.15, 131.73, 131.39, 131.23, 130.91, 130.24, 129.06, 128.73, 128.61, 128.59, 128.56, 71.20, 69.56. ^{31}P NMR (202 MHz; D_2O) δ -6.57. ESI MS: m/z 374.2 $[\text{M}-\text{Na}]^-$ (calcd for $[\text{C}_{22}\text{H}_{17}\text{NO}_3\text{P}]^-$ 374.10). Acidification results in oxazoline ring opening.^[271]

Route B

Preparation of (S)-N-(2-Hydroxy-1-carboxymethyl-ethyl)-2-iodo-benzamide (5). To a stirred solution of 2-iodo-benzoic acid **2b** (1.5 g, 6.05 mmol, 1.1 equiv) and L-serine methyl ester hydrochloride **3** (0.856 g, 5.50 mmol) in CH₂Cl₂ (40 mL) were added TEA (0.84 mL, 6.05 mmol, 1.1 equiv) and EDC (1.16 g, 6.05 mmol, 1.1 equiv). The reaction mixture was stirred 2 h at r.t., until the starting material was consumed according to TLC (EA/*n*-hex 3:7). The mixture was diluted with 100 mL CH₂Cl₂, washed with 5% NaHCO₃ (50 mL), 1 M HCl (50 mL) and brine (2 × 50 mL), dried over Na₂SO₄, filtered and concentrated under reduced pressure. The product was chromatographed on silica gel eluting with EA/*n*-hex 3:7 to yield the amide **5** (1.8 g, 5.16 mmol, 93%) as a white, amorphous solid. ¹H NMR (300 MHz; CDCl₃) δ 7.87 (m, 1H), 7.46-7.36 (m, 2H), 7.23 (ddd, *J* = 8.0, 7.2, 1.9 Hz, 1H), 6.77 (bd, 1H), 4.86 (td, *J* = 7.2, 3.4, 1H), 4.11 (d, *J* = 3.2, 2H), 3.83 (s, 3H), 2.51 (bs, 1H). ¹³C NMR (126 MHz; CDCl₃) δ 170.52, 169.31, 144.18, 139.93, 131.49, 128.37, 128.24, 92.41, 63.11, 55.13, 52.90. FAB MS: *m/z* 349.9 [M]⁺ (calcd for [C₁₁H₁₂INO₄]⁺ 349.98).

Preparation of (S)-Methyl-2-(2-iodo-phenyl)-4,5-dihydrooxazolo-4-carboxylate (6). To a stirred solution of **5** (1.5 g, 4.3 mmol) in dry THF (25 mL) was added (methoxycarbonylsulfamoyl)triethylammonium hydroxide, inner salt (Burgess' reagent, 1.23 g, 5.16 mmol, 1.2 equiv). After being refluxed for 4 hours (TLC control: EA/*n*-hex 1:4), the reaction mixture was allowed to cool down to room temperature and diluted with 200 mL EA. The resulting solution was washed with water (2 × 100 mL) and brine (100 mL), and dried over Na₂SO₄. Removal of the solvent under reduced pressure afforded the crude product as brownish oil. Purification by flash chromatography (elution with EA/*n*-hex 1:4, column preconditioned with the eluent containing 1% TEA) gave oxazoline **6** as colorless oil (0.852 g, 1.13 mmol, 60%). ¹H NMR (300 MHz; CDCl₃) δ 7.93 (dd, *J* = 8.0, 1.2 Hz, 1H), 7.66 (dd, *J* = 7.7, 1.7 Hz, 1H), 7.38 (dt, *J* = 7.6, 7.6, 1.2 Hz, 1H), 7.09-7.15 (m, 1H), 5.00 (dd, *J* = 10.6 Hz, 8.0 Hz, 1H), 4.62 (dd, *J* = 10.6, 8.8 Hz, 1H), 3.83 (s, 3H). ¹³C NMR (126 MHz; CDCl₃) δ 171.22, 166.87, 140.49, 132.79, 132.01, 131.02, 127.78, 94.49, 69.79, 68.67, 52.72. EI MS: *m/z* 331.0 [M]⁺ (calcd for [C₁₁H₁₀INO₃]⁺ 330.97).

Preparation of (S)-Methyl-2-(2-diphenylphosphino-phenyl)-4,5-dihydrooxazolo-4-

carboxylate (L5). In a Schlenk flask, **6** (800 mg, 2.42 mmol), dry DMF (4 mL) and TEA (370 μ L, 2.66 mmol, 1.1 equiv) were charged together and the resulting solution degassed. After addition of diphenylphosphine **7** (500 μ L, 2.90 mmol, 1.2 equiv), the solution was heated up to 80°C. A solution of Pd(OAc)₂ (10.87 mg, 48.4 μ mol) in 2 mL DMF was separately prepared and degassed. 1 mL from this solution (1 mol% final concentration of Pd catalyst) was added to the reaction mixture. The deep purple solution was further heated at 80°C until completion (monitored by TLC: EA/*n*-hex 3:7; 4 h). The reaction mixture was allowed to cool down at room temperature and diluted with 100 mL EA. The resulting solution was washed with brine (2 x 50 mL), the organic phase transferred via a stainless steel cannula in a Schlenk flask, and dried over Na₂SO₄. The solvent was removed under vacuum, and the residue loaded onto a silicagel column (elution with EA/*n*-hex 3:7, column preconditioned with the eluent containing 1% TEA) to obtain phosphinooxazoline **L5** a colorless oil (1.77 mmol, 688 mg, 73%).

5.2.3 Synthesis of Palladium(II)- and Platinum(II)-Phosphine Complexes

Dichlorobis[(4-carboxyphenyl)diphenylphosphine]-palladium(II) (8). Reaction of **L1** (49.0 mg, 0.16 mmol, 2.0 equiv) with PdCl₂(PhCN)₂ (30.7 mg, 0.08 mmol) in 4 mL acetonitrile, overnight, at room temperature, gave a yellow powder. The solid was filtered, washed with diethylether and dried, yielding 46.0 mg (0.06 mmol, 73%) Pd(**L1**)₂Cl₂ complex **8**. ¹H NMR (300 MHz; DMSO-*d*₆) δ 13.71 (bs, 2H), 7.99-7.97 (d, 4H), 7.76-7.31 (m, 24H). ³¹P NMR (122 MHz; DMSO-*d*₆) δ 24.58.

Dichlorobis[(4-carboxyphenyl)diphenylphosphine]-platinum(II) (9). The platinum complex was synthesized according to published procedure,^[314] using [Pt(cod)Cl]₂ and monophosphine **L1**. ¹H NMR (300 MHz; CD₃OD) δ 7.80-7.73 (bd, 4H), 7.60-7.57 (m, 8H), 7.47-7.40 (m, 8H), 7.32-7.29 (m, 8H). ³¹P NMR (122 MHz; CD₃OD) δ 14.34 (satellite due to 34% ¹⁹⁵Pt, *J*_{Pt,P} = 1852.2 Hz).

A similar procedure was used to prepare Pt(**L1**)₂Cl₂ complex **9** in 9:1 acetonitrile/H₂O. [Pt(cod)Cl]₂ (29.9 mg, 0.08 mmol) was dissolved in 0.6 ml acetonitrile and then treated with 3.4 mL aqueous solution (1:0.7 acetonitrile/100 mM TEAA in 80% acetonitrile

(buffer B)) of **L1** (98.0 mg, 0.32 mmol, 4.0 equiv) overnight, at room temperature, until a yellow precipitate was formed. The mixture was filtered, the resulting pale yellow solid washed with diethylether and dried, yielding 82.5 mg (0.10 mmol, 62%) Pt(**L1**)₂Cl₂ complex **9**. ¹H NMR (300 MHz; DMSO-*d*₆) δ 8.04-6.55 (m, aromatic). ³¹P NMR (122 MHz; DMSO-*d*₆) δ 18.44.

5.2.4 Synthesis of Platinum(II)-, Palladium(II)- and Rhodium(I)-PYRPHOS Complexes

Dichlorobis[(*R,R*)-*N*-(4-carboxylbutanoyl)-3,4-bis(diphenylphosphino)pyrrolidine]-palladium(II) (10**).** To a solution of Pd(PhCN)Cl₂ (38.4 mg, 0.1 mmol) in dichloromethane (2 mL), under argon, was added solid PYRPHOS **L2** (55.3 mg, 0.1 mmol) (1.0 equiv bisphosphine unit per Rh). The resulting yellow-orange solution was stirred at room temperature for 18 h. After filtration over Celite (2 cm), the solution was concentrated to 0.5 mL under reduced pressure. Upon addition of diethyl ether, an orange solid precipitated which was then filtered, washed with diethyl ether, and dried under vacuum (**10**: yield 78%, 56 mg, 0.07 mmol). ¹H NMR (250 MHz; DMSO-*d*₆) δ 7.96-7.48 (m, 20H), 3.46-3.31 (m, 4H), 2.90 (m, 1H), 2.65 (m, 1H), 2.12-1.88 (m, 4H), 1.52 (m, 2H). ³¹P NMR (101 MHz; DMSO-*d*₆) δ 42.45.

Dichlorobis[(*R,R*)-*N*-(4-carboxylbutanoyl)-3,4-bis(diphenylphosphino)pyrrolidine]-platinum(II) (11**).** To a solution of [Pt(cod)Cl]₂ (37.4 mg, 0.10 mmol) in dichloromethane (2 mL), under argon, was added solid PYRPHOS **L2** (110.6 mg, 0.20 mmol). The resulting yellow mixture was stirred at room temperature for 18 h and then passed through Celite (2 cm). The solvent was partially removed under reduced pressure and an identical amount of diethyl ether was added. The resulting yellow solid was filtered, washed with ether and dried under vacuum (**11**: yield 83%, 68 mg, 0.08 mol). ¹H NMR (250 MHz; CD₃OD) δ 7.77-7.39 (m, 20H), 3.61-3.39 (m, 4H), 2.88 (m, 1H), 2.68 (m, 1H), 2.09-1.89 (m, 4H), 1.61-1.46 (m, 2H). ³¹P NMR (101 MHz; CD₃OD) δ 26.38 (satellite $J_{\text{Pt,P}} = 1162.5$ Hz).

Dichlorobis[(*R,R*)-*N*-(4-carboxylbutanoyl)-3,4-bis(diphenylphosphino)pyrrolidine]-rhodium(I) (12**).** To a degassed solution of [Rh(cod)Cl]₂ (24.6 mg, 0.05 mmol) in acetonitrile (1 mL) was added a solution of **L2** (55.3 mg, 0.1 mmol, 1.0 equiv

bisphosphine unit per Rh) in degassed acetonitrile/water (6:4, 1 mL). The resulting solution was stirred overnight, at room temperature. An orange solid precipitated which was then filtered, washed with diethylether and dried, yielding 52.0 mg (0.07 mmol, 72%) Rh(L2)₂Cl₂ complex **12**. ¹H NMR (250 MHz; CD₃OD) δ 7.66-7.21 (m, 20H), 3.43-3.38 (m, 4H), 2.82 (t, 1H), 2.64 (t, 1h), 2.08-1.91 (m, 4H), 1.60-1.54 (m, 2H). ³¹P NMR (101 MHz; CD₃OD) δ 38.16 (m, 1P), 36.84 (m, 1P).

[(Bicyclo[2.2.1]hepta-2,5-diene)-[(R,R)-N-(4-carboxylbutanoyl)-3,4-bis(diphenylphosphino)pyrrolidine]-rhodium(I) (13). [Rh(nbd)Cl]₂ (20.8 mg, 45.2 μmol) and AgBF₄ (17.6 mg, 90.3 μmol, 2.0 equiv) were dissolved in freshly degassed acetone (5.5 mL) and stirred for 45 min at room temperature. The precipitated AgCl was filtered off (G4) and the filtrate was immediately degassed. To the resulting yellow solution was added solid PYRPHOS L2 (50.0 mg, 90.3 μmol, 2.0 equiv). The solution turned immediately deep orange. After stirring for 2 h at room temperature, the mixture was concentrated under reduced pressure and treated with diethyl ether until weak turbidity appeared. After overnight storage at -20°C, an orange solid was formed. The precipitate was filtered, washed with ether, and dried under vacuum. The desired [Rh(nbd)L2]⁺BF₄⁻ complex **13** was obtained as yellow-orange powder, in 72% yield (60 mg, 71 μmol). ¹H NMR (300 MHz; Acetone-*d*₆) δ 10.43 (bs, 1H), 8.07-7.24 (m, 20H), 5.66 (bs, 1H, nbd), 5.11 (bs, 1H, nbd), 4.22-3.86 (m, 2H, nbd), 3.40 (dd, 4H), 3.05 (bs, 1H), 2.83 (bs, 2H, nbd), 2.61 (bs, 1H), 2.25-2.18 (m, 4H), 1.95-1.64 (m, 2H), 1.19 (m, 2H, nbd). ³¹P NMR (122 MHz; Acetone-*d*₆) δ 36.92 (m, 1P), 35.63 (m, 1P). ESI MS (sample dissolved in acetonitrile): *m/z* 738.15 [M]⁺ (calcd for Rh(L2)(acetonitrile)₂⁺ [C₃₇H₃₉N₃O₃P₂Rh]⁺ 738.16).

5.2.5 Synthesis of Rhodium(I)- and Iridium(I)-PHOX Complexes

[(Bicyclo[2.2.1]hepta-2,5-diene)-[(S)-methyl-2-(2-diphenylphosphino-phenyl)-4,5-dihydrooxazolo-4-carboxylate]rhodium(I)]-tetrafluoroborate (14). In a Schlenk flask (under argon), 2,5-norbornadiene-rhodium(I) chloride dimer, [Rh(nbd)Cl]₂ (115.3 mg, 0.25 mmol), was dissolved in degassed acetone (20 mL). After addition of AgBF₄ (97.84 mg, 0.5 mmol, 2.0 equiv), the mixture was stirred at room temperature for 1 hour and then AgCl was filtered off. The resulting solution of [Rh(nbd)Solv₂]⁺BF₄⁻

was immediately degassed. Separately, PHOX ligand **L5** (101 mg, 0.26 mmol, 1.04 equiv) was dissolved in degassed acetone (2 mL) and pre-formed $[\text{Rh}(\text{nbd})\text{Solv}_2]^+\text{BF}_4^-$ in acetone (10 mL, 0.25 mmol) added. The resulting mixture was stirred at room temperature, for 14 hours, and then concentrated to small volume under reduced pressure.

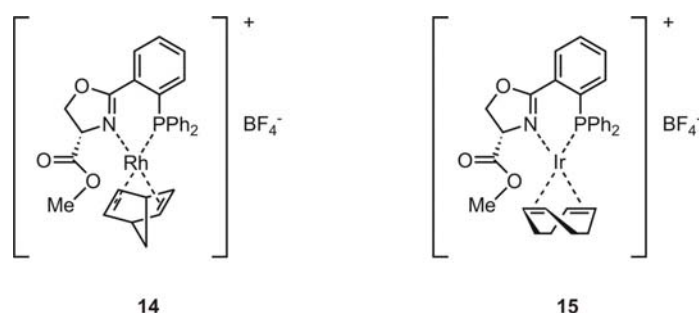


Figure 5.4. Phosphino-oxazoline-rhodium(I) and -iridium(I) complexes.

Addition of diethyl ether resulted in precipitation of an orange solid that was filtered in air, without protection against oxygen, washed with ether and dried under vacuum, affording $[\text{Rh}(\text{nbd})\text{L5}]^+\text{BF}_4^-$ complex **14** in 65% yield (95 mg, 0.16 mmol). ^1H NMR (300 MHz; CDCl_3) δ 8.20 (m, 1H), 7.83 (m, 1H), 7.34-7.63 (m, 11H), 7.12 (m, 1H), 5.92 (bs, 1H, nbd), 5.73 (bd, 1H, nbd), 5.06 (t, 1H), 4.95 (m, 1H), 4.70 (m, 1H), 3.96 (bs, 2H, nbd), 3.58 (bs, 1H, nbd), 3.44 (m, 1H, nbd), 1.50 (m, 2H, nbd). ^{31}P NMR (122 MHz; CDCl_3) δ 31.91 (d, $J_{\text{P,Rh}} = 168.9$ Hz). ESI MS: m/z 584.09 $[\text{M}]^+$ (calcd for $[\text{C}_{30}\text{H}_{28}\text{NO}_3\text{PRh}]^+$ 584.09).

[(1,5-cyclooctadiene)-[(S)-methyl-2-(2-diphenylphosphino-phenyl)-4,5-dihydro-oxazolo-4-carboxylate]iridium(I)]-tetrafluoroborate (15). Similar procedure as for the preparation of the complex **14**: $[\text{Ir}(\text{cod})\text{Cl}]_2$ (215.3 mg, 0.32 mmol) and AgBF_4 (250.1 mg, 0.64 mmol, 2.0 equiv) dissolved together in acetone (28 mL), then stirring for 1 hour at room temperature. After filtration of AgCl , the resulting solution of $[\text{Rh}(\text{nbd})\text{Solv}_2]^+\text{BF}_4^-$ (23 mL) was added to **L5** (300 mg, 0.77 mmol, 1.2 equiv per iridium ion). The complex formation was carried out at room temperature, for 1 hour. The workup was performed as described (see complex **14**), affording $[\text{Ir}(\text{cod})\text{L5}]^+\text{BF}_4^-$ complex **15** as red solid, in 78% yield (384.1 mg, 0.50 mmol). ^1H NMR (500 MHz; $\text{DMSO}-d_6$) δ 8.70-8.68 (m, 1H), 8.28-8.26 (m, 2H), 8.12-7.92 (m, 9H), 7.54-7.50 (m, 2H), 5.60 (dd, $J = 10.1, 4.1$ Hz, 1H), 5.42 (dd, $J = 9.3, 4.1$ Hz, 1H), 5.24 (m, 1H), 3.97

(s, 2H, cod), 3.75 (bs, cod), 2.92 (m, 4H, cod). ^{31}P NMR (122 MHz; DMSO- d_6) δ 14.95.

General procedure for the *in situ* preparation of (phosphinooxazoline)iridium(I) complexes in 100% dioxane and 3:7 dioxane/H₂O . Under argon atmosphere, 2.5 μmol $[\text{Ir}(\text{cod})\text{Cl}]_2$ (6.7 mg) were added to a solution of 5.5 μmol phosphinooxazoline ligand (8.2 mg **L4** or 8.5 mg **L5**, 2.2 equiv) in 0.5 ml degassed dioxane or 3:7 dioxane/H₂O mixture. The redish purple resulting solution was stirred for 30 min, at room temperature and then directly subjected to ^{31}P NMR analysis.

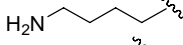
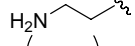
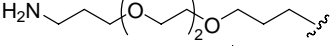
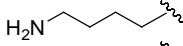
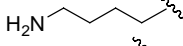
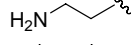
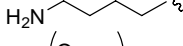
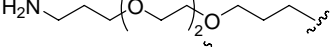
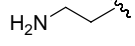
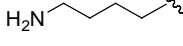
Phosphinooxazoline(L4)iridium (I) complex. ^{31}P NMR (202 MHz) δ 10.27 (dioxane, 10% CDCl_3); 15.64 (3:7 dioxane/H₂O, 10% D_2O).

Phosphinooxazoline(L5)iridium (I) complex. ^{31}P NMR (202 MHz) δ 8.84 (dioxane, 10% CDCl_3); 15.16 (3:7 dioxane/H₂O, 10% D_2O).

5.3 Oligonucleotides

DNA and RNA sequences employed in this work for preparation of single and double-stranded constructs carrying metal chelating moieties are shown in Table 5.1, in 5' to 3' orientation. Oligodeoxynucleotides **ODN1-5** (19mer) and their complementary strands **cDNA1-3** (19, 23, and 16mers) were prepared by standard automated solid-phase synthesis. Unmodified complementary 19mer sequences **cDNA4** ($\epsilon = 195700 \text{ L}\cdot\text{mol}^{-1}\cdot\text{cm}^{-1}$), **cRNA1** ($\epsilon = 173\,800 \text{ L}\cdot\text{mol}^{-1}\cdot\text{cm}^{-1}$), and **cRNA** ($\epsilon = 181900 \text{ L}\cdot\text{mol}^{-1}\cdot\text{cm}^{-1}$) were obtained from IBA in 1 μmol scale synthesis, as double HPLC purified solution.

Table 5.1. Oligonucleotide sequences.

ODN	Sequence	R
ODN1a		
ODN1b	5'-GC AGT GAA GGC ^R TGA GCT CC-3'	
ODN1c		
ODN2	5'-GC AGT GAA GGC TGA GCT CCT AC ^R C-3'	
ODN3 ^[a]	5'-GC AGT GAA GGC TGA GCT CCS C ^R C-3'	
ODN4a		
ODN4b	5'-GC AGC GAT AAC ^R TAA GCG CT-3'	
ODN4c		
ODN5a ^[b]	5'-GC AGT GAA XXC ^R TXA GCT CC-3'	
ODN5b ^[b]	5'-GC AGT GAA XXC ^R TXA GCT CC-3'	
cDNA1	5'-GG AGC TCA GCC TTC ACT GC-3'	-

cDNA2	5'-GG AGC TCA CAA GTC CTT CAC TGC-3'	-
cDNA3	5'-GG AGC TCC TTC ACT GC-3'	-
cDNA4	5'-AG CGC TTA GTT ATC GCT GC-3'	-
cRNA1	5'-GG AGC UCA GCC UUC UCA GC-3'	-
cRNA	5'-AG CGC UUA GUU AUC GCU GC-3'	-

[a] A decaethylene glycol spacer **S** was incorporated during solid phase synthesis. [b] **X** = 7-deaza-riboG

5.3.1 Automated Solid-Phase Synthesis

Solid-phase DNA synthesis was performed on an ExpediteTM 8909 automated synthesizer using the conventional phosphoramidite chemistry,^[315] dC or dG (*t*-butyl-phenoxyacetyl, TAC) controlled pore glass support (40 $\mu\text{mol/g}$, 500 \AA) and β -cyanoethyl-phosphoramidites containing base-labile TAC-protecting groups (Proligo). The decaethyleneglycol phosphoramidite **S** was prepared in our lab.^[250] 4-Triazolyl-deoxyuridine phosphoramidite was purchased from Glen Research and 7-deaza-guanosine phosphoramidite was obtained from ChemGenes. The exocyclic amine in 7-deaza-guanosine phosphoramidite was protected with the standard *iso*-butyryl group. The 2'-hydroxyl group was protected as a *t*-butyldimethylsilylether. Standard reagents employed in DNA solid-phase synthesis (deblocking reagent - dichloroacetic acid in dichloromethane, activator - dicyanoimidazole, oxidizing reagent - iodine in THF/H₂O, and capping reagent - *t*-butyl-phenoxyacetanhydride in acetonitrile), as well as acetonitrile (water content ≤ 10 ppm) were purchased from Proligo and Sigma Aldrich Fine Chemicals.

Solid-phase synthesis of ODNs was performed on 1 μmol or 15 μmol scale synthesis, usually leaving the terminal 4,4'-dimethoxytrityl (DMT) group on. The phosphoramidites were used as 0.067 M (DNA monomers), and 0.1 M (RNA monomer) acetonitrile solutions. The standard protocols provided by Applied Biosystems were optimized (Tables 5.2 and 5.3).

Table 5.2. Protocol for 1 μmol scale solid-phase DNA synthesis (dA cycle).^[a]

Step	Function	Mode ^[b]	Amount (pulse)	Time (sec)	Description
Deblocking	144 /*Index Fract. Coll.	NA	1	0	“Event out ON”
	0 /*Default	WAIT	0	1.5	“Wait”
	38 /*Diverted Wsh A	PULSE	15	0	“Flush system with Wsh A”
	141 /*Trityl Mon. On/Off	NA	1	1	“START data collection”
	16 /*Dblk	PULSE	20	0	“Dblk to column”
	0 /*Default	WAIT	0	20	“Default”
	16 /*Dblk	PULSE	40	40	“Deblock”
	38 /*Diverted Wsh A	PULSE	60	0	“Flush system with Wsh A”
	141 /*Trityl Mon. On/Off	NA	0	1	“STOP data collection”
	38 /*Diverted Wsh A	PULSE	20	0	“Flush system with Wsh A”
	144 /*Index Fract. Coll.	NA	2	0	“Event out OFF”
Coupling	1 /*Wsh	PULSE	8	0	“Flush system with Wsh”
	2 /*Act	PULSE	5	0	“Flush system with Act”
	18 /*A + Act	PULSE	5	0	“Monomer + Act to column”
	18 /*A + Act	PULSE	3	24	“Couple monomer”
	2 /*Act	PULSE	3	24	“Couple monomer”
	18 /*A + Act	PULSE	2	16	“Couple monomer”
	2 /*Act	PULSE	3	24	“Couple monomer”
	0 /*Default	WAIT	0	20	“Default”
	1 /*Wsh	PULSE	7	56	“Couple monomer”
	1 /*Wsh	PULSE	21	0	“Flush system with Wsh”
Capping	12 /*Wsh A	PULSE	20	0	“Flush system with Wsh A”
	13 /*Caps	PULSE	8	0	“Caps to column”
	12 /*Wsh A	PULSE	9	23	“Cap”
	12 /*Wsh A	PULSE	21	0	“Flush system with Wsh A”
Oxidizing	15 /*Ox	PULSE	35	0	“Ox to column”
	0 /*Default	WAIT	0	20	“Default”
	12 /*Wsh A	PULSE	60	0	“Flush system with Wsh A”
Capping	13 /*Caps	PULSE	7	0	“Caps to column”
	12 /*Wsh A	PULSE	45	0	“End of cycle wash”

[a] Deblocking reagent = dblk, acetonitrile = Wsh, WshA, activator = act, capping reagents = Caps, oxidizer = Ox. [b] 1 PULSE = 16 μL .

Table 5.3. Protocol for 15 μmol scale solid-phase DNA synthesis (dA cycle).^[a]

Step	Function	Mode ^[b]	Amount (pulse)	Time (sec)	Description
Deblocking	144 /*Index Fract. Coll.	NA	1	0	“Event out ON”
	0 /*Default	WAIT	0	1.5	“Wait”
	141 /*Trityl Mon. On/Off	NA	1	1	“START data collection”
	38 /*Diverted Wsh A	PULSE	50	0	“Flush system with Wsh A”
	16 /*Dblk	PULSE	500	0	“Dblk to column”
	0 /*Default	WAIT	0	20	“Default”
	16 /*Dblk	PULSE	500	0	“Dblk to column”
	0 /*Default	WAIT	0	20	“Default”
	38 /*Diverted Wsh A	PULSE	50	0	“Flush system with Wsh A”
	141 /*Trityl Mon. On/Off	NA	0	1	“STOP data collection”
	144 /*Index Fract. Coll.	NA	2	0	“Event out OFF”
	12 /* Wsh A	PULSE	400	0	“Flush system with Wsh A”
Coupling	1 /*Wsh	PULSE	40	0	“Flush system with Wsh”
	2 /*Act	PULSE	35	0	“Flush system with Act”
	41 /*Gas B	PULSE	1	20	“Gas B”

	18 /*A + Act	PULSE	25	0	“Monomer + Act to column”
	0 /*Default	WAIT	0	60	“Couple monomer”
	18 /*A + Act	PULSE	25	0	“Monomer + Act to column”
	0 /*Default	WAIT	0	60	“Couple monomer”
	2 /*Act	PULSE	20	30	“Couple monomer”
	1 /*Wsh	PULSE	40	0	“Flush system with Wsh”
	41 /*Gas B	PULSE	1	20	“Gas B”
	18 /*A + Act	PULSE	8	0	“Monomer + Act to column”
	0 /*Default	WAIT	0	60	“Couple monomer”
	2 /*Act	PULSE	20	30	“Couple monomer”
	1 /*Wsh	PULSE	100	0	“Flush system with Wsh”
Capping	12 /*Wsh A	PULSE	100	0	“Flush system with Wsh A”
	13 /*Caps	PULSE	75	0	“Caps to column”
	13 /*Caps	PULSE	25	15	“Cap”
	12 /*Wsh A	PULSE	15	40	“Cap”
	12 /*Wsh A	PULSE	100	0	“Flush system with Wsh A”
Oxidizing	15 /*Ox	PULSE	125	0	“Ox to column”
	0 /*Default	WAIT	0	20	“Default”
	12 /*Wsh A	PULSE	100	0	“Flush system with Wsh A”
Capping	13 /*Caps	PULSE	50	0	“Caps to column”
	12 /*Wsh A	PULSE	340	0	“End of cycle wash”

[a] Deblocking reagent = dblk, acetonitrile = Wsh and WshA, argon = Gas B, activator = act, capping reagents = Caps, oxidizer = Ox. [b] 1 PULSE = 16 μ L.

5.3.2 General Procedure for the Synthesis of Amino-Modified ODNs

For the preparation of amino-modified oligonucleotides (ODN), the “convertible nucleoside approach”^[255, 256] was adapted and optimized. 4-Triazolyl-deoxyuridine phosphoramidite was assembled at varying internal positions on DNA during automated solid phase synthesis, in combination with other non-standard phosphoramidite building blocks (*e.g.*, a decaethyleneglycol spacer molecule **S** as for **ODN3**). Base-labile TAC (*t*-butyl-phenoxyacetyl) protecting groups were used for all natural nucleoside monomers. Treatment of the fully protected, resin-bound ODN with 1 mL aqueous solution of ethylenediamine (5 M) or 1,4-butanediamine (5 M) at room temperature for 4 h, afforded the one-pot cleavage from support, deprotection and conversion of the 4-triazolyl-dU to different 4-alkylamino-dC. In the case of 1,13-diamino-4,7,10-trioxatridecane, the treatment with 0.8 mL neat amine (4 h) was followed by additional stirring in the presence of 0.5 mL water (5 h). The cleaved products were filtered (0.22 μ m membrane filter) and the CPG washed with H₂O (3 \times 0.5 mL). The resulting fractions (~2.5 mL) were combined, and after CHCl₃ extraction (3 \times 1 mL) the DNA material was passed through a Sephadex G-25 NAP column (Amersham Biosciences)

for removal of remaining organic residues, using water as eluent. The crude ODN was then purified by reversed-phase HPLC. Fractions containing the tritylated ODN were collected and lyophilized. The terminal DMT group was removed by treatment with 2% v/v TFA (1 mL) for 2 min at room temperature. After quenching the acid with NaHCO₃, the ODNs were ethanol precipitated. Desalting on Sephadex G-25 column afforded pure fully detritylated ODNs (>95% purity), as confirmed by analytical reversed-phase HPLC. The amount of DNA was quantified by UV spectroscopy ($\lambda_{\text{max}} = 260 \text{ nm}$, $\epsilon_{\text{ODN1a-c}} = 181300 \text{ L}\cdot\text{mol}^{-1}\cdot\text{cm}^{-1}$, $\epsilon_{\text{ODN2}} = 220600 \text{ L}\cdot\text{mol}^{-1}\cdot\text{cm}^{-1}$, $\epsilon_{\text{ODN3}} = 195700 \text{ L}\cdot\text{mol}^{-1}\cdot\text{cm}^{-1}$, $\epsilon_{\text{ODN4a-c}} = 186000 \text{ L}\cdot\text{mol}^{-1}\cdot\text{cm}^{-1}$), resulting in overall yields of 21-42%.

Table 5.4. Isolated yields and MALDI-TOF analysis of **ODN1-4**.

Entry	Isolated yield (%)	m/z ^[a]	
		calcd	obsd
ODN1a	35	5921	5928
ODN1b	42	5895	5898
ODN1c	40	6055	6059
ODN2	32	7120	7125
ODN3	33	7024	7029
ODN4a	25	5866	5856
ODN4b	21	5894	5887
ODN4c	22	6026	6019

[a] **ODN1a**, **ODN2** and **ODN3** detected in negative mode ($[\text{M-H}]^-$), **ODN1b-c** and **ODN4a-c** in positive mode ($[\text{M+H}]^+$).

5.3.3 General Procedure for the Synthesis of 7-deaza-riboG - containing Amino-Modified ODNs

Chimeric DNA sequences were synthesized using extended coupling times (10 min) for for more efficient incorporation of the 7-deaza-riboG monomer. The 7-deaza-riboG coupling cycle performed for 1 μmol scale synthesis is shown in Table 5.5. Deprotection, cleavage from solid-support and conversion of the triazolyl group were carried out by treatment with 1 mL aqueous solution of ethylenediamine (5 M) or 1,4-butanediamine (5 M) at room temperature, overnight.

Table 5.5. Coupling cycle of 7-deaza-riboG used in 1 μ mol scale DNA synthesis.

Step	Function	Mode	Amount (pulse)	Time (sec)	Description
Deblocking	144 /*Index Fract. Coll.	NA	1	0	“Event out ON”
	0 /*Default	WAIT	0	1.5	“Wait”
	38 /*Diverted Wsh A	PULSE	15	0	“Flush system with Wsh A”
	141 /*Trityl Mon. On/Off	NA	1	1	“START data collection”
	16 /*Dbk	PULSE	20	0	“Dbk to column”
	0 /*Default	WAIT	0	20	“Default”
	16 /*Dbk	PULSE	40	40	“Deblock”
	38 /*Diverted Wsh A	PULSE	60	0	“Flush system with Wsh A”
	141 /*Trityl Mon. On/Off	NA	0	1	“STOP data collection”
	38 /*Diverted Wsh A	PULSE	20	0	“Flush system with Wsh A”
144 /*Index Fract. Coll.	NA	2	0	“Event out OFF”	
Coupling ^[a]	1 /*Wsh	PULSE	8	0	“Flush system with Wsh”
	2 /*Act	PULSE	5	0	“Flush system with Act”
	23 /*6 + Act	PULSE	5	0	“Monomer + Act to column”
	23 /*6 + Act	PULSE	5	150	“Couple monomer”
	2 /*Act	PULSE	8	150	“Couple monomer”
	23 /*6 + Act	PULSE	2	120	“Couple monomer”
	2 /*Act	PULSE	3	120	“Couple monomer”
	0 /*Default	WAIT	0	20	“Default”
	1 /*Wsh	PULSE	7	40	“Couple monomer”
	1 /*Wsh	PULSE	21	0	“Flush system with Wsh”
Capping	12 /*Wsh A	PULSE	20	0	“Flush system with Wsh A”
	13 /*Caps	PULSE	8	0	“Caps to column”
	12 /*Wsh A	PULSE	9	23	“Cap”
	12 /*Wsh A	PULSE	21	0	“Flush system with Wsh A”
Oxidizing	15 /*Ox	PULSE	35	0	“Ox to column”
	0 /*Default	WAIT	0	20	“Default”
	12 /*Wsh A	PULSE	60	0	“Flush system with Wsh A”
Capping	13 /*Caps	PULSE	7	0	“Caps to column”
	12 /*Wsh A	PULSE	45	0	“End of cycle wash”

[a] In the coupling step, 6 stands for 7-deaza-riboG monomer.

The cleaved products were filtered (0.22 μ m membrane filter) and the CPG washed with acetonitrile/ethanol/H₂O 3:1:1 (3 \times 0.5 mL).

The resulting fractions (~2.5 mL) were combined and passed through a Sephadex G-25 NAP-25 column for removal of remaining organic residues, using water as eluent. After lyophilization, the 2'-O-TBDMS was removed by treatment with 1 ml of 0.1 M tetrabutylammonium fluoride in THF for 24 h at room temperature. The solution of the crude oligomer was diluted with 1.5 ml water, desalted on a Sephadex G-25 NAP column, and purified by reversed-phase HPLC. Tritylated oligonucleotides were collected and lyophilized. The terminal DMT group was removed using the protocol previously described. The purity of the detritylated oligomers was confirmed by analytical reversed-phase HPLC. The amount of DNA was quantified by UV

spectroscopy ($\lambda_{\max} = 260 \text{ nm}$, $\epsilon_{\text{ODN5a,b}} = 181300 \text{ L}\cdot\text{mol}^{-1}\cdot\text{cm}^{-1}$), resulting in overall yields of 14% **ODN5a** and 5% **ODN5b**, respectively. The MALDI-TOF MS analysis (positive mode $[\text{M}+\text{H}]^+$) of the isolated oligomers is shown in Table 5.6.

Table 5.6. Isolated yields and MALDI-TOF analysis of **ODN5a,b**.

Entry	Isolated yield (%)	$[\text{M}+\text{H}]^+$	
		calcd	obsd
ODN5a	14	5945	5945
ODN5b	5	5973	5980

5.3.4 General Procedure for the Synthesis of Complementary DNA

Unmodified ODNs were prepared by 1 μmol scale synthesis. Treatment of the fully protected, resin-bound ODN with 1 mL ammonium hydroxide 28% for 1 h at room temperature afforded the cleavage from solid-support and removal of the protection groups. The cleaved products were filtered (0.22 μm membrane filter) and the CPG washed with H_2O ($3 \times 0.5 \text{ mL}$). The resulting fractions ($\sim 2.5 \text{ mL}$) were combined, and after CHCl_3 extraction ($3 \times 1 \text{ mL}$) the DNA material was passed through a Sephadex G-25 NAP column for removal of remaining organic residues, using water as eluent. The crude ODN was then purified by reversed-phased HPLC. Fractions containing the tritylated ODN were collected and lyophilized. The terminal DMT group was removed by treatment with 2% v/v TFA (1 mL) for 2 min at room temperature. After quenching the acid with NaHCO_3 , the ODNs were ethanol precipitated. Desalting on Sephadex G-25 column afforded pure fully detritylated ODNs (>95% purity), as confirmed by analytical reversed-phase HPLC. The amount of DNA was quantified by UV spectroscopy ($\lambda_{\max} = 260 \text{ nm}$, $\epsilon_{\text{cDNA1}} = 170200 \text{ L}\cdot\text{mol}^{-1}\cdot\text{cm}^{-1}$, $\epsilon_{\text{cDNA2}} = 211700 \text{ L}\cdot\text{mol}^{-1}\cdot\text{cm}^{-1}$, $\epsilon_{\text{cDNA3}} = 140700 \text{ L}\cdot\text{mol}^{-1}\cdot\text{cm}^{-1}$), resulting in overall yields of 20-37%.

Table 5.7. Isolated yields and MALDI-TOF analysis of **cDNA1-3**.

Entry	Isolated yield (%)	$[\text{M}+\text{H}]^+$	
		calcd	obsd
cDNA1	20	5765	5767
cDNA2	37	6986	6982
cDNA3	25	4834	4835

5.4 Synthesis of DNA-Based Ligands

5.4.1 Incorporation of Phosphite Moiety by DNA Solid-phase Synthesis

General procedure for solid-phase synthesis of DNA-phosphite conjugates. Synthesis of modified oligodeoxynucleotides **sODN1-3** (Table 5.8) carrying a terminal phosphite moiety (Scheme 3.2) was attempted by the phosphoramidite approach on the Expedite synthesizer, on 0.2 μ mole scale synthesis, using nucleotide precursor phosphoramidites with standard protecting groups (acetyl for dG, benzoyl for dA and dC). Phosphoramidite **P2** precursor (0.1 M solution in acetonitrile) was assembled at the 5' terminus on short DNA sequences, using a modified coupling protocol. The coupling time was extended and the standard dicyanoimidazole activator was replaced with 5-benzylthio-(1*H*)-tetrazole (BTT, 0.25 M solution in acetonitrile), and the oxidation step was omitted. Final deblocking was not necessary in this case.

Table 5.8. 5'-Functionalization of **ODN1-3** with phosphoramidite moieties.^[a]

ODN	Sequence	Coupling of R moiety to the 5'-end	Spacer S
sODN1	5'-TA CGC-3'		-
sODN2	5'-STA CGC-3'		-
sODN3	5'-TSA CGC-3'		

[a] Attempted solid-phase coupling of **P1** or **P2** to oligonucleotides didn't lead to the desired conjugates, and only 5'-OH unmodified **sODN1-3** were obtained. **sODN1-P2** could be isolated as DNA-phosphate conjugate **sODN1-P2(O)**.

After the synthesis, the oligonucleotides were deprotected and cleaved from the solid support by treatment with 1 mL of 28% aqueous ammonia overnight at room temperature.

Table 5.9. Isolated yields and MALDI-TOF analysis of **sODN1-3**.

Entry	Isolated yield (%)	sODN ^[a]		sODN-P2(O) ^[b]	
		calcd	obsd	[M-H] ⁺	calcd
sODN1	43	1675	1462	1691	1710
sODN2	28	2195	1982	-	-
sODN3	46	2195	1982	-	-

[a] Conjugates **sODN1-3** were isolated as 5'-OH unmodified oligonucleotides, when no oxidation was performed after **P2** coupling during solid phase synthesis. [b] sODN(O) was obtained by carrying out complete coupling cycle (including oxidation) for **P2**. Isolated yield refers to the DNA product obtained after solid phase synthesis and HPLC purification.

The cleaved products were filtered (0.22 μm membrane filter) and the CPG washed with H₂O (3 \times 0.5 mL). The ammonia solution was removed by evaporation in a speedvac.

The crude oligonucleotide was redissolved in 0.5 mL H₂O and purified by reversed-phase HPLC. The fractions containing the major peak were collected and lyophilized. The isolated DNA products corresponded to the 5'-unmodified oligonucleotides, as confirmed by MALDI-TOF mass spectrometry. The amount of DNA was quantified by UV spectroscopy ($\lambda_{\text{max}} = 260 \text{ nm}$, $\epsilon_{\text{sODN1-3}} = 45900 \text{ L}\cdot\text{mol}^{-1}\cdot\text{cm}^{-1}$), resulting in overall yields of 28-46% of **sODN1-3**.

Synthesis of DNA-appended biphenyl-phosphate ester conjugate sODN1-P2(O).

The incorporation of **P2** residue at the 5'-end **sODN1** by solid phase synthesis was re-attempted by carrying out the complete **P2** coupling cycle, including oxidation step. After ammonia deprotection and cleavage from the solid support, the crude oligonucleotide was purified by reversed-phase HPLC. The fractions containing the major peak were collected, lyophilized, resuspended in H₂O, and analyzed by MALDI-TOF mass spectrometry. The isolated DNA conjugate corresponded to 5'-biphenyl-phosphotriester-containing oligonucleotide **sODN1-P2(O)** (see Table 5.9). The amount of DNA was quantified by UV spectroscopy ($\lambda_{\text{max}} = 260 \text{ nm}$, $\epsilon_{\text{sODN1}} = 45900 \text{ L}\cdot\text{mol}^{-1}\cdot\text{cm}^{-1}$), resulting in an overall yield of 48%.

Attempted solid-phase synthesis of sODN1-P2-rhodium(I) complex. DNA-phosphite oligonucleotide **sODN1-P2** was prepared by standard solid-phase synthesis on a 0.2 μmol scale as previously described. The phosphoramidite **P2** was assembled on the solid support-bound DNA by automated coupling, no oxidation being performed. The

DNA-coated beads were transferred from the synthesis column to an Eppendorf tube and a solution of $[\text{Rh}(\text{cod})\text{Cl}]_2$ (9.8 mg, 20.0 nmol) in acetonitrile (0.2 mL) was added. After vigorously mixing the resulting suspension for 30 minutes at room temperature, the solution of metal complex was removed, the resin washed with acetonitrile (3×0.5 mL) and dried. The beads-supported DNA was then combined with 1.0 mL 28% ammonium hydroxide. After 30 minutes of incubation at 65°C , an aliquot (50 μL) from the deprotection mixture was removed, cooled down to room temperature, filtered and analyzed by reversed-phase HPLC. Beside several peaks eluting in the time range of the unmodified DNA ($t_{\text{R}} = 18.0$ min) and high-eluting organic residues ($t_{\text{R}} > 36.0$ min) released in the deprotection step, a distinct DNA peak was observed ($t_{\text{R}} = 27.8$ min). The fraction corresponding to this DNA product was collected and lyophilized. MALDI-TOF mass spectrometry confirmed the formation of the **sODN1-P2** conjugate (calc. $[\text{M}-\text{H}]^-$ 1675, found 1685).

5.4.2 Synthesis of DNA-Phosphine Conjugates

General procedure for the functionalization of amino-ODNs with phosphine ligands. The phosphine derivatives **L1-3** and **L6** (1.0 equiv) were converted to the corresponding activated esters in degassed DMF in 45-60 min at room temperature by reaction with NHS (1.0 equiv) in the presence of EDC (1.2 equiv). In parallel, **ODN1a-c**, **ODN2,3**, **ODN4a,b**, and **ODN5a** were dissolved in NaHCO_3 (0.1 M, pH 8.3) and the resulting solutions were degassed. The coupling reactions were performed by combining the solutions of the in situ generated NHS-ester (200-600 equiv) and the amino-modified DNA (final DMF/ H_2O ratio 2:1 v/v) to achieve final **ODN1a**, **ODN2**, and **ODN3** concentration of 115, 103, and 104 μM , respectively, for coupling with **L1** (22 mM), and final **ODN1a** concentration of 35, 45, and 45 μM , respectively, for coupling with **L2**, **L3** and **L6** (17 mM in all cases).

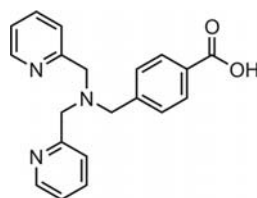
MALDI-TOF mass spectrometry of the HPLC purified **ODN6-11a**, however, gave in general only the mass of the oxidized products **ODN6-8(O)**, **ODN9,10(O)₂**, and **ODN11a(O)**. While MALDI mass spectrometry was found unsuitable for the direct detection of phosphine conjugates, ESI-MS gave in the only attempted case (**ODN9**) the main peak corresponding to the non-oxidized phosphine.

Sulphide-protection of the DNA-phosphine conjugates. To prove the identity of the HPLC high-eluting oligonucleotides as phosphine-DNA conjugates **ODN6-11a**, the HPLC eluate was collected and immediately treated with elemental sulfur. After incubating the resulting mixture for 1h at room temperature, the solution was filtered (0.22 μm membrane filter), lyophilized and redissolved in water (20 μL), yielding the air-stable phosphine sulfide analogues **ODN6-8(S)**, **ODN9,10(S)₂**, and **ODN11a(S)** as confirmed by MALDI-TOF MS (Table 5.11).

In case of bisphosphines **L2** and **L3** coupling, HPLC chromatograms showed the formation of a second oligonucleotide peak (<10%), eluting earlier than the main product. The fractions containing these oligonucleotides were also isolated and reacted with sulfur. They corresponded to byproducts generated by partial oxidation and were characterized by MALDI mass spectrometry as monoxide-monosulfide (Table 5.11).

5.4.3 Synthesis of DNA-Appended *N,N*-bis(2-picolyl)amine Conjugates

Chelating nitrogen ligand derived from *N,N*-bis(2-picolyl)amine, namely $(\text{PyCH}_2)_2\text{N-CH}_2\text{-}p\text{-C}_6\text{H}_4\text{-COOH}$ (**bpa**) (Figure 5.5), obtained from Dr. Srecko Kirin, Prof. Dr. Nils Metzler-Nolte,^[268] was reacted with alkylamino-modified oligonucleotides (**ODN1a**, **ODN2** and **ODN3**).

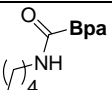
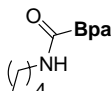
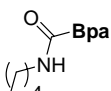


Bpa

Figure 5.5. $(\text{PyCH}_2)_2\text{N-CH}_2\text{-}p\text{-C}_6\text{H}_4\text{-COOH}$ Ligand.

Bpa (1.0 equiv) was first dissolved in DMF and activated with NHS (1.0 equiv) in the presence of EDC (1.2 equiv.), for 1 h, at room temperature. The *in situ* generated active ester (100-250 equiv) was then directly added to an ODN solution in NaHCO₃ (100 mM, pH 8.3) to achieve final DMF/H₂O ratio 2:1 v/v and DNA concentrations of 56.4 (**ODN1a**), 46.3 (**ODN2**), and 119.7 μM (**ODN3**) respectively. The final concentration of bipyridine ligand was maintained in all cases 11.11 mM. After slow shaking for 16 h at room temperature, the coupling solution was mixed with an equal amount of formamide-loading buffer and analyzed by 18% polyacrylamide gel electrophoresis (Figure 3.8, Chapter 3.1.2.3). The coupling reaction proceeded to completion, leading to only one band with lower electrophoretic mobility compared with the amino-modified oligonucleotide, as observed by UV illumination ($\lambda = 254$ nm) of the gel (UV-Transilluminator CAMAC Reprostar II).

Table 5.12. Sequences and MALDI-TOF analysis of **ODN14-16**.

Entry	Sequence	[M-H] ⁻	
		calcd	obsd
ODN14	 5'-GC AGT GAA GGC TGA GCT CC-3'	6235	6242
ODN15	 5'-GC AGT GAA GGC TGA GCT CCT ACC-3'	7434	7440
ODN16 ^[a]	 5'-GC AGT GAA GGC TGA GCT CCS CC-3'	7338	7341

[a] S = decaethylene glycol spacer

The bands were excised and the DNA recovered by elution with ammonium acetate (0.5 M, 0.5 mL) overnight, at room temperature. After ethanol precipitation, the DNA conjugates **ODN14-16** (25% isolated yield) were redissolved in water (50 μL) and analyzed by MALDI-TOF mass spectrometry (Table 5.12).

5.5 High-Pressure Liquid Chromatography

5.5.1 Reversed-Phase HPLC Purification of Oligodeoxynucleotides

Oligonucleotides purification was performed on reversed-phase HPLC. By purifying with the DMT group still attached at the 5'-terminus of the synthetic oligonucleotide, failure sequences that contain no DMT groups are weakly bound to the column and easily separated from the product which is more strongly retained and eluted later. The buffers used in reversed-phase HPLC technique are volatile and the purified product can be rapidly recovered by lyophilization of the volatile solvent.

HPLC analyses were performed on an Agilent 1100 Series HPLC system equipped with an diode array detector using a Phenomenex[®] Luna 5 μ m C18 column (4.6 \times 250 mm) and eluting with a gradient of 100 mM triethylammonium acetate (TEAA) pH 7.0 (buffer A) and 100 mM TEAA in 80% acetonitrile (buffer B) at 1 mL/min flow-rate. Preparative HPLC runs were carried out using Phenomenex[®] Luna 5 μ m C18 column (15.0 \times 250 mm) and eluting with a gradient of buffer A and buffer B, followed by a gradient of water and acetonitrile, at 6 mL/min flow-rate.

Reversed-phase HPLC analysis of ODN1 conversion, deprotection and cleavage (DMT-on). Treatment of the DMT-on resin-bound *ODN1a* with a 5 M aqueous solution of diaminobutane was monitored by reversed-phase HPLC (Gradient: 3 min at 15% B, increase to 29% B over 11 min, isocratic for 29 min; detection at 260 nm). Reaction times longer than 4 hours did not improve the yields of deprotection, cleavage and conversion (see Figure 3.4, Chapter 3.1.2.1).

Reversed-phase HPLC purification of amino-modified ODN1a-c, ODN2,3, ODN4a-c, ODN5a,b, and their complementary strands cDNA1-3 (DMT-on). Gradient: 3 min at 2% B, increase to 29% B over 8 min, isocratic for 7 min; change elution system to water / acetonitrile: change to 23% acetonitrile over 1min, increase from 23% acetonitrile to 30% acetonitrile over 6 min, isocratic for 3 min; detection at 260 nm; 6 mL/min flow-rate; 55°C.

Characterization of ODN1-5, and cDNA1-3 (DMT-off). The purity of detritylated amino-modified oligonucleotides *ODN1-5* and of their complementary, unmodified DNA sequences *cDNA1-3* was confirmed by analytical HPLC, using a gradient of

buffer B from 1% to 25% within 40 min. The observed retention times are shown in Table 5.13.

Table 5.13. Retention times of **ODN1-5** and **cODN1-3**.

ODN	Retention time (DMT-on)	Retention time (DMT-off)
	[min]	[min]
ODN1a	23.7	25.5
ODN1b	23.5	24.7
ODN1c	24.0	25.9
ODN2	-	26.5
ODN3	-	32.8
ODN4a	23.7	24.8
ODN4b	23.6	24.9
ODN4c	23.5	26.4
ODN5a	23.9	22.8
ODN5b	24.1	22.9
cDNA1	26.5	24.3
cDNA2	26.4	25.1
cDNA3	23.4	27.2

Reversed-phase HPLC purification of phosphine and phosphinoxazoline-functionalized ODN6-13. Gradients used in the HPLC purification were as follows:

1) increase from 5% B to 15% B over 20 min, increase from 15% B to 25% B over 10 min, increase from 25% B to 40% over 5 min, increase from 40% B to 100% B over 10 min (**ODN6-8**);

2) increase from 10% B to 62% B over 52 min (**ODN9,10**);

3) increase from 1% B to 75% B over 40 min (**ODN11-13**); detection at 260 nm, 1 mL/min flow-rate, 45°C column oven.

Retention times of **ODN6-13** and their oxidized species are reported in Table 5.14.

Table 5.14. Retention times of phosphine- and phosphinoxazoline-DNA conjugates **ODN6-11**.

Entry	Retention time [min]		
	ODN(O) ₂	ODN(O)	ODN
ODN6	-	34.4	39.0
ODN7	-	35.1	39.1
ODN8	-	35.7	39.2
ODN9	22.9	30.4	37.5
ODN10	32.2	43.5	50.7
ODN11a	-	20.3	27.9
ODN11b	-	18.3	24.6
ODN11c	-	23.1	32.2
ODN12a	-	19.3	26.2
ODN12b	-	18.3	27.6
ODN12c	-	25.4	31.4
ODN13	-	21.7	29.0

Reversed-phase HPLC analysis of the attempted coupling reaction between P1 or P2 phosphoramidites and sODN1-3. Gradient: increase from 1%B to 15% B over 20 min, increase from 15% B to 40% B within 10 min; detection at 260 nm).

Table 5.15. Retention times of sODN1-3.

Entry	Retention time [min]	
	5'-HO-ODN	sODN-P2(O) ^[a]
sODN1	18.0	27.9
sODN2	26.5	-
sODN3	26.2	-

[a] sODN1-P2 was isolated in the oxidized form.

5.6 Mass Spectrometry Analysis of Oligonucleotides

Conditions for MALDI-TOF MS analysis. Oligonucleotides were dissolved in water to a final concentration of 10 μ M (commonly 100 pmol, 10 μ L) and desalted by using C₁₈ZipTips (Millipore Corporation, Bedford, MA, USA). The C18 resin was wetted using 50% aqueous acetonitrile solution (2 x 10 μ L) and then equilibrated by washing with 0.1 M TEAA (3 x 10 μ L). For binding of the oligonucleotide to the resin, the sample was aspirated and dispensed (approx. 5-10 times). The salts were removed by washing with 0.1 M TEAA. The desalted DNA was eluted by aspirating and dispensing about 5 times 5 μ L 50% acetonitrile/water in a separate vial.

The samples for analysis were prepared using the dried droplet method with the following matrix solutions: 1) 6-aza-2-thiothymine/diammonium hydrogen citrate in 1:2 v/v water/acetonitrile (detection in negative mode); 2) 3-hydroxy-picolinic acid/diammonium hydrogen citrate in 1.2:1 v/v water/acetonitrile (detection in positive mode).

Conditions for ESI MS analysis of ODN9. ESI mass spectra were recorded in the negative mode on a Bruker APEX IV Fourier-transform ion cyclotron resonance (FT-ICR) mass spectrometer with a 7.05 T magnet and an Apollo electrospray (ESI) ion source equipped with an off-axis 70° stainless steel spray needle. Typically, 50 μ M analyte solutions (ACN/H₂O 1:1) were introduced into the ion source with a syringe pump (Cole-Parmer Instruments, Series 74900) at flow rates of 3 to 4 μ L/min. Ion transfer into the first of three differential pump stages in the ion source occurred through a glass capillary with 0.5 mm inner diameter and nickel coatings at both ends.

Ionization parameters were adjusted as follows: capillary voltage: 4.1 kV; end plate voltage 3.6 kV; capexit voltage: -280 V; skimmer voltages: -5 to -7.5 V; temperature of drying gas: 40 °C. Nitrogen was used as tir ssive (25 psi) and drying gas (5 psi). The ions were accumulated in the instruments n-hexapole for 1-1.5 s, introduced into the FT-ICR cell which was operated at pressures below 10^{-10} mbar, and detected by a standard excitation and detection sequence. For each measurement, up to 128 scans were averaged to improve the signal-to-noise ratio.

5.7 5'-Radioactive Labelling of Oligonucleotides

Synthetic oligonucleotides are labelled in phosphorylation reactions catalyzed by bacteriophage T4 polynucleotide kinase (PNK). The γ -phosphate is transferred from ATP to the free 5'-hydroxyl group of the target oligonucleotide, affording the radioactive labelling of DNA. Standard 5'-kinase labelling reaction included the DNA to be labelled, [γ - ^{32}P]-ATP, T4 PNK, and buffer.

Table 5.16. Standard 5'-radioactive labelling of oligonucleotides.

	Amount (pmol)	Volume (μL)	Observations
DNA	6-7.5	2-3	From chemical synthesis
10xBuffer		1.5	Fermentas
γ - ^{32}P -ATP		5	3000 Ci/mmol, 10 mCi/mL (Amersham)
T4-PNK		1	10 U/ μL (Fermentas)
H ₂ O		to 15 μL	

After incubation at 37°C for 2 h, the labelled oligonucleotide was purified by 20% polyacrylamide gel electrophoresis, under denaturing conditions, using a sequencing gel apparatus. The reaction mixture was mixed with an equal volume of formamide-loading buffer and loaded to the gel. After electrophoresis, the gel was exposed to autoradiographic film. The gel band corresponding to the desired product was excised, transferred to an eppendorf tube and incubated with ammonium acetate (pH 7, 0.5 M, 0.4 mL) overnight, at 37°C. The resulting solution containing the oligonucleotide was then filtered (spin filters, 0.22 μm cellulose acetate membrane, 3 min centrifugation at 12000 rpm), and the labelled oligonucleotide isolated by ethanol precipitation. After rinsing with 70% ethanol, the DNA pellet was resuspended in water (0.4 mL) and the incorporated radioactivity estimated by scintillation counter measurements.

5.8 Analysis and Quantification of DNA

5.8.1 Quantification of Oligonucleotides by UV Absorbance

The nucleobases in DNA and RNA absorb light with a maximum absorbance of 260 nm. Oligonucleotides were the most accurately and conveniently quantified, after synthesis, by measuring their absorbance at 260 nm in a spectrophotometer.

The DNA samples were measured with a Shimadzu UV-160A UV-spectrophotometer, in quartz cuvettes (Quarzglas HELLMMA) or with NanoDrop ND-100 Spectrophotometer (PeqLab Biotechnologie GmbH) and blanked with the same solution used to dissolve the oligonucleotide (usually water). The absorbance of a DNA sample at 260 nm was used to calculate the DNA concentration when the extinction coefficient ε was known. The molar extinction coefficient describes the amount of absorbance at 260nm (A_{260}) of 1 mol·L⁻¹ DNA solution measured in 1 cm path-length cuvette. This definition is derived from the Beer-Lambert law showed in the following equation:

$$A = \log(I_0/I) = \varepsilon \cdot c \cdot l \quad \text{Equation 5.1}$$

where A is the absorbance, I_0 and I are the intensities of incident and transmitted light, respectively, c is the molar concentration of the oligonucleotide (mol·L⁻¹), l is the length of the light path through the sample (cm), and ε is the molar extinction coefficient of the molecule (L·mol⁻¹·cm⁻¹).

The extinction coefficient is a physical constant that is unique for each DNA sequence, since each nucleotide constituent has a different absorbance at 260 nm. The extinction coefficient was calculated for each oligonucleotide using an equation that incorporates the contribution of each base (Equation 5.2):

$$\varepsilon = A(15.2) + C(7.05) + G(12.01) + T(8.4) \quad \text{Equation 5.2}$$

at pH 8, where A, C, G, T are the numbers of dAs, dCs, dG, and dTs, respectively, and the numbers in parentheses are the molar extinction coefficients for each nucleotide.

5.8.2 Analysis of DNA Duplexes by Thermal Melting Curves

The stability of a DNA-DNA duplex was measured by thermal denaturation experiments on a UV-visible spectrophotometer, by recording the absorbance at 260 nm as a function of temperature. Heating a DNA sample results in a change in absorbance properties, which reflects a conformational change of the molecule in solution, and allows the determination of DNA secondary structure stability. Duplex denaturation leads to a hyperchromism of 15-20%. Cooling the sample leads to a renaturation of the structure.

A thermal denaturation experiment of duplex DNA yields the melting temperature value T_m , which corresponds to the temperature at which half of the sample is base-paired (double-helical state), and half is unwinded. T_m determination implies the measurement of the absorbance properties of the folded and unfolded forms as a function of temperature.

Such an assay was used to study hybridization between an amino-modified oligonucleotide (**ODN1a**) and its complementary target (**cdNA1**). The stability of the resulting double-stranded structure was investigated in aqueous solutions containing various concentrations of dioxane. A final DNA concentration of 2 μM (strand concentration) and an optical pathlength of 1 cm were used in order to obtain an absorbance value around 0.6 (in the linearity range of the instrument).

The samples were prepared by mixing equimolar amounts of the two DNA strands (2 nmol) in HEPES buffer (15 mM, 0.64 mL, pH 7.5 at 25°C) containing 150 mM NaClO_4 and 7.5 mM $\text{Mg}(\text{ClO}_4)_2$, followed by addition of water or/and dioxane up to 0, 5, 10, 20, and 30% final concentration) and 1 mL final volume. The samples were degassed by sonication (15 min) in order to remove air bubbles eventually formed in solution, which might alter the absorbance measurements. The solutions were then placed in cuvettes and sealed by carefully adding a thin layer of mineral oil on the top of solution to prevent partial evaporation of the analyte solution occurring at high temperature. The multisample cell holder accommodated 6 cuvettes. For each sample, a melting curve experiment consisted of one fast reversible heating/cooling cycle (15°C \rightarrow 90°C \rightarrow 15°C with a thermal gradient of 5°C/min, maintaining 90°C for 5 min and, at the end, 15°C for 5 min), followed by two cycles performed with 0.5°C/min thermal gradient..

The heating (dissociation state) and cooling (initial state) profiles are superimposable, indicating that the transition is kinetically reversible.

Melting temperatures were observed by following the change in UV absorbance as the temperature was increased and determined by computer fit, followed by calculation of the maximum of the first derivative of the absorbance signal (dA/dT). Uncertainty in T_m values was estimated to be ± 0.6 - 0.8 .

5.8.3 Polyacrylamide Gel Electrophoresis (PAGE)

Denaturing polyacrylamide gels were used for purification and separation of single-stranded DNA. The gel was polymerized in the presence of urea as denaturing agent.

Denaturing PAGE was used to purify ^{32}P -radioactive labelled 19mer DNAs, **cDNA1**, **ODN1a**, **ODN9(O)₂**, **ODN9(O)(S)** and **ODN9(S)₂** and to assay the synthesis of bipyridine-DNA conjugates **ODN14-16**. A 20% gel solution was prepared by diluting a stock solution of acrylamide: bisacrylamide (19:1 (% w/v), 120 mL) with 10 x TBE buffer (boric acid 0.89 M, Na₂EDTA 0.02 M, TRIS 0.89 M, 15 mL), followed by addition of urea solution (7 M, 15 mL). The gel polymerization was initiated by addition of *N,N,N',N'*-tetramethylene diamine (TEMED) (50 μL) and ammonium persulfate (APS) (10% in water, 0.75 mL) and was completed in 30-60 minutes at room temperature. The DNA samples (30 μL / well) were loaded together with gel tracking dyes (xylene cyanol and bromphenol blue) on the gel which has been pre-run for 15-20 min at 240 V. The PAGE electrophoresis was carried out in TBE buffer, using a sequencing gel apparatus, at 1200 V, for 8 h, until the bromophenyl blue indicator dye that comigrates with the DNA sequence was about $\frac{3}{4}$ of the way to the bottom. The oligonucleotides were then visualized using the PhosphorImager instrument for ^{32}P -5'-radioactive labelled or by UV shadowing (shining 254 nm UV light from a hand held lamp).

Nondenaturing polyacrylamide gel was used for analysis of double-stranded DNAs formed between **ODN1a**, **ODN9(O)₂**, **ODN9(O)(S)** and **ODN9(S)₂** and the complementary **cDNA1** and **cRNA1**, respectively. The duplexes were prepared by combining trace amounts of ^{32}P -radioactive labeled 19mer DNA or RNA (100,000 cpm) with excess of the corresponding complementary strand (typically 100 pmol), and dissolving them in buffer (100 mM Hepes pH 7.5, 200 mM NaCl, and 1 mM EDTA).

The final volume was adjusted to 20 μL by addition of water (5 μM final concentration). The oligonucleotides were heated for 10 min at 75°C, and allowed to hybridize by slowly cooling down first to 55°C and stirring for 20 min, followed by cooling down to 37°C within 1 h. After mixing with an equal volume of glycerol 20% containing tracking dye, the duplex solutions were loaded on nondenaturing 16% polyacrylamide gel (60 mL solution acrylamide: bisacrylamide (19:1 (% w/v), 90 mL 1 x TBE buffer, 50 μL TEMED, 0.75 mL APS, no urea). The gel was run at low voltage (400 V) to prevent heating that might cause melting of the strands, for 16 h, until complete migration of the bromphenolblue dye.

5.9 Transition Metal-Catalyzed Reactions

5.9.1 Conjugate Addition

5.9.1.1 Synthesis of 3-Phenyl-1-cyclohexanone

In a Schlenk flask, under argon, $[\text{Rh}(\text{cod})\text{Cl}]_2$ (60.4 mg, 0.12 mmol, 3 mol%) and trimethylphosphite (80.0 μL , 0.60 mmol, 2.8 equiv per Rh) were dissolved in 20 mL of dioxane. After addition of water (2 mL), the resulting mixture was stirred for 10 min at room temperature. Phenylboronic acid **16** (3.0 g, 24.0 mmol, 3.0 equiv) was added to the solution. The mixture was heated at 100°C and 2-cyclohexen-1-one **17** (0.8 g, 8.0 mmol) was added. The resulting solution was additionally stirred for 2 hours at 100°C, then allowed to cool down to room temperature, quenched with saturated NaHCO_3 (15 mL) and extracted with diethyl ether (2×25 mL). The organic phase was then washed with brine (2×20 mL) and dried over Na_2SO_4 . Removal of the solvent under reduced pressure afforded the crude product as brownish oil. Purification by flash chromatography (elution with EA/*n*-hex 1:9) gave compound **18** as colorless oil (0.9 mg, 5.6 mmol, 70%). ^1H NMR (300 MHz; CDCl_3) δ 7.38-7.22 (m, 5H), 3.04 (m, 1H), 2.64-2.33 (m, 4H), 2.02-2.21 (m, 2H), 2.06-1.74 (m, 2H).

5.9.1.2 General Procedure for 1,4-Addition of Phenylboronic Acid to 2-Cyclohexen-1-one

• **Phosphoramidite ligands.** For each catalytic experiment, $[\text{Rh}(\text{cod})\text{Cl}]_2$ (6.0 mg, 12.0 μmol , 3 mol%) was added to a solution of phosphoramidite **P1** (12.3 mg, 60.0 μmol , 2.5 equiv per Rh) or **P2** (17.3 mg, 60.0 μmol , 2.5 equiv per Rh) in 2.2 mL dioxane/water (10:1, 1:5 or 1:10) placed in a Schlenk flask containing, if the case, a reflux condenser. After being stirred for 10 min at room temperature, phenylboronic acid **16** (300.0 mg, 2.4 mmol, 3.0 equiv) was added. The resulting mixture was heated at 60°C or stirred for 10 min at room temperature before addition of the enone substrate. The flask was then charged with 2-cyclohexen-1-one **17** (77.0 mg, 0.8 mmol). The progress of the reaction was monitored by TLC (elution with EA/*n*-hex 1:9). The reaction mixture was stirred for 24-72 hours at 60°C or at room temperature (36.4 mM final substrate concentration and 10.9 mM final [Rh] catalyst concentration) and then quenched by addition of saturated NaHCO_3 (2 mL). The reaction product was extracted with diethyl ether (2×5 mL), washed with brine (2×5 mL) and dried over Na_2SO_4 . The residual solvent was evaporated under reduced pressure. The yields were estimated by ^1H NMR spectroscopy (CDCl_3) with isopropanol as internal standard (5-80% conversion).

Catalytic experiments using lower Rh catalyst loading, $[\text{Rh}(\text{cod})\text{Cl}]_2$ (1.2 mg, 2.0 μmol , 0.5 mol%), were performed in the presence of **P1** ligand (2.1 mg, 10.0 μmol , 2.5 equiv per Rh) in 1:10 dioxane/water (2.2 mL), following the previously described procedure. The reaction mixture was stirred for 24 hours at room temperature. In this case, the final [Rh] catalyst concentration was 1.8 mM, while the enone substrate **17** was maintained at 36.4 mM concentration.

Duplicated control experiments of 1,4-addition in the presence of only $[\text{Rh}(\text{cod})\text{Cl}]_2$ precursor were also carried out. In a Schlenk flask, under argon, $[\text{Rh}(\text{cod})\text{Cl}]_2$ (6.0 mg, 12.0 μmol , 3 mol%) was dissolved in dioxane (0.2 mL). Upon addition of water (2 mL) and phenylboronic acid **16** (300.0 mg, 2.4 mmol, 3.0 equiv), the resulting solution was stirred for 10 min at room temperature. 2-Cyclohexen-1-one **17** (77.0 mg, 0.8 mmol) was then added and the reaction mixture stirred for 24 hours at room temperature. The product **18** formation was monitored by TLC (elution with EA/*n*-hex 1:9) (5%

conversion).

- **Monophosphine ligands.** A solution of $[\text{Rh}(\text{cod})\text{Cl}]_2$ (0.5 mg, 1.0 μmol) in dioxane (0.2 mL) was added to a solution of commercially available phosphine TPPDS **L7** (2.0 mg, 4.0 μmol , 4.0 equiv) in water (2.0 mL), containing K_2CO_3 (150.6 mg, 1.1 mmol, 2.1 equiv), or Tris buffer (2.0 mL, 20 mM, pH 8.0) to achieve final $[\text{Rh}]$ concentration of 9.1, 0.91 and 0.23 mM, respectively. The resulting mixture was stirred under argon for 30 min, at room temperature. After addition of sodium dodecyl sulfate SDS surfactant (78.0 mg, 0.27 mmol, 0.5 equiv), phenylboronic acid **16** (158.5 mg, 1.3 mmol, 2.5 equiv) and 2-cyclohexen-1-one **17** (49.6 mg, 0.52 mmol), the reaction mixture was heated at 37°C and the stirring continued for 48 hours.

Control experiment with $[\text{Rh}(\text{cod})\text{Cl}]_2$ catalyst and no ligand was also carried out. $[\text{Rh}(\text{cod})\text{Cl}]_2$ (6.2 mg, 12.5 μmol) was dissolved in dioxane (8 mL). From this solution, 0.2 mL was diluted with Tris buffer (2.0 mL, 20 mM, pH 8.0) to achieve 0.23 mM final $[\text{Rh}]$ concentration. After addition of SDS (78.0 mg, 0.27 mmol, 0.5 equiv), phenylboronic acid (158.5 mg, 1.3 mmol, 3.0 equiv) and 3-phenyl-1-cyclohexanone **18** (49.6 mg, 0.52 mmol), the resulting mixture was stirred for 48 hours at 37°C.

When phosphine **L1** was used, the 1,4-addition reaction was performed in 50% water. $[\text{Rh}(\text{cod})\text{Cl}]_2$ (4.9 mg, 10.0 μmol , 3.85 mol%) was added to a solution **L1** (12.2 mg, 40.0 μmol , 2.0 equiv per Rh) in dioxane or methanol (1.1 mL). SDS (78.0 mg, 0.27 mmol, 0.5 equiv) and water (1.1 mL) were added and the whole mixture stirred for 30 min at room temperature. To the flask were then added successively phenylboronic acid **16** (158.5 mg, 1.3 mmol, 3.0 equiv) and 2-cyclohexen-1-one **17** (49.6 mg, 0.52 mmol). The reaction mixture was heated at 50°C and then stirred at 50°C for 19 hours. After extraction with diethyl ether (2×2 mL), the organic phase was filtered through a short silicagel plug (20×6 mm, in a 6 mm pipette). After evaporation of the solvent under reduced pressure, the residue was dissolved in 2:1 acetonitrile/water (3 mL). The yields were determined by reversed-phase HPLC analysis (C18 column (4.6×250 mm), elution with 70% acetonitrile and 30% water, detection wavelength 254 nm; $t_{\text{R}} = 5.6$ min (3-phenyl-cyclohexanone)). A calibration curve was obtained by plotting the integrated peak area versus various product concentrations (2.25, 4.50, 9.00, 13.50 and 18 mM concentration 3-phenyl-1-cyclohexanone; $c_{\text{P}} = 0.0036 \cdot \text{Area} + 0.0929$, $R^2 = 0.9902$). Conversion: 7-42%.

• **Bisphosphine L2 and L8 ligands.** To a degassed solution of $[\text{RhL2}(\text{nbD})]^+\text{BF}_4^-$ complex **13** (27.1 mg, 0.03 mmol) or $[\text{RhL8}(\text{nbD})]^+\text{BF}_4^-$ (24.0 mg, 0.03 mmol) in dioxane (3.0 mL), phenylboronic acid **16** (183.0 mg, 1.5 mmol, 1.5 equiv) and water (0.5 mL) were added. The resulting mixture was further degassed by two freeze-thaw cycles. After stirring for 30 min at room temperature, TEA (0.14 mL, 1.0 mmol, 1.0 equiv) was added and the reaction started by addition of 2-cyclohexen-1-one **17** (97.0 μL , 1.0 mmol). The resulting mixture was stirred for 6 hours at room temperature. The final concentration of Rh complex was in all cases 10 mM, corresponding to 3 mol% catalyst loading.

Test reactions were setup and performed also in air. Control experiments only with $[\text{Rh}(\text{cod})\text{Cl}]_2$ pre-catalyst were carried out in the absence and presence of base (0.1 equiv NaHCO_3) under the conditions described above. Reactions with the *in situ* generated Rh complex were performed by addition of $[\text{Rh}(\text{nbD})\text{Cl}]_2$ (6.9 mg, 0.015 mmol) to a degassed solution of BINAP ligand **L8** (28.0 mg, 0.045 mmol, 1.5 equiv per Rh) in 6:1 dioxane/water (3 mL) and then similarly to the other catalytic reactions.

In all cases, after filtration through a syringe filter (0.2 μm , PTFE), the crude product was diluted with water to 3.5 mL and analyzed by reversed-phase HPLC (C18 column (4.6 \times 250 mm), elution with 50% water, 50% acetonitrile, detection wavelength 260 nm, $t_{\text{R}}(\mathbf{18}) = 11.0$ min). Conversions: 0-80%.

• **PHOX L5 ligand.** 1,4-Addition with the isolated Rh-PHOX complex **14** or with the *in situ* prepared complex was carried out in 3:7 dioxane/water. The following stock solutions in dioxane were used: 1) solution of 0.41 M 2-cyclohexen-1-one, 0.40 M TEA and 0.02 M benzophenone as internal standard, 2) 0.60 M phenylboronic acid **16**, and 3) 0.01 M $[\text{RhL5}(\text{nbD})]^+\text{BF}_4^-$ complex **14**. Additionally, Rh(I) complex was *in situ* prepared by weighing $[\text{Rh}(\text{C}_2\text{H}_4)_2\text{Cl}]_2$ pre-catalyst (3.9 mg, 0.010 mmol) and ligand **L5** (8.6 mg, 0.022 mmol, 1.1 equiv ligand per Rh) into a Schlenk flask, under argon atmosphere. Degassed dioxane was then added (2.0 mL) to generate 10 mM stock solution of catalyst. The resulting mixture turned immediately deep red and was used in catalytic reactions without further purification.

For each catalytic experiment, a Schlenk flask was charged with degassed water (0.7 mL). To the flask were added successively degassed solutions of $[\text{RhL5}(\text{nbD})]^+\text{BF}_4^-$ (0.01 mL, 1.0 μmol), or the *in situ* prepared Rh(I) catalyst (0.1 mL, 1.0 μmol), 2-

cyclohexen-1-one **17** and TEA (0.1 mL, 41.0 μmol enone substrate, 20.0 μmol internal standard and 40.0 μmol base, respectively), and finally phenylboronic acid **16** (0.1 mL, 60.0 μmol , 1.5 equiv), yielding 1.0 mM final catalyst concentration and 2.4 mol% catalyst loading, respectively. The reaction mixture was stirred for 4 hours at room temperature. After extraction with diethyl ether (2×1 mL), the organic phase was passed through a short silica gel plug (10×6 mm, in a 6 mm pipette). The eluate was then evaporated to dryness under reduced pressure. The residue was dissolved in 1:1 water/acetonitrile and analyzed by reversed-phase HPLC (C18 column (4.6×250 mm), elution with 50% water and 50% acetonitrile, detection wavelength 260 nm, $t_{\text{R}}(\mathbf{18}) = 11.0$ min).

5.9.2 Allylic Amination

5.9.2.1 Synthesis and Stability of the Allylic Substrate

The branched monosubstituted allylic substrate, racemic mixture, was prepared by esterification of 1-phenylprop-2-en-1-ol **19**. The linear allylic substrate, cinnamyl acetate **20**, is commercially available.

Synthesis of 1-phenyl-2-propenyl acetate (21). A solution of commercially available 1-phenylprop-2-en-1-ol **19** (2.0 g, 14.9 mmol) and DMAP (0.18 g, 1.5 mmol, 0.1 equiv) at 0°C was slowly treated with acetic anhydride (7.1 mL, 74.5 mmol, 5 equiv) and then allowed to warm up to 25°C overnight. The conversion of allylic alcohol to allylic acetate was complete (TLC control 1:9 EA/*n*-hex). After quenching with saturated solution of NaHCO₃ (60 mL), the resulting solution was further stirred for additional 30 min at room temperature. The mixture was extracted with diethylether (2×60 mL) and the combined organic fractions were washed with 5% NaHCO₃ (100 mL), 1 M HCl (100 mL) and brine (100 mL) before being dried (Na₂SO₄) and concentrated in vacuo. Chromatography on silica gel (column preconditioned with the eluent containing 1% TEA, elution with 5:95 EA/*n*-hex) afforded compound **21** as colorless oil (1.8 g, 10.4 mmol, 82%). ¹H NMR (300 MHz; CDCl₃) δ 7.28-7.22 (m, 5H), 6.18 (td, $J = 5.8, 1.3$, 1H), 5.92 (ddd, $J = 17.2, 10.4, 5.9$ Hz, 1H), 5.19 (m, 2H), 2.02 (s, 3H). ¹³C NMR (126 MHz; CDCl₃) δ 169.84, 138.81, 136.21, 128.47, 128.08, 127.06, 116.80, 76.09, 21.15. EI MS: m/z 176.1 [M]⁺ (calcd for [C₁₁H₁₂O₂]⁺ 176.08).

Stability of the allylic substrate in aqueous (basic) environment. The stability of branched allylic acetate **21** in water and under basic conditions was investigated. Stock solutions of the two substrates were prepared by weighing 1-phenyl-2-propenyl acetate **21** (35.2 mg, 0.2 mmol) into a vial and adding 10 mL acetonitrile. Samples from the resulting solution were diluted with an equal volume of water or aqueous 0.1 M NaHCO₃ solution, affording 10.0 mM final concentration of **21**. The resulting solutions were stored at room temperature for 9 hours. Aliquots (20 μ L) were withdrawn at regular time intervals and analyzed by reversed-phase HPLC (C18 column (4.6 \times 250 mm), elution with 50% water and 50% acetonitrile, detection wavelength 260 nm, t_R (**21**) = 14.4 min) (Figure 3.21, Chapter 3.2.3.1).

5.9.2.2 Synthesis of Linear and Branched Allylic Amines

Synthesis of 4-(1-phenyl-2-propenyl)-morpholine (24). Allyl substrate 1-phenyl-2-propenyl acetate **21** (0.5 g, 2.8 mmol) was weighed into a Schlenk flask equipped with a reflux condenser, dissolved in ethanol (10 mL) and the resulting solution degassed (3 cycles). [Rh(cod)Cl]₂ (28.1 mg, 0.06 mmol, 4.3 mol%) and triphenyl phosphite (63.0 μ L, 0.24 mmol, 2.0 equiv/Rh) were then added and the mixture immediately degassed (one cycle). After addition of morpholine **22** (0.75 mL, 8.5 mmol, 3.0 equiv), the reaction mixture was heated at 40°C and stirred overnight until the ester was fully converted to the amine (TLC control 1:9 EA/*n*-hex). After cooling the solution at room temperature, the crude was extracted with diethyl ether (20 mL), and the organic layer washed with saturated aqueous NaHCO₃ solution (ca 20 mL) until the pH of the organic layer was 8.0. The organic layer was then dried over Na₂SO₄, the solvent was evaporated under reduced pressure and the product purified by column chromatography (eluent 1:9 EA/*n*-hex). The allylic amine **24** was obtained as colorless oil (0.55 g, 2.7 mmol, 96%). ¹H NMR (300 MHz; CDCl₃) δ 7.27-7.13 (m, 5H), 5.81 (ddd, J = 17.1, 10.1, 8.8 Hz, 1H), 5.14 (ddd, J = 17.1, 1.6, 0.7 Hz, 1H), 5.00 (dd, J = 10.1, 1.8, 1H), 3.59 (m, 4H), 3.53 (d, J = 8.8 Hz, 1H), 2.43-2.36 (m, 2H), 2.27-2.20 (m, 2H). ¹³C NMR (76 MHz; CDCl₃) δ 141.48, 139.66, 128.47, 127.83, 127.13, 116.48, 75.39, 67.02, 51.88. EI MS: m/z 203.2 [M]⁺ (calcd for [C₁₃H₁₇NO]⁺ 203.13).

Synthesis of 4-(3-phenyl-2-propenyl)-morpholine (25). In a Schlenk flask, Pd(PPh₃)₄ (0.11 mmol, 0.13 g, 2 mol%) was dissolved in degassed dry THF (15 mL). Cinnamyl

acetate **20** (1.0 g, 5.7 mmol) and morpholine **22** (1.5 mL, 17.1 mmol, 3.0 equiv) were then added to the reaction mixture. The resulting solution was heated to 50°C and allowed to stir at 50°C for 6 hours until complete conversion of the allylic substrate (TLC control 3:7 EA/*n*-hex). After cooling down to room temperature, the crude product was extracted with diethyl ether (20 mL) and washed 5% aqueous NaHCO₃ solution (20 mL), and brine (20 mL). The organic phase was dried over Na₂SO₄, concentrated under reduced pressure and the product purified by flash column chromatography (elution 1:4 EA/*n*-hex) to give linear allylic amine **25** as colorless oil (0.97 g, 4.7 mmol, 84%). ¹H NMR (300 MHz; CDCl₃) δ 7.62-7.11 (m, 5H), 6.44 (dd, *J* = 15.9, 1H), 6.16 (td, *J* = 15.9, 6.8, 1H), 3.64 (m, 4H), 3.05 (dd, *J* = 6.8, 1.3, 2H), 2.40 (m, 4H). ¹³C NMR (76 MHz; CDCl₃) δ 136.65, 133.21, 128.43, 127.42, 126.17, 125.93, 66.83, 61.33, 53.56. EI MS: *m/z* 203.3 [M]⁺ (calcd for [C₁₃H₁₇NO]⁺ 203.13).

Synthesis of N-(1-phenyl-2-propenyl) glycine ethyl ester (26). In a Schlenk flask, 1-phenyl-2-propenyl acetate **21** (0.5 g, 2.8 mmol) was dissolved in acetonitrile (4 mL) and the solution degassed. To this solution were added [Rh(cod)Cl]₂ (56.0 mg, 0.11 mmol) and trimethylphosphite (70.5 mg, 71.0 μL, 0.57 mmol, 2.6 equiv per Rh). Separately, glycine ethyl ester hydrochloride **23** (0.6 g, 4.0 mmol, 1.4 equiv) was charged into a Schlenk flask. After addition of water (4 mL) and NaHCO₃ (0.47 g, 5.6 mmol, 2.0 equiv), the resulting solution was degassed, transferred to the reaction mixture and stirred at room temperature overnight (TLC control 3:7 EA/*n*-hex). The crude product was extracted with diethyl ether (2 × 20 mL) and the combined extracts washed with 1 M HCl (2 × 20 mL), 5% NaHCO₃ (20 mL) and brine (20 mL). After adjusting the pH to 7 with 5% NaHCO₃ (15 mL), the aqueous layer was one more time extracted with diethyl ether (40 mL). The combined organic phase was dried over Na₂SO₄. The solvent was evaporated and the residue chromatographed on silica gel (elution 1:9 EA/*n*-hex), affording amine **26** as colorless oil (0.26 mg, 1.2 mmol, 41%). ¹H NMR (300 MHz; CDCl₃) δ 7.31-7.17 (m, 5H), 5.83 (m, 1H), 5.18 (d, *J* = 16.2 Hz, 1H), 5.06 (m, 1H), 4.14 (m, 2H), 3.29 (s, 2H), 1.19 (t, 3H). ¹³C NMR (76 MHz; CDCl₃) δ 172.52, 142.06, 140.24, 128.61, 127.45, 127.36, 126.37, 115.69, 65.45, 60.75, 48.54, 14.22.

5.9.2.3 Allylic Amination Catalyzed by Ir-PHOX Complexes

Stock solutions of $[\text{Ir}(\text{cod})\text{Cl}]_2$ (50 mM), and phosphinooxazolines **L4** and **L5** (6.3 mM) were prepared by weighing $[\text{Ir}(\text{cod})\text{Cl}]_2$ (33.6 mg, 0.05 mmol) into a volumetric flask and adding 1 mL dioxane, and **L4** (4.5 mg, 12.0 μmol) and **L5** (4.7 mg, 12.0 μmol) into Schlenk flasks and adding to each 1.8 mL degassed dioxane, respectively. Ir-catalyst was prepared by adding with a syringe 0.2 mL stock solution $[\text{Ir}(\text{cod})\text{Cl}]_2$ to each Schlenk flask containing the ligand (1.25 equiv ligand per Ir), affording a final volume of 2 mL. The resulting solutions turned immediately deep red indicating the *in situ* formation of Ir-**L4** and Ir-**L5** complexes (10.0 mM). From each solution, 0.2 and 0.3 mL were transferred into separate Schlenk flasks and diluted with degassed dioxane (up to 2.0 and 5.0 mL, respectively) to give 1.0 mM and 0.6 mM Ir-**L4** and Ir-**L5** stock solutions. The Ir-PHOX stock solutions were stored at -20°C and used for multiple catalytic experiments.

Stock solutions of $[\text{Ir}(\text{cod})\text{Cl}]_2$ were prepared by weighing 4.9 mg (12.5 μmol) in volumetric flasks by adding the appropriate amount of dioxane to achieve a range of 5.0, 0.5, 0.3, 0.25, and 0.1 mM final concentrations. $[\text{Ir}(\text{cod})\text{Cl}]_2$ stock solutions were each time newly prepared, degassed (by at least three freeze-thaw cycles) and used for single set of experiments.

Allylic substrate stock solution was prepared by weighing dodecane (489.4 mg, 2.88 mmol), as internal standard, together with 1-phenyl-2-propenyl acetate **21** (885.6 mg, 5.0 mmol) or cinnamyl acetate **20** (885.6 mg, 5.0 mmol) into two vials and adding 10.0 mL dioxane to each vial to make the final concentration of 0.50 M allylic substrate and 0.28 M internal standard.

Two aqueous stock solutions of morpholine **22** were prepared by weighing each time 163.4 mg (1.88 mmol) into a volumetric flask and adding 1:7 dioxane/water or dioxane/aqueous 125 mM NaClO_4 , 6.25 mM $\text{Mg}(\text{ClO}_4)_2$ solution (10 mL), and yielding 0.18 M final morpholine concentration. Stock solution of morpholine in neat dioxane was also prepared by dissolving **22** (480.0 mg, 5.5 mmol) in 10 mL dioxane to a final concentration of 0.55 M.

Stock solution of glycine ethyl ester hydrochloride **23** containing NaHCO_3 was prepared by weighing the aminoacid ester (195.4 mg, 1.4 mmol) and the base (176.4 mg, 2.1

mmol, 1.5 equiv) in a volumetric flask and adding water (10 mL) to give 0.14 M final concentration of glycine ethyl ester **23** in 0.21 M aqueous NaHCO₃ solution.

All stock solutions were then placed in Schlenk flasks, stored under argon (at -20°C) and degassed every time before using in allylic amination reactions.

Gas chromatography analysis. The course of the catalytic allylic aminations was monitored by gas chromatography performed with a Shimadzu GC-2014 instrument. Capillary column FS-Supreme-5, 30 m × 0.38 mm AD × 0.25 mm, carrier gas helium. GC-method: T_{injector} = 200°C, T_{detector} = 250°C, 1.03 mL/min flow rate, 120.0 kPa column pressure, 1 µL injected volume, split ratio 40.0. Temperature program: 2 min at 150°C, increase to 230°C with 15°C/min; t_R = 3.3 min (dodecane), 3.9 min (**21**), 5.5 min (**20**), 6.4 min (**24**) and 8.0 min (**25**). The products and the substrates were quantified using internal standard. Internal standard (dodecane) concentration was maintained 1.44 mM in all cases, while concentrations of substrates and products were ranging between 0.028-0.690 mM (**21**, fitted equation: $A/A_{\text{standard}} = 0.8958 \cdot (c/c_{\text{standard}}) + 0.0005$, R² = 0.9978), 0.051-2.537 mM (**20**, fitted equation: $A/A_{\text{standard}} = 0.8139 \cdot (c/c_{\text{standard}}) + 0.0127$, R² = 0.9976), 2.509-0.050 mM (**24**, fitted equation: $A/A_{\text{standard}} = 0.9346 \cdot (c/c_{\text{standard}}) + 0.0122$, R² = 0.9977) and 0.625-0.025 mM (**25**, fitted equation: $A/A_{\text{standard}} = 0.9825 \cdot (c/c_{\text{standard}}) - 0.0070$, R² = 0.9976).

HPLC analysis. The determination of the enantiomeric excesses of 4-(1-phenyl-2-propenyl)-morpholine **24** was effected by Agilent 1100 Series HPLC system equipped with a diode array detector, using a Diacel CHIRALCEL OJ-H (0.46 cm × 25 cm) and eluting with *n*-hexane/*i*-propanol = 99:1 at 0.7 mL/min flow-rate (detection wavelength = 220, 254 nm; t_R (**24**) = 10.8, 12.5 min).

General procedure for iridium(I)-catalyzed allylic amination reaction. All reactions were performed in the presence of 1.0 and 0.05-0.1 mM Ir catalyst, on 1.0 mL scale. Stock solution of Ir catalyst (0.1 mL) was added to 0.1 mL degassed stock solution of branched **21** or linear allylic substrate **20** (0.05 mmol, 8.8 mg) in a Schlenk flask containing a stirring bar. Aqueous solution of morpholine **22** (0.8 mL, 13.1 mg, 0.15 mmol, 3.0 equiv) was added with a syringe, and the reaction was stirred at various temperatures (25, 37, 50°C) for 1-16 hours (TLC control 3:7 EA/*n*-hex). The crude product was extracted with diethyl ether (3 × 1 mL) and the combined organic layers were dried over Na₂SO₄. After partial removal of the solvent under reduced pressure,

the mixture was filtered over a layer of silica gel (20 × 6 mm, in a 6 mm pipette). The solvent was then evaporated under light vacuum and the residue was dissolved in 1,2-dichloroethane (2 mL) and analyzed by gas chromatography. The crude reaction mixture was then purified by preparative TLC (elution 3:7 EA/*n*-hex) and the desired product was subjected to determination of enantiomeric excess by HPLC.

The same general procedure was also used with 0.1 mL of the stock solution of Ir-**L5** complex (10.0 mM, in acetonitrile), 0.1 mL stock solution of branched allylic acetate **21** (0.5 M, acetonitrile), 0.3 mL acetonitrile and 0.5 mL of the stock solution of glycine ethyl ester **23** (0.14 M, in 0.14 M aqueous NaHCO₃). The amination reaction was conducted at room temperature for 16 hours. The crude reaction mixture was diluted to 5 mL by addition of 1:1 water/acetonitrile, filtered (0.22 μm, PTFE) and analyzed by reversed-phase HPLC (injected volume 20 μL, C18 column (4.6×250 mm), elution with 50% water and 50% acetonitrile, 1 mL/min flow rate, 25°C column temperature, detection wavelength 260 nm, *t_R*(**26**) = 12.4 min).

Iridium(I)-catalyzed allylic amination in the presence of unmodified DNA. All control reactions were carried out at 0.05-0.1 mM Ir catalyst, in 3:7 dioxane/water (100 μL) and in the presence of 23mer **cDNA2**. Typically, in a PCR or Eppendorf tube placed under argon and containing a stirring bar (Figure 5.6), DNA (5.33-13.3 nmol) was dissolved in aqueous solution of morpholine **22** (80 μL, 15.0 μmol), containing NaClO₄ and Mg(ClO₄)₂ (see preparation of morpholine stock solutions). The resulting solution was then mixed with 5-10 μL stock solution of [Ir(cod)Cl]₂ (0.5 mM) or preformed catalyst Ir-**L5** (1.0 mM) in a volume of 90 μL, yielding 1.1-1.3 equiv DNA per Ir. After stirring the resulting solution for 30 min at room temperature, the reaction was started with the addition of allylic substrate **21** (10 μL, 5.0 μmol) and mixed by continuous stirring for 14-18 hours at room temperature. After addition of diethyl ether (200 μL), the reaction mixture was passed over a silica gel plug (20 × 6 mm, in a 6 mm Pasteur pipette) and the crude product eluted with diethyl ether. The solvent was removed under light vacuum, the residue dissolved in 1,2-dichloroethane (0.5-0.7 mL) and analyzed by gas-chromatography for estimating the reaction conversion. The product was then purified by preparative TLC (elution 3:7 EA/*n*-hex, product recovery in ethyl acetate) and the enantiomeric excess determined by chiral HPLC.



Figure 5.6. Reaction set-up for Ir(I)-catalyzed amination using DNA-based PHOX ligands.

Iridium(I)-catalyzed allylic amination with single-stranded DNA-PHOX ligands ODN11a-c and ODN12a,b. The HPLC fraction containing the desired DNA-PHOX conjugate was collected in a 25 mL Greiner tube, under argon atmosphere and immediately degassed. A known volume of eluate, typically 0.6-0.8 mL, was transferred in an Eppendorf tube (1.5 mL), purged several times with argon and lyophilized overnight. The remaining eluate was used in UV measurements to determine the amount of isolated DNA-PHOX conjugate and implicitly the amount of DNA-ligand to be used for the catalytic experiment (typically 1.5-5.2 nmol). The lyophilized DNA was then redissolved in thoroughly degassed 143.0 mM NaClO₄, 7.0 mM Mg(ClO₄)₂ aqueous solution (35-70 μL) and combined with the corresponding amount of 0.5 mM, 0.3 mM, or 0.25 mM [Ir(cod)Cl]₂ stock solution (5.0-10.0 μL, 1.5-5.0 nmol) to generate *in situ* the DNA-Ir catalyst (1.1-1.3 equiv DNA-PHOX/Ir). After stirring for 20-30 min under argon, an aliquot of stock solution of allylic acetate substrate **21** (5.0-10.0 μL) was added to the DNA solution to a final concentration of 50 mM and the stirring continued for 10 min. Finally, degassed solution of morpholine **22** (0.55 M, 5.0-10.0 μL, 1.1 equiv amine to the allylic substrate) was added and the amination reaction conducted for 16-19 hours, at room temperature, with a final Ir catalysts concentration ranging between 20 and 100 μM. The reaction mixture was then diluted with diethyl ether (0.2 mL) and the reaction vial washed with diethyl ether (2 × 0.2 mL). The resulting solution was filtered through a short silica gel plug that was thoroughly washed with diethyl ether,

concentrated under light vacuum and subjected to GC and chiral HPLC analysis as described in the paragraph “General procedure for Ir-catalyzed allylic amination reaction”.

In parallel, the stability of the DNA-PHOX conjugates upon addition of Ir precatalyst and under the conditions employed in allylic amination reaction was investigated. To a **ODN11a-c** solution (1.1-1.3 equiv per metal ion) was added stock solution of $[\text{Ir}(\text{cod})\text{Cl}]_2$ to a final volume of 0.1 mL 3:7 dioxane/water and 0.1 mM final Ir(I) catalyst concentration. The resulting mixture was sampled (approx. 25 μL) at various time points and analyzed by reversed-phase HPLC (gradient: increase from 1% B to 75% B over 40 min; detection at 260 nm, 1 mL/min flow-rate, 45°C column oven).

Iridium(I)-catalyzed allylic amination with double-stranded DNA-PHOX ligands.

Catalytic experiments using DNA/DNA or DNA/RNA duplexes were carried at room temperature, in 3:7 dioxane/water and 0.05-0.1 mL reaction scale. Concentrations of Ir(I) catalysts were maintained between 20 and 50 μM , unless otherwise stated. The double-stranded constructs were prepared by mixing equimolar quantities of DNA-PHOX conjugate **ODN11-13** and complementary **cdNA1-4** or **cRNA** sequence in an aqueous solution containing 143.0 mM NaClO_4 and 7.0 mM $\text{Mg}(\text{ClO}_4)_2$, at room temperature. Complementary DNA and RNA strands (2.0-4.0 nmol) were lyophilized, resuspended in degassed water with salts (35.0-70.0 μL) and added to an Eppendorf tube (Figure 5.6) containing the freshly lyophilized DNA-PHOX ligand. The resulting solution was immediately purged with argon. The two nucleic acid strands were then allowed to anneal at room temperature over 30-45 min and then treated with degassed $[\text{Ir}(\text{cod})\text{Cl}]_2$ solution (5.0-10.0 μL , 1.1-1.3 equiv DNA-PHOX per iridium ion). After stirring for 30 min at room temperature, stock solutions of allylic acetate **21** and respectively morpholine **22** substrates (5.0-10.0 μL each, final concentrations 50 mM and 55 mM respectively) were added and stirring continued for 16-19 hours, under argon atmosphere. Work-up of the crude reaction mixture followed the procedure described in the preceding paragraph.

6 Appendices

6.1 List of Abbreviations

δ	Chemical shift
ϵ	Molar extinction coefficient
λ	Wavelength
A	Adenosine; Peak area
A_{260}	Absorbance at 260 nm
Ac	Acetyl
ACN	Acetonitrile
ATP	Adenosine triphosphate
bd	Broad doublet
BINAP	2,2'-Bis(diphenylphosphino)-1,1'-binaphthyl
BINOL	1,1'-Bi-2-naphthol
bpa	<i>N,N'</i> -Bis(2-picoyl)amine
bpy	2,2'-Bipyridine
bs	Broad singlet
BTT	5-Benzylthio-(1 <i>H</i>)-tetrazole
c	Concentration
C	Cytidine
cDNA	Complementary DNA
Ci	Curie; 1Ci = 37 MBq
CID	Collision-induced dissociation
cod	1,5-cyclooctadiene
CPG	<u>C</u> ontrolled pore <u>g</u> lass
d	Doublet
dA	2'-Deoxy-adenosine
dC	2'-Deoxycytidine
DCM	Dichloromethane

DEA	Diethylamine
dG	2'-Deoxy-guanosine
DIPA	Diisopropylamine
DMAP	4-(Dimethylamino)pyridine
DMF	<i>N,N'</i> -Dimethylformamide
DMSO	Dimethyl sulfoxide
DMT	4,4'-Dimethoxytrytil
DNA	Deoxyribonucleic acid
dppz	Dipyridophenazine
EA	Ethylacetate
EDC	<i>N</i> -(3-Dimethylaminopropyl)- <i>N'</i> -ethylcarbodiimide hydrochloride
EDTA	Ethylenediamine tetraacetate
ee	Enantiomeric excess
EI	Electron impact
equiv	Equivalent
ESI	Electrospray ionization
EtOH	Ethanol
FAB	<u>F</u> ast <u>a</u> tom <u>i</u> c <u>b</u> ombardment
FT-ICR	<u>F</u> ourier- <u>t</u> ransform <u>i</u> on <u>c</u> yclotron <u>r</u> esonance
g	Gram
G	Guanosine
h	Hour
Hepes	4-(2-Hydroxyethyl)-1-piperazineethanesulfonic acid
hex	Hexane
HPLC	<u>H</u> igh <u>P</u> ressure <u>L</u> iquid <u>C</u> hromatography
<i>I</i>	Spin quantum number
<i>I</i>	Light intensity
<i>J</i>	Coupling constant
<i>K</i>	Reaction rate constant
<i>l</i>	Length of the light path
L	Liter; Ligand
LG	Leaving group

m	Meter; Multiplet
M	Mol/L; Molar; Transition metal
MALDI-TOF	<u>M</u> atrix <u>a</u> ssisted <u>l</u> aser <u>d</u> esorption <u>i</u> onization <u>t</u> ime- <u>o</u> f- <u>f</u> light
Me	Methyl
Me ₂ -dppz	7,8-Dimethyldipyridophenazine
min	Minute
MS	<u>M</u> ass <u>s</u> pectrometry
nbd	Bicyclo[2.2.1]hepta-2,5-diene; norbornadiene
NHS	<i>N</i> -hydroxysuccinimide, <i>N</i> -hydroxysuccinimidyl
nm	Nanometer
NMR	<u>N</u> uclear <u>m</u> agnetic <u>r</u> esonance
Nu	Nucleophile
ODN	Oligodeoxynucleotide
Pa	Pascal
PAGE	Polyacrylamide gel electrophoresis
PCR	Polymerase chain reaction
PG	Protecting group
Ph	Phenyl
PhCN	Benzonitrile
phen	1,10-Phenanthroline
phi	9,10-Phenanthrenequinone diimine
PHOX	2-(2-Diphenylphosphino-phenyl)-4,5-dihydrooxazole
PNK	Polynucleotide kinase
ppm	Parts per milion
Pr	Propyl
PTFE	Polytetrafluoroethane
PYRPHOS	3,4-Bis-diphenylphosphino-pyrrolidine
RNA	Ribonucleic acid
rpm	<u>R</u> otations <u>p</u> er <u>m</u> inute
rt	Room temperature
RT	Reverse transcription
s	Singlet

SDS	Sodiumdodecyl sulfate
sec	Second
SELEX	<u>S</u> ystematic <u>e</u> volution of <u>l</u> igands by <u>e</u> xponential <u>e</u> nrichment
S _N	Nucleophilic substitution
Solv	Solvent
t	Triplet
T	Thymidine; Temperature
TAC	(<i>t</i> -Butyl)phenoxyacetyl
tap	1,4,5,8-Tetraazaphenanthrene
TBE	Tris-borate-EDTA buffer
TCA	Trichloroacetic acid
TEA	Triethylamine
TEAA	Triethylammonium acetate
TFA	Trifluoroacetic acid
THF	Tetrahydrofuran
TLC	<u>T</u> hin <u>l</u> ayer <u>c</u> hromatography
T _m	Melting temperature
TPPDS	Bis(4-sulfonatophenyl)phenylphosphine
tpy	2,2':6',2''-Terpyridine
t _R	Retention time
Tris	Trishydroxymethylaminomethane; 2-amino-2-hydroxymethyl-1,3-propanediol
U	Uridine; Unit
UV	Ultraviolet

6.2 Instruments and Special Materials

Analytical balance	AX 204 and B3001-S Mettler Toledo
Centrifuges	Eppendorf 5804 R and Mikro 120 Hettich
Electrophoresis chamber	GIBCO BRL Sequencing System LIFE TECHNOLOGIES™

Eppendorf and PCR tubes, siliconized	Biozym
Exposure cassettes	For 35 × 43 cm Kodak imaging screens
Freeze dryer	BenchTop K Series, VirTis Ismatec
Gas chromatograph	Schimadzu GC-2014
- capillary column FS-Supreme-5, 30 m × 0.38 mm	
Gel Documentation equipment	AlphaImager™ 2200 Alpha Innotech
Greiner tubes	CellStar
HPLC	Agilent 1100 Series
HPLC Columns:	
- Luna C ₁₈ , 5 μm, 4.6 250 mm and 15.0 × 250 mm	Phenomenex®
- Chiralcel OJ-H, 4.6 × 250 mm	Daicel
Mass Spectrometer:	
- MALDI-TOF	Bruker BIFLEX III
- FAB and EI	JEOL JMS-700
- ESI	Finnigan MAT TSQ 700
- ESI FT-ICR	Bruker APEX IV
Minicentrifuges	Kiesker
NAP columns, Sephadex G-25	GE Healthcare (Amersham Biosciences)
NMR Spectrometer	Mercury Plus 300, Varian VNMR S 500, Bruker AC-300, DRX-300
pH-Meter	MP 220 Mettler Toledo
Phosphorimager	Typhoon 9400 Amersham Biosciences
Pipettes	Abimed P2, P20, P200, P1000
Scintillation counter	Beckman LS 6500
Silica gel 40 μm	J.T. Baker
Silica gel plates Polygram® Sil G/UV ₂₅₄ 40 × 80 mm	Macherey-Nagel
Speed vac	Univapo 100 ECH
Spin filters	Nanosep® MF Centrifugal devices, 0.2 μm PALL, Life Sciences

Synthesizer	Applied Biosystems Expedite™ 8909
Syringe filters	PTFE, 13 mm, 0.2 µm, Carl Roth
Thermomixer	Eppendorf, Thermomixer 5436
Ultrapure Water Purification System	Milli-Q, Millipore
UV Cuvettes	Quarzglas SUPRASIL, HELLMMA
UV-Lamp 254 nm	Benda NU-8 KL
UV-Transilluminator	254 nm, 300 × 200 mm Carl Roth
UV/VIS Spectrophotometer	
- Ultrospac 2100 pro	Amersham Pharmacia Biotech
- NanoDrop ND-1000	Peqlab Biotechnologie
- Cary 100 Bio	Varian
X-ray film	Fuji, Medical X-ray Film RXOG (Safety)
X-ray film cassettes	Kodak, X-OMATIC

7 References

- [1] R. Noyori, Asymmetric catalysis: science and opportunities (Nobel Lecture). *Angew. Chem., Int. Ed. Engl.* **2002**, *41*, 2008-22.
- [2] W. A. Bonner, The origin and amplification of biomolecular chirality. *Origins Life Evol. Biosphere* **1991**, *21*, 59-111.
- [3] W. A. Bonner, Chirality and life. *Origins Life Evol. Biosphere* **1995**, *25*, 175-90.
- [4] B. L. Feringa, R. A. Van Delden, Absolute asymmetric synthesis: the origin, control, and amplification of chirality. *Angew. Chem., Int. Ed. Engl.* **1999**, *38*, 3419-38.
- [5] C. M. Thomas, T. R. Ward, Artificial metalloenzymes: proteins as hosts for enantioselective catalysis. *Chem. Soc. Rev.* **2005**, *34*, 337-46.
- [6] H. E. Schoemaker, D. Mink, M. G. Wubbolts, Dispelling the Myths-Biocatalysis in Industrial Synthesis. *Science* **2003**, *299*, 1694-98.
- [7] K. A. Powell, S. W. Ramer, S. B. Del Cardayre, W. P. C. Stemmer, M. B. Tobin, P. F. Longchamp, G. W. Huisman, Directed evolution and biocatalysis. *Angew. Chem., Int. Ed. Engl.* **2001**, *40*, 3948-59.
- [8] E. N. Jacobsen, A. Pfaltz, H. Yamamoto, *Comprehensive Asymmetric Catalysis, Vol. 1-3*, Springer, Berlin, **1999**.
- [9] K. Muniz, C. Bolm, Configurational control in stereochemically pure ligands and metal complexes for asymmetric catalysis. *Chem. Eur. J.* **2000**, *6*, 2309-16.
- [10] W. S. Knowles, Asymmetric hydrogenations (Nobel Lecture). *Angew. Chem., Int. Ed. Engl.* **2002**, *41*, 1998-2007.
- [11] K. B. Sharpless, Searching for new reactivity (Nobel Lecture). *Angew. Chem., Int. Ed. Engl.* **2002**, *41*, 2024-32.
- [12] K. V. L. Crepy, T. Imamoto, New P-chirogenic phosphine ligands and their use in catalytic asymmetric reactions. *Top. Curr. Chem.* **2003**, *229*, 1-40.
- [13] R. Noyori, H. Takaya, BINAP: an efficient chiral element for asymmetric catalysis. *Acc. Chem. Res.* **1990**, *23*, 345-50.
- [14] J. A. Osborn, F. H. Jardine, J. F. Young, G. Wilkinson, Preparation and properties of tris(triphenylphosphine)halorhodium(I) and some reactions thereof including catalytic homogeneous hydrogenation of olefins and acetylenes and their derivatives. *J. Chem. Soc., A: Inorg. Phys. Theor.* **1966**, 1711-32.
- [15] U. Nagel, Asymmetric hydrogenation of α -(acetylamino)cinnamic acids with a new rhodium complex; the concept of an optimal ligand. *Angew. Chem.* **1984**,

- 96, 425-6.
- [16] M. J. Burk, C₂-symmetric bis(phospholanes) and their use in highly enantioselective hydrogenation reactions. *J. Am. Chem. Soc.* **1991**, *113*, 8518-19.
- [17] M. J. Burk, Modular Phospholane Ligands in Asymmetric Catalysis. *Acc. Chem. Res.* **2000**, *33*, 363-72.
- [18] G. D. Engel, L. H. Gade, Construction and probing of multisite chiral catalysts: dendrimer fixation of C₂-symmetrical diphosphinerhodium complexes. *Chem. Eur. J.* **2002**, *8*, 4319-29.
- [19] U. Nagel, E. Kinzel, Enantioselective catalysis. 4. Synthesis of N-substituted (R,R)-3,4-bis(diphenylphosphino)pyrrolidines. The use of their rhodium complexes for the asymmetric hydrogenation of α -(acylamino)acrylic acid derivatives. *Chem. Ber.* **1986**, *119*, 3326-43.
- [20] Q. H. Fan, G. J. Deng, C. C. Lin, A. S. C. Chan, Preparation and use of MeO-PEG-supported chiral diphosphine ligands: soluble polymer-supported catalysts for asymmetric hydrogenation. *Tetrahedron: Asymmetry* **2001**, *12*, 1241-47.
- [21] T. Belser, M. Stoehr, A. Pfaltz, Immobilization of Rhodium Complexes at Thiolate Monolayers on Gold Surfaces: Catalytic and Structural Studies. *J. Am. Chem. Soc.* **2005**, *127*, 8720-31.
- [22] Y. Ribourdouille, G. D. Engel, M. Richard-Plouet, L. H. Gade, A strongly positive dendrimer effect in asymmetric catalysis: allylic aminations with Pyrphos-palladium functionalised PPI and PAMAM dendrimers. *Chem. Commun.* **2003**, 1228-29.
- [23] A. Miyashita, A. Yasuda, H. Takaya, K. Toriumi, T. Ito, T. Souchi, R. Noyori, Synthesis of 2,2'-bis(diphenylphosphino)-1,1'-binaphthyl (BINAP), an atropisomeric chiral bis(triaryl)phosphine, and its use in the rhodium(I)-catalyzed asymmetric hydrogenation of α -(acylamino)acrylic acids. *J. Am. Chem. Soc.* **1980**, *102*, 7932-4.
- [24] A. Miyashita, H. Takaya, T. Souchi, R. Noyori, 2,2'-Bis(diphenylphosphino)-1,1'-binaphthyl (BINAP). A new atropisomeric bis(triaryl)phosphine. Synthesis and its use in the rhodium(I)-catalyzed asymmetric hydrogenation of α -(acylamino)acrylic acids. *Tetrahedron* **1984**, *40*, 1245-53.
- [25] U. Schmidt, J. Langner, B. Kirschbaum, C. Braun, Synthesis and enantioselective hydrogenation of α -acyloxyacrylates. *Synthesis* **1994**, 1138-40.
- [26] W. D. Lubell, M. Kitamura, R. Noyori, Enantioselective synthesis of β -amino acids based on BINAP-ruthenium(II) catalyzed hydrogenation. *Tetrahedron: Asymmetry* **1991**, *2*, 543-54.

- [27] M. Kitamura, Y. Hsiao, M. Ohta, M. Tsukamoto, T. Ohta, H. Takaya, R. Noyori, General asymmetric synthesis of isoquinoline alkaloids. Enantioselective hydrogenation of enamides catalyzed by BINAP-ruthenium(II) complexes. *J. Org. Chem.* **1994**, *59*, 297-310.
- [28] D. M. Tschaen, L. Abramson, D. Cai, R. Desmond, U.-H. Dolling, L. Frey, S. Karady, Y.-J. Shi, T. R. Verhoeven, Asymmetric Synthesis of MK-0499. *J. Org. Chem.* **1995**, *60*, 4324-30.
- [29] T. Ohta, H. Takaya, M. Kitamura, K. Nagai, R. Noyori, Asymmetric hydrogenation of unsaturated carboxylic acids catalyzed by BINAP-ruthenium(II) complexes. *J. Org. Chem.* **1987**, *52*, 3174-6.
- [30] H. Takaya, T. Ohta, N. Sayo, H. Kumobayashi, S. Akutagawa, S. Inoue, I. Kasahara, R. Noyori, Enantioselective hydrogenation of allylic and homoallylic alcohols. *J. Am. Chem. Soc.* **1987**, *109*, 1596-7.
- [31] R. Noyori, T. Ohkuma, M. Kitamura, H. Takaya, N. Sayo, H. Kumobayashi, S. Akutagawa, Asymmetric hydrogenation of β -keto carboxylic esters. A practical, purely chemical access to β -hydroxy esters in high enantiomeric purity. *J. Am. Chem. Soc.* **1987**, *109*, 5856-8.
- [32] S. Jeulin, S. D. De Paule, V. Ratovelomanana-Vidal, J.-P. Genet, N. Champion, P. Dellis, Chiral biphenyl diphosphines for asymmetric catalysis: stereoelectronic design and industrial perspectives. *Proc. Natl. Acad. Sci. USA* **2004**, *101*, 5799-804.
- [33] K. Tani, J.-i. Onouchi, T. Yamagata, Y. Kataoka, Iridium(I)-catalyzed asymmetric hydrogenation of prochiral imines; protic amines as catalyst improvers. *Chem. Lett.* **1995**, 955-6.
- [34] Y. Sato, M. Sodeoka, M. Shibasaki, Catalytic asymmetric carbon-carbon bond formation: asymmetric synthesis of cis-decalin derivatives by palladium-catalyzed cyclization of prochiral alkenyl iodides. *J. Org. Chem.* **1989**, *54*, 4738-9.
- [35] F. Ozawa, Y. Kobatake, A. Kubo, T. Hayashi, Palladium-catalyzed asymmetric hydroalkenylation of norbornene. *J. Chem. Soc., Chem. Commun.* **1994**, 1323-4.
- [36] F. Ozawa, A. Kubo, Y. Matsumoto, T. Hayashi, E. Nishioka, K. Yanagi, K. Moriguchi, Palladium-catalyzed asymmetric arylation of 2,3-dihydrofuran with phenyl triflate. A novel asymmetric catalysis involving a kinetic resolution process. *Organometallics* **1993**, *12*, 4188-96.
- [37] Y. Nakamura, S. Takeuchi, S. Zhang, K. Okumura, Y. Ohgo, Preparation of a fluorous chiral BINAP and application to an asymmetric Heck reaction. *Tetrahedron Lett.* **2002**, *43*, 3053-56.

- [38] D. Kiely, P. J. Guiry, A comparative study of diphosphine and phosphinamine palladium complexes on a new substrate for the intramolecular asymmetric Heck reaction. *Tetrahedron Lett.* **2002**, *43*, 9545-47.
- [39] O. Loiseleur, P. Meier, A. Pfaltz, Chiral phosphanyldihydrooxazoles in asymmetric catalysis: enantioselective Heck reactions. *Angew. Chem., Int. Ed. Engl.* **1996**, *35*, 200-2.
- [40] Y. Takaya, M. Ogasawara, T. Hayashi, M. Sakai, N. Miyaura, Rhodium-Catalyzed Asymmetric 1,4-Addition of Aryl- and Alkenylboronic Acids to Enones. *J. Am. Chem. Soc.* **1998**, *120*, 5579-80.
- [41] S. Sakuma, M. Sakai, R. Itooka, N. Miyaura, Asymmetric Conjugate 1,4-Addition of Arylboronic Acids to α,β -Unsaturated Esters Catalyzed by Rhodium(I)/(S)-binap. *J. Org. Chem.* **2000**, *65*, 5951-55.
- [42] Y. Takaya, T. Senda, H. Kurushima, M. Ogasawara, T. Hayashi, Rhodium-catalyzed asymmetric 1,4-addition of arylboron reagents to α,β -unsaturated esters. *Tetrahedron: Asymmetry* **1999**, *10*, 4047-56.
- [43] T. Hayashi, T. Senda, Y. Takaya, M. Ogasawara, Rhodium-Catalyzed Asymmetric 1,4-Addition to 1-Alkenylphosphonates. *J. Am. Chem. Soc.* **1999**, *121*, 11591-92.
- [44] M. Sakai, H. Hayashi, N. Miyaura, Rhodium-Catalyzed Conjugate Addition of Aryl- or 1-Alkenylboronic Acids to Enones. *Organometallics* **1997**, *16*, 4229-31.
- [45] T. Hayashi, T. Senda, M. Ogasawara, Rhodium-Catalyzed Asymmetric Conjugate Addition of Organoboronic Acids to Nitroalkenes. *J. Am. Chem. Soc.* **2000**, *122*, 10716-17.
- [46] K. Fagnou, M. Lautens, Rhodium-catalyzed carbon-carbon bond forming reactions of organometallic compounds. *Chem. Rev.* **2003**, *103*, 169-96.
- [47] T. Hayashi, K. Yamasaki, Rhodium-Catalyzed Asymmetric 1,4-Addition and Its Related Asymmetric Reactions. *Chem. Rev.* **2003**, *103*, 2829-44.
- [48] P. Guerreiro, V. Ratovelomanana-Vidal, J. P. Genet, P. Dellis, Recyclable diguanidinium-BINAP and PEG-BINAP supported catalysts: syntheses and use in Rh(I) and Ru(II) asymmetric hydrogenation reactions. *Tetrahedron Lett.* **2001**, *42*, 3423-26.
- [49] T. Lamouille, C. Saluzzo, R. ter Halle, F. Le Guyader, M. Lemaire, Hydrogenation of ethyl acetoacetate catalyzed by hydrosoluble BINAP derivatives. *Tetrahedron Lett.* **2001**, *42*, 663-64.
- [50] Y. Otomaru, T. Senda, T. Hayashi, Preparation of an Amphiphilic Resin-Supported BINAP Ligand and Its Use for Rhodium-Catalyzed Asymmetric 1,4-

- Addition of Phenylboronic Acid in Water. *Org. Lett.* **2004**, *6*, 3357-59.
- [51] C. J. Chapman, C. G. Frost, M. P. Gill-Carey, G. Kociok-Kohn, M. F. Mahon, A. S. Weller, M. C. Willis, Diphosphine mono-sulfides: readily available chiral monophosphines. *Tetrahedron: Asymmetry* **2003**, *14*, 705-10.
- [52] J. W. Faller, J. C. Wilt, J. Parr, Kinetic Resolution and Unusual Regioselectivity in Palladium-Catalyzed Allylic Alkylations with a Chiral P,S Ligand. *Org. Lett.* **2004**, *6*, 1301-04.
- [53] J. W. Faller, C. Wilt Jeremy, Palladium/BINAP(S)-catalyzed asymmetric allylic amination. *Org. Lett.* **2005**, *7*, 633-6.
- [54] J. W. Faller, J. C. Wilt, Regioselectivity in the Palladium/(S)-BINAP(S)-Catalyzed Asymmetric Allylic Amination: Reaction Scope, Kinetics, and Stereodynamics. *Organometallics* **2005**, *24*, 5076-83.
- [55] G. Helmchen, S. Kudis, P. Sennhenn, H. Steinhagen, Enantioselective catalysis with complexes of asymmetric P,N-chelate ligands. *Pure Appl. Chem.* **1997**, *69*, 513-18.
- [56] J. Sprinz, G. Helmchen, Phosphinoaryl- and phosphinoalkyloxazolines as new chiral ligands for enantioselective catalysis: very high enantioselectivity in palladium catalyzed allylic substitutions. *Tetrahedron Lett.* **1993**, *34*, 1769-72.
- [57] G. Helmchen, A. Pfaltz, Phosphinoxazolines-A New Class of Versatile, Modular P,N-Ligands for Asymmetric Catalysis. *Acc. Chem. Res.* **2000**, *33*, 336-45.
- [58] A. Lightfoot, P. Schnider, A. Pfaltz, Enantioselective hydrogenation of olefins with iridium-phosphanodihydrooxazole catalysts. *Angew. Chem., Int. Ed. Engl.* **1998**, *37*, 2897-99.
- [59] D. G. Blackmond, A. Lightfoot, A. Pfaltz, T. Rosner, P. Schnider, N. Zimmermann, Enantioselective hydrogenation of olefins with phosphinoxazoline-iridium catalysts. *Chirality* **2000**, *12*, 442-49.
- [60] S. P. Smidt, N. Zimmermann, M. Studer, A. Pfaltz, Enantioselective hydrogenation of alkenes with iridium-PHOX catalysts: A kinetic study of anion effects. *Chem. Eur. J.* **2004**, *10*, 4685-93.
- [61] A. Pfaltz, J. Blankenstein, R. Hilgraf, E. Hormann, S. McIntyre, F. Menges, M. Schonleber, S. P. Smidt, B. Wustenberg, N. Zimmermann, Iridium-catalyzed enantioselective hydrogenation of olefins. *Adv. Synth. Catal.* **2003**, *345*, 33-44.
- [62] P. Schnider, G. Koch, R. Pretot, G. Wang, F. M. Bohnen, C. Kruger, A. Pfaltz, Enantioselective hydrogenation of imines with chiral (phosphanodihydrooxazole)iridium catalysts. *Chem. Eur. J.* **1997**, *3*, 887-92.
- [63] O. Loiseleur, M. Hayashi, M. Keenan, N. Schmees, A. Pfaltz, Enantioselective

- Heck reactions using chiral P,N-ligands. *J. Organomet. Chem.* **1999**, *576*, 16-22.
- [64] G. Helmchen, Enantioselective palladium-catalyzed allylic substitutions with asymmetric chiral ligands. *J. Organomet. Chem.* **1999**, *576*, 203-14.
- [65] P. von Matt, O. Loiseleur, G. Koch, A. Pfaltz, C. Lefeber, T. Feucht, G. Helmchen, Enantioselective allylic amination with chiral (phosphino-oxazoline)palladium catalysts. *Tetrahedron: Asymmetry* **1994**, *5*, 573-84.
- [66] R. N. Constantine, N. Kim, R. C. Bunt, Hammett Studies of Enantiocontrol by PHOX Ligands in Pd-Catalyzed Allylic Substitution Reactions. *Org. Lett.* **2003**, *5*, 2279-82.
- [67] J. P. Janssen, G. Helmchen, First enantioselective alkylations of monosubstituted allylic acetates catalyzed by chiral iridium complexes. *Tetrahedron Lett.* **1997**, *38*, 8025-26.
- [68] C. Garcia-Yebra, J. P. Janssen, F. Rominger, G. Helmchen, Asymmetric Iridium(I)-Catalyzed Allylic Alkylation of Monosubstituted Allylic Substrates with Phosphinooxazolines as Ligands. Isolation, Characterization, and Reactivity of Chiral (Allyl)iridium(III) Complexes. *Organometallics* **2004**, *23*, 5459-70.
- [69] H. Rieck, G. Helmchen, Palladium complex catalyzed asymmetric allylic substitutions with nitromethane: enantioselectivities exceeding 99.9% ee. *Angew. Chem., Int. Ed. Engl.* **1996**, *34*, 2687-9.
- [70] H. Eichelmann, H.-J. Gais, Palladium-catalyzed asymmetric allylic sulfonylation. *Tetrahedron: Asymmetry* **1995**, *6*, 643-6.
- [71] C. Welter, O. Koch, G. Lipowsky, G. Helmchen, First intramolecular enantioselective iridium-catalyzed allylic aminations. *Chem. Commun.* **2004**, 896-97.
- [72] G. Helmchen, A. Dahnz, P. Duebon, M. Schelwies, R. Weihofen, Iridium-catalyzed asymmetric allylic substitutions. *Chem. Commun.* **2007**, 675-91.
- [73] K. N. Gavrilov, O. G. Bondarev, A. V. Korostylev, A. I. Polosukhin, V. N. Tsarev, N. E. Kadilnikov, S. E. Lyubimov, A. A. Shiryaev, S. V. Zheglov, H.-J. Gais, V. A. Davankov, Novel P,N-bidentate phosphite ligands in asymmetric catalysis. *Chirality* **2003**, *15*, S97-S103.
- [74] J. Ansell, M. Wills, Enantioselective catalysis using phosphorus-donor ligands containing two or three P-N or P-O bonds. *Chem. Soc. Rev.* **2002**, *31*, 259-68.
- [75] R. Takeuchi, M. Kashio, Iridium Complex-Catalyzed Allylic Alkylation of Allylic Esters and Allylic Alcohols: Unique Regio- and Stereoselectivity. *J. Am. Chem. Soc.* **1998**, *120*, 8647-55.
- [76] R. Takeuchi, N. Ue, K. Tanabe, K. Yamashita, N. Shiga, Iridium complex-

- catalyzed allylic amination of allylic esters. *J. Am. Chem. Soc.* **2001**, *123*, 9525-34.
- [77] B. Bartels, C. Garcia-Yebra, F. Rominger, G. Helmchen, Iridium-catalysed allylic substitution: Stereochemical aspects and isolation of Ir(III) complexes related to the catalytic cycle. *Eur. J. Inorg. Chem.* **2002**, 2569-86.
- [78] B. Bartels, G. Helmchen, Ir-catalyzed allylic substitution: mechanistic aspects and asymmetric synthesis with phosphorus amidites as ligands. *Chem. Commun.* **1999**, 741-42.
- [79] K. Fuji, N. Kinoshita, T. Kawabata, K. Tanaka, Enantioselective allylic substitution catalyzed by an iridium complex: remarkable effects of the counter cation. *Chem. Commun.* **1999**, 2289-90.
- [80] O. Pamies, M. Dieguez, G. Nieto, A. Ruiz, C. Claver, Highly Enantioselective Rh-Catalyzed Hydrogenation Based on Phosphine-Phosphite Ligands Derived from Carbohydrates. *J. Org. Chem.* **2001**, *66*, 8364-69.
- [81] M. T. Reetz, G. Mehler, Highly enantioselective Rh-catalyzed hydrogenation reactions based on chiral monophosphite ligands. *Angew. Chem., Int. Ed. Engl.* **2000**, *39*, 3889-90.
- [82] M. T. Reetz, J.-A. Ma, R. Goddard, BINOL-derived monodentate phosphites and phosphoramidites with phosphorus stereogenic centers: Novel ligands for transition-metal catalysis. *Angew. Chem., Int. Ed. Engl.* **2005**, *44*, 412-15.
- [83] B. L. Feringa, M. Pineschi, L. A. Arnold, R. Imbos, A. H. M. De Vries, Highly enantioselective catalytic conjugate addition and tandem conjugate addition - aldol reactions of organozinc reagents. *Angew. Chem., Int. Ed. Engl.* **1997**, *36*, 2620-23.
- [84] A. Alexakis, S. Rosset, J. Allamand, S. March, F. Guillen, C. Benhaim, Novel biphenol phosphoramidite ligands for the enantioselective copper-catalyzed conjugate addition of dialkyl zincs. *Synlett* **2001**, 1375-78.
- [85] A. Alexakis, C. Benhaim, S. Rosset, M. Humam, Dramatic Improvement of the Enantiomeric Excess in the Asymmetric Conjugate Addition Reaction Using New Experimental Conditions. *J. Am. Chem. Soc.* **2002**, *124*, 5262-63.
- [86] E. Keller, J. Maurer, R. Naasz, T. Schader, A. Meetsma, B. L. Feringa, Unexpected enhancement of enantioselectivity in copper(II) catalyzed conjugate addition of diethylzinc to cyclic enones with novel TADDOL phosphorus amidite ligands. *Tetrahedron: Asymmetry* **1998**, *9*, 2409-13.
- [87] R. Imbos, M. H. G. Brillman, M. Pineschi, B. L. Feringa, Highly Enantioselective Catalytic Conjugate Additions to Cyclohexadienones. *Org. Lett.* **1999**, *1*, 623-25.

- [88] L. A. Arnold, R. Imbos, A. Mandoli, A. H. M. De Vries, R. Naasz, B. L. Feringa, Enantioselective catalytic conjugate addition of dialkylzinc reagents using copper-phosphoramidite complexes; ligand variation and non-linear effects. *Tetrahedron* **2000**, *56*, 2865-78.
- [89] C. Monti, C. Gennari, U. Piarulli, Rh-catalyzed enantioselective conjugate addition of arylboronic acids with a dynamic library of chiral tropos phosphorus ligands. *Chem. Eur. J.* **2007**, *13*, 1547-58.
- [90] U. T. Bornscheuer, Methods to increase enantioselectivity of lipases and esterases. *Curr. Opin. Biotechnol.* **2002**, *13*, 543-47.
- [91] R. D. Schmid, R. Verger, Lipases: interfacial enzymes with attractive applications. *Angew. Chem., Int. Ed. Engl.* **1998**, *37*, 1609-33.
- [92] M. T. Reetz, Lipases as practical biocatalysts. *Curr. Op. Chem. Biol.* **2002**, *6*, 145-50.
- [93] F. H. Arnold, Combinatorial and computational challenges for biocatalyst design. *Nature* **2001**, *409*, 253-57.
- [94] D. Rotticci, J. C. Rotticci-Mulder, S. Denman, T. Norin, K. Hult, Improved enantioselectivity of a lipase by rational protein engineering. *ChemBioChem* **2001**, *2*, 766-70.
- [95] U. T. Bornscheuer, M. Pohl, Improved biocatalysts by directed evolution and rational protein design. *Curr. Op. Chem. Biol.* **2001**, *5*, 137-43.
- [96] D. Qi, C. M. Tann, D. Haring, M. D. Distefano, Generation of new enzymes via covalent modification of existing proteins. *Chem. Rev.* **2001**, *101*, 3081-111.
- [97] M. T. Reetz, Strategies for the development of enantioselective catalysts. *Pure Appl. Chem.* **1999**, *71*, 1503-09.
- [98] E. T. Farinas, T. Bulter, F. H. Arnold, Directed enzyme evolution. *Curr. Opin. Biotechnol.* **2001**, *12*, 545-51.
- [99] F. H. Arnold, Design by directed evolution. *Acc. Chem. Res.* **1998**, *31*, 125-31.
- [100] P. A. Patten, R. J. Howard, W. P. C. Stemmer, Applications of DNA shuffling to pharmaceuticals and vaccines. *Curr. Opin. Biotechnol.* **1997**, *8*, 724-33.
- [101] K.-E. Jaeger, M. T. Reetz, Directed evolution of enantioselective enzymes for organic chemistry. *Curr. Op. Chem. Biol.* **2000**, *4*, 68-73.
- [102] M. T. Reetz, Combinatorial and Evolution-Based Methods in the Creation of Enantioselective Catalysts. *Angew. Chem., Int. Ed. Engl.* **2001**, *40*, 284-310.
- [103] M. T. Reetz, A. Zonta, K. Schimossek, K. Liebeton, K.-E. Jaeger, Creation of enantioselective biocatalysts for organic chemistry by in vitro evolution. *Angew. Chem., Int. Ed. Engl.* **1998**, *36*, 2830-32.
- [104] M. T. Reetz, K.-E. Jaeger, Enantioselective enzymes for organic synthesis

- created by directed evolution. *Chem. Eur. J.* **2000**, *6*, 407-12.
- [105] M. T. Reetz, S. Wilensek, D. Zha, K. E. Jaeger, Directed Evolution of an Enantioselective Enzyme through Combinatorial Multiple-Cassette Mutagenesis. *Angew. Chem., Int. Ed. Engl.* **2001**, *40*, 3589-91.
- [106] S. A. Funke, A. Eipper, M. T. Reetz, N. Otte, W. Theil, G. Van Pouderoyen, B. W. Dijkstra, K.-E. Jaeger, T. Eggert, Directed Evolution of an Enantioselective *Bacillus subtilis* Lipase. *Biocat. Biotransform.* **2003**, *21*, 67-73.
- [107] G. P. Horsman, A. M. F. Liu, E. Henke, U. T. Bornscheuer, R. J. Kazlauskas, Mutations in distant residues moderately increase the enantioselectivity of *Pseudomonas fluorescens* esterase towards methyl 3-bromo-2-methylpropanoate and ethyl 3-phenylbutyrate. *Chem. Eur. J.* **2003**, *9*, 1933-39.
- [108] G. J. Williams, S. Domann, A. Nelson, A. Berry, Modifying the stereochemistry of an enzyme-catalyzed reaction by directed evolution. *Proc. Natl. Acad. Sci. USA* **2003**, *100*, 3143-48.
- [109] M. T. Reetz, B. Brunner, T. Schneider, F. Schulz, C. M. Clouthier, M. M. Kayser, Asymmetric catalysis: Directed evolution as a method to create enantioselective cyclohexanone monooxygenases for catalysis in Baeyer-Villiger reactions. *Angew. Chem., Int. Ed. Engl.* **2004**, *43*, 4075-78.
- [110] M. T. Reetz, Directed evolution of selective enzymes and hybrid catalysts. *Tetrahedron* **2002**, *58*, 6595-602.
- [111] M. T. Reetz, M. Rentzsch, A. Pletsch, M. Maywald, Towards the directed evolution of hybrid catalysts. *Chimia* **2002**, *56*, 721-23.
- [112] M. E. Wilson, G. M. Whitesides, Conversion of a protein to a homogeneous asymmetric hydrogenation catalyst by site-specific modification with a diphosphinerhodium(I) moiety. *J. Am. Chem. Soc.* **1978**, *100*, 306-07.
- [113] C.-C. Lin, C.-W. Lin, A. S. C. Chan, Catalytic hydrogenation of itaconic acid in a biotinylated Pyrphos-rhodium(I) system in a protein cavity. *Tetrahedron: Asymmetry* **1999**, *10*, 1887-93.
- [114] J. Collot, J. Gradinaru, N. Humbert, M. Skander, A. Zocchi, T. R. Ward, Artificial Metalloenzymes for Enantioselective Catalysis Based on Biotin-Avidin. *J. Am. Chem. Soc.* **2003**, *125*, 9030-31.
- [115] C. M. Thomas, T. R. Ward, Artificial metalloenzymes: proteins as hosts for enantioselective catalysis. *Chem. Soc. Rev.* **2005**, *34*, 337-46.
- [116] C. Letondor, A. Pordea, N. Humbert, A. Ivanova, S. Mazurek, M. Novic, T. R. Ward, Artificial Transfer Hydrogenases Based on the Biotin-(Strept)avidin Technology: Fine Tuning the Selectivity by Saturation Mutagenesis of the Host Protein. *J. Am. Chem. Soc.* **2006**, *128*, 8320-28.

- [117] A. Mahammed, Z. Gross, Albumin-Conjugated Corrole Metal Complexes: Extremely Simple Yet Very Efficient Biomimetic Oxidation Systems. *J. Am. Chem. Soc.* **2005**, *127*, 2883-87.
- [118] C. Letondor, T. R. Ward, Artificial metalloenzymes for enantioselective catalysis: Recent advances. *ChemBioChem* **2006**, *7*, 1845-52.
- [119] M. T. Reetz, N. Jiao, Copper-phthalocyanine conjugates of serum albumins as enantioselective catalysts in Diels-Alder reactions. *Angew. Chem., Int. Ed. Engl.* **2006**, *45*, 2416-19.
- [120] M. Ohashi, T. Koshiyama, T. Ueno, M. Yanase, H. Fujii, Y. Watanabe, Preparation of artificial metalloenzymes by insertion of chromium(III) Schiff base complexes into apomyoglobin mutants. *Angew. Chem., Int. Ed. Engl.* **2003**, *42*, 1005-8.
- [121] M. T. Reetz, J. J. P. Peyralans, A. Maichele, Y. Fu, M. Maywald, Directed evolution of hybrid enzymes: Evolving enantioselectivity of an achiral Rh-complex anchored to a protein. *Chem. Commun.* **2006**, 4318-20.
- [122] R. R. Davies, M. D. Distefano, A Semisynthetic Metalloenzyme Based on a Protein Cavity That Catalyzes the Enantioselective Hydrolysis of Ester and Amide Substrates. *J. Am. Chem. Soc.* **1997**, *119*, 11643-52.
- [123] M. T. Reetz, Controlling the enantioselectivity of enzymes by directed evolution: practical and theoretical ramifications. *Proc. Natl. Acad. Sci. USA* **2004**, *101*, 5716-22.
- [124] L. Panella, J. Broos, J. Jin, M. W. Fraaije, D. B. Janssen, M. Jeronimus-Stratingh, B. L. Feringa, A. J. Minnaard, J. G. De Vries, Merging homogeneous catalysis with biocatalysis; papain as hydrogenation catalyst. *Chem. Commun.* **2005**, 5656-58.
- [125] R. Corradini, S. Sforza, T. Tedeschi, R. Marchelli, Chirality as a tool in nucleic acid recognition: principles and relevance in biotechnology and in medicinal chemistry. *Chirality* **2007**, *19*, 269-94.
- [126] S. M. Hecht, Editor, *Bioorganic Chemistry: Nucleic Acids*. Oxford, UK: Oxford University Press, **1996**.
- [127] R. E. Dickerson, H. R. Drew, B. N. Conner, R. M. Wing, A. V. Fratini, M. L. Kopka, The anatomy of A-, B-, and Z-DNA. *Science* **1982**, *216*, 475-85.
- [128] R. Wing, H. Drew, T. Takano, C. Broka, S. Tanaka, K. Itakura, R. E. Dickerson, Crystal structure analysis of a complete turn of B-DNA. *Nature* **1980**, *287*, 755-8.
- [129] C. A. Frederick, G. J. Quigley, M. K. Teng, M. Coll, G. A. Van der Marel, J. H. Van Boom, A. Rich, A. H. Wang, Molecular structure of an A-DNA decamer

- d(ACCGGCCGGT). *Eur. J. Biochem.* **1989**, *181*, 295-307.
- [130] D. M. J. Lilley, R. M. Clegg, S. Diekmann, N. C. Seeman, E. von Kitzing, P. J. Hagerman, A nomenclature of junctions and branchpoints in nucleic acids. *Nucleic Acids Res.* **1995**, *23*, 3363-4.
- [131] D. M. J. Lilley, All change at Holliday junction. *Proc. Natl. Acad. Sci. USA* **1997**, *94*, 9513-15.
- [132] D. S. Wilson, J. W. Szostak, In vitro selection of functional nucleic acids. *Annu. Rev. Biochem.* **1999**, *68*, 611-47.
- [133] R. R. Breaker, DNA aptamers and DNA enzymes. *Curr. Op. Chem. Biol.* **1997**, *1*, 26-31.
- [134] G. R. Zimmermann, R. D. Jenison, C. L. Wick, J.-P. Simorre, A. Pardi, Interlocking structural motifs mediate molecular discrimination by a theophylline-binding RNA. *Nat. Struct. Biol.* **1997**, *4*, 644-49.
- [135] T. Hermann, D. J. Patel, Adaptive recognition by nucleic acid aptamers. *Science* **2000**, *287*, 820-25.
- [136] M. Famulok, Oligonucleotide aptamers that recognize small molecules. *Curr. Opin. Struct. Biol.* **1999**, *9*, 324-29.
- [137] Y. Wang, R. R. Rando, Specific binding of aminoglycoside antibiotics to RNA. *Chem. Biol.* **1995**, *2*, 281-90.
- [138] Y. Tor, Targeting RNA with small molecules. *ChemBioChem* **2003**, *4*, 998-1007.
- [139] M. Sassanfar, J. W. Szostak, An RNA motif that binds ATP. *Nature* **1993**, *364*, 550-3.
- [140] D. Kiga, Y. Futamura, K. Sakamoto, S. Yokoyama, An RNA aptamer to the xanthine/guanine base with a distinctive mode of purine recognition. *Nucleic Acids Res.* **1998**, *26*, 1755-60.
- [141] R. D. Jenison, S. C. Gill, A. Pardi, B. Polisky, High-resolution molecular discrimination by RNA. *Science* **1994**, *263*, 1425-9.
- [142] A. Geiger, P. Burgstaller, H. von der Eltz, A. Roeder, M. Famulok, RNA aptamers that bind L-arginine with sub-micromolar dissociation constants and high enantioselectivity. *Nucleic Acids Res.* **1996**, *24*, 1029-36.
- [143] I. Majerfeld, D. Puthenvedu, M. Yarus, RNA Affinity for Molecular L-Histidine; Genetic Code Origins. *J. Mol. Evol.* **2005**, *61*, 226-35.
- [144] A. Shoji, M. Kuwahara, H. Ozaki, H. Sawai, Modified DNA Aptamer That Binds the (R)-Isomer of a Thalidomide Derivative with High Enantioselectivity. *J. Am. Chem. Soc.* **2007**, *129*, 1456-64.
- [145] P. B. Dervan, Molecular recognition of DNA by small molecules. *Bioorg. Med.*

- Chem.* **2001**, *9*, 2215-35.
- [146] G. Roelfes, B. L. Feringa, DNA-based asymmetric catalysis. *Angew. Chem., Int. Ed. Engl.* **2005**, *44*, 3230-32.
- [147] R. Wombacher, S. Keiper, S. Suhm, A. Serganov, D. J. Patel, A. Jäschke, Control of stereoselectivity in an enzymatic reaction by backdoor access. *Angew. Chem., Int. Ed. Engl.* **2006**, *45*, 2469-72.
- [148] Liu and co-workers tethered the same phosphane derivative L1 to a 3'-amino terminated DNA sequence and used the resulting conjugate in a DNA-templated Wittig olefination. See: , X. Li, D. R. Liu, Stereoselectivity in DNA-templated organic synthesis and its origins. *J. Am. Chem. Soc.* **2003**, *125*, 10188-9.
- [149] X. Li, D. R. Liu, DNA-templated organic synthesis: Nature's strategy for controlling chemical reactivity applied to synthetic molecules. *Angew. Chem., Int. Ed. Engl.* **2004**, *43*, 4848-70.
- [150] S. K. Silverman, Deoxyribozymes: DNA catalysts for bioorganic chemistry. *Org. Biomol. Chem.* **2004**, *2*, 2701-6.
- [151] M. Famulok, A. Jenne, Catalysis based on nucleic acid structures. *Top. Curr. Chem.* **1999**, *202*, 101-31.
- [152] C. Hammann, D. M. J. Lilley, Folding and activity of the hammerhead ribozyme. *ChemBioChem* **2002**, *3*, 690-700.
- [153] D. M. J. Lilley, Structure, folding and mechanisms of ribozymes. *Curr. Opin. Struct. Biol.* **2005**, *15*, 313-23.
- [154] B. T. Wimberly, D. E. Brodersen, W. M. Clemons, Jr., R. J. Morgan-Warren, A. P. Carter, C. Vornrhein, T. Hartsch, V. Ramakrishnan, Structure of the 30S ribosomal subunit. *Nature* **2000**, *407*, 327-39.
- [155] A. P. Carter, W. M. Clemons, D. E. Brodersen, R. J. Morgan-Warren, B. T. Wimberly, V. Ramakrishnan, Functional insights from the structure of the 30S ribosomal subunit and its interactions with antibiotics. *Nature* **2000**, *407*, 340-48.
- [156] V. Ramakrishnan, Ribosome structure and the mechanism of translation. *Cell* **2002**, *108*, 557-72.
- [157] G. F. Joyce, Directed evolution of nucleic acid enzymes. *Annu. Rev. Biochem.* **2004**, *73*, 791-836.
- [158] R. Green, A. D. Ellington, J. W. Szostak, In vitro genetic analysis of the Tetrahymena self-splicing intron. *Nature* **1990**, *347*, 406-8.
- [159] G. F. Joyce, In vitro evolution of nucleic acids. *Curr. Opin. Struct. Biol.* **1994**, *4*, 331-6.
- [160] A. Jäschke, Artificial ribozymes and deoxyribozymes. *Curr. Opin. Struct. Biol.*

- 2001**, *11*, 321-26.
- [161] A. Jäschke, S. Keiper, SELEX: systematic evolution of ligands by exponential enrichment. *Highlights in Bioorganic Chemistry* **2004**, 433-35.
- [162] R. Fiammengo, A. Jäschke, Nucleic acid enzymes. *Curr. Opin. Biotechnol.* **2005**, *16*, 614-21.
- [163] R. R. Breaker, G. F. Joyce, A DNA enzyme that cleaves RNA. *Chem. Biol.* **1994**, *1*, 223-9.
- [164] N. Carmi, L. A. Shultz, R. R. Breaker, In vitro selection of self-cleaving DNAs. *Chem. Biol.* **1996**, *3*, 1039-46.
- [165] B. Cuenoud, J. W. Szostak, A DNA metalloenzyme with DNA ligase activity. *Nature* **1995**, *375*, 611-14.
- [166] R. L. Coppins, S. K. Silverman, A DNA enzyme that mimics the first step of RNA splicing. *Nat. Struct. Mol. Biol.* **2004**, *11*, 270-74.
- [167] Y. Li, D. Sen, A catalytic DNA for porphyrin metallation. *Nat. Struct. Biol.* **1996**, *3*, 743-7.
- [168] P. Travascio, A. J. Bennet, D. Y. Wang, D. Sen, A ribozyme and a catalytic DNA with peroxidase activity: active sites versus cofactor-binding sites. *Chem. Biol.* **1999**, *6*, 779-87.
- [169] Y. Li, R. R. Breaker, Phosphorylating DNA with DNA. *Proc. Natl. Acad. Sci. USA* **1999**, *96*, 2746-51.
- [170] Y. Li, Y. Liu, R. R. Breaker, Capping DNA with DNA. *Biochemistry* **2000**, *39*, 3106-14.
- [171] T. L. Sheppard, P. Ordoukhanian, G. F. Joyce, A DNA enzyme with N-glycosylase activity. *Proc. Natl. Acad. Sci. USA* **2000**, *97*, 7802-07.
- [172] G. M. Emilsson, R. R. Breaker, Deoxyribozymes: new activities and new applications. *Cellular and Molecular Life Sciences* **2002**, *59*, 596-607.
- [173] C. R. Geyer, D. Sen, Lanthanide probes for a phosphodiester-cleaving, lead-dependent, DNzyme. *J. Mol. Biol.* **1998**, *275*, 483-9.
- [174] G. J. Narlikar, D. Herschlag, Mechanistic aspects of enzymic catalysis: Lessons from comparison of RNA and protein enzymes. *Annu. Rev. Biochem.* **1997**, *66*, 19-59.
- [175] A. Roth, R. R. Breaker, An amino acid as a cofactor for a catalytic polynucleotide. *Proc. Natl. Acad. Sci. USA* **1998**, *95*, 6027-31.
- [176] R. Ting, J. M. Thomas, L. Lermer, D. M. Perrin, Substrate specificity and kinetic framework of a DNzyme with an expanded chemical repertoire: a putative RNaseA mimic that catalyzes RNA hydrolysis independent of a divalent metal cation. *Nucleic Acids Res.* **2004**, *32*, 6660-72.

- [177] A. V. Sidorov, J. A. Grasby, D. M. Williams, Sequence-specific cleavage of RNA in the absence of divalent metal ions by a DNAzyme incorporating imidazolyl and amino functionalities. *Nucleic Acids Res.* **2004**, *32*, 1591-601.
- [178] J. P. May, R. Ting, L. Lermer, J. M. Thomas, Y. Roupioz, D. M. Perrin, Covalent Schiff Base Catalysis and Turnover by a DNAzyme: A M²⁺-Independent AP-Endonuclease Mimic. *J. Am. Chem. Soc.* **2004**, *126*, 4145-56.
- [179] K. Kruger, P. J. Grabowski, A. J. Zaug, J. Sands, D. E. Gottschling, T. R. Cech, Self-splicing RNA: autoexcision and autocyclization of the ribosomal RNA intervening sequence of Tetrahymena. *Cell* **1982**, *31*, 147-57.
- [180] C. Guerrier-Takada, K. Gardiner, T. Marsh, N. Pace, S. Altman, The RNA moiety of ribonuclease P is the catalytic subunit of the enzyme. *Cell* **1983**, *35*, 849-57.
- [181] S. Tsukiji, S. B. Pattnaik, H. Suga, An alcohol dehydrogenase ribozyme. *Nat. Struct. Biol.* **2003**, *10*, 713-17.
- [182] D. Nieuwlandt, M. West, X. Cheng, G. Kirshenheuter, B. E. Eaton, The first example of an RNA urea synthase: Selection through the enzyme active site of human neutrophil elastase. *ChemBioChem* **2003**, *4*, 651-54.
- [183] P. J. Unrau, D. P. Bartel, RNA-catalyzed nucleotide synthesis. *Nature* **1998**, *395*, 260-63.
- [184] M. W. L. Lau, K. E. C. Cadieux, P. J. Unrau, Isolation of Fast Purine Nucleotide Synthase Ribozymes. *J. Am. Chem. Soc.* **2004**, *126*, 15686-93.
- [185] W. K. Johnston, P. J. Unrau, M. S. Lawrence, M. E. Glasner, D. P. Bartel, RNA-catalyzed RNA polymerization: accurate and general RNA-templated primer extension. *Science* **2001**, *292*, 1319-25.
- [186] M. S. Lawrence, D. P. Bartel, Processivity of ribozyme-catalyzed RNA polymerization. *Biochemistry* **2003**, *42*, 8748-55.
- [187] H. Murakami, H. Saito, H. Suga, A Versatile tRNA Aminoacylation Catalyst Based on RNA. *Chem. Biol.* **2003**, *10*, 655-62.
- [188] N. Li, F. Huang, Ribozyme-Catalyzed Aminoacylation from CoA Thioesters. *Biochemistry* **2005**, *44*, 4582-90.
- [189] T. M. Tarasow, S. L. Tarasow, B. E. Eaton, RNA-catalysed carbon-carbon bond formation. *Nature* **1997**, *389*, 54-57.
- [190] B. Seelig, A. Jäschke, A small catalytic RNA motif with Diels-Alderase activity. *Chem. Biol.* **1999**, *6*, 167-76.
- [191] B. Seelig, S. Keiper, F. Stuhlmann, A. Jäschke, Enantioselective ribozyme catalysis of a bimolecular cycloaddition reaction. *Angew. Chem., Int. Ed. Engl.* **2000**, *39*, 4576-79.

- [192] G. Sengle, A. Eisenfuhr, P. S. Arora, J. S. Nowick, M. Famulok, Novel RNA catalysts for the Michael reaction. *Chem. Biol.* **2001**, *8*, 459-73.
- [193] S. Fusz, A. Eisenfuehr, S. G. Srivatsan, A. Heckel, M. Famulok, A Ribozyme for the Aldol Reaction. *Chem. Biol.* **2005**, *12*, 941-50.
- [194] L. Jaeger, The new world of ribozymes. *Curr. Opin. Struct. Biol.* **1997**, *7*, 324-35.
- [195] M. Zivarts, Y. Liu, R. R. Breaker, Engineered allosteric ribozymes that respond to specific divalent metal ions. *Nucleic Acids Res.* **2005**, *33*, 622-31.
- [196] T. M. Tarasow, S. L. Tarasow, C. Tu, E. Kellogg, B. E. Eaton, Characteristics of an RNA Diels-Alderase Active Site. *J. Am. Chem. Soc.* **1999**, *121*, 3614-17.
- [197] T. M. Tarasow, E. Kellogg, B. L. Holley, D. Nieuwlandt, S. L. Tarasow, B. E. Eaton, The Effect of Mutation on RNA Diels-Alderases. *J. Am. Chem. Soc.* **2004**, *126*, 11843-51.
- [198] A. Serganov, S. Keiper, L. Malinina, V. Tereshko, E. Skripkin, C. Höbartner, A. Polonskaia, T. Phan Anh, R. Wombacher, R. Micura, Z. Dauter, A. Jäschke, D. J. Patel, Structural basis for Diels-Alder ribozyme-catalyzed carbon-carbon bond formation. *Nat. Struct. Mol. Biol.* **2005**, *12*, 218-24.
- [199] G. Roelfes, A. J. Boersma, B. L. Feringa, Highly enantioselective DNA-based catalysis. *Chem. Commun.* **2006**, 635-37.
- [200] G. Roelfes, DNA and RNA induced enantioselectivity in chemical synthesis. *Mol. Biosyst.* **2007**, *3*, 126-35.
- [201] L. Ropartz, N. J. Meeuwenoord, G. A. van der Marel, P. W. N. M. van Leeuwen, A. M. Z. Slawin, P. C. J. Kamer, Phosphine containing oligonucleotides for the development of metallodeoxyribozymes. *Chem. Commun.* **2007**, 1556-58.
- [202] J. Reedijk, Improved understanding in platinum antitumor chemistry. *Chem. Commun.* **1996**, 801-6.
- [203] A. Anagnostopoulou, E. Moldrheim, N. Katsaros, E. Sletten, Interaction of cis- and trans-RuCl₂(DMSO)₄ with the nucleotides GpA, d(GpA), ApG, d(ApG) and d(CCTGGTCC): high-field NMR characterization of the reaction products. *J. Biol. Inorg. Chem.* **1999**, *4*, 199-208.
- [204] C. X. Zhang, S. J. Lippard, New metal complexes as potential therapeutics. *Curr. Op. Chem. Biol.* **2003**, *7*, 481-89.
- [205] K. E. Erkkila, D. T. Odom, J. K. Barton, Recognition and Reaction of Metallointercalators with DNA. *Chem. Rev.* **1999**, *99*, 2777-95.
- [206] M. B. Fleisher, K. C. Waterman, N. J. Turro, J. K. Barton, Light-induced cleavage of DNA by metal complexes. *Inorg. Chem.* **1986**, *25*, 3549-51.

- [207] L. Jacquet, J. M. Kelly, A. Kirsch-De Mesmaeker, Photoadduct between tris(1,4,5,8-tetraazaphenanthrene)ruthenium(II) and guanosine monophosphate - a model for a new mode of covalent binding of metal complexes to DNA. *J. Chem. Soc., Chem. Commun.* **1995**, 913-14.
- [208] R. E. Molmlin, P. J. Dandliker, J. K. Barton, Charge transfer through the DNA base stack. *Angew. Chem., Int. Ed. Engl.* **1998**, *36*, 2715-30.
- [209] A. E. Friedman, J. C. Chambron, J. P. Sauvage, N. J. Turro, J. K. Barton, A molecular light switch for DNA: Ru(bpy)₂(dppz)²⁺. *J. Am. Chem. Soc.* **1990**, *112*, 4960-2.
- [210] D. S. Sigman, Nuclease activity of 1,10-phenanthroline-copper ion. *Acc. Chem. Res.* **1986**, *19*, 180-6.
- [211] K. J. Humphreys, K. D. Karlin, S. E. Rokita, Efficient and specific strand scission of DNA by a dinuclear copper complex: Comparative reactivity of complexes with linked tris(2-pyridylmethyl)amine moieties. *J. Am. Chem. Soc.* **2002**, *124*, 6009-19.
- [212] C. A. Claussen, E. C. Long, Nucleic acid recognition by metal complexes of bleomycin. *Chem. Rev.* **1999**, *99*, 2797-816.
- [213] M. Balaz, M. De Napoli, A. E. Holmes, A. Mammana, K. Nakanishi, N. Berova, R. Purrello, A cationic zinc porphyrin as a chiroptical probe for Z-DNA. *Angew. Chem., Int. Ed. Engl.* **2005**, *44*, 4006-09.
- [214] J. K. Barton, L. A. Basile, A. Danishefsky, A. Alexandrescu, Chiral probes for the handedness of DNA helixes: enantiomers of tris(4,7-diphenylphenanthroline)ruthenium(II). *Proc. Natl. Acad. Sci. USA* **1984**, *81*, 1961-5.
- [215] I. Dubey, G. Pratviel, B. Meunier, Synthesis and DNA cleavage of 2'-O-amino-linked metalloporphyrin-oligonucleotide conjugates. *J. Chem. Soc., Perkin Trans. I* **2000**, 3088-95.
- [216] J. Telser, K. A. Cruickshank, K. S. Schanze, T. L. Netzel, DNA oligomers and duplexes containing a covalently attached derivative of tris(2,2'-bipyridine)ruthenium(II): synthesis and characterization by thermodynamic and optical spectroscopic measurements. *J. Am. Chem. Soc.* **1989**, *111*, 7221-26.
- [217] I. Ortman, S. Content, N. Boutonnet, A. Kirsch-De Mesmaeker, W. Bannwarth, J. F. Constant, E. Defrancq, J. Lhomme, Ru-labeled oligonucleotides for photoinduced reactions on targeted DNA guanines. *Chem. Eur. J.* **1999**, *5*, 2712-21.
- [218] D. Ossipov, S. Gohil, J. Chattopadhyaya, Synthesis of the DNA-[Ru(tpy)(dppz)(CH₃CN)]²⁺ conjugates and their photo cross-linking studies

- with the complementary DNA strand. *J. Am. Chem. Soc.* **2002**, *124*, 13416-33.
- [219] C. H. B. Chen, D. S. Sigman, Sequence-specific scission of RNA by 1,10-phenanthroline-copper linked to deoxyoligonucleotides. *J. Am. Chem. Soc.* **1988**, *110*, 6570-2.
- [220] J. Gallagher, C.-h. B. Chen, C. Q. Pan, D. M. Perrin, Y.-M. Cho, D. S. Sigman, Optimizing the Targeted Chemical Nuclease Activity of 1,10-Phenanthroline-Copper by Ligand Modification. *Bioconjugate Chem.* **1996**, *7*, 413-20.
- [221] Liu and co-workers tethered the same phosphine derivative **2a** to a 3'-amino terminated DNA sequence and used the resulting conjugate in a DNA-templated Wittig olefination. See: Z. J. Gartner, M. W. Kanan, D. R. Liu, Multistep small-molecule synthesis programmed by DNA templates. *J. Am. Chem. Soc.* **2002**, *124*, 10304-06.
- [222] K. Sakurai, T. M. Snyder, D. R. Liu, DNA-Templated Functional Group Transformations Enable Sequence-Programmed Synthesis Using Small-Molecule Reagents. *J. Am. Chem. Soc.* **2005**, *127*, 1660-61.
- [223] O. Lentzen, E. Defrancq, J.-F. Constant, S. Schumm, D. Garcia-Fresnadillo, C. Moucheron, P. Dumy, A. Kirsch-De Mesmaeker, Determination of DNA guanine sites forming photo-adducts with Ru(II)-labeled oligonucleotides; DNA polymerase inhibition by the resulting photo-crosslinking. *J. Biol. Inorg. Chem.* **2004**, *9*, 100-08.
- [224] T. Ihara, Y. Maruo, S. Takenaka, M. Takagi, Ferrocene-oligonucleotide conjugates for electrochemical probing of DNA. *Nucleic Acids Res.* **1996**, *24*, 4273-80.
- [225] R. E. Holmlin, P. J. Dandliker, J. K. Barton, Synthesis of Metallointercalator-DNA Conjugates on a Solid Support. *Bioconjugate Chem.* **1999**, *10*, 1122-30.
- [226] A. E. Beilstein, M. W. Grinstaff, On-column derivatization of oligodeoxynucleotides with ferrocene. *Chem. Commun.* **2000**, 509-10.
- [227] A. E. Beilstein, M. W. Grinstaff, Synthesis and characterization of ferrocene-labeled oligodeoxynucleotides. *J. Organomet. Chem.* **2001**, *637-639*, 398-406.
- [228] S. I. Khan, M. W. Grinstaff, Palladium(0)-Catalyzed Modification of Oligonucleotides during Automated Solid-Phase Synthesis. *J. Am. Chem. Soc.* **1999**, *121*, 4704-05.
- [229] K. Wiederholt, L. W. McLaughlin, A 2,2'-bipyridine ligand for incorporation into oligodeoxynucleotides: synthesis, stability and fluorescence properties of ruthenium-DNA complexes. *Nucleic Acids Res.* **1999**, *27*, 2487-93.
- [230] W. C. Putnam, A. T. Daniher, B. N. Trawick, J. K. Bashkin, Efficient new ribozyme mimics: direct mapping of molecular design principles from small

- molecules to macromolecular, biomimetic catalysts. *Nucleic Acids Res.* **2001**, *29*, 2199-204.
- [231] G. B. Dreyer, P. B. Dervan, Sequence-specific cleavage of single-stranded DNA: oligodeoxynucleotide-EDTA X Fe(II). *Proc. Natl. Acad. Sci. USA* **1985**, *82*, 968-72.
- [232] D. E. Bergstrom, N. P. Gerry, Precision Sequence-Specific Cleavage of a Nucleic Acid by a Minor-Groove-Directed Metal-Binding Ligand Linked through N-2 of Deoxyguanosine. *J. Am. Chem. Soc.* **1994**, *116*, 12067-68.
- [233] S. T. Gaballah, C. E. Kerr, B. E. Eaton, T. L. Netzel, Synthesis of 5-(2,2'-bipyridinyl and 2,2'-bipyridinediiumyl)-2'-deoxyuridine nucleosides: precursors to metallo-DNA conjugates. *Nucleosides Nucleotides Nucleic Acids* **2002**, *21*, 547-60.
- [234] D. J. Hurley, Y. Tor, Ru(II) and Os(II) Nucleosides and Oligonucleotides: Synthesis and Properties. *J. Am. Chem. Soc.* **2002**, *124*, 3749-62.
- [235] C. J. Yu, H. Yowanto, Y. Wan, T. J. Meade, Y. Chong, M. Strong, L. H. Donilon, J. F. Kayyem, M. Gozin, G. F. Blackburn, Uridine-Conjugated Ferrocene DNA Oligonucleotides: Unexpected Cyclization Reaction of the Uridine Base. *J. Am. Chem. Soc.* **2000**, *122*, 6767-68.
- [236] E. S. Krider, J. J. Rack, N. L. Frank, T. J. Meade, Automated Synthesis of 3'-Metalated Oligonucleotides. *Inorg. Chem.* **2001**, *40*, 4002-09.
- [237] E. Meggers, P. L. Holland, W. B. Tolman, F. E. Romesberg, P. G. Schultz, A Novel Copper-Mediated DNA Base Pair. *J. Am. Chem. Soc.* **2000**, *122*, 10714-15.
- [238] H. Weizman, Y. Tor, 2,2'-Bipyridine Ligandose: A Novel Building Block for Modifying DNA with Intra-Duplex Metal Complexes. *J. Am. Chem. Soc.* **2001**, *123*, 3375-76.
- [239] J. L. Czapinski, T. L. Sheppard, Nucleic Acid Template-Directed Assembly of Metallosalen-DNA Conjugates. *J. Am. Chem. Soc.* **2001**, *123*, 8618-19.
- [240] M. Shionoya, K. Tanaka, Artificial metallo-DNA: a bio-inspired approach to metal array programming. *Curr. Op. Chem. Biol.* **2004**, *8*, 592-97.
- [241] G. H. Clever, K. Polborn, T. Carell, A highly DNA-duplex-stabilizing metal-salen base pair. *Angew. Chem., Int. Ed. Engl.* **2005**, *44*, 7204-08.
- [242] K. Tanaka, A. Tengeiji, T. Kato, N. Toyama, M. Shionoya, A Discrete Self-Assembled Metal Array in Artificial DNA. *Science* **2003**, *299*, 1212-13.
- [243] G. H. Clever, T. Carell, Controlled stacking of 10 transition-metal ions inside a DNA duplex. *Angew. Chem., Int. Ed. Engl.* **2007**, *46*, 250-53.
- [244] J. D. Vaught, T. Dewey, B. E. Eaton, T7 RNA polymerase transcription with 5-

- position modified UTP derivatives. *J. Am. Chem. Soc.* **2004**, *126*, 11231-7.
- [245] O. Thum, S. Jager, M. Famulok, Functionalized DNA: a new replicable biopolymer. *Angew. Chem., Int. Ed. Engl.* **2001**, *40*, 3990-93.
- [246] S. Jaeger, G. Rasched, H. Kornreich-Leshem, M. Engeser, O. Thum, M. Famulok, A Versatile Toolbox for Variable DNA Functionalization at High Density. *J. Am. Chem. Soc.* **2005**, *127*, 15071-82.
- [247] H. Sawai, A. Ozaki-Nakamura, M. Mine, H. Ozaki, Synthesis of New Modified DNAs by Hyperthermophilic DNA Polymerase: Substrate and Template Specificity of Functionalized Thymidine Analogues Bearing an sp³-Hybridized Carbon at the C5 α -Position for Several DNA Polymerases. *Bioconjugate Chem.* **2002**, *13*, 309-16.
- [248] H. Weizman, Y. Tor, Redox-active metal-containing nucleotides: Synthesis, tunability, and enzymatic incorporation into DNA. *J. Am. Chem. Soc.* **2002**, *124*, 1568-69.
- [249] S. A. Benner, Understanding Nucleic Acids Using Synthetic Chemistry. *Acc. Chem. Res.* **2004**, *37*, 784-97.
- [250] Unpublished data Dr. R. Fiammengo, University of Heidelberg, 2004-2005. The decaethyleneglycol spacer **S**, the ligands **L3**, **L8** and the complex [Rh(BINAP)(nbd)]BF₄ were kindly provided by Dr. R. Fiammengo.
- [251] M. A. Said, K. C. K. Swamy, M. Veith, V. Huch, Reactivity of cyclic arsenites and phosphites: x-ray structures of bis(5,5-dimethyl-1,3,2-dioxarsenan-2-yl) ether and bis(2,4,8,10-tetra-tert-butyl-12H-dibenzo[d,g][1,3,2]dioxarsenocin-6-yl) ether. *J. Chem. Soc., Perkin Trans. 1* **1995**, 2945-51.
- [252] J.-G. Boiteau, R. Imbos, A. J. Minnaard, B. L. Feringa, Rhodium-Catalyzed Asymmetric Conjugate Additions of Boronic Acids Using Monodentate Phosphoramidite Ligands. *Org. Lett.* **2003**, *5*, 681-84.
- [253] C. Monti, C. Gennari, U. Piarulli, Enantioselective conjugate addition of phenylboronic acid to enones catalyzed by a chiral tropos/atropos rhodium complex at the coalescence temperature. *Chem. Commun.* **2005**, 5281-83.
- [254] M. Caprioara, R. Fiammengo, M. Engeser, A. Jäschke, DNA-based phosphane ligands. *Chem. Eur. J.* **2007**, *13*, 2089-95, S89/1-S89/10.
- [255] A. M. MacMillan, G. L. Verdine, Synthesis of functionally tethered oligodeoxynucleotides by the convertible nucleoside approach. *J. Org. Chem.* **1990**, *55*, 5931-33.
- [256] Y. Z. Xu, Q. Zheng, P. F. Swann, Synthesis of DNA containing modified bases by post-synthetic substitution. Synthesis of oligomers containing 4-substituted thymine: O4-alkylthymine, 5-methylcytosine, N4-dimethylamino-5-

- methylcytosine, and 4-thiothymine. *J. Org. Chem.* **1992**, *57*, 3839-45.
- [257] N. Haginoya, A. Ono, Y. Nomura, Y. Ueno, A. Matsuda, Nucleosides and Nucleotides. 160. Synthesis of Oligodeoxyribonucleotides Containing 5-(N-Aminoalkyl)carbamoyl-2'-deoxyuridines by a New Postsynthetic Modification Method and Their Thermal Stability and Nuclease-Resistance Properties. *Bioconjugate Chem.* **1997**, *8*, 271-80.
- [258] O. Gorchs, M. Hernandez, L. Garriga, E. Pedroso, A. Grandas, J. Farras, A New Method for the Preparation of Modified Oligonucleotides. *Org. Lett.* **2002**, *4*, 1827-30.
- [259] R. Narukulla, D. E. G. Shuker, Y.-Z. Xu, Post-synthetic and site-specific modification of endocyclic nitrogen atoms of purines in DNA and its potential for biological and structural studies. *Nucleic Acids Res.* **2005**, *33*, 1767-78.
- [260] A. M. MacMillan, G. L. Verdine, Engineering tethered DNA molecules by the convertible nucleoside approach. *Tetrahedron* **1991**, *47*, 2603-16.
- [261] R. S. Coleman, E. A. Kesicki, Synthesis and Postsynthetic Modification of Oligodeoxynucleotides Containing 4-Thio-2'-deoxyuridine (ds4U). *J. Am. Chem. Soc.* **1994**, *116*, 11636-42.
- [262] C. A. Frederick, G. J. Quigley, G. A. Van der Marel, J. H. Van Boom, A. H. J. Wang, A. Rich, Methylation of the EcoRI recognition site does not alter DNA conformation: the crystal structure of d(CGCGAm6ATTCGCG) at 2.0-Å resolution. *J. Biol. Chem.* **1988**, *263*, 17872-9.
- [263] <http://www.sigmaaldrich.com/catalog/search/TablePage/14572938>.
- [264] J.-L. Mergny, L. Lacroix, Analysis of thermal melting curves. *Oligonucleotides* **2003**, *13*, 515-37.
- [265] G. Bonner, A. M. Klibanov, Structural stability of DNA in nonaqueous solvents. *Biotechnol. Bioeng.* **2000**, *68*, 339-44.
- [266] G. Lober, H. Schutz, V. Kleinwachter, Effect of organic solvents on the properties of the complexes of DNA with proflavine and similar compounds. *Biopolymers* **1972**, *11*, 2439-59.
- [267] J. Casey, N. Davidson, Rates of formation and thermal stabilities of RNA:DNA and DNA:DNA duplexes at high concentrations of formamide. *Nucleic Acids Res.* **1977**, *4*, 1539-52.
- [268] S. I. Kirin, P. Duebon, T. Weyhermueller, E. Bill, N. Metzler-Nolte, Amino Acid and Peptide Bioconjugates of Copper(II) and Zinc(II) Complexes with a Modified N,N-Bis(2-picolyl)amine Ligand. *Inorg. Chem.* **2005**, *44*, 5405-15.
- [269] S. R. Gilbertson, G. Chen, M. McLoughlin, Versatile Building Block for the Synthesis of Phosphine-Containing Peptides: The Sulfide of

- Diphenylphosphinoserine. *J. Am. Chem. Soc.* **1994**, *116*, 4481-2.
- [270] O. Herd, A. Hessler, M. Hingst, M. Tepper, O. Stelzer, Water soluble phosphines. VIII. Palladium-catalyzed P-C cross coupling reactions between primary or secondary phosphines and functional aryl iodides - a novel synthetic route to water soluble phosphines. *J. Organomet. Chem.* **1996**, *522*, 69-76.
- [271] Acidifying results in oxazoline ring opening. See: A. Laaziri, J. Uziel, S. Juge, Electrophilic ring opening of oxazolines derived from serine and threonine: a practical entry to N(N)-protected α -halogeno α -amino esters. *Tetrahedron: Asymmetry* **1998**, *9*, 437-47.
- [272] B. M. Novak, R. H. Grubbs, Catalytic organometallic chemistry in water: the aqueous ring-opening metathesis polymerization of 7-oxanorbornene derivatives. *J. Am. Chem. Soc.* **1988**, *110*, 7542-3.
- [273] B. Cornils, W. A. Herrmann, Editors, *Aqueous-Phase Organometallic Catalysis: Concepts and Applications*, **1998**.
- [274] D. Sinou, Asymmetric organometallic-catalyzed reactions in aqueous media. *Adv. Synth. Catal.* **2002**, *344*, 221-37.
- [275] S. P. Smidt, Iridium-Catalysed Enantioselective Hydrogenation - New P,N Ligands and Mechanistic Investigations. *Inauguraldissertation* **2003**.
- [276] S. P. Smidt, A. Pfaltz, E. Martinez-Viviente, P. S. Pregosin, A. Albinati, X-ray and NOE Studies on Trinuclear Iridium Hydride Phosphino Oxazoline (PHOX) Complexes. *Organometallics* **2003**, *22*, 1000-09.
- [277] J.-G. Boiteau, A. J. Minnaard, B. L. Feringa, High Efficiency and Enantioselectivity in the Rh-Catalyzed Conjugate Addition of Arylboronic Acids Using Monodentate Phosphoramidites. *J. Org. Chem.* **2003**, *68*, 9481-84.
- [278] R. Itooka, Y. Iguchi, N. Miyaura, Rhodium-Catalyzed 1,4-Addition of Arylboronic Acids to α,β -Unsaturated Carbonyl Compounds: Large Accelerating Effects of Bases and Ligands. *J. Org. Chem.* **2003**, *68*, 6000-04.
- [279] M. Lautens, A. Roy, K. Fukuoka, K. Fagnou, B. Martin-Matute, Rhodium-Catalyzed Coupling Reactions of Arylboronic Acids to Olefins in Aqueous Media. *J. Am. Chem. Soc.* **2001**, *123*, 5358-59.
- [280] T. Hayashi, M. Takahashi, Y. Takaya, M. Ogasawara, Catalytic Cycle of Rhodium-Catalyzed Asymmetric 1,4-Addition of Organoboronic Acids. Arylrhodium, Oxa- p -allylrhodium, and Hydroxorhodium Intermediates. *J. Am. Chem. Soc.* **2002**, *124*, 5052-58.
- [281] B. M. Trost, M. L. Crawley, Asymmetric Transition-Metal-Catalyzed Allylic Alkylations: Applications in Total Synthesis. *Chem. Rev.* **2003**, *103*, 2921-43.
- [282] F. Glorius, A. Pfaltz, Enantioselective Molybdenum-Catalyzed Allylic

- Alkylation Using Chiral Bisoxazoline Ligands. *Org. Lett.* **1999**, *1*, 141-44.
- [283] B. M. Trost, K. Dogra, I. Hachiya, T. Emura, D. L. Hughes, S. Krska, R. A. Reamer, M. Palucki, N. Yasuda, P. J. Reider, Designed ligands as probes for the catalytic binding mode in mo-catalyzed asymmetric allylic alkylation. *Angew. Chem., Int. Ed. Engl.* **2002**, *41*, 1929-32.
- [284] O. Belda, C. Moberg, Molybdenum-Catalyzed Asymmetric Allylic Alkylations. *Acc. Chem. Res.* **2004**, *37*, 159-67.
- [285] G. C. Lloyd-Jones, A. Pfaltz, Chiral phosphinodihydrooxazoles in asymmetric catalysis: tungsten-catalyzed allylic substitution. *Angew. Chem., Int. Ed. Engl.* **1995**, *34*, 462-4.
- [286] P. A. Evans, J. D. Nelson, Conservation of Absolute Configuration in the Acyclic Rhodium-Catalyzed Allylic Alkylation Reaction: Evidence for an Enyl (s + p) Organorhodium Intermediate. *J. Am. Chem. Soc.* **1998**, *120*, 5581-82.
- [287] D. Enders, B. Jandeleit, S. von Berg, G. Raabe, J. Runsink, Iron-Mediated Allylic Substitution Reactions with Chirality Transfer. Stereochemistry of the Formation of Diastereo- and Enantiomerically Enriched Olefinic and Allylic Tetracarbonyl Iron Complexes. *Organometallics* **2001**, *20*, 4312-32.
- [288] Y. Morisaki, T. Kondo, T. Mitsudo, Ruthenium-Catalyzed Allylic Substitution of Cyclic Allyl Carbonates with Nucleophiles. Stereoselectivity and Scope of the Reaction. *Organometallics* **1999**, *18*, 4742-46.
- [289] B. M. Trost, P. L. Fraise, Z. T. Ball, A stereospecific ruthenium-catalyzed allylic alkylation. *Angew. Chem., Int. Ed. Engl.* **2002**, *41*, 1059-61.
- [290] R. Takeuchi, M. Kashio, Highly selective allylic alkylation with a carbon nucleophile at the more substituted allylic terminus catalyzed by an iridium complex: an efficient method for constructing quaternary carbon centers. *Angew. Chem., Int. Ed. Engl.* **1997**, *36*, 263-65.
- [291] R. Takeuchi, N. Shiga, Complete Retention of Z Geometry in Allylic Substitution Catalyzed by an Iridium Complex. *Org. Lett.* **1999**, *1*, 265-67.
- [292] T. Ohmura, J. F. Hartwig, Regio- and Enantioselective Allylic Amination of Achiral Allylic Esters Catalyzed by an Iridium-Phosphoramidite Complex. *J. Am. Chem. Soc.* **2002**, *124*, 15164-65.
- [293] F. Lopez, T. Ohmura, J. F. Hartwig, Regio- and Enantioselective Iridium-Catalyzed Intermolecular Allylic Etherification of Achiral Allylic Carbonates with Phenoxides. *J. Am. Chem. Soc.* **2003**, *125*, 3426-27.
- [294] C. A. Kiener, C. Shu, C. Incarvito, J. F. Hartwig, Identification of an Activated Catalyst in the Iridium-Catalyzed Allylic Amination and Etherification. Increased Rates, Scope, and Selectivity. *J. Am. Chem. Soc.* **2003**, *125*, 14272-73.

- [295] A. Leitner, S. Shekhar, M. J. Pouy, J. F. Hartwig, A Simple Iridium Catalyst with a Single Resolved Stereocenter for Enantioselective Allylic Amination. Catalyst Selection from Mechanistic Analysis. *J. Am. Chem. Soc.* **2005**, *127*, 15506-14.
- [296] A. Leitner, C. Shu, J. F. Hartwig, Editing the stereochemical elements in an iridium catalyst for enantioselective allylic amination. *Proc. Natl. Acad. Sci. USA* **2004**, *101*, 5830-33.
- [297] D. Polet, A. Alexakis, Kinetic Study of Various Phosphoramidite Ligands in the Iridium-Catalyzed Allylic Substitution. *Org. Lett.* **2005**, *7*, 1621-24.
- [298] D. Polet, A. Alexakis, K. Tissot-Croset, C. Corminboeuf, K. Ditrich, Phosphoramidite ligands in iridium-catalyzed allylic substitution. *Chem. Eur. J.* **2006**, *12*, 3596-609.
- [299] U. M. Lindstroem, Stereoselective Organic Reactions in Water. *Chem. Rev.* **2002**, *102*, 2751-71.
- [300] Y. Uozumi, H. Danjo, T. Hayashi, Palladium-catalyzed asymmetric allylic substitution in aqueous media using amphiphilic resin-supported MOP ligands. *Tetrahedron Lett.* **1998**, *39*, 8303-06.
- [301] S. dos Santos, Y. Tong, F. Quignard, A. Choplin, D. Sinou, J. P. Dutasta, Supported Aqueous-Phase Palladium Catalysts for the Reaction of Allylic Substitution: Toward an Understanding of the Catalytic System. *Organometallics* **1998**, *17*, 78-89.
- [302] M. Feuerstein, D. Laurenti, H. Doucet, M. Santelli, Palladium-tetraphosphine catalysed allylic substitution in water. *Tetrahedron Lett.* **2001**, *42*, 2313-15.
- [303] T. Hashizume, K. Yonehara, K. Ohe, S. Uemura, A Novel Amphiphilic Chiral Ligand Derived from D-Glucosamine. Application to Palladium-Catalyzed Asymmetric Allylic Substitution Reaction in an Aqueous or an Organic Medium, Allowing for Catalyst Recycling. *J. Org. Chem.* **2000**, *65*, 5197-201.
- [304] B. Wiese, G. Helmchen, Chiral phosphinooxazolines with a bi- or tricyclic oxazoline moiety - applications in Pd-catalyzed allylic alkylations. *Tetrahedron Lett.* **1998**, *39*, 5727-30.
- [305] W. S. Sheldrick, B. Guenther, Synthesis and structure of the mixed bridged diene-rhodium(I) complex [(COD)Rh(m-Cl)(m-OAc)Rh(COD)]. Reactions with the modified purine bases N⁶,N⁶-dimethyladenine and 8-aza-9-methyladenine. *J. Organomet. Chem.* **1989**, *375*, 233-43.
- [306] J. D. Engel, P. H. von Hippel, Effects of methylation on the stability of nucleic acid conformations: studies at the monomer level. *Biochemistry* **1974**, *13*, 4143-58.

- [307] C. R. Allerson, S. L. Chen, G. L. Verdine, A Chemical Method for Site-Specific Modification of RNA: The Convertible Nucleoside Approach. *J. Am. Chem. Soc.* **1997**, *119*, 7423-33.
- [308] J. Sambrook, D. W. Russell, *Molecular Cloning. A Laboratory Manual, Vol. 1-3*, Cold Spring Harbor, New York, **2001**.
- [309] F. M. Ausubel, R. Brent, R. E. Kingston, M. D. D., J. G. Seidman, J. A. Smith, K. Struhl, *Current Protocols in Molecular Biology, Vol. 1*, John Wiley & Sons, Inc., **2004**.
- [310] H. Hocke, Y. Uozumi, A simple synthetic approach to homochiral 6- and 6'-substituted 1,1'-binaphthyl derivatives. *Tetrahedron* **2003**, *59*, 619-30.
- [311] A. Rimkus, N. Sewald, First Synthesis of a β -Homoamino Acid by Enantioselective Catalysis. *Org. Lett.* **2003**, *5*, 79-80.
- [312] J. Duran, M. Gulias, L. Castedo, J. L. Mascarenas, Ligand-Induced Acceleration of the Intramolecular [3 + 2] Cycloaddition between Alkynes and Alkylidenecyclopropanes. *Org. Lett.* **2005**, *7*, 5693-96.
- [313] J. Hu, M. J. Miller, Total Synthesis of a Mycobactin S, a Siderophore and Growth Promoter of Mycobacterium Smegmatis, and Determination of its Growth Inhibitory Activity against Mycobacterium tuberculosis. *J. Am. Chem. Soc.* **1997**, *119*, 3462-68.
- [314] V. Ravindar, H. Schumann, H. Hemling, J. Blum, Synthesis and structure determination of some platinum(II) complexes with hydrophilic carboxylated tertiary phosphine ligands. *Inorg. Chim. Acta* **1995**, *240*, 145-52.
- [315] S. L. Beaucage, R. P. Iyer, The functionalization of oligonucleotides via phosphoramidite derivatives. *Tetrahedron* **1993**, *49*, 1925-63.

List of publications

Papers

M. Caprioara, R. Fiammengo, M. Engeser, A. Jäschke, DNA-Based Phosphane Ligands, *Chemistry - A European Journal*, **2007**, *13*, 2089-2095

Posters

- R. Fiammengo, M. Caprioara, P. Fournier, K. Musilek, N. Sauer, A. Jäschke - Towards RNA-based hybrid catalysts, Joint Workshop "Templates meet Catalysis", June 7-8 2004 Bonn, Germany

- M. Caprioara, R. Fiammengo, C. Kuhmann, A. Jäschke - Functionalized DNA and RNA as Ligands for Asymmetric Catalysis, Nucleic Acid Chemical Biology (NACB) PhD Summer School, June 19-23 2005 Odense, Denmark

- Roberto Fiammengo, Mihaela Caprioara, Pierre Fournier, Andres Jäschke - Selective hybrid catalysts based on nucleic acids, Heidelberg Forum of Molecular Catalysis, 8th July 2005, Heidelberg, Germany

- M. Caprioara, R. Fiammengo, P. Fournier, A. Jäschke - Functionalized DNA and RNA as Ligands for Asymmetric Catalysis and in vitro selection of Hybrid Catalysts, "Concepts and Advances in Modern Catalysis" Joint Workshop, University of California, Berkley, Northwestern University, Evanston, University of Heidelberg, May 5-6 2006, Heidelberg, Germany

- M. Caprioara, P. Fournier, R. Fiammengo, A. Jäschke - DNA-Based Ligands for Transition Metals and Use in Asymmetric Catalysis, Heidelberg Forum of Molecular Catalysis, June 2007, Heidelberg, Germany

Oral presentations

M. Caprioara, P. Fournier, R. Fiammengo, A. Jäschke - Towards RNA-based Hybrid Catalysts, Groningen Meets Heidelberg - Catalysis and More, 13rd June 2007, Heidelberg, Germany